Reliability Assessment of Shear Design Provisions for Reinforced Concrete Beams with Stirrups

By

Oladimeji Benedict Olalusi

Dissertation presented for the degree of Doctor of Philosophy
in the Faculty of Engineering at Stellenbosch University

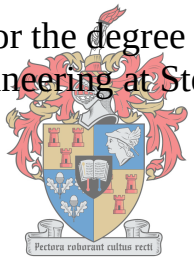

Department of Civil Engineering,
University of Stellenbosch,
Private Bag X1, Matieland 7602, South Africa.

Promoter

Prof. C. Viljoen

December 2018

Declaration

By submitting this dissertation electronically, I declare that the entirety of the work contained therein is my own, original work, that I am the sole author thereof (save to the extent explicitly otherwise stated), that reproduction and publication thereof by Stellenbosch University will not infringe any third party rights and that I have not previously in its entirety or in part submitted it for obtaining any qualification.

Signature: . . . . . .
O.B. Olalusi

December 2018
Date: . . . . . .

UNIVERSITEIT·STELLENBOSCH·UNIVERSITY
jou kennisvennoot • your knowledge partner

Plagiaatverklaring / Plagiarism *Declaration*

1 Plagiaat is die oorneem en gebruik van die idees, materiaal en ander intellektuele eiendom van ander persone asof dit jou eie werk is.
Plagiarism is the use of ideas, material and other intellectual property of another's work and to present is as my own.

2 Ek erken dat die pleeg van plagiaat 'n strafbare oortreding is aangesien dit 'n vorm van diefstal is.
I agree that plagiarism is a punishable offence because it constitutes theft.

3 Ek verstaan ook dat direkte vertalings plagiaat is.
also understand that direct translations are plagiarism.

4 Dienooreenkomstig is alle aanhalings en bydraes vanuit enige bron (ingesluit die internet) volledig verwys (erken). Ek erken dat die woordelikse aanhaal van teks sonder aanhalingstekens (selfs al word die bron volledig erken) plagiaat is.
Accordingly all quotations and contributions from any source whatsoever (including the internet) have been cited fully. I understand that the reproduction of text without quotation marks (even when the source is cited) is plagiarism.

5 Ek verklaar dat die werk in hierdie skryfstuk vervat, behalwe waar anders aangedui, my eie oorspronklike werk is en dat ek dit nie vantevore in die geheel of gedeeltelik ingehandig het vir bepunting in hierdie module/werkstuk of 'n ander module/werkstuk nie.
declare that the work contained in this assignment, except where otherwise stated, is my original work and that I have not previously (in its entirety or in part) submitted it for grading in this module/assignment or another module/assignment.

O.B OLALUSI	**DECEMBER 2018**
Voorletters en van / *Initials and surname*	**Datum / *Date***

Abstract

EN 1992-1-1: Design of concrete structures (EC2) has been accepted for adoption by South Africa to replace SANS 10100-1. EC2 shear design formulation is based on the Variable Strut Inclination Method (VSIM). The mean value predictions of the operational EC2 VSIM have been shown to underestimate shear capacity at low stirrup quantities. Conversely, the model overestimates shear capacity at high stirrup quantities (Cladera & Mari, 2007). There is a concern regarding sufficient safety performance at high levels of stirrup reinforcement, and over conservatism at low stirrup reinforcement is uneconomical.

The systematic sensitivity of EC2 VSIM mean value predictions to the amount of stirrup reinforcement motivates the assessment of the consistency and uniformity of the reliability index of EC2 shear design formulation over the range of practical design situations i.e. shear reinforcements $\rho_w f_{ywm}$, concrete strengths f_{cm}, beam depths d and type of beam cross section.

Quantification of model uncertainty and bias is an important first step since these contribute significantly to reliability performance (Holicky *et al*, 2015). The study characterised model factors for various shear resistance models by comparing unbiased predictions of the models to experimental test results. The derived model factors were investigated parametrically against important shear design parameters. The model factors related to the operational EC2 VSIM shear capacity predictions were found to be sensitive to the amount of shear reinforcement with model factors significantly above one (underpredicting capacity) at low levels of stirrup reinforcement. Correlation and regression assessments uncovered milder sensitivities to other vital parameters affecting shear strength.

Based on the results obtained from the model factor characterisation, two shear resistance models were considered suitable as general probabilistic model GPMs for the reliability assessment of EC2 shear design procedure and alternative shear design procedures. The principal GPM was established based on the probabilistic representation of the Modified Compression Field Theory (MCFT). MCFT capacity predictions were obtained from the implementation sectional analysis program Response-2000 (R2k). As a validation procedure, an alternative GPM based on the Compression Chord Capacity Model (CCC) was implemented.

The First Order Reliability Method (FORM) was used to compute the reliability index for representative test sections. The outcome of EC2 reliability assessment indicated uneconomically high reliability at low levels of shear reinforcement, high concrete strength and large beam depth, and actively reducing reliability with increased levels of shear reinforcement, reduced concrete strength

and reduced beam depth for both rectangular and I-shaped beams. EC2 underestimates design shear resistance for I-beams due to the neglect of shear contributions from compression flanges and longitudinal reinforcements (dowel action), thereby resulting in higher reliability values for such beams. Reliability indices of all the test sections investigated meet the target reliability requirement for Reliability Class 2 structures prescribed by basis of design standards SANS 10160-1 and EN 1990, for the design range considered.

The inconsistent reliability performance of EC2 VSIM shear design formulation across practical ranges of main shear design parameters motivated the assessment of alternative approaches (ACI and Fib Model Code 2010 (III)) to identify other suitable design formulations in terms of achieving the target reliability index consistently. The reliability performance of ACI and MC-10 (III) shear design provisions was assessed at parametric variations of shear reinforcement $\rho_w f_{ywm}$, concrete strength f_{cm} and beam depth d; and compared to that of the EC2 shear design formulation. The reliability levels of ACI and MC-10 (III) decrease as the amount of shear reinforcement increases and increase as the concrete strength increases. MC-10 (III) and ACI predict less conservative reliability estimates at low amount of shear reinforcement compared to EC2 VSIM, indicating that MC-10 (III) and ACI are more economical at this design situation. MC-10 (III) and ACI reliability levels drastically decrease with increasing beam depth. The reliability of small beams designed according to MC-10 (III) and ACI shear design formulations substantially exceeded the target reliabilities. However, the reliability of MC-10 (III) for deep beams with low concrete strengths falls quite significantly below the target reliability values.

Opsomming

EN 1992-1-1: Ontwerp van betonstrukture (EC2) is aanvaar vir aanneming deur Suid-Afrika om SANS 10100-1 te vervang. EC2 gebruik 'n skuifontwerp metode wat bekend staan as die Veranderlike Stut Hoek Metode (VSHM). Die gemiddelde waarde voorspellings van die operasionele EC2 VSHM toon dat die skuifkapasiteit by lae skuifbewapening hoeveelhede onderskat word. Aan die ander kant oorskat die model skuifkapasiteit by hoë skuifbewapening hoeveelhede (Cladera & Mari, 2007). Daar bestaan kommer oor genoegsame veiligheidsoptrede by hoë vlakke van skuifbewapening versterkings; en oor-konserwatisme by lae skuifbewapening is onekonomies.

Die sistematiese sensitiwiteit van EC2 VSHM gemiddelde waarde voorspellings met skuifbewapening motiveer die noodsaaklikheid om die konsekwentheid van die betroubaarheidsindeks van EC2 skuifontwerp formulering te evalueer oor die omvang van praktiese ontwerp situasies dit wil sê skuifversterkings $\rho_w f_{ywm}$, beton sterkte f_{cm}, balkdieptes d asook dwarssnit tipes.

Kwantifisering van model onsekerheid en vooroordeel is 'n belangrike eerste stap aangesien dit aansienlik bydra tot betroubaarheidsprestasie (Holicky et al, 2015). Die studie het modelfaktore vir verskillende skuifweerstandmodelle karakteriseer deur onbevooroordeelde voorspellings van die modelle te vergelyk met eksperimentele toets resultate. Die modelfaktore is parametries ondersoek teen belangrike skuifontwerp parameters. Die modelfaktore wat verband hou met die operasionele EC2 VSHM skuifkapasiteit voorspellings, is sensitief vir die hoeveelheid skuifversterking met modelfaktore aansienlik hoër as een (onder-voorspelden kapasiteit) by hoë vlakke van skuifbewapening versterkings. Korrelasie- en regressie-assesserings het matiger sensitiwiteit met ander belangrike parameters wat skuifsterkte beïnvloed.

Op grond van die modelfaktor karakterisering, is twee geskikte algemene waarskynlikheid modelle AWM's identifiseer vir die betroubaarheids evaluering van die skuifontwerp prosedures. Die hoof AWM is ‘n waarskynlikheids voorstelling van die Aangepaste Drukveld Teorie (ADT). ADT kapasiteit voorspellings is gemaak deur die implementerings snit-analise program Response-2000 (R2k). As 'n geldigings prosedure, is 'n alternatiewe AWM gebaseer op die Druk Koord Kapasiteitsmodel (DKK) geïmplementeer.

Die eerste orde betroubaarheids metode (EOBM) is gebruik om die betroubaarheidsindeks vir verteenwoordigende toetsafdelings te bereken. Vir VSHM dui die uitkoms op onekonomiese hoë betroubaarheid by lae vlakke van skuifversterking, hoë beton sterkte, en groot balkdieptes.

Betroubaarheid verminder aktief met verhoogde vlakke van skuifversterking, verminderde beton sterkte en verminderde balkdiepte vir beide reghoekige en I-vormige balke. EC2 onderskat ontwerp skuifweerstand vir I-balke omdat skuifbydraes vanaf die drukflense en langstaal buite rekening gelaat word wat sodoende hoër betroubaarheids waardes vir sulke balke tot gevolg het. Betroubaarheids indekse van al die toets snitte wat ondersoek is haal die teiken betroubaarheid vir Betroubaarheids Klas 2 strukture volgens beide SANS 10160-1 en EN 1990.

Die onkonstante betroubaarheidsprestasie van EC2 VSHM skuifontwerp formulering oor praktiese omvang van hoofskuif ontwerpparameters het die assessering van alternatiewe benaderings (ACI en Fib Model Kode 2010 (III)) gemotiveer om ontwerpformulering te vind wat beter presteer ten opsigte van die konsekwente behaling van die teiken betroubaarheidsindeks. Die betroubaarheidsprestasie van ACI en MC-10 (III) skuifontwerp voorsienings is beoordeel by parametriese variasies van skuifversterking $p_w f_{ywm}$, betonsterkte f_{cm} en balkdiepte d; en vergelyk met dié van die EC2 skuifontwerp formulering. Die betroubaarheidsvlakke van ACI en MC-10 (III) neem af soos die hoeveelheid skuifversterking $p_w f_{ywm}$ verhoog, en neem toe namate die beton sterkte verhoog. MC-10 (III) en ACI voorspel minder konserwatiewe betroubaarheidsberamings by lae hoeveelheid skuifversterking in vergelyking met EC2 VSHM, wat aandui dat MC-10 (III) en ACI meer ekonomies is in hierdie ontwerpsituasie. MC-10 (III) en ACI se betroubaarheidsvlakke neem drasties af met toenemende balkdiepte. Die betroubaarheid van klein balke wat volgens MC-10 (III) en ACI-skuifontwerp formules ontwerp is, het die geteikende betroubaarhede aansienlik oorskry. Die betroubaarheid van MC-10 (III) vir diep balke met lae beton sterkte val egter beduidend onder die teiken betroubaarheidswaardes.

Acknowledgements

I am grateful to God my creator, for blessing me with the opportunity and the potential to complete this research work, may He receive all the glory. I would like to appreciate the following people for making significant contributions towards the success of this research work.

- My promoter, Prof Celeste Viljoen whose drive for excellence spurred me to work diligently throughout the study. Her excellent guidance and invaluable support made an enormous impact on this dissertation. I want to thank her for her time and patience. Besides, this study would not have been possible without her financial support which she offered me from her research funds, for which I am immensely grateful.

- The Water Research Council, for funding the study.

- Prof. Dr.-Ing. Karl-Heinz Reineck of University of Stuttgart, for providing me with the database for shear tests on reinforced concrete beams with stirrups used in my study.

- My parents, for their constant love, prayers and support throughout my entire academic career. I could not have achieved any of my goals without them.

- My friends and colleagues, John, Toyosi, Mohammed, for the coffee breaks, encouragement and motivation.

Dedications

This thesis is dedicated to my beautiful and intelligent wife Boluwatife. Thank you for the sacrifice of carrying the pregnancy of our first daughter (Tanitoluwa) alone while I was away most of the time during my studies. Without your unending love, patience, prayers, encouragement and support over the past few years, I would not have been able to successfully complete this project.

Contents

List of Figures

CHAPTER 2

CHAPTER 3

CHAPTER 4

CHAPTER 5

CHAPTER 6

List of Tables

CHAPTER 5

CHAPTER 6

CHAPTER 7

CHAPTER 8

List of Symbols

a	shear span
A_v	stirrup area within the distance of the stirrup spacing
$A_{w,min}$	minimum stirrup reinforcement ratio
A_{sw}	area of shear reinforcement within spacing, s
$b_{v,eff}$	effective shear width
b_w	beam width
β_{cr}	the crack inclination
β	reliability index
β_T	target reliability index
$\beta_{T,RC}$	target level of reliability for Reliability Class
c	depth of the compression zone
d	effective depth of the beam
d_v	effective shear depth
ε_x	strain along the transverse direction
ε_z	strain along the longitudinal direction
ε_1	principal tensile strain
ε_2	principal compressive strain
E_s	modulus of elasticity of the reinforcement steel
E_c	modulus of elasticity of the concrete
f_2	the crushing strength of the diagonally compressed strut
f_2	principal compressive stress in concrete
f_1	principal tensile stress in concrete
f_x	stress in concrete in x-direction
f_z	stress in concrete in z-direction
f_{yx}	the yield point of the reinforcement in the x direction
f_{yz}	the yield point of the reinforcement in the z direction
f_{sx}	the service stress in the reinforcement in x direction
f_{sz}	the service stress in the reinforcement in z direction
f_v	stress in the shear reinforcement
f_{cr}	the principal compressive stress at initial cracking
f_{yw}	yield strength of the stirrups

f_{ywm}	mean value of steel yield strength of stirrups
f_{ywk}	characteristic strength of the stirrup reinforcement
f_c	concrete compressive cylinder strength
f_{ck}	characteristic value of concrete compressive cylinder strength
f_{cm}	mean value of concrete compressive cylinder strength
f_{cu}	characteristic value of concrete cube strength
$f_x(X)$	joint probability density distribution of the vector of basic variables X
ϕ	strength reduction factor
θ	concrete compressive strut angle
θ_d	design value of concrete strut angle
θ_m	mean value of concrete strut angle
V_{Rd}	design value of shear resistance force
$\mathrm{V}_{Rd,c}$	concrete contribution to design shear resistance
$\mathrm{V}_{Rd,s}$	stirrup contribution to design shear resistance
$\mathrm{V}_{Rd,max}$	upper limit of design shear resistance
V_c	contribution of the uncracked compression to resisting shear force
V_l	contribution of the longitudinal reinforcement/dowel action to shear resistance
V_w	shear transfer force across web cracks
$\mathrm{V}_{Rd,cmin}$	minimum shear strength contribution by concrete to design shear resistance
V_u	design value of acting shear force
V_{cc}	shear in compression zone
V_d	contribution of dowel action to shear resistance
V_{ca}	contribution of aggregate interlock to shear resistance
V_{cr}	residual tensile stress in concrete
V_p	vertical component of prestressing steel
v_1	strength reduction factor
N_V	tension in the longitudinal direction
s	stirrup spacing
s_x	the perpendicular spacing of cracks inclined at angle θ
ϕ	the angle of the initial inclined cracks.
ζ	size and slenderness effect factor
x	neutral axis depth of the cracked section

ρ_l	longitudinal reinforcement ratio
ρ_w	shear reinforcement ratio
σ_{fyw}	standard deviation of steel yield strength
$\rho_{w,min}$	minimum stirrup reinforcement ratio
$\rho_w f_{yw}$	stirrup reinforcement quantity in MPa
$\rho_w f_{ywm}$	mean value of the stirrup reinforcement quantity
$\rho_w f_{ywd}$	design value of the stirrup reinforcement quantity
M_u	factored design moment
MF	Model factor
γ_c	partial material factor for concrete
γ_s	partial material factor for steel
z	internal lever arm
α_{cw}	coefficient accounting for stress in the compression chord
ρ_x	reinforcement ratio in x direction
ρ_y	reinforcement ratio in y directions
X	basic random variables on which the resistance and loads depend.
X_k	characteristic value of material strength
X_m	mean value of variable X
$g(\mathrm{X})$	limit state function of random variables (X)
Φ	probability distribution.
α_{x_i}	sensitivity factor of x_i
P_f	probability of failure
$\mathrm{P}_{f,T}$	target probability of failure
μ_{MF}	mean value of the model factor
σ_x	normal stress in x direction
σ_y	normal stress in y direction
σ_{MF}	standard deviation of the model factor
Ω_{MF}	coefficient of variation of the model factor
η_{MF}	skewness of the model factor
r	Pearson's correlation coefficient
$\propto$	the angle of stirrups

R^2	coefficient of determination
τ_{xy}	shear stress in $x-y$ coordinate
λ	modification factor

Abbreviations

FORM	First Order Reliability Method
JCSS	Joint Committee on Structural Safety
LN	Lognormal distribution
N	Normal distribution
GPM	General probabilistic model
LSF	Limit State Function
MCFT	Modified Compression Field Theory (for concrete shear resistance)
R2k	Response 2000 (for MCFT shear resistance prediction)
CCC	Compression Chord Capacity (for concrete shear resistance)
PMC	Probabilistic Model Code
LSF	Limit state function
DP	Demerit Point
TDP	Total Demerit Point
VSIM	Variable Strut Inclination Method (for concrete shear resistance)
VSIM-A	Variable Strut Inclination Method as modified (for concrete shear resistance)
LoA	Level of Approximation

Chapter 1

Introduction

Through the span of history, structural engineers have made exceptional contributions and changes to the world we live in today. They design vital structures and facilities that are necessary for our regular lives with the primary goal of producing safe, economical and functional buildings. To accomplish this goal, reference to a standard code of practice is useful. The standard code of practice serves as a reference document with relevant guidance, recognised and accepted design basis with procedures and rules for assessment of structural performance. The design methodologies recommended by standard design codes of practice should be valid, easy to use and economical in the application regarding time and money. According to Ellingwood (1994), a design code should reflect a long-standing method of engineering practice that has been adequately substantiated. The calibration of a standard code of practice should be carried out extensively to be used across various applications in practice. Some countries with no particular code of practices adopt established standard codes as the national reference. One of the significant factors that determine the type of code to be adopted by a country is the suitability and extent of the application of the code with respect to their culture and environmental conditions.

1.1 Background to study

Reinforced concrete (RC) is an extensively used construction material for fast infrastructural development. It is widely used in the industry today due to its apparent benefits, which includes high modulus of elasticity, freeze-thaw resistance, chemical resistance and permeability. Different types of failure occur in RC beams and other structural components. Amongst them, a dominant failure mode is the shear failure.

Shear failure of a reinforced concrete member can be sudden and catastrophic. Several experimental tests on the shear failure of beams have been performed in the past 60 years. Theoretical models and simple semi-empirically based expressions have also been derived for shear strength prediction. However, there is still disagreement concerning the shear mechanism in reinforced concrete beams and the difficulty of accurately predicting shear resistance is widely researched.

The principal aim of any beam shear design is to achieve a proper level of safety for the designed beam. Structural design decisions are enclosed by significant uncertainties that arise from the random nature of the loadings, structural resistance and prediction models (Idris *et al.*, 2014). The uncertainties involved in the shear transfer mechanism is instrumental in the difficulty in predicting shear capacity accurately. As a result of this, quantification of model uncertainties accounting for the systematic differences between the models and the experimental observations is necessary. The underestimation of these uncertainties sometimes lead to grave consequences such as collapse as reported in Carino *et al.* (1983). Thus, safety and performance are critical issues.

Model uncertainties and bias reveal the accuracy of the shear predictions of un-calibrated shear resistance models and thus significantly affect reliability performance. Previous studies have demonstrated that efficient shear reliability assessment can be conducted by the proper modelling of these uncertainties (Mensah, 2015). Researchers have also shown that the effect of uncertainties can be accounted for in shear design procedures through the calibration of appropriate safety factors (Retief, 2015).

Models on which shear provisions in most current design standards are based vary from the empirical or semi-empirical truss-based approaches, the Variable Strut Inclination Method (VSIM), complex rational models based on Modified Compression Field Theory (MCFT) and models based on General Stress Field Approach. USA (ACI 318) still adopt the semi-empirical truss-based approaches while others like Canada (CSA) have revised their standards based on the more current MCFT. The European standard (EN 1992-1-1) shear design provisions for beams with stirrups are still based on the VSIM without concrete contribution. Other models that have attempted to model the shear strength of beams include the tooth model (Reineck, 1991), the critical crack theory (Muttoni and Ruiz, 2008), the splitting test analogy model (Desai, 2004) and the Compression Chord Capacity model (CCC) (Cladera *et al.*, 2016).

1.2 Motivation and problem statement

Eurocode is recognised as advanced, wholly integrated set of structural codes which can be adjusted and modified for use in any region in the world. Several countries have based their national codes on European standards. Some of these countries include Singapore, Malaysia, New Zealand, Sri Lanka, India and Saudi Arabia. The Eurocode Standard for Design of Concrete Structures EN 1992-1-1 (EN1992-1-1, 2004) has been accepted for adoption by South Africa to replace the operational South African Standard for Structural Use of Concrete SANS 10100-1 (SANS 10100-1, 2000).

Eurocode 2 (EN1992-1-1) uses a method of shear design known as the Variable Strut Inclination Method (VSIM); hence the VSIM based shear design procedure will be adopted as well. The VSIM for shear is a truss model allowing the variable inclination of concrete struts θ within the confines of $1 \leq \cot\theta \leq 2.5$ (Mosley *et al.,* 2007). Recent studies have shown that the best-estimate predictions of the VSIM, which provide conceptual basis for operational Eurocode 2 (EC2) design procedures, are relatively high for heavily shear reinforced concrete members and, conversely, are very low for lightly shear reinforced concrete members when compared to experimental observations (Cladera and Mari, 2007; Todisco *et al.,* 2016; Mari *et al.,* 2015; Sagaseta and Vollum, 2011; Collins *et al.,* 2007; Mensah, 2015). It offers scatter of results when the ratio of the experimentally determined shear resistance and predicted shear resistance was plotted against the amount of shear reinforcement.

The inability of VSIM to accurately capture trends witnessed from experimental observations attests to the presence of significant uncertainties in the shear strength model. The need was therefore clear to quantify the model uncertainties and bias associated with VSIM shear model, accounting for the systematic differences between the model and the physical tests. Holicky *et al.* (2015) stated that the currently used model factor statistics are mostly based on instinctive discernment and limited data which may result in an unrealistic description of model uncertainties. Therefore, improved description and quantification of model uncertainties are needed, especially where these significantly affect reliability performance.

The systematic sensitivity of EC2 VSIM shear capacity predictions to the amount of stirrup reinforcement motivates the need for subsequent reliability assessment of the design procedure, to appraise the uniformity and consistency of its performance in terms of the reliability index over the range of practical design situations. No evidence has been found from background documents and relevant literature that VSIM has been calibrated to account for systematic trends associated with

stirrup quantities. The design formulation of EC2 introduces safety bias through the use of partial factors, characteristic values and limits on the strut angle. Given this, four apparent questions may be asked which briefly define the problem statement of this research:

1. What are the model uncertainties in shear resistance models?
2. Which of these models is most suitable as a general probabilistic model (GPM) for shear resistance?
3. Over the range of practical design situations, does the EC2 shear design formulation consistently meet reliability targets?
4. What is the reliability performance of alternative shear design provisions (Fib Model Code 2010 and ACI-318) compared to EC2?

To answer these questions, comprehensive investigation and reliability assessment of EC2 VSIM shear design formulation is critical to assess performance over the range of practical design situations. Such characterisation and assessment may serve as the basis for subsequent evaluation of other available prediction models and their model factors, to identify other suitable candidates in terms of consistent reliability performance. The study is focused on the reliability analysis of the resistance part only. This is generally based on the principle of separating resistance calibration from actions by requiring resistance reliability $\beta_R = \propto_R \beta_T$ where $\propto_R = 0.8$ and β_T is the target level of reliability (EN 1990). The major feature of reliability separation is that material codes or resistance performance, can be calibrated independent of loading codes and loading considerations in general.

1.3 Research aim and objectives

The ultimate goal of this research is to evaluate the reliability performance of the EC2, ACI 318 and Fib Model Code 2010 (III) shear design formulations for stirrup failure. Towards the effective performance assessment of the design procedure, quantification of model uncertainty and bias is vital for its explicit inclusion in reliability assessment. Specific objectives are:

a. To review the current available literature on shear failure in beams to gain understanding of the underlying shear transfer mechanisms and the effect of critical shear parameters such as the shear span depth ratio, the shear reinforcement, the longitudinal reinforcement, the size effect and the concrete strength, on the behaviour of reinforced concrete beams with stirrups.

b. To compare the capacity prediction of VSIM model to alternative shear models like Modified Compression Field Theory (MCFT), the ACI-318 shear model, Fib Model Code 2010 (III) model and the Compression Chord Capacity model (Claderal *et al.*, 2016) and experimental test results.

c. To quantify and characterise model factors for shear resistance models, by considering five prediction models of shear capacity, namely (1) the EC2 VSIM best-estimate model (EN 1992-1-1, 2004), (2) MCFT (Bentz, 2000), (3) Fib Model Code 2010 (III) best estimate model (Fib, 2010), (4) ACI 318 best estimate model (ACI 318, 2011) and (5) Compression Chord Capacity Model (Claderal *et al.*, 2016)). The characterised model factors are investigated parametrically against essential shear parameters.

d. To assess the suitability of these prediction models as general probabilistic models (GPMs) (i.e. the best estimate of predicted shear capacity, including bias and uncertainty characteristics of such prediction) for shear resistance that can be used for the reliability assessment of EC2 shear design procedure and any other available shear design procedure for representative case studies.

e. To use two of the suitable GPMs in (d) (principal and alternative GPM) and their respective model factor statistics to assess the reliability performance of EC2 shear design formulation across a parametric variation of concrete strength, amount of shear reinforcement and beam depth.

f. To assess the reliability performance of alternative shear design provisions (Model Code 2010 and ACI-318) across practical ranges of stirrup reinforcement, concrete strength and beam depth, and compare the results to that of EC2 shear design provisions.

g. To conclude with the reliability performance of EC2, ACI 318 and Model Code 2010 shear design provisions in terms of meeting reliability targets and the consistency of reliability achieved.

1.4 Structure of the dissertation

This dissertation is structured into nine chapters as follows.

Chapter 2 reviews the mechanisms of shear resistance in reinforced concrete beams. The modelling of the contributions of aggregate interlock, dowel action and the flexural compression zone are

discussed in detail. Different shear parameters like shear span to depth ratio, shear reinforcement, longitudinal reinforcement and concrete strength were reviewed, and their influence on reinforced concrete beams is discussed. Salient features of the different models that have been developed for predicting shear capacity of beams with shear reinforcements are presented in the chapter. Different modes of shear failures and factors affecting shear strength modelling in RC beams are identified and discussed. The existing shear strength models and recently published authorial shear strength equations from the literature are discussed in this chapter. The chapter also presents a description of the computer program Response 2000 and its implementation of the MCFT. The underlying assumptions in the program and the types of analysis performed are also described.

Chapter 3 reviews the shear design provisions of beams with shear reinforcement in well-established codes of practices, focusing on six well-known national codes of practice: ACI 318 building code, AASHTO LRFD bridge design specification, Fib Model Code 2010 Level of Approximation III, Canadian Standards Association CSA A23.3, Eurocode 2 and the South African National Standard SANS 10100-1. The various shear design equations are illustrated and compared by means of a specific example at parametric variations of shear reinforcements (low to high), concrete strength (low to high) and beam depths (small to large); and the observations are presented.

Chapter 4 compares EC2 VSIM mean and design value predictions and the predictions from alternative shear procedures to experimental results to provide a general overview of the performance of their unbiased mean value predictions and to assess their accuracy. The design value analysis is conducted to reveal the impact of the safety bias incorporated in the different shear design provisions. It is shown that the capacity predictions from the different methods differ considerably from one another and from the experimental results.

Chapter 5 presents reliability principles and its application in deriving structural design guidelines. The First Order Reliability Method (FORM) used for the performance evaluation is also discussed.

Chapter 6 focuses on the statistical quantification and characterisation of model factors for various shear resistance models. In general, five resistance models were considered, namely: (1) the EC2 VSIM best-estimate model, (2) best-estimate predictions offered by analysis program R2k which represents practical application of the MCFT, (3) Fib Model Code 2010 (III) best estimate model, (4) ACI 318 best estimate model and (5) Compression Chord Capacity Model (CCC). The chapter elaborates on the database of compiled experimental observations to which statistical methods are

applied to characterise the relevant model uncertainties and bias. As part of the statistical characterisation, model factors were investigated parametrically against essential shear parameters using correlation and regression assessments. Based on these, suitable general probabilistic models (GPMs) for shear resistance were identified for the reliability assessment of shear design procedures. MCFT is identified as the best predictor of shear resistance in terms of the characterised model uncertainty and bias, and trend with shear parameters.

Chapter 7 presents the reliability performance assessment of the EC2 shear design formulation. The principally derived GPM for the reliability assessment is based on the probabilistic representation of MCFT (R2k). This was validated by means of a similar reliability analysis using the CCC based GPM. Both reliability analyses indicate uneconomically high reliability for low levels of shear reinforcement, high concrete strength and large beam depth, and actively reducing reliability (but still adequate) with increased levels of shear reinforcement, reduced concrete strength and reduced beam depth.

Chapter 8 presents the reliability performance assessment of alternative and established shear design provisions. The design provisions assessed include shear design procedures in Fib Model Code 2010 and ACI 318. The reliability performance of EC2 is compared to that of the alternative shear design approaches, and the observations are presented in this chapter. The reliability levels of ACI and MC-10 (III) decrease as the amount of shear reinforcement increases and increase as the concrete strength increases. MC-10 (III) and ACI reliabilities drastically decrease with increasing beam depth.

Chapter 9 summarises the thesis, presents the main conclusions of the dissertation regarding the level of reliability of EC2, ACI and MC-10 (III) shear design formulations; and makes recommendations for future work. The four research questions raised in the problem statement are answered with a discussion of how the research objectives are accomplished.

Chapter 2

Literature Review

This chapter provides an overview of the literature and state of knowledge related to the shear mechanism in beams. It discusses the basis of the different models developed for predicting shear capacity of beams with stirrups. Different modes of shear failures and parameters affecting shear strength modelling in reinforced concrete (RC) beams are identified and discussed.

2.6 Review of shear in concrete beams

Investigating shear behaviour is one of the most complex aspects of reinforced concrete design (Victor *et al*., 2013). The complexity of shear behaviour has made shear strength modelling an area of critical research in reinforced design today (Slowik, 2014; Victor *et al*., 2013; Collins *et al*., 2007). The aim of developing an adequate and useful model for the shear capacity prediction of RC beams has been the ultimate goal of a significant worldwide research effort over the years (Collins *et al*., 2007; Braestrup *et al*., 1976). Different theories have been proposed, some of which include the truss model, compression field theory and non-linear fracture mechanics (Farooq *et al*., 2014). Most of all the developed shear models are either empirical or semi-empirical and are developed from experimental results through regression analysis (Shah & Ahmad, 2009; Kassem, 2015; Ghafar *et al*., 2016), application of genetic algorithm (Ashour *et al*., 2003; Perra & Vique, 2009; Gandomi *et al*., 2013) and artificial neural network (Mansour *et al*., 2004; Arafa *et al*., 2011; Amani & Moeini, 2012; Cladera *et al*., 2004; Farooq *et al*., 2014).

Several researchers have conducted experimental tests on RC beams and found that the following parameters affect the shear behaviour of beams. The parameters include: longitudinal steel ratio, aggregate type, shear span to effective depth ratio, loading type, strength of concrete and support conditions (Bazant *et al*., 1987; Rajagopalan *et al*.; 1968, Yoon *et al*., 1996; Lee *et al*., 2008; Grebovic

et al., 2015). All the researchers aim to substantiate the shear strength capacity of RC beams with the most acceptable theory, which is developed based on their experiments. Shear failure in beams is initiated by inclined cracks triggered by combined stresses emanating from the shear force in conjunction with axial loads and bending moments. The shear failure load in a beam depends on the structural properties of the beam, loading, geometry and dimensions. As a result of the number of variables involved, shear behaviour in a RC beam is complicated and a general shear theory has been evasive (Frosch & Wolf, 2003).

2.2 Basic shear transfer mechanisms

The mechanism of shear failure in RC beams is complicated and a number of factors affect it (Kuchma *et al*., 2004). This is one of the reasons a general shear strength formulation has not been created. Several components contribute to the shear strength of RC beams and it is difficult to define the contribution of each part completely. There have been differences with respect to these components and their influence on shear strength. ACI-ASCE Committee 445 (2009) identified six crucial shear resistance components for shear reinforced concrete beams, which are widely accepted in the research community today. They include interface shear transfers, dowel action, shear in the uncracked compression zone, residual tensile stresses, shear reinforcement and arch action. Each of these shear mechanisms are discussed in the next sections and illustrated in Figure 2.1.

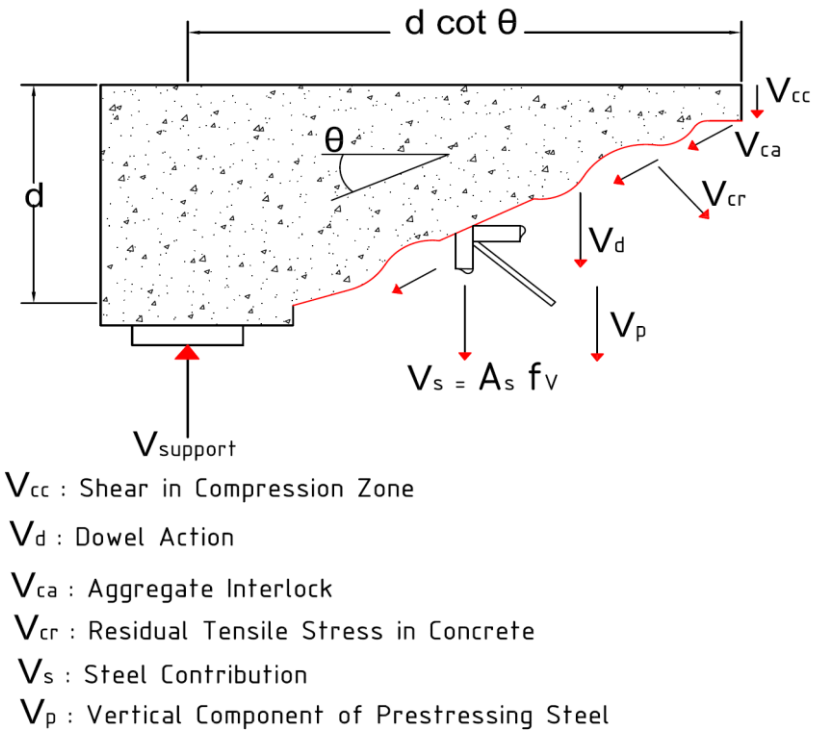

Figure 2.1 Shear transfer mechanism and forces contributing to shear resistance (taken from Kuchma *et al*. (2004))

2.2.1 Shear stress in the un-cracked compression zone:

The un-cracked concrete zone contributes to the shear strength in a cracked concrete beam. In the un-cracked compression zone, shear force is transferred by the tensile and compressive stresses (Kuchma *et al*., 1998; Kim *et al*., 1994). The degree of the shear strength is restricted by the depth of the compression zone (Frosch & Wolf, 2003). Thus, the shear contribution by the un-cracked concrete in a slender beam with no axial compression becomes insignificant as the depth of the concrete section decreases (Kuchma *et al*., 1998; Kim *et al*., 1996).

2.2.2 Interface shear transfer

Some earlier experimental studies have shown that the bulk of the total shear force on a beam without web reinforcement is carried across the cracks through interface shear transfer, also referred to as aggregate interlock. The interface shear transfer is the force resulting from aggregate projecting from the crack surface. The aggregate projecting provides friction and resistance against relative slippage

of the concrete sections. The influence of aggregate interlock on shear strength depends on the aggregate size and crack width. Consequently, its contribution increases as the aggregate size increases and as the crack width decreases (Kuchma *et al*., 2004). Nilson *et al*. (1991) reported that the interlock forces developing at the interface could resist about one-third of the total shear force in the beam.

2.2.3 Dowel action of longitudinal reinforcement

Shear force is transmitted using dowel action of the longitudinal reinforcement when shear displacement occurs along the cracks. The longitudinal bars provide resistance averting slippage of the concrete sections. The tensile strength of the concrete cover supporting the reinforcement limits the dowel action (Frosch & Wolf, 2003). The effect of dowel action on shear resistance is dependent on the supporting concrete cover, the spacing of flexural cracks and the amount and distribution of longitudinal reinforcement (Kuchma *et al*., 2004; Kim *et al*., 1996; Ramirez *et al*., 1998).

2.2.4 Residual tensile stresses across cracks

When a concrete beam is cracked, concrete tensile stresses are transferred across cracks by small pieces of concrete at the tips of the inclined cracks. According to ACI-ASCE Committee 445 (2009), tensile forces can exist until cracks exceed widths of 0.05-0.15 mm. Concrete acts as a bridge between narrow cracks and provides tensile strength across the crack. The resistance provided by the residual tensile stresses in a narrow crack opening is significant. However, for large beams, residual tensile stresses do not contribute greatly to shear resistance due to the scale of the crack width in such beams.

2.2.5 Shear reinforcement

Shear reinforcement, traditionally called stirrups, is provided to resist shear by traversing cracks. The stirrups do not only carry shear but also restrain cracks in the concrete from widening. They prevent the growth of inclined cracks, and therefore help to ensure a more ductile behaviour. Stirrups also increase the shear transferred through dowel action and interface shear transfer. Thus, the presence of shear reinforcement affects the individual contributions of the various shear resisting mechanisms.

2.2.6 Arch action

In addition to the above shear transfer mechanisms, the arch action is a principal shear transfer mechanism in deep or short beams. As the depth of a beam increases, shear is transferred to the support by an inclined strut. The combination of the compression strut and the longitudinal reinforcement produce tied arch action which aids shear resistance. The main factors motivating this behaviour are the concrete strength, the span to depth ratio and the area of longitudinal reinforcement (Kim *et al*., 1996). Figure 2.2 illustrates the arch action mechanism.

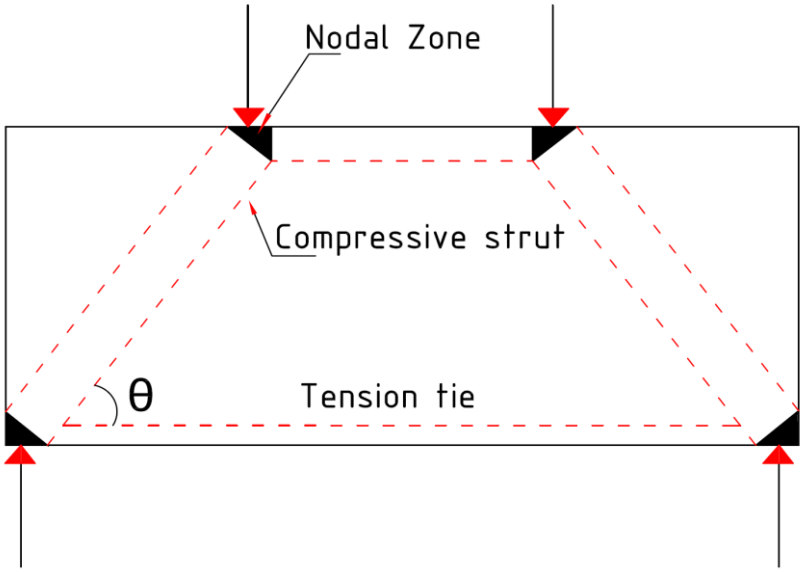

Figure 2.2. Arch action (taken from Yousif & Ken (2016))

2.3 Modes of beam shear cracking

The propagation of inclined crack initiates beam shear failure. This crack can be categorised into two types, namely web-shear cracks and flexure-shear cracks.

2.3.1 Web-shear cracks (diagonal tension cracks)

This type of crack occurs in short span beams which are relatively deep with thin webs, subjected to high shear stresses and low flexural stresses. Web-shear cracking starts from the inner part of the beam and moves diagonally to the tension face when the principal tensile stresses produced exceed

the tensile strength of concrete. They occur near the supports or at points of inflexion in continuous beams. Adequate stirrup reinforcement is needed to avert the initiation of diagonal tension crack in a RC beam. A typical web-shear crack is illustrated in Figure 2.3(a).

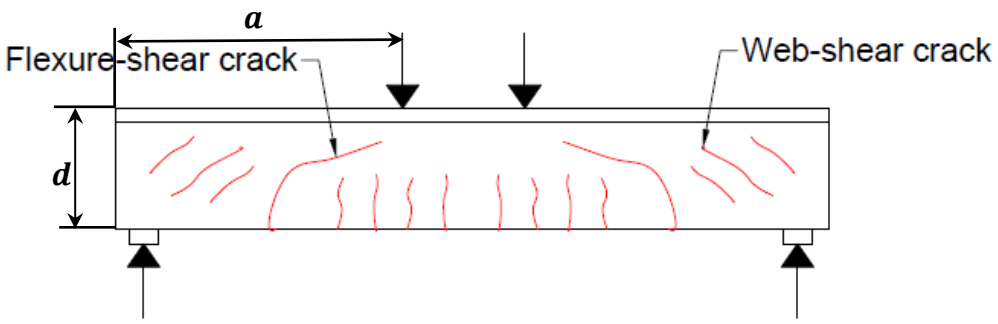

Figure 2.3(a). Web-shear and flexure-shear crack (taken from Kuchma *et al* (2004))

2.3.2 Flexure-shear cracks

Flexural cracking initiates flexural-shear cracks. The occurrence of a flexural crack in addition to a diagonal tension crack results in the flexure-shear crack. Flexural cracks are vertical cracks that occur due to flexural stresses. They initiate from the bottom of the beam where flexural stresses are the greatest and extend into a diagonal tension crack (inclined towards the loading point). Sometimes the inclined cracks extend along the tension reinforcement towards the support and weaken the anchorage of the reinforcement. Such cracks are called secondary cracks (see Figure 2.3(b)). A flexure-shear crack is illustrated in Figure 2.3(a).

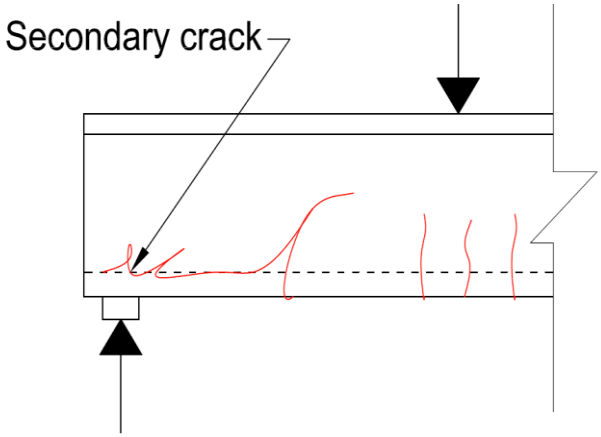

Figure 2.3(b). Secondary crack (taken from Kuchma *et al* (2004))

2.4 Classification of beams and modes of failures

Shear resistance of RC beams is influenced by a several parameters, some of which include the percentage of reinforcement steel, aggregate size, shear reinforcement and shear span to depth ratio. Investigation of the shear strength of RC beams portrays shear span to depth ratio (a/d) as a very important parameter (Arun, 2014; Grebovic, 2015). The classification of beams and their modes of shear failure according to ASCE-ACI Committee 426 (1973) and Pillai (1983) are described in the next sections.

2.4.1 Very slender beams $(a/d > 6)$

The a/d ratio above which flexural failure is certain is in the neighbourhood of 6. It also depends on the amount of tension steel area and the strength of concrete and steel. Reinforced concrete beams with a/d in this region fail in flexure before the propagation of inclined shear cracks.

2.4.2 Normal beams/slender beams $(2.5 < a/d < 6)$

Reinforced concrete beams in this region fail either in shear or flexure. Shear failure occurs by the formation of inclined flexure-shear cracks. Flexural vertical cracks develop first, and the cracks proliferate to the top of the beam. This type of failure is usually sudden and without warning (in beams without stirrup reinforcements) and is referred to as ***diagonal tension failure*** (see Figure 2.4).

Addition of shear reinforcement improves the shear strength significantly. This enables loads to be carried until failure occurs in a ***shear tension mode*** or a ***shear compression mode***, or in a ***flexural mode***. Shear compression failure occurs in beams containing sufficient amount of shear reinforcement. A shear compression failure (see Figure 2.5) occurs when the compressive strength is exceeded.

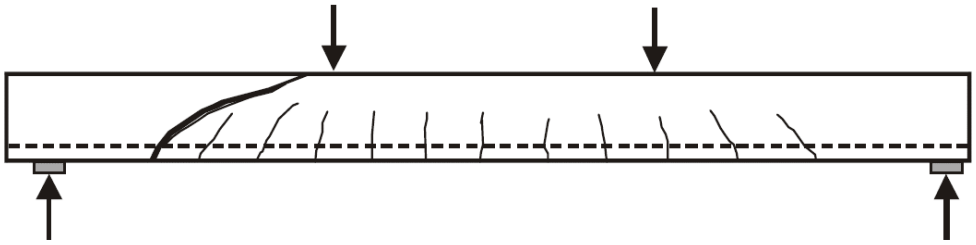

Figure 2.4. Diagonal tension failure (taken from Kuchma *et al* (2004))

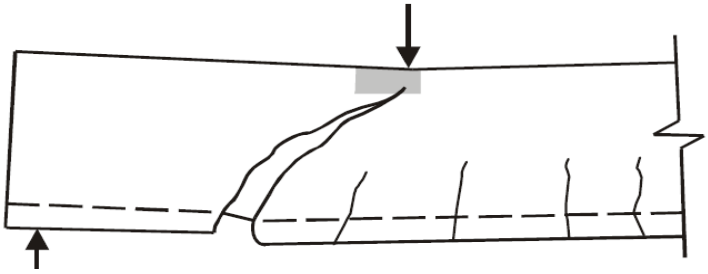

Figure 2.5. Shear compression failure (taken from Kuchma *et al* (2004))

2.4.3 Short beams ($1 < a/d < 2.5$)

In reinforced concrete short beams, the beam failure is propagated by an inclined flexure-shear crack. The inclined flexure-shear crack propagates towards the topmost part of the beam resulting in the crushing of the compression zone (***shear compression failure***) or development of secondary cracks along the tension reinforcement resulting in loss of bond and anchorage of the tension reinforcement or splitting between the concrete and the longitudinal reinforcement, termed ***shear tension failure*** (see Figure 2.6). These types of failures usually occur before the flexural strength of the section is reached.

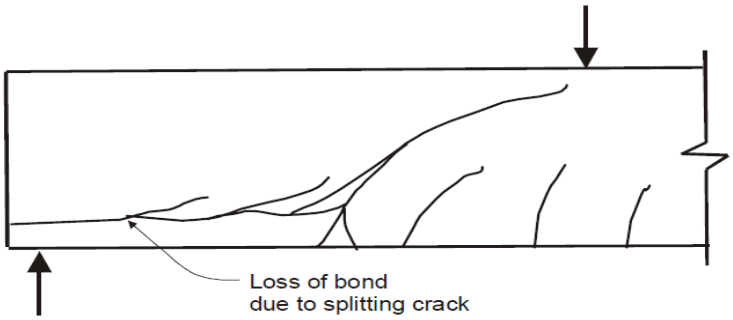

Figure 2.6. Shear tension failure (taken from Kuchma *et al* (2004))

2.4.4 Deep beams ($a/d < 1$)

In reinforced concrete deep beams, most of the shear force is transferred by arch action as shown in Figure 2.7. Inclined cracks develop along the line between reaction and load. The web may buckle and subsequently crush which is termed ***arch rib failure***. Other types of failure that may also occur includes ***flexural failure*** due to the yielding of the tension bars, ***shear compression failure*** due to crushing of the compression zone, ***anchorage failure*** of the tension steel and ***bearing failure*** due to the crushing of concrete above the support. The different failure modes in a deep beam are illustrated in Figure 2.8.

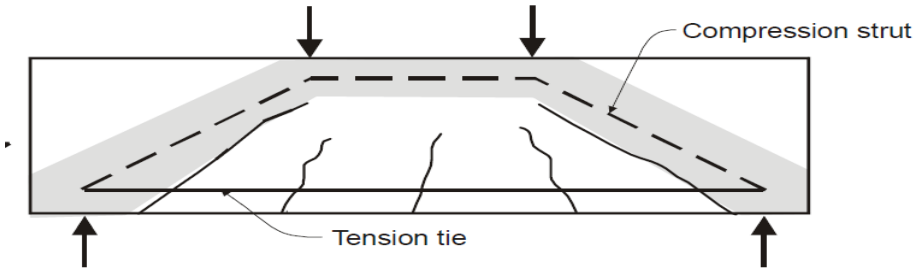

Figure 2.7. Tied-arch structural system (taken from Kuchma *et al* (2004))

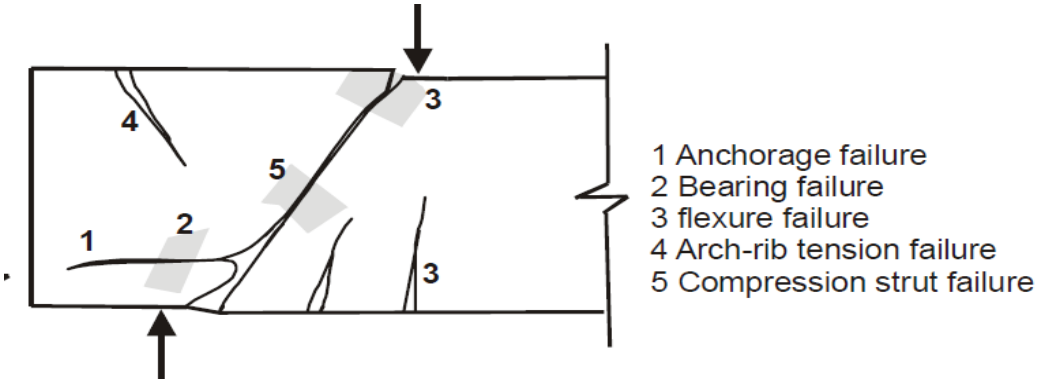

Figure 2.8. Modes of failure for deep beams (taken from Kuchma *et al* (2004))

2.4.5 Thin-webbed beams with web reinforcement

In addition to the modes of failure discussed above, thin-webbed beams with stirrup reinforcement may fail by web-crushing. The shear stresses in the webs of thin webbed beams are much higher than in rectangular beams, thereby resulting in different modes of failure. Web-crushing failure is the dominant mode of failure in thin webbed beams. All the previously described failure modes are also possible for thin webbed beams. This is illustrated in Figure 2.9.

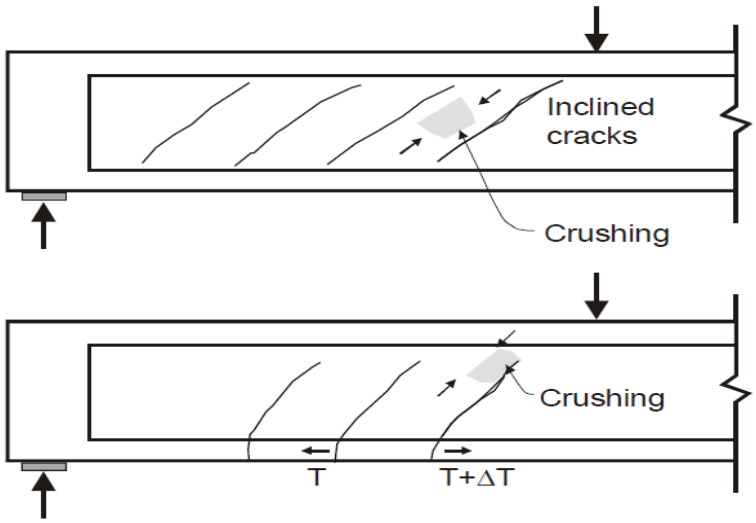

Figure 2.9. Web-crushing failure in thinned-webbed beams (taken from Kuchma *et al* (2004))

The occurrence of a particular mode of failure is depends on the span to depth ratio, loading, amount and anchorage of reinforcement and the beam cross-section. The aim of shear design is to prevent shear failure. Beam design involves the provision of an adequate amount of shear reinforcement,

concrete strength, providing an adequate thickness of the web and the proper amount of longitudinal bars. Generally, shear failure occurs in beams with a low span to depth ratio or a few stirrups.

2.5 Parameters influencing shear strength

Researchers have identified several characteristics of beams significantly affecting the contributions of the various shear transfer mechanisms and thus the ultimate shear strength. It is essential to evaluate the influence of different shear design factors on the structural behaviour of RC beams in shear to improve their shear capacity. The most dominant parameters according to ASCE-ACI Committee 445 (2009) includes the shear span to depth ratio (a/d), the concrete strength, size effect and the amount of longitudinal tension bar. The influence of each parameter is discussed in the next sections.

2.5.1 Concrete strength

The concrete strength plays a unique role in the structural behaviour of reinforced concrete beams. Researchers have reported that concrete tensile strength has a more significant effect than compressive strength on shear strength (Collins & Kuchma, 1999; Angelakos *et al*., 2001). Concrete strength increases the shear strength of RC beams (Moody *et al*., 1954; Yoon *et al*., 1996; Mphonde *et al*., 1984). Shear cracks occur when the tensile stresses surpass the tensile strength of concrete (Frosch & Wolf, 2003). The capacity of the uncracked compression zone and dowel action increases with increasing concrete strength.

The influence of concrete strength on shear strength becomes more substantial as the a/d ratio decreases. The failures become more sudden and explosive as the concrete strength increases (Attard & Mendis, 1993), especially at lower a/d values. In the tests on large, lightly reinforced beams and high strength concretes conducted by Angelakos *et al*. (2001) and Collins & Kuchma (1999), increase in shear strength with concrete strength was not achieved as revealed by other researchers. According to them, the shear stress at failure for beams with shear reinforcement decreases significantly as concrete strength increases, as the beam size increases and as the longitudinal reinforcement ratio decreases. The researchers attributed the change in this trend to high concrete strength which reduces the efficiency of the interface shear transfer mechanism.

Johnson & Ramirez (1989) revealed that an increase in concrete compressive strength increases the diagonal tension-cracking load. Higher strength concrete develops smooth crack surfaces which result in a decrease in interface shear transfer and hence affect the shear resistance contributed by the concrete. Roller & Russell (1990) showed that at concrete compressive strength exceeding 117 MPa, the ACI 318-83 code provisions overestimate the nominal shear strength contributed by the concrete.

2.5.2 Size effect

The shear strength of reinforced concrete beams (RC) in shear decreases as the beam depth increases, and this is referred to as the size effect. The shear stress at inclined cracking tends to decrease for a given percentage of longitudinal reinforcement, concrete strength, breadth and shear span to depth ratio (a/d). As the depth of the beam increases, the inclined crack width tends to increase resulting in a reduction in the aggregate interlock across the crack. Size effect is less significant in beams with stirrup reinforcement because the crack widths are controlled by stirrup reinforcement. The shear reinforcement binds the crack faces together so that the aggregate interlock is better maintained than in beams without shear reinforcement (Kuchma *et al*., 2004).

Tan & Cheng (2006) concluded that size effect in a reinforced concrete beam is controlled by strut geometry as well as the spacing and diameter of the shear reinforcement. The experiment conducted by Słowik & Nowicki (2012) showed that size effect influences failure mode. The influence of size effect in reinforced concrete beams undergoing shear was also reported in the investigations conducted by Kani (1967), Walraven & Lehwalter (1994), Ožbolt & Eligehausen (1996), Karihaloo *et al* (2003), Wang *et al* (2006), Sherwood *et al* (2007) and Hassan *et al* (2008) and they confirmed that shear capacity decreases as the absolute member's depth increases. Rao & Sundaresan (2014), Zhang & Tan (2007), Tang & Tan (2004), Rao & Injaganeri (2011) further proposed models incorporating size effect. Collins & Kuchma (1999) and Reineck (1991), explained that size effect in large beams results in a reduction in interface shear transfer due to the development of larger crack widths.

2.5.3 Shear span to depth ratio (a/d)

The shear span is described as the distance (a) between a point of axial load and a support. Shear strength increases as the shear span to depth ratio (a/d) decreases. The a/d affects the inclined

cracking shears of lower shear span beams, while for longer shear spans it has little effect on the inclined cracking shear (Kuchma *et al*., 1997). When the a/d ratio is less than 2.5, arch action dominates, increasing the shear resistance of the section. As the a/d ratio increases, beam action dominates, increasing the likelihood of the occurrence of a flexural failure. Large a/d ratios increase the crack width, making it complicated to transmit shear across cracks through dowel action and aggregate interlock and thus decreasing shear strength (ASCE-ACI Committee 445, 2009).

Andermatt & Lubell (2013) investigated the shear behaviour of deep concrete beams with shear reinforcement. The result showed that the normalised shear strength of the specimens increased as the (a/d) decreased with all other variables held constant. Tan *et al*. (1995) conducted experiments on nineteen reinforced concrete deep beams with seven different shear span depth ratios (a/d) and four different effective span depth ratios. The result showed that at an increasing effective span to depth ratio and $a/d > 1.0$, flexural behaviour dominates. As the (a/d) ratio increases, the shear failure mode was accompanied by flexure, and at high effective span-depth ratios the flexural failure mode was prevailing. Shin *et al*. (1999) reported that the mode of RC beam failure was influenced by the a/d ratio. The shear compression failure mode tends to change to shear tension failure at $a/d = 2$. Kong & Rangan (1998) revealed that the a/d did not have a substantial effect on shear strength when it exceeded 2.5. However, when the $a/d < 2.5$, the shear strength increases due to arch action.

2.5.4 Longitudinal reinforcement ratio

The shear strength of a RC beam is affected in several ways by the longitudinal steel ratio. Increasing the amount of longitudinal steel reduces the length and width of the flexural cracks. Reduction in the crack width increases the dowel action and interface shear transfer, thus increasing the overall shear capacity of the concrete section significantly (Kong & Rangan, 1998; Lee & Kim, 2008). For a given loading, the effect of decreasing the longitudinal steel ratio increases the flexural stresses and strains resulting in wider flexural cracks and thus leading to a decrease in the shear strength of the section. (ASCE-ACI Committee 445, 2009; Rahal & Al-Shaleh, 2004). Collins & Kuchma (1999) observed that beams having longitudinal reinforcement distributed over beam depth have closely spaced and narrower cracks with significant shear strengths.

2.5.5 Axial force

The shear strength of reinforced concrete beam reduces when subjected to axial tension. Axial tensile forces tend to make the crack angle more inclined and hasten the onset of critical failure in the section. Contrarily, axial compression increases shear strength (Kuchma *et al*., 2004).

2.5.6 Web reinforcement

Shear reinforcements, also called stirrups, are used to increase the shear resistance of reinforced concrete beams and also to change the mode of failure to a more ductile failure (Collins *et al*., 2008). Shear reinforcement comes into play after the formation of cracks. Stirrups do not prevent inclined cracks from forming, but following the development of inclined cracks, stirrups resist a portion of the shear and contribute significantly to the ultimate shear capacity of the concrete section. Web reinforcement restricts the widening of the cracks and helps maintain the aggregate interlock resistance of shear (Aguilar *et al*., 2002). The web reinforcement also improves the dowel action of the longitudinal tension reinforcement (Wang, 2002).

Smith & Vantsiotis, (1982) state that horizontal shear reinforcement in deep beams used near bottom faces of beams is more efficient than vertical shear reinforcement. Tan *et al*. (1997) reported that the combination of both horizontal and vertical shear reinforcement are instrumental in increasing beam stiffness, restraining the growth of diagonal cracks and in increasing the ultimate shear strength. ACI-ASCE Committee (2008) concludes that vertical shear reinforcement is more efficient than horizontal shear reinforcement in providing shear resistance in deep beams.

2.6 Existing shear strength models

2.6.1 Historical development of shear strength models

Ritter (1899) developed a shear strength model known as 45^0 truss model for the assessment of post-cracking behaviour which was later advanced by Morsch (1909) by introducing the use of the model for torsion. The truss model was widely used as the shear strength model to comprehend the shear behaviour of RC beams with stirrups. In the experiments conducted by Withey (1908) and Talbot

(1909), it was revealed that the 45^0 truss model underpredicted capacity when compared to physical tests.

In 1974, Collins and Mitchell developed the Compression Field Theory (CFT) for beams subjected to torsion and shear. Shear stress conditions in this model are based on compatibility conditions, equilibrium conditions and constitutive relationships. Vecchio & Collins (1986) modified the CFT and named it the Modified Compression Field Theory (MCFT). The modification was done by accounting for the contribution of the concrete in tension.

The work of Nielsen (1984) and Thürlimann *et al*. (1983) proposed plasticity theory for predicting shear strength. They assume that at failure both the stirrups and longitudinal reinforcement yield. Hsu *et al*. (1992) developed two shear strength models named Rotating Angle Softened Truss Model (RASTM) and the Fixed Angle Softened Truss Model (FASTM). The assumption in RASTM is that both the direction of the principal stress and strain coincide whereas FASTM assumes that the principal stress in concrete struts and crack direction does not coincide after cracking. Detailed descriptions of the various shear strength models are presented in the next sections.

2.6.2 45^0 Truss model

Truss models were the traditional approach towards understanding the shear behaviour and estimating the shear capacity of reinforced concrete beams with stirrups in the early 1900's. Ritter (1899), in his model, considers the 45^0 diagonal concrete struts as the diagonal members of the truss, shear reinforcement forms the vertical tension ties of the truss, the longitudinal bar forms the bottom chord of the truss, and the compression chord serves as the top chord of the truss. Morsch, in 1922, assumes that the inclined compressive struts extended across more than one shear reinforcement. He explained that there was a continuous field of diagonal concrete strut resisting the shear (see Figure 2.10) in stead of having discrete diagonal concrete struts. Ritter (1899) assumed that shear failure occurs in the beam when the stirrup has yielded, or when there is a failure of the inclined concrete strut in compression.

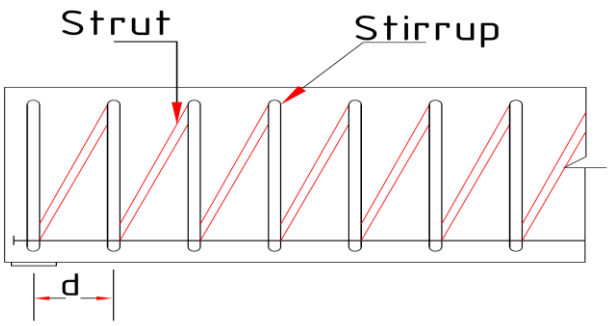

a) Discrete diagonal compressive struts

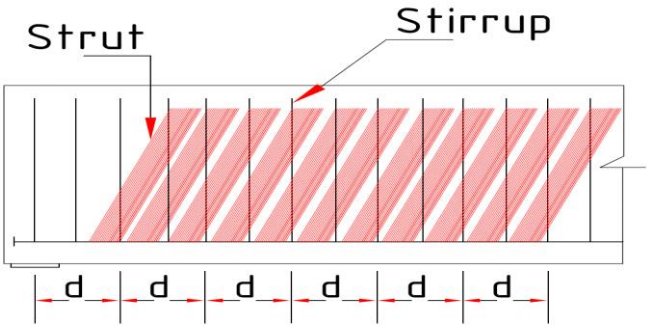

b) Continuous field of diagonal compression

Figure 2.10. Truss model (taken from Sun & Kuchma (2007))

The assumptions made in the 45^0 model include the following:

- The crack angle coincides with the diagonal compression stress, and the angle remains 45^0 after initial cracking.
- It neglects the tensile stresses in the direction perpendicular to the diagonal compression.
- The top and bottom chords carry shear, and shear stresses are distributed uniformly over an effective shear area with width b_w and depth d.

Figure 2.11 presents the equilibrium conditions used in the truss model. Assuming diagonal compression struts are inclined to the beam axis at an angle of $\theta = 45^0$, three equilibrium equations were developed as shown in Equations 2.1 to 2.3.

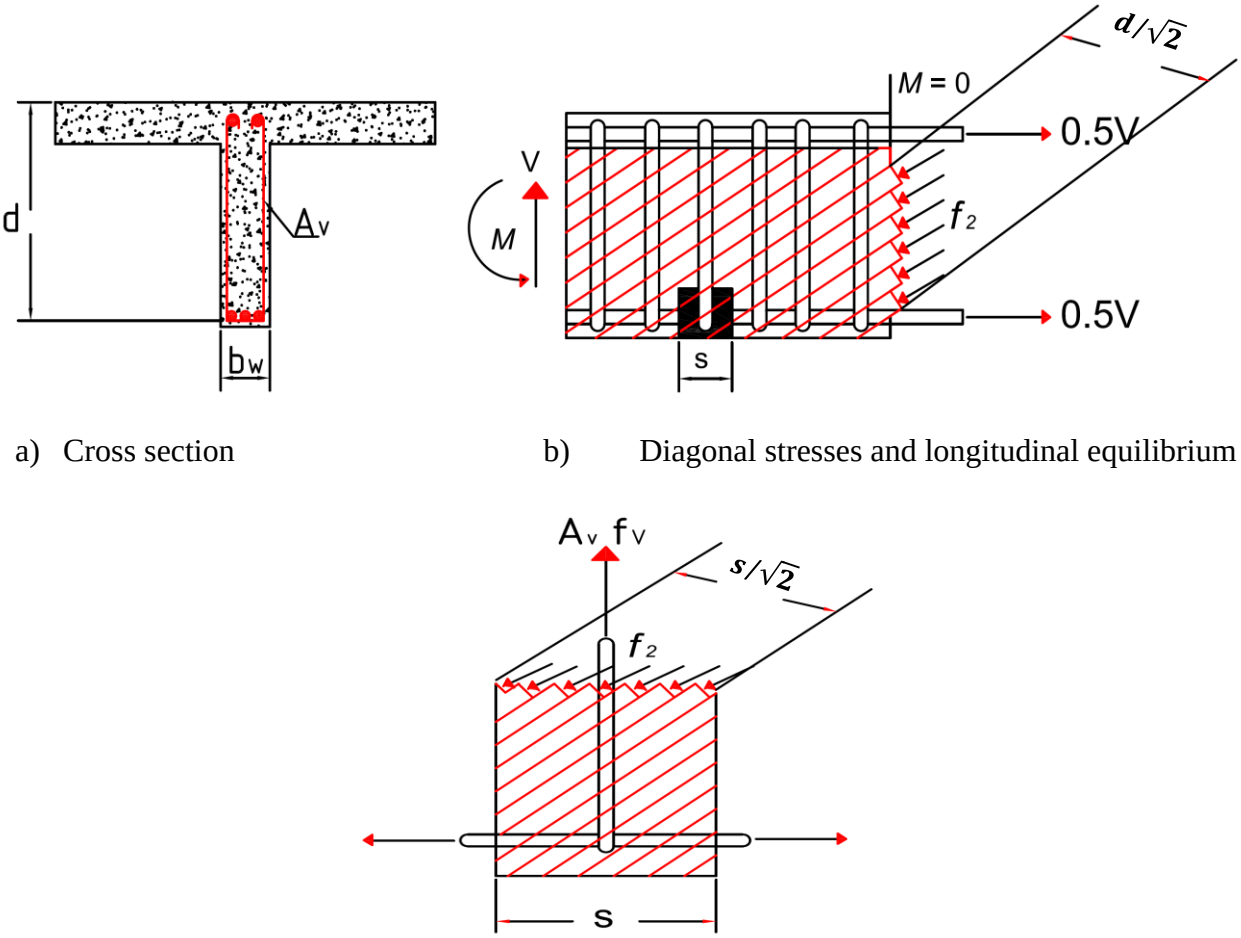

a) Cross section b) Diagonal stresses and longitudinal equilibrium

c) Force in stirrup

Figure 2.11 Equilibrium conditions for 45 degrees truss model (taken from Collins & Mitchell (1996))

$$f_2 = {}^{2V}/_{b_w d} \tag{2.1}$$

$$N_V = V \tag{2.2}$$

$$A_v f_v /_s = {}^{V}/_{d} \tag{2.3}$$

where f_2 is the principal compressive stress

V is the total shear force

N_v is the tension in the longitudinal direction

f_v is the stresses in the shear reinforcement

A_v is the stirrup area within the distance of the stirrup spacing s

Most building codes at present accept Ritter's 45° truss model with an addition of an empirical concrete contribution factor. Examples of such building codes include SANS 10100-1: 2003 and ACI-318. Ritter's model assumes that shear resistance in the beam is only carried by the shear reinforcement supplied in the beam with no contribution from the concrete. Previous researchers (Sun & Kuchma, 2007; Sagaseta & Vollum, 2012; Kuchma *et al*., 2008) proved that shear strength predictions based on only the post-cracking shear reinforcement contribution to shear resistance underestimate the overall shear strength of the section. This was corrected by introducing a concrete contribution factor, determined empirically to shear resistance. This approach was employed in BS8110-1 (1997) and also adapted to the current South African operational concrete design standard SANS 10100-1.

2.6.3 Variable-angle truss model

Ritter's truss analogy model can be made more accurate by varying the strut angle (θ). The variable-angle truss model is a modified version of the 45° truss model allowing the strut angle (θ) to vary within a certain boundary. The model is also known as the plasticity truss model, and it is established based on the plasticity theory for reinforced concrete (Hsu, 1992). The model assumes that both the shear reinforcement and the longitudinal reinforcement (provided to resist bending) must yield before failure. The three equilibrium equations in this model can be derived in a similar way as the 45° truss model. Equations 2.4 to 2.6 present the equilibrium conditions.

$$f_2 = {}^{V}/_{b_w d}\,(cot\ \theta + \tan\theta) \tag{2.4}$$

$$N_V = V\ cot\ \theta \tag{2.5}$$

$${A_v f_v}/_{s} = {}^{V}/_{d}\,(tan\theta) \tag{2.6}$$

where θ is the strut angle

The model assumes that in the ultimate limit state the shear reinforcement yields. In this state, the maximum compressive stress f_2 is attained or diagonal compression reaches its limit. With this

assumption, the strut angle can be derived and the shear strength determined. This model is used in some design standards, such as Eurocode 2 and German Code DIN 1045.

2.6.4 Basic- and Modified Compression Field Theory

The Modified Compression Field Theory (MCFT) (Vecchio & Collins 1986) derives from Compression Field Theory (Collins 1978), which in turn derives from Tension Field Theory (Wagner 1929). Each of these are rational theories that satisfy equilibrium of stress, compatibility and uniaxial stress-strain relationships.

Tension Field Theory (TFT) was developed for analysis of metallic membranes. The theory postulates that after buckling occurs in a membrane loaded in shear, the stress is transferred by a diagonal tension strut. Additional stress transfer methods, like bending of the buckling plate, are neglected.

Compression Field Theory (CFT) states that after a reinforced concrete element has cracked, tension in the concrete can be neglected. Axial stress transfers stress in the reinforcement and compressive stress in the concrete parallel to the direction of cracking. CFT is a crack modelling approach which treats the cracked reinforced concrete as a new material with its constitutive relationships. In a reinforced concrete beam, the cracked web transmits shear in a sophisticated way. Increasing load creates new cracks while the old cracks spread and change inclination. The longitudinal strains and the crack inclinations change over the depth of the beams because the section resists moment as well as shear (Vecchio & Collins, 1993). The analogous truss models proposed by Ritter (1899) and Mörsch (1909) approximated this behaviour with the assumption that diagonal compressive stresses can carry shear in the concrete inclined at 45 degrees to the longitudinal and dismiss tensile stresses in the diagonally cracked concrete (ACI Committee 445, 2009).

The MCFT generalises the compression field theory and also accounts for the stress that concrete carries between cracks, a phenomenon called ***tension stiffening***. The MCFT model was formulated considering equilibrium, compatibility as well as relative stress-strain relationships of the steel and concrete. The compressive struts angle at failure point is estimated by considering many factors some of which includes cross-sectional dimensions, bending moments, transverse reinforcement and longitudinal reinforcement (Cladera & Mari, 2007). The MCFT is considered an advanced model with a wide range of literature and studies in where it was proven to make better predictions of shear strength than any alternative shear design theory in use today.

2.6.4.1 MCFT assumptions

The MCFT makes the following assumptions:

- Cracks are free to rotate over time, and their direction coincides with the second principal direction of stress at the given load step.
- Steel is entirely bonded to concrete at the boundaries of the element.
- Reinforcement is uniformly distributed and can be represented as being smeared across the element.
- Stresses can be represented as average values across multiple cracks.
- The direction of principal stress in concrete coincides with the direction of principal strain of the element.

2.6.4.2 Analytical formulation of the MCFT

Considering a two-dimensional small concrete beam element with the axis (x, z), where the longitudinal (x-axis) and transverse (z-axis) coincide with the reinforcement directions, the element will contain the axial stresses f_x and f_z and the shear stress $\mathcal{V}_{xz}$. If the edges remain straight and parallel upon deformation, the new shape can be defined by the normal strains $\mathcal{E}_x$ and $\mathcal{E}_z$ and the shear strain γ_{xz}. The equations of MCFT are discussed in the next sections.

2.6.4.3 Equilibrium condition

The force applied to the reinforced concrete element is resisted by the combination of stresses in both the concrete and the steel reinforcement. The equilibrium equations relate the stress in the reinforcements to the stress in the cracked concrete through the Mohr circles of MCFT. From Figure 2.12, the following equations were derived:

$$\rho_z f_{sz} = f_z + \mathcal{V} tan\theta - f_1 \tag{2.7}$$

$$\rho_x f_{sx} = f_x + \mathcal{V} cot\theta - f_1 \tag{2.8}$$

$$f_2 = \mathcal{V}(tan\theta + cot\theta) - f_1 \tag{2.9}$$

where f_x and f_z are stresses in concrete in x and z-direction respectively

f_1 and f_2 are the principal tensile and principal compressive stresses in concrete respectively

$\mathcal{V}$ is the shear stress

θ is the angle of inclination

ρ_x, ρ_z is the reinforcement ratios in x and z directions respectively

2.6.4.4 Compatibility condition

In order to satisfy the compatibility condition, strain experienced by concrete at a point must be equivalent to the strain experienced by reinforcement at that point. Any change in concrete strain must show the same change in steel strain. It further states that,

For the transverse direction, $\mathcal{E}_{sz} = \mathcal{E}_{cz} = \mathcal{E}_z$ and
For the transverse direction, $\mathcal{E}_{sx} = \mathcal{E}_{cx} = \mathcal{E}_x$

$$\mathcal{E}_x + \mathcal{E}_z = \mathcal{E}_1 + \mathcal{E}_2 \tag{2.10}$$

$$\tan^2\theta = \frac{\mathcal{E}_x + \mathcal{E}_2}{\mathcal{E}_z + \mathcal{E}_2} \tag{2.11}$$

where $\mathcal{E}_x, \mathcal{E}_z$ are the strains along the transverse and longitudinal directions respectively

$\mathcal{E}_1$, $\mathcal{E}_2$ are the principal tensile strain and the compressive strain

2.6.4.5 Stress-strain relationship

The stresses presented in Equations 2.7 to 2.9 are related to the strains presented in Equations 2.10 and 2.11 through the stress-strain relationship for steel and cracked concrete. The stress-strain relationship for reinforcement is taken to be bilinear. The traditional linear relationship is stated in Equation 2.12 and 2.13.

$$f_{sx} = E_S\,\mathcal{E}_x \leq f_{yx} \tag{2.12}$$

$$f_{sz} = E_S\,\mathcal{E}_z \leq f_{yz} \tag{2.13}$$

where f_{yx} and f_{yz} are the yield points of the reinforcement in the x and z-directions respectively

E_S is the modulus of elasticity of the reinforcement steel

f_{sx} and f_{sz} are the service stresses in the reinforcement in x and z direction respectively

The stress-strain relationship for cracked concrete is expressed in Equation 2.14 (Collins *et al*., 2007).

$$\varepsilon_2 = -0.002\ (1 - \sqrt{1 - f_{2/} f_{2,max}}) \tag{2.14}$$

where;

$$f_{2,max} = f_c\ /\ (0.8 + 170\ \varepsilon_1) \tag{2.15}$$

$$f_1 = \frac{f_{cr}}{1 + \sqrt{500\ \varepsilon_1}} \tag{2.16}$$

f_2 is the crushing strength of the diagonally compressed strut

f_{cr} is the principal compressive stress at initial cracking taken as $0.33\sqrt{f_{c,max}}$ in MPa

s_x is the perpendicular spacing of cracks inclined at angle θ

The reinforcement and concrete stress-strain relationship graphs are presented in Figure 2.12. It summarises the geometric conditions, equilibrium equations and stress-strain relationships used in the MCFT.

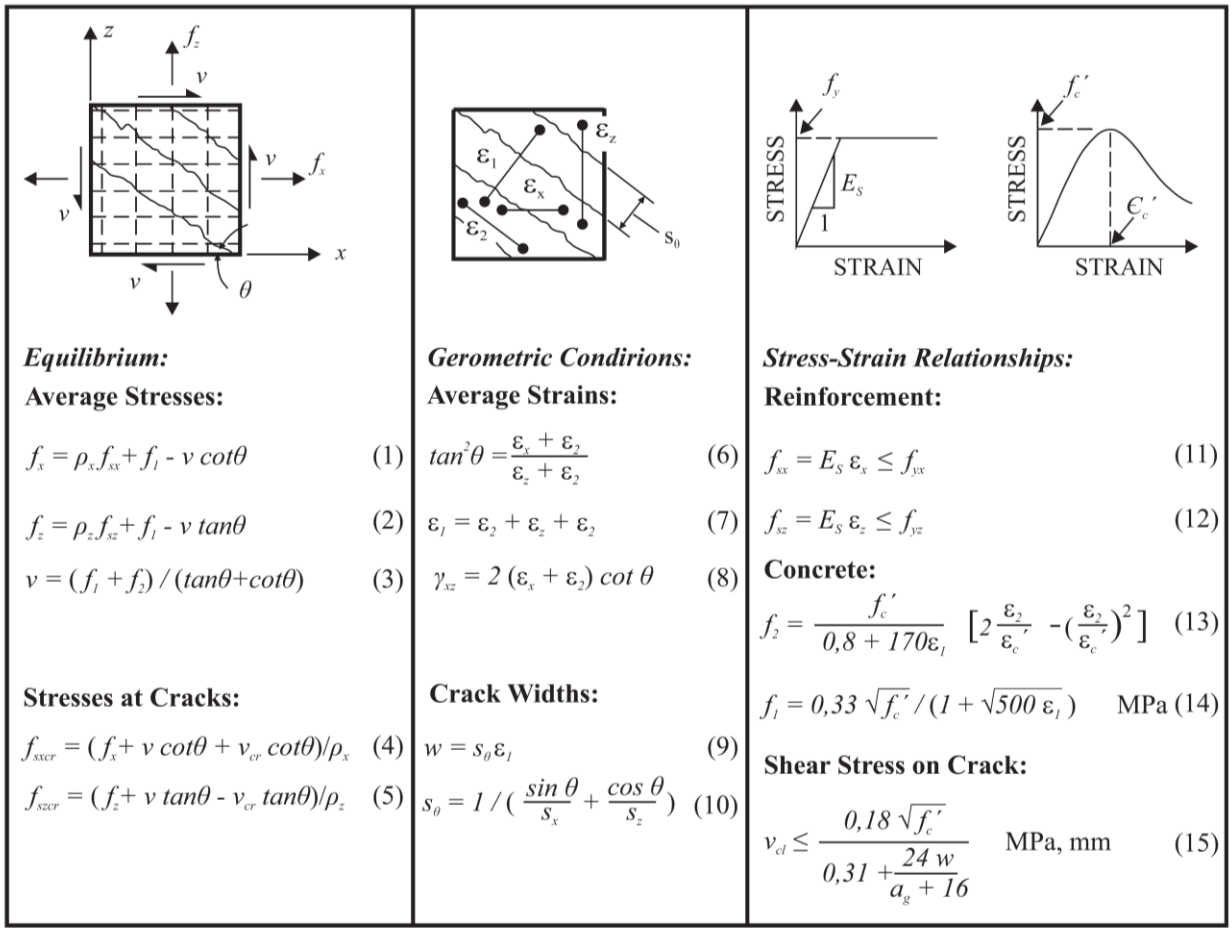

Equilibrium:

Average Stresses:

$$f_x = \rho_x f_{sx} + f_1 - v \cot\theta \quad (1)$$

$$f_z = \rho_z f_{sz} + f_1 - v \tan\theta \quad (2)$$

$$v = (f_1 + f_2) / (\tan\theta + \cot\theta) \quad (3)$$

Stresses at Cracks:

$$f_{sxcr} = (f_x + v \cot\theta + v_{cr} \cot\theta)/\rho_x \quad (4)$$

$$f_{szcr} = (f_z + v \tan\theta - v_{cr} \tan\theta)/\rho_z \quad (5)$$

Gerometric Condirions:

Average Strains:

$$\tan^2\theta = \frac{\varepsilon_x + \varepsilon_2}{\varepsilon_z + \varepsilon_2} \quad (6)$$

$$\varepsilon_1 = \varepsilon_2 + \varepsilon_z + \varepsilon_2 \quad (7)$$

$$\gamma_{xz} = 2 (\varepsilon_x + \varepsilon_2) \cot\theta \quad (8)$$

Crack Widths:

$$w = s_\theta \varepsilon_1 \quad (9)$$

$$s_\theta = 1 / \left(\frac{\sin\theta}{s_x} + \frac{\cos\theta}{s_z} \right) \quad (10)$$

Stress-Strain Relationships:

Reinforcement:

$$f_{sx} = E_S \varepsilon_x \le f_{yx} \quad (11)$$

$$f_{sz} = E_S \varepsilon_z \le f_{yz} \quad (12)$$

Concrete:

$$f_2 = \frac{f_c'}{0{,}8 + 170\varepsilon_1} \left[2 \frac{\varepsilon_2}{\varepsilon_c'} - \left(\frac{\varepsilon_2}{\varepsilon_c'} \right)^2 \right] \quad (13)$$

$$f_1 = 0{,}33 \sqrt{f_c'} / (1 + \sqrt{500\,\varepsilon_1}) \quad \text{MPa} \quad (14)$$

Shear Stress on Crack:

$$v_{cl} \le \frac{0{,}18 \sqrt{f_c'}}{0{,}31 + \frac{24\,w}{a_g + 16}} \quad \text{MPa, mm} \quad (15)$$

Figure 2.12 Summarized Modified Compression Field Theory equations (taken from Bentz *et al.* (2006))

2.6.5 Rotating Angle Softened Truss Model (RASTM)

Similar to MCFT, the RASTM model assumes that the directions of the principal stress and strain coincide with the crack angle after cracking of concrete. For typical elements, this angle will decrease as the shear is increased, hence the name rotating angle. It is assumed that the loading or material response results in a gradual reorientation in the direction of the cracks, as well as that of the principal stress and principal strain in the concrete.

The expression for the model is based on two coordinate systems, the x and y-axes representing the longitudinal and transverse directions, respectively. The equilibrium equations are developed by superposing the stresses in the steel and concrete with the steel resisting the axial stresses only. The resultant equations are presented in Equation 2.17 to 2.19.

$$\sigma_x = \sigma_d \cos^2\theta + \sigma_r \sin^2\theta + \rho_x f_x \tag{2.17}$$

$$\sigma_y = \sigma_d \sin^2\theta + \sigma_r \cos^2\theta + \rho_y f_y \tag{2.18}$$

$$\tau_{xy} = (\sigma_d - \sigma_r)\sin\theta\cos\theta \tag{2.19}$$

where r, d denote the principal tensile and compressive directions respectively

σ_x, σ_y, τ_{xy} are normal and shear stresses in each direction in $x - y$ coordinate

σ_d, σ_r are principal stresses in d and r directions, respectively

ρ_x, ρ_y are reinforcement ratios in the x and y-directions, respectively

f_x, f_y are steel stresses in the x and y-directions, respectively

The compatibility relationships as derived from Mohr's strain circle are presented in Equations 2.20 to 2.22 below.

$$\varepsilon_x = \varepsilon_d \cos^2\theta + \varepsilon_r \sin^2\theta \tag{2.20}$$

$$\varepsilon_y = \varepsilon_d \sin^2\theta + \varepsilon_r \cos^2\theta \tag{2.21}$$

$$\gamma_{yy} = 2(\varepsilon_d - \varepsilon_r)\sin\theta\cos\theta \tag{2.22}$$

where $\mathcal{E}_x$ and $\mathcal{E}_y$ denote the strains along the transverse and longitudinal directions respectively

$\mathcal{E}_r$ and $\mathcal{E}_d$ are the principal tensile strain and the compressive strain respectively

The stress-strain relationships presented in Equation 2.23 to 2.25 account for concrete softening (Belarbi & Hsu, 1995).

$$\sigma_d = \xi_{\sigma 0} {f_c'}^{1} \left[2\left({\varepsilon_d}/{\xi_{\varepsilon 0}\varepsilon_c'}\right) - \left({\varepsilon_d}/{\xi_{\varepsilon 0}\varepsilon_c'}\right)^2\right] \quad \text{if } {\varepsilon_d}/{\xi_{\varepsilon 0}\varepsilon_c'} \leq 1 \tag{2.23a}$$

$$\sigma_d = \xi_{\sigma 0} {f_c'}^{1} \left[1 - \left(\frac{{\varepsilon_d}/{\xi_{\varepsilon 0}\varepsilon_c'} - 1}{{2}/{\xi_{\varepsilon 0}} - 1}\right)^2\right] \quad \text{if } {\varepsilon_d}/{\xi_{\varepsilon 0}\varepsilon_c'} > 1 \tag{2.23b}$$

where for proportional loading

$$\xi_{\sigma 0} = \frac{0.9}{\sqrt{1+400\varepsilon_r}} \text{ and } \xi_{\varepsilon 0} = \frac{1}{\sqrt{1+500\varepsilon_r}} \tag{2.24}$$

and for sequential loading

$$\xi_{\sigma 0} = \frac{0.9}{\sqrt{1+250\varepsilon_r}} \text{ and } \xi_{\varepsilon 0} = 1 \tag{2.25}$$

RASTM predicts similar shear strength to that of MCFT for slightly shear reinforced concrete beams but predicts lower shear strength than that of MCFT for heavily shear reinforced concrete beams. As a result of the assumption that the direction of principal stress in cracked concrete and the crack angle coincides, the contribution of concrete to shear is not accounted for in the RASTM model. In order to consider the contribution of concrete to shear, Hsu (1992) and his researchers developed the Fixed Angle Softened Truss Model (FASTM).

2.6.6 Fixed Angle Softened Truss Model (FASTM)

The Fixed Angle Softened Truss Model (FASTM) assumes that the concrete struts remain parallel to the initial cracks. This initial crack direction depends on the principal concrete stress directions just before cracking. The model is referred to as the Fixed Angle Softened Truss Model (FASTM) because the crack angle remains constant after the concrete has cracked. With FASTM, the directions of the cracks remain the same as the direction of the first cracking. By transforming the stresses and strains into the two coordinate systems as presented in Equation 2.26 to 2.28, the FASTM equilibrium and compatibility equations are developed.

$$\sigma_x = \sigma_2{}^c \cos^2 \emptyset + \sigma_1{}^c \sin^2 \emptyset + \tau_{21} 2 \sin\emptyset\cos\emptyset + \rho_x f_x \tag{2.26}$$

$$\sigma_y = \sigma_2{}^c \sin^2 \emptyset + \sigma_1{}^c \cos^2 \emptyset + \tau_{21} 2 \sin\emptyset\cos\emptyset + \rho_y f_y \tag{2.27}$$

$$\tau_{xy} = (-\sigma_2{}^c + \sigma_1{}^c)\sin\emptyset\cos\emptyset + \tau_{21}{}^c(\sin^2\emptyset - \cos^2\emptyset) \tag{2.28}$$

where, σ_x, σ_y, τ_{xy} are the normal and shear stresses in $x - y$ coordinate

$\sigma_2{}^c$, $\sigma_1{}^c$, $\tau_{21}{}^c$ are the normal and shear stresses in the concrete in the 2-1 directions

$\emptyset$ is the angle of the initial inclined cracks.

The compatibility relationships are presented in Equation 2.29 to 2.31.

$$\varepsilon_x = \varepsilon_2{}^c \cos^2 \emptyset + \varepsilon_1{}^c \sin^2 \emptyset + \gamma_{21} 2 sin\emptyset cos\emptyset \tag{2.29}$$

$$\sigma_y = \varepsilon_2{}^c \sin^2 \emptyset + \varepsilon_1{}^c \cos^2 \emptyset + \gamma_{21} 2 sin\emptyset cos\emptyset \tag{2.30}$$

$$\tau_{xy} = (-\varepsilon_2{}^c + \varepsilon_1{}^c) sin\emptyset cos\emptyset + \gamma_{21}{}^c (sin^2\emptyset - cos^2\emptyset) \tag{2.31}$$

where, $\varepsilon_2{}^c$, $\varepsilon_1{}^c$, $\gamma_{21}{}^c$ are the normal and shear strain in 2-1 coordinate

Pang & Hsu (1996) developed the shear strength of a structural element subjected to pure shear as expressed in Equation 2.32.

$$\tau_{xy} = \frac{(\tau_{21}{}^c)^2 + (\sigma_1{}^c)^2 + (\rho_x f_x + \rho_y f_y)\sigma_1{}^c}{2\sqrt{\rho_x f_x \rho_y f_y}} + \sqrt{\rho_x f_x \rho_y f_y} \tag{2.32}$$

The first term in Equation 2.32 represents the concrete contribution (V_c), whereas the second term represents the stirrup contribution (V_s).

2.6.7 Disturbed Stress Field Model (DSFM)

The DSFM can be described as the further development of the MCFT where the consideration of the influence of crack slip resulted in the removal of the restriction of the orientation of average stress and strain. Vecchio (2000) introduced DSFM for describing the behaviour of cracked reinforced concrete elements. The theory is an extension of MCFT with advancements made with the inclusion of crack shear slip modelling. DSFM combines its improved representation of crack mechanisms with aspects of rotating-crack and fixed-crack models, resulting in better accuracy. The equilibrium equations are presented in Equation 2.33 to 2.36.

$$\sigma_x = f_{cx} + \rho_s f_{sx} \tag{2.33}$$

$$\sigma_y = f_{cy} + \rho_s f_{sy} \tag{2.34}$$

$$\tau_{xy} = v_{cxy} \tag{2.35}$$

$$\varepsilon_x{}^s = -\gamma_s/2.\sin(2\theta) \tag{2.36}$$

$$\varepsilon_y{}^s = -\gamma_s/2.\sin(2\theta) \tag{2.37}$$

$$\gamma_{xy}{}^s = \gamma_s.\cos(2\theta) \tag{2.38}$$

The concrete stresses f_{cx}, f_{cy} and v_{cxy} are determined from the principal stresses using the Mohr's circle of stress. The compatibility condition is expressed in Equation 2.37 and 2.38.

2.6.8 Proposed authorial shear strength equations

Several researchers have developed empirical and semi-empirical formulations for predicting the shear resistance of RC beams with shear links using compilations of experimental test results obtained from the literature.

2.6.8.1 Gambarova and Dei Poli shear strength model

Gambarova (1988) and Dei Poli *et al.* (1990) developed a truss model based on the theory that the forces transferred across cracks by friction is dependent on the crack displacement, slip and crack width. Equation 2.39 was proposed as the contribution of the stirrup in resisting shear in reinforced concrete beams:

$$V_s = \frac{A_v f_y cot\beta_{cr}}{s} \tag{2.39}$$

where β_{cr} is the crack inclination

s is the stirrup spacing

2.6.8.2 Zararis shear strength model

Zararis (2003) developed the model expressions presented in Equation 2.40 and 2.42. According to him, the shear strength of reinforced concrete beams with stirrups can be predicted by using the combination of the following two equations:

$$V_c = \left[1.2 - 0.2\left(\frac{a}{d}\right)d\right]\left(\frac{c}{d}\right)f_{ct}bd \tag{2.40}$$

where f_{ct} is given by Equation 2.41

$$f_{ct} = 0.3(f_c')^{\frac{2}{3}} \tag{2.41}$$

$$V_s = \left[0.5 + 0.25\left(\frac{a}{d}\right)\right]\rho_y f_{vy} bd \tag{2.42}$$

where c is the depth of the compression zone

V_c is the concrete contribution

V_s is the steel contribution.

2.6.8.3 Russo *et al*. shear strength model

Russo *et al*. (2004) proposed the expression in Equation 2.43 for predicting the ultimate shear strength of reinforced concrete beams with stirrups. He applied the equation to 116 experimental beams with stirrups and found that the proposed expression predicts the test results better than ACI 318, Eurocode 2 and CEB/FIP Model Code. The proposed formula was found to be adequately conservative and accurate.

$$V_{uv} = \zeta\left[0.97\rho^{0.46}f_c'^{1/2} + 0.2\rho^{0.91}f_c'^{0.38}f_{yl}^{0.95}\left(\frac{a}{d}\right)^{-2.33}\right] + 1.75 I_b \rho_v f_{yv} \tag{2.43}$$

where the factor I_b is given by Equation 2.44

$$I_b = \frac{0.97\rho^{0.46} {f_c}'^{1/2}}{0.97\rho^{0.46} {f_c}'^{1/2} + 0.2\rho^{0.91} {f_c}'^{0.38} {f_{yl}}^{0.95} \left(\frac{a}{d}\right)^{-2.33}} \quad (2.44)$$

2.6.8.4 Tureyen & Frosch shear strength model

Tureyen & Frosch (2003) calculated shear strength using the model of a cracked concrete beam under the effect of shear stress and axial compression. They proposed the following simplified expressions in Equation 2.45 to 2.47 for the nominal shear strength (V_n) of the concrete members.

$$V_n = V_s + V_c \quad (2.45)$$

$$V_c = 5\sqrt{f_c'} b_w c \quad (2.46)$$

$$V_s = \frac{A_v f_v d}{s} \quad (2.47)$$

where c represents the neutral axis depth

2.6.8.5 Shah & Ahmad shear strength model

Shah & Ahmad (2009) proposed a linear regression model for predicting the shear strength of beams with stirrups as presented in Equation 2.48. The developed regression equation predicts the shear strength of beams as reasonably well compared to the other shear models like ACI 318 and Russo *et al*. (2004).

$$V_n = \zeta \left[0.01 f_c' + 0.507\rho - 0.208\left(\frac{a}{d}\right) + 4.53\rho_v f_y\right] bd \quad (2.48)$$

2.6.8.6 Compression Chord Capacity shear strength model (CCC)

Cladera *et al*. (2016) developed a simplified model for shear strength prediction of RC beams named Compression Chord Capacity model (CCC). According to the proposal of Cladera *et al*. (2016), the shear resistance (V_{CCC}) of a reinforced concrete member with stirrup reinforcement is described as the sum of the concrete $V_{Rd,c}$ and stirrup contributions $V_{Rd,s}$ expressed as Equation 2.51. The shear

reinforcement contributions $V_{Rd,s}$ is expressed as Equation 2.49. The constant 1.4 is not a calibrating factor but a term to account for the confinement of the concrete in the compression chord caused by the stirrups.

$$V_{Rd,s} = 1.4\frac{A_{sw}}{s}\frac{f_{ywk}}{\gamma_s}(d_s - x)cot\theta \tag{2.49}$$

The shear resisted by concrete $V_{Rd,c}$ in Equation 2.50, considers different contributions which includes the contribution of the uncracked compression head V_c, longitudinal reinforcement V_l and shear transfer across web cracks V_w.

$$V_{Rd,c} = V_c + V_w + V_l = 0.3\zeta\frac{x}{d}\left({f_{ck}}/{\gamma_c}\right)^{2/3} b_{v,eff} \tag{2.50}$$

$$V_{CCC} = 1.4\frac{A_{sw}}{s}\frac{f_{ywk}}{\gamma_s}(d_s - x)cot\theta + 0.3\zeta\frac{x}{d}\left({f_{ck}}/{\gamma_c}\right)^{2/3} b_{v,eff} \leq V_{Rd,max} \tag{2.51}$$

The web crushing capacity $V_{Rd,max}$ is expressed as Equation 2.52.

$$V_{Rd,max} = \frac{b_w z v_1 \alpha_{cw}\left({f_{ck}}/{\gamma_c}\right)cot\theta}{(1 + cot\theta^2)} \tag{2.52}$$

The inclination of the compression strut is considered equal to the mean inclination of the shear crack and expressed as Equation 2.53

$$cot\theta = \frac{0.85\,d}{d - x} \leq 2.50 \tag{2.53}$$

where x is the neutral axis depth of the cracked section. The equation for x is expressed as Equation 2.54.

$$\frac{x}{d} = 0.75(\propto_e \rho_l)^{1/3} \tag{2.54}$$

where $\propto_e = \frac{E_s}{E_c}$ is the modular ratio between steel and concrete and ρ_l the longitudinal reinforcement ratio. The minimum shear strength contribution by concrete $V_{Rd,cmin}$ is given in Equation 2.55.

$$V_{Rd,cmin} = 0.25\left(\zeta\frac{x}{d} + \frac{20}{d}\right)\left({f_{ck}}/{\gamma_c}\right)^{2/3} b_w d \tag{2.55}$$

When computing $V_{Rd,cmin}$ the relative neutral axis depth ${x}/{d}$ must not be greater than 0.20. ζ is the size and slenderness effect factor given in Equation 2.56

$$\zeta = \frac{2}{\sqrt{1+\frac{d}{200}}}\left(\frac{d}{a}\right)^{0.2} \leq 0.45 \tag{2.56}$$

The influence of the compression flange is accounted for using effective shear width $b_{v,eff}$ given in Equations 2.57 and 2.58

$$\text{If } x \leq h_f \; b_{v,eff} = b_w + 2h_f \leq b \tag{2.57}$$

$$\text{If } x > h_f \; b_{v,eff} = b_w + (b_v - b_w)\left(\frac{h_f}{x}\right)^{3/2} \tag{2.58}$$

2.6.9 Response-2000

Response 2000 (R2k) is a two-dimensional sectional analysis program that evaluates the shear strength of RC beams subjected to shear, moment and axial load using the basis of MCFT. The computer program was developed by Evan Bentz (2000). MCFT (R2k) provides a prediction of shear which compares well to experimental results (Bentz, 2000; Kuchma *et al*., 2004; Metwally, 2012). The capacity predictions of MCFT can be classified as LoA IV (highest level of approximation) estimates of shear resistance according to the Fib MC 2010 classification system (Kuchma *et al*., 2008 and Bentz, 2010). Example capabilities are illustrated in Figure 2.13 and 2.14. The key features and analytical modelling decisions of Response-2000 are discussed here. Additional information is available in Bentz (2000).

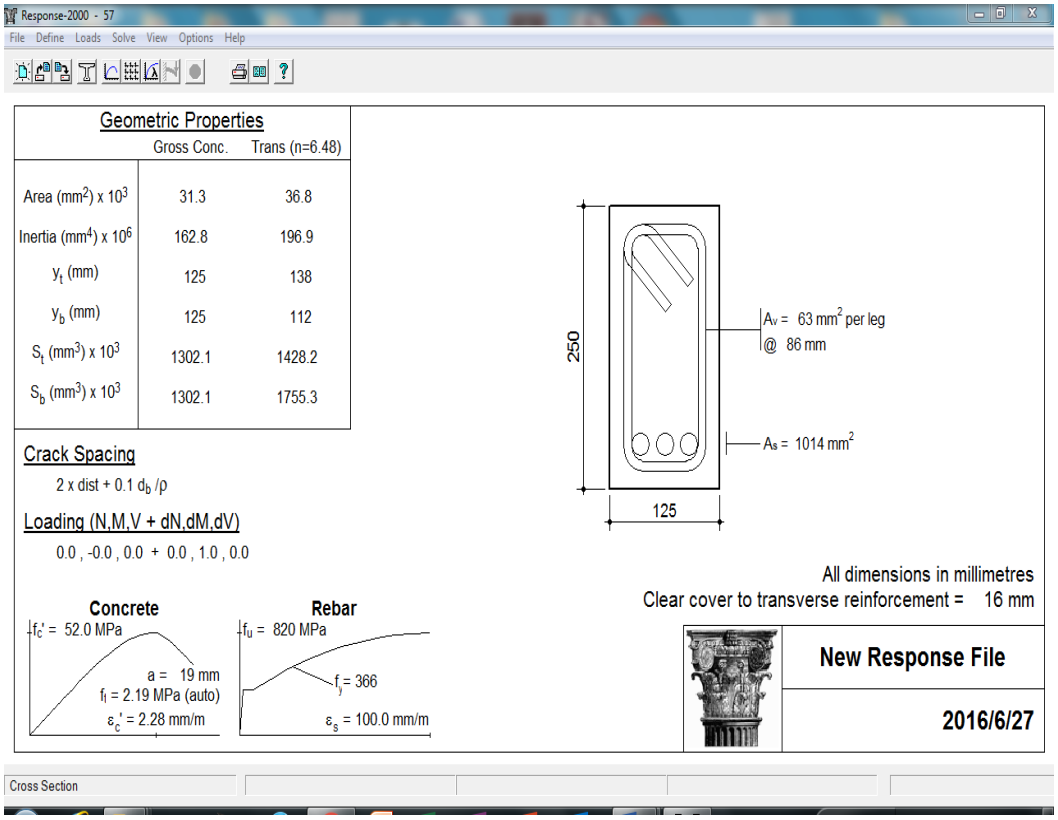

Figure 2.13 Produced cross-section of a beam from Response-2000

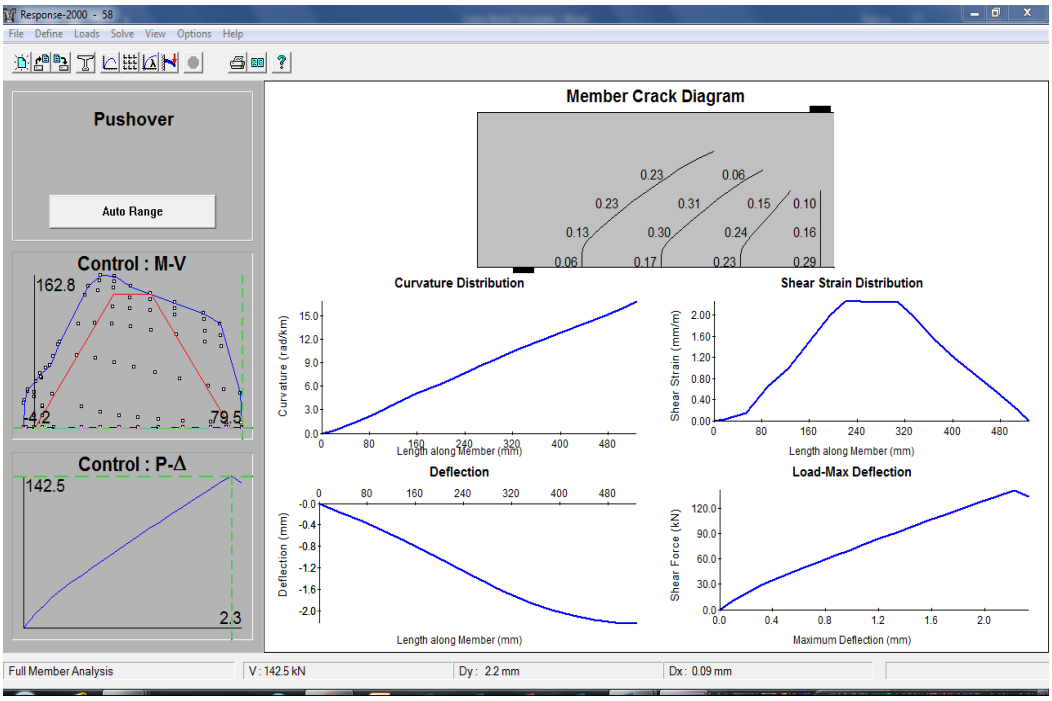

Figure 2.14 Response-2000 results from member analysis of a reinforced concrete beam.

2.6.9.1 Assumptions in R2k

According to Bentz (2010), the following assumptions are considered in R2k:

1. The beam theory assumption that plane sections remain plane.
2. There is no substantial nett stress in the transverse direction acting through the depth of the beam. Both the concrete and transverse steel forces must balance at each point through the depth of the beam. This indicates that if there is transverse clamping stress, the actual strength of the beam will exceed that predicted by R2k.
3. R2k is based on independent constitutive relationships of the MCFT which can be used for biaxial stress-strain behaviour throughout the depth of the beam.

2.6.9.2 Sectional analysis in R2k

Finding the sectional response at any point along the length of the member is an iterative process. The three unknowns at the section are the shear-strain profile, the curvature and the strain at the top fibre of the section. Compatibility is enforced by maintaining that plane sections remain plane (note that this ignores the constraint that strain compatibility does not permit a non-constant shear strain profile when plane sections remain plane). Equilibrium is enforced for axial and shear forces while maintaining a user-specified shear to moment ratio (Bentz, 2010).

The model allows shear stress and strain to vary over the length of the section, despite the assumption that plane sections remain plane (Metwally, 2012). The sectional analysis provides a variety of output. Notable output data include the moment-curvature relationship, moment-shear interaction envelope, longitudinal stress-strain data at fibre nodes, shear stress-strain data at fibre nodes and cracking information.

2.6.9.3 Member analysis in R2k

R2k determines the force-deflection behaviour of a simple beam subject to different load and support conditions. The program incorporates the longitudinal stiffness method formulated by Bentz (2010). The load vs deformation response is determined by the following procedures:

1. The first step is the determination of the full moment-shear (M-V) interaction response for the section

2. The member section is divided into twenty segments as integration points
3. The internal shear and moment at individual segment is determined for each load step
4. The shear-strain and curvature are calculated at each segment by interpolating the data points from the moment-shear (M-V) interaction diagram
5. Using the resultant shear-strains and curvature values, the displacements are calculated by the moment-area method.

2.6.9.4 MCFT (R2k) input parameters

For shear analysis based on MCFT using R2k, loads, some geometry and other member properties have to be specified. The input parameters include:

a) Concrete cylinder compressive strength
b) Aggregate size
c) Number of bars and area of longitudinal reinforcement
d) Stirrup spacing
e) Area of shear reinforcement
f) Section breadth
g) Yield strength of tension reinforcement
h) Yield strength of stirrup reinforcement
i) Concrete cover
j) Section height
k) Stirrup type

2.6.9.5 Mode of failure in R2k

The methods of determining the mode of failure in R2k are discussed below.

1. Moment-shear interaction diagram

The mode of failure in R2k can be determined by comparing the assumed moment-shear envelope of the member to the moment-shear interaction failure envelope. Flexural failure occurs when the member curve intersects the failure envelope where the moment is at its maximum, and shear is zero (that is if it touches on the far right side). Conversely, shear effects influence the member's failure, if the member curve intersects anywhere else. These two scenarios are shown in Figure 2.15 and 2.16.

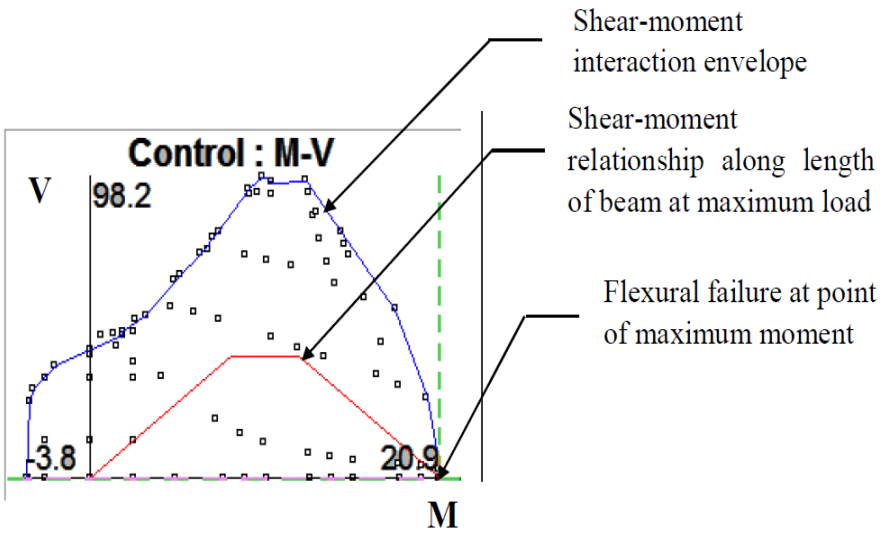

Figure 2.15 Flexural failure in Response 2000

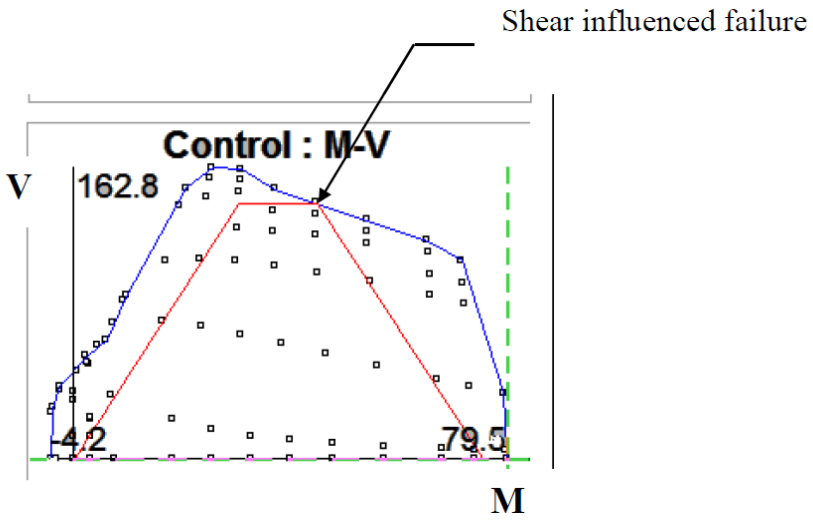

Figure 2.16 Shear failure in Response 2000

2 Principal compressive stress plot

The principal compressive stress plot in R2k is shown in Figure 2.17. The maximum allowable stress is shown in red at left, and the applied stress in the concrete beam is shown in blue line on the right side. In beams with shear reinforcement, if the blue and red lines touch, or about to touch concrete strut crushing failure is predicted in the section.

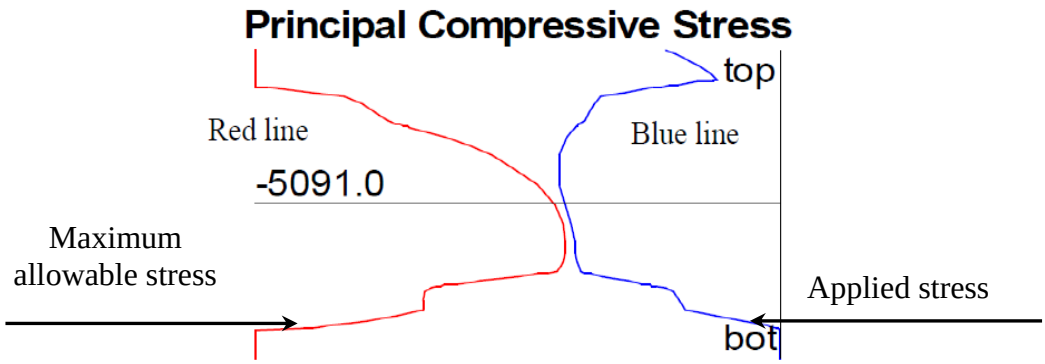

Figure 2.17 Principal compressive stress plot indicating web-crushing failure

2.6.9.6 Response-2000 results

Response 2000 is an advanced research tool that provides a detailed output of results including concrete and steel stresses and strains, concrete angle of principal compression, crack spacing at all layers and force-deformation plots as well as shear-moment interaction diagrams. Figure 2.14 presents some example output plots from Response 2000 for a typical rectangular reinforced concrete beam. MCFT (R2k) provides best-estimate predictions of shear resistance that are derived based on mean values of the input parameters. It is not a design procedure for shear. MCFT (R2k) predictions are not connected to the design safety bias introduced by partial material factors and characteristic values, as it is introduced in a design procedure to achieve sufficient safety performance.

Bentz (2000) verified Response 2000 against 534 experimental tests reported in the literature on a variety of member types and found a mean ratio of measured to predicted shear strength of 1.05 and a C.O.V of 12%. In the report presented by Hawkins *et al*. (2005), MCFT (R2k) predictions were compared with the results of 149 experimental shear tests. The database included 85 prestressed concrete girders. They obtained the mean ratio of experimental to the predicted shear strength of 1.02 and 1.11, and a C.O.V of 11% and 17% for reinforced and prestressed girders, respectively.

2.7 Summary

This chapter presented an outline of the current understanding of shear behaviour of reinforced concrete beams, different modes of shear failure and available shear models. In order to better understand the behaviour of shear, shear transfer mechanisms are discussed in detail in this chapter. Shear is resisted through the contributions of the aggregate interlock, dowel action, shear in the

uncracked compression zone, residual tensile stresses, shear reinforcement and arch action. There have been differences with respect to these components and their influence on shear strength. As discussed in the chapter, different shear parameters like shear span to depth ratio, shear reinforcement, longitudinal reinforcement and concrete strength can have a significant influence on shear strength of reinforced concrete beams.

Existing shear strength models on which shear provisions in most current design standards are based are reviewed in this chapter. The models include the truss-based approach, the Variable Strut Inclination Method (VSIM), the Modified Compression Field Theory (MCFT), the Disturbed Stress Field Approach, the Fixed Angle Softened Truss model and the Rotating Angle Softened model.

The truss-based approach is the traditional method towards determining the shear resistance of reinforced concrete members with shear reinforcement. In the model, diagonal concrete struts are considered to be the diagonal members of the truss, the stirrups are the vertical members of the truss, the longitudinal reinforcement served as the bottom chord of the truss, and the flexural compression zone served as the top chord of the truss. The variable-angle truss model is a modified version of the 45° truss model allowing the strut angle (θ) to vary within a certain boundary.

The MCFT generalises the compression field theory and also accounts for the stress that concrete carries between cracks, a phenomenon called tension stiffening. The MCFT model was formulated considering equilibrium, compatibility as well as relative stress-strain relationships of the steel and concrete. The Disturbed Stress Field Model (DSFM) theory is an extension of MCFT with advancements made with the inclusion of crack shear slip modelling

The Rotating-Angle Softened-Truss Model (RASTM) and the Fixed-Angle Softened-Truss Model (FASTM) utilize equilibrium, compatibility and stress-strain relationships for softened concrete. RASTM model assumes that the crack angle in post-cracking concrete coincides with the principal stress and strain directions. The Fixed Angle Softened Truss Model (FASTM) assumes that the concrete struts remain parallel to the initial cracks. This initial crack direction depends on the principal concrete stress directions just before cracking.

Other recently published authorial shear strength equations from published literature such as the Tureyen & Frosch shear strength model, Compression Chord Capacity model, are discussed. The chapter presented a description of the computer program Response 2000 and its implementation of the MCFT. Response 2000 (R2k) is a two-dimensional sectional analysis program that evaluates the shear strength of RC beams subjected to shear, moment and axial load using the basis of MCFT.

Chapter 3

Review of available shear design approaches

3.1 Introduction

Given the numerous shear strength theories and developments discussed in Chapter 2, shear strength prediction of slender reinforced concrete beams is still an intricate and elaborate topic. Consensus has not been achieved internationally on the essential parameters and mechanisms governing shear behaviour (Collins *et al*., 2008). Different shear design methods and guidelines use different theories in shear modelling such as truss model, Modified Compression Field Theory (MCFT) and fracture mechanics approach.

This chapter reviews the shear design provisions of beams with shear reinforcement in well-established codes of practices, focusing on six well-known international codes: ACI building code (ACI 318-11), AASHTO LRFD design specification, Canadian Standards Association (CSA A23.3-04), Eurocode 2 (EN 1992-1-1), the South African National Standard (SANS 10100-1) and Fib Model Code LoA III (2010). Their stipulations on shear design differ considerably from one another, resulting in different design procedures and safety performance. Salient features of some of the shear methods were identified, their weaknesses and limitations were also discussed.

3.2 Overview of shear design provisions in design codes

3.2.1 ACI 318-11 shear design provision

The 45^0 truss analogy is adopted in the ACI 318 building standard to estimate the shear reinforcement contribution to shear resistance. The estimated shear force at inclined cracking is taken as the concrete contribution. The design shear resistance V_{Rd} is computed as the addition of the concrete contribution,

V_c (Equation 3.1 or 3.2) and shear reinforcement contribution, V_s (Equation 3.3) as expressed in Equation 3.4a.

$$V_c = \frac{\lambda}{6}\sqrt{f_c'}\,b_w d \tag{3.1}$$

$$V_c = \left[0.16\sqrt{f_c'} + 17\rho_l {V_u d}/{M_u}\right] b_w d \leq 0.3\sqrt{f_c'}\,b_w d \tag{3.2}$$

where $f_{c,}$ is the concrete compressive cylinder strength

ρ_l is the flexural reinforcement ratio

b_w is the beam width

d is the effective depth of the beam

V_u and M_u are factored shear force and bending moment occurring simultaneously in the critical section considered

λ is a modification factor taken as 1.0 for normal weight concrete.

The steel contribution V_s is calculated based on the 45^0 truss model as Equation 3.3.

$$V_s = \frac{A_v f_v d}{s} \tag{3.3}$$

where f_v is the yield strength of the transverse reinforcement (MPa)

s is the spacing of the transverse reinforcement (mm)

A_v is the area of shear reinforcement (mm^2)

$$\mathrm{V}_n = V_s + V_c = \frac{\lambda\sqrt{f_c'}\,b_w d}{6} + \frac{A_v f_v d}{s} \tag{3.4a}$$

In the ACI 318, the strength design philosophy states that the design shear capacity of a member must exceed the shear demand as expessed in Equation 3.4b. ACI 318 does not use partial factors but resistance reduction factor (Load and Resistance Factor Design LRFD format).

$$\phi V_n \geq V_u \tag{3.4b}$$

where ϕ is the shear strength reduction factor and is given as 0.75 (ACI 318, 2011).

3.2.1.1 Minimum amount of shear reinforcement

ACI 318 specifies the minimum shear reinforcement in all reinforced concrete members to prevent the sudden failure at the occurrence of inclined cracks. The minimum area of shear reinforcement $A_{w,min}$ is expressed as Equation 3.5.

$$A_{w,min} = 0.062\sqrt{f_c'}\frac{b_w s}{f_{yw}} \geq 0.35\frac{b_w s}{f_{yw}} \tag{3.5}$$

f_c' represents a 9% fractile and the following relationship (3.6) can be derived

$$f_c' = f_{ck} + 1.60 \tag{3.6}$$

ACI 318 does not allow the use of a concrete compressive strength f_c'exceeding 69 MPa. For shear strength calculation, $\sqrt{f_c'}$ is limited to 8.30 MPa so that the influence of concrete strength f_c' greater than 69 MPa is neglected. The shear strength provided by shear reinforcement is limited to the value of Equation 3.7 to prevent crushing of the concrete before yielding of transverse reinforcement.

$$V_s \leq V_{Rd,max} = 0.830\sqrt{f_c'}b_w d \tag{3.7}$$

3.2.2 AASHTO LRFD design specifications (2002)

AASHTO (American Association of State Highway and Transportation Officials) LRFD shear design provision was developed based on the MCFT. Equations 3.8 to 3.10 presents the nominal shear resistance V_n.

$$V_n = V_S + V_c \leq 0.25 f_c' b_w d_v \tag{3.8}$$

$$V_c = 0.083\beta\sqrt{f_c'}\, b_w d_v \tag{3.9}$$

$$V_s = \frac{A_v f_v d \cot\theta}{s} \tag{3.10}$$

where b_w is the effective web width

d_v is the effective shear depth

s is the spacing of stirrups

β is the factor indicating the ability of diagonally cracked concrete to transmit tension

V_s is the contribution from shear reinforcement

V_c is the concrete contribution

θ is the angle of inclination of diagonal compressive stresses

Values for β and θ for members that contain the minimum required amount of shear reinforcement and for members that contain less than that amount are provided in AASHTO LRFD. The AASHTO LRFD follows the ACI approach of applying an overall resistance factor denoted, ϕ instead of partial material factor. The overall resistance of a member is given by $\phi V_n \geq V_u$, where ϕ has a value of 0.9.

3.2.3 Canadian Standards Association (CSA A23.3-04) shear design provision

The general shear provisions of the Canadian Standards Association Code (CSA-04) were developed based on the MCFT. The CSA A23.3-04 introduced an approach that significantly simplifies the MCFT procedure. The CSA specifications were developed to offer an easy way to obtain β which is the factor portraying the ability of diagonally cracked concrete to transmit tension. θ is the angle of inclination of diagonal compressive stresses. In CSA, the iteration procedure was removed for easy design purposes by taking $\theta = 30$ degrees. The nominal shear strength is determined using similar equations as AASHTO LRFD (Equations 3.8 to 3.10).

3.2.4 SANS 10100-1. (2000) shear design provision

SANS 10100 is based on the 45° truss model with the inclusion of a concrete contribution term developed empirically. The nominal shear stress, v_n is the sum of the shear reinforcement

contribution v_s and the concrete contribution v_c. Thus the nominal shear stress is expressed as Equation 3.11 and 3.12.

$$v_n = v_s + v_c \tag{3.11}$$

$$v_n = \frac{0.75}{\gamma_{m,c}}\left(\frac{f_{cu}}{25}\right)^{1/3}\left(\frac{100A_S}{b_w \mathrm{d}}\right)^{1/3}\left(\frac{400}{\mathrm{d}}\right)^{1/4} + \frac{A_v f_v d}{\gamma_{m,s} b_w s} \tag{3.12}$$

where $\gamma_{m,c}$ is the partial material safety factor for concrete

$\gamma_{m,s}$ is the partial material safety factor for steel

$\frac{100A_S}{b_w \mathrm{d}}$ is the reinforcement ratio.

f_v is the yield strength of shear reinforcement

A_v is the area of shear reinforcement

f_{cu} is the characteristic concrete cube strength

SANS apply a partial material factor for concrete of $\gamma_{m,c} = 1.4$ and $\gamma_{m,s} = 1.15$ for steel.

3.2.5 Fib Model Code 2010 (MC-10(III))

The shear design provisions based on the stipulations of Model code 2010 are more complicated compared to other design codes presented in this study. The shear resistance prediction is categorised based on three different Levels of Approximation (LoA). Only LoA III is considered in this study. The complexity, effort, detail and level of accuracy increases as the LoA increases. Model Code 2010 provides an opportunity to take into account the shear force contributed by concrete at LoA III. The design shear resistance $\mathrm{V}_{Rd}\,(\mathrm{X}_k, \gamma)$ or $\mathrm{V}_{MC-10(III)}\,(\mathrm{X}_k, \gamma)$ for a beam with shear reinforcement can be derived using the state equation expressed as Equation 3.15. Components of the design shear resistance include the resistance attributed to the concrete $V_{Rd,c}$ (Equation 3.14) and the shear strength provided by the stirrup reinforcement $\mathrm{V}_{Rd,S}$ (Equation 3.13).

$$V_{Rd,s} = 0.9\frac{A_{sw}}{s_w} f_{ywk}/\gamma_s \, d(cot\theta + cot\alpha)sin\alpha \tag{3.13}$$

$$V_{Rd,c} = 0.9K_v\sqrt{f_{ck}/\gamma_c}\, b_w d \tag{3.14}$$

$$\mathrm{V}_{MC-10(III)}\,(\mathrm{X}_k, \gamma) = 0.9\frac{A_{sw}}{S_w}\frac{f_{ywk}}{\gamma_s} d(cot\theta + cot\alpha)sin\alpha + 0.9K_v\sqrt{f_{ck}/\gamma_c}\, b_w d \tag{3.15}$$

where f_{ck} is the characteristic value of concrete compressive strength

b_w is the width of the web

d is the effective depth of the section

γ_c is the partial safety factor of the concrete according to the design situation

γ_s is the partial safety factor of the steel according to the design situation

K_v is the first parameter of the model defined by the levels of approximation (Fib, 2010; 2013; Walraven, 2011).

For calculating the design shear resistance attributed to the concrete ($\mathrm{V}_{Rd,c}$), K_v (Equation 3.16) is dependent on the calculated longitudinal strain ε_x and is defined by Equation 3.17.

$$K_v = \frac{0.4}{(1 + 1500\varepsilon_x)}\left(1 - {V_{Ed}}/{V_{Rd,max}(\theta_{min})}\right) \geq 0 \tag{3.16}$$

$$\varepsilon_x = \frac{{M_{Ed}}/{z} + V_{Ed}}{2E_S A_S} < 0.003 \tag{3.17}$$

where ε_x is the longitudinal strain which must not exceed 0.003.

A_S comprises the main longitudinal reinforcing bars in the tension chord.

z is the lever arm and its taken as $0.9d$.

The angle of inclination of the compressive stress field θ is determined using Equation 3.18(a) (Fib, 2010). The inclination of the compressive stress field must be within the range specified in Equation 3.18(b) (Fib, 2013).

$$\theta = 29^0 + 7000\varepsilon_x \tag{3.18a}$$

$$20^0 + 10000\varepsilon_x \leq \theta \leq 45^0 \tag{3.18b}$$

3.2.5.1 MC-10 (III) web-crushing strength capacity ($V_{Rd,max}$)

The shear strength is limited by the crushing of the concrete $V_{Rd,max}$ calculated as Equation 3.19. The equation of $V_{Rd,max}$ has a strength reduction factor $K_c = K_\varepsilon \eta_{fc}$ composed of a factor for the strain effect K_ε (Equation 3.21) and a brittleness factor η_{fc} described in Equation 3.20. The brittleness factor reduces the strength for $f_{ck} > 30$ MPa due to increased brittle failure behaviour of such concrete.

$$V_{Rd,max} = 0.9K_c \, {f_{ck}}/{\gamma_c} \, b_w d \frac{cot\theta + cot\alpha}{1 + cot^2\theta} \tag{3.19}$$

$$\eta_{fc} = \left(\frac{30}{f_{ck}}\right)^{1/3} \leq 1.0 \tag{3.20}$$

where θ is defined by the different levels of approximation and indicates the angle of the principal compressive stress in the web

$\propto$ is the angle of the stirrups

K_c is the concrete strength reduction factor taking into consideration the effect of cracked concrete.

$$K_\varepsilon = \frac{1}{1.2 + 55\varepsilon_1} \leq 0.65 \tag{3.21}$$

ε_1 is the principal strain defined by Mohr's circle of strain, taken as Equation 3.22

$$\varepsilon_1 = \varepsilon_x + (\varepsilon_x + 0.002)cot^2\theta \tag{3.22}$$

3.2.5.2 Minimum amount of shear reinforcement

The minimum stirrup reinforcement ratio $A_{w,min}$ is defined by Equation 3.23 which is similar to that of Eurocode 2.

$$A_{w,min} = 0.08 \frac{\sqrt{f_{ck}}}{f_{ywk}} b_w s \tag{3.23}$$

Model Code 10 LoA III assumes the same partial material safety factor for concrete γ_c and steel γ_s as stated in Eurocode 2.

3.2.6 EN 1992 Eurocode 2: 2004 shear design provision

Eurocode 2 is based on a method of shear design known as the Variable Strut Inclination Method. The method assumes that shear reinforcement carries all the shear force. The VSIM allows the concrete compressive struts angle (which is determined based on the theory of plasticity) to be varied (Braestrup *et al.*, 1976; Jensen & Lapko, 2009).

3.2.6.1 Capacity based on shear reinforcement of links ($V_{Rd,s}$)

Two primary shear forces are represented in EC2 for design purposes, namely $V_{Rd,max}$ and $V_{Rd,s}$. Where $V_{Rd,max}$ represents web-crushing strength capacity and $V_{Rd,s}$ denotes the shear capacity of the member with stirrup failure. Figure 3.1 shows an analogous truss representing the action of a reinforced concrete beam in shear.

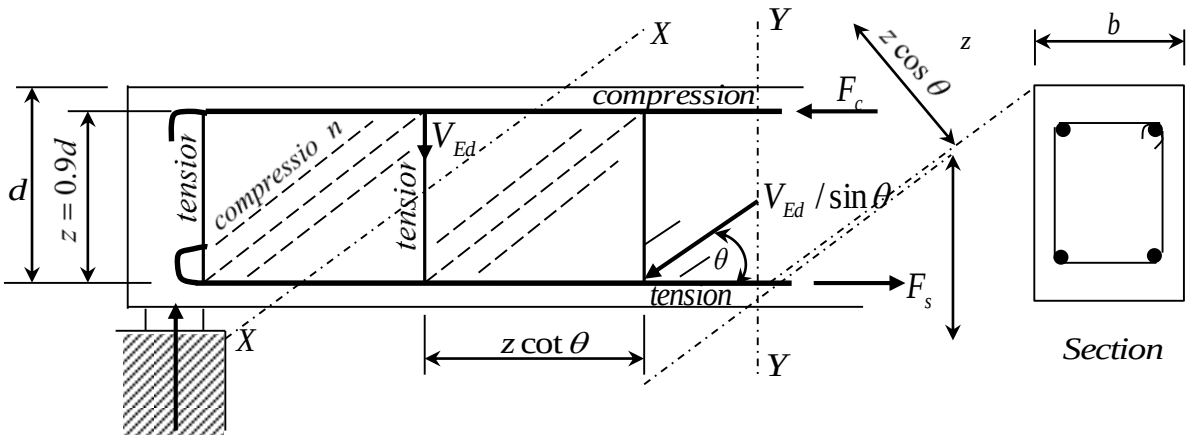

Figure 3.1 Truss model for VSIM (taken from Mosley *et al.*, 2007)

$$V_{Rd,s} = f_{ywd}\, A_{sw} = \frac{f_{ywk}}{1.15} A_{sw} \tag{3.24}$$

Assuming the shear links are spaced at a distance s apart, the force in each link is given by Equation 3.25.

$$V_{Rd,S}\frac{s}{zcot\theta} = f_{ywd}A_{sw} \tag{3.25}$$

Equation 3.25 can be rearranged to give the design shear resistance $V_{Rd,s}$. Thus:

$$\mathrm{V}_{Rd,s}\,(\mathrm{X}_k,\gamma) = \mathrm{V}_{VSIM-L\theta}(\mathrm{X}_k,\gamma) = \frac{A_{sw}}{s}z\frac{f_{ywk}}{\gamma_s = 1.15}cot\theta \tag{3.26}$$

As the magnitude of the maximum shear force on the beam increases, the strut angle θ also increases. This further results in an increase in the compressive forces in the diagonal concrete members. EC2 sets the angle to have a value between 21.8 and 45 degrees. Equation 3.25 is used to determine the amount and spacing of the shear links, which further depends on the value of θ used in the design.

3.2.6.2 Web-crushing strength capacity ($V_{Rd,max}$)

The applied shear force must be restricted to prevent excessive compressive stresses in the concrete struts to avoid concrete compressive failure. Therefore, the maximum design shear force $V_{Rd,max}$ is restricted by the ultimate strength of the strut and its vertical component. $\mathrm{V}_{Rd,max}$ is calculated as Equation 3.27.

$$V_{Rd,max} = \frac{\left(\frac{f_{ck}}{\gamma_c}\right)b_w\,zv_1\,\alpha_{cw}}{(cot\theta + tan\theta)} \tag{3.27}$$

where:

$$v_1 = 0.6(1 - \frac{f_{ck}}{250}) \tag{3.28}$$

where s is the spacing of the links

f_{ck} is the characteristic strength of concrete

γ_c is the partial material factor for concrete, recommended value = 1.5

γ_s is the partial material factor for steel, recommended value = 1.15

f_{ywk} is the characteristic strength of the link reinforcement

A_{sw} is the cross-sectional area of the two legs of the link

v_1 is the strength reduction factor

α_{cw} is the coefficient accounting for stress in the compression chord

3.2.6.3 Minimum amount of shear reinforcement

The minimum amount of shear reinforcement to be provided is a parameter open for national choice. EC 2 specifies a minimum value for $\frac{A_{sw}}{s}$ such that:

$$\frac{A_{sw,min}}{s} = \frac{0.08{f_{ck}}^{0.5} b_w}{f_{ywk}} \tag{3.29}$$

3.2.6.4 Maximum capacity design for VSIM

As expressed in Equation 3.26, as the strut angle θ decreases the shear capacity based on the stirrups increases. Conversely, as the strut angle θ decreases with values below 45 degrees, the shear crushing strength capacity given by Equation 3.27 decreases. According to Beeby & Narayanan (1995), the state where the stirrup capacity equals the concrete strut capacity is the point of the maximum capacity. This means that the real conditions at failure may be developed by equating Equation 3.26 and 3.27 ($V_{Rd,S} = V_{Rd,max}$). From this, the equation to determine the strut angle θ is derived as presented in Equation 3.30. Using the calculated value of θ from Equation 3.30 will give the required amount of shear reinforcement.

$$\theta = \sin^{-1}\sqrt{\frac{A_{sw}\left(\frac{f_{ywk}}{\gamma_s}\right)}{\alpha_{cw} b_w s v_1 \left(\frac{f_{ck}}{\gamma_c}\right)}} \tag{3.30}$$

3.2.6.5 Influence of concrete strut inclination angle θ on EC2 VSIM capacity predictions

The performance of EC2 VSIM is to certain degree depending on the limits governing the concrete compressive strut angle (θ). Based on the equation of EC2 design shear resistance $V_{Rd,s}$, a smaller value of concrete strut inclination angle θ allows for a reduction in the amount of shear reinforcement

ratio necessary to achieve the same shear reinforcement contribution. Figure 3.2 shows the plot of the design concrete strut angle θ_d for variation in shear reinforcement for a subset of the database of beam experiments developed by Reineck *et al* (2014) (Section 6.2). Figure 3.3 presents the variation of design strut angle θ_d for specific test sections at the parametric range of design shear reinforcement $\rho_w f_{ywd}$ and characteristic concrete strength f_{ck}. The test sections considered, have the following characteristics: $b_w = 200$, $d = 300$, $a/d = 2.5$, $\rho_l = 4\%$.

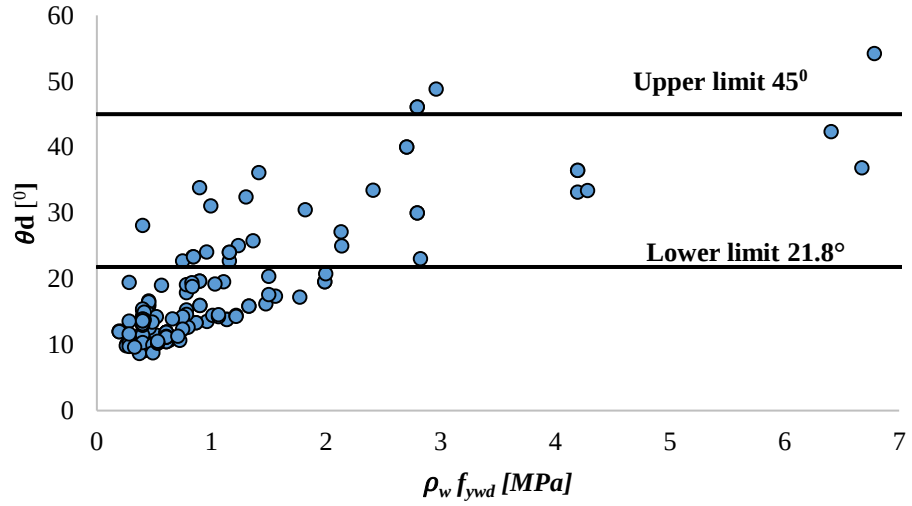

Figure 3.2. Variation of θ_d with $\rho_w f_{ywd}$ using a database of experimental test

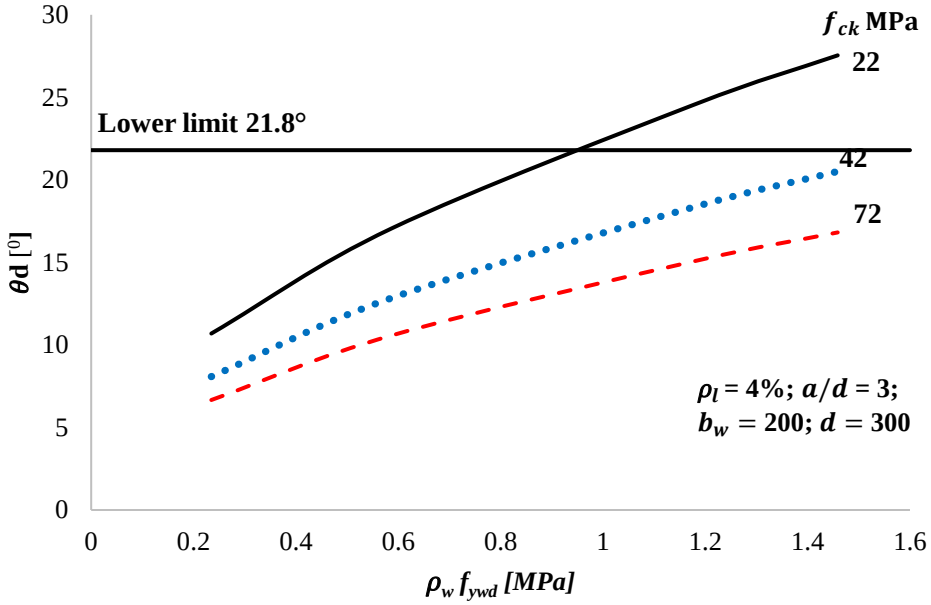

Figure 3.3. Variation of θ_d with $\rho_w f_{ywd}$ and f_{ck}

From Figures 3.2 and 3.3, it can be seen that VSIM predicts θ_d to be much lower than the 21.8^0, the lower limit recommended by Eurocode 2. This clearly reveals that the unbiased and unconstrained analytical formulation of VSIM (i.e. without the concrete strut angle θ limitation) naturally predicts a flatter concrete strut θ angle (< 21.8^0) especially at lower levels of shear reinforcement (Mensah, 2015). It can be seen from Figure 3.3 that θ_d only exceeded 21.8^0 at combined situations of low concrete strength f_{ck} (22 MPa) and high shear reinforcement $\rho_w f_{ywd} > 1\ MPa$. This is an indication that the limited strut angle as stated in the operational EC2 VSIM shear design function is a form of bias imposed on the concrete compressive strut angle to build conservatism in the model. The lower limit of 21.8^0 is enforced to achieve a more conservative estimate of shear predictions, significantly influencing the performance of VSIM for lower levels of shear reinforcement while the upper limit of 45^0 is to prevent overly conservative estimates. The 21.8° lower limit is introduced into the operational EC2 VSIM procedures to avert flatter angles/lower angles predicted by the unconstrained analytical version of VSIM (denoted V_{VSIM-A}).

3.2.6.6 Influence of concrete strength on EC2 VSIM predictions

Concrete strength is a critical parameter affecting the shear behaviour of beams with shear reinforcement. The effect of concrete strength on the normalised shear capacity of experimental RC beams is shown in Figure 3.4. A subset of the database of beam experiments developed by Reineck *et al*. (2014) (Section 6.2) is categorised into ranges of increasing concrete strength in Figure 3.4. From the figure, it can be noted that shear strength increases with increasing shear reinforcement and concrete strength, also noted by other researchers (Moody *et al*., 1954; Yoon *et al*., 1996). As reflected in Figure 3.5, concrete strength only affects EC2 VSIM predictions ($V_{VSIM-L\theta}$) at the combination of low concrete strength f_{ck} and high amount of shear reinforcement $\rho_w f_{ywd}$. This can be attributed to the limitation imposed on the concrete strut angle. The design concrete strut angle θ_d predicted by $V_{VSIM-L\theta}$ in this design situation exceeds 21.8°.

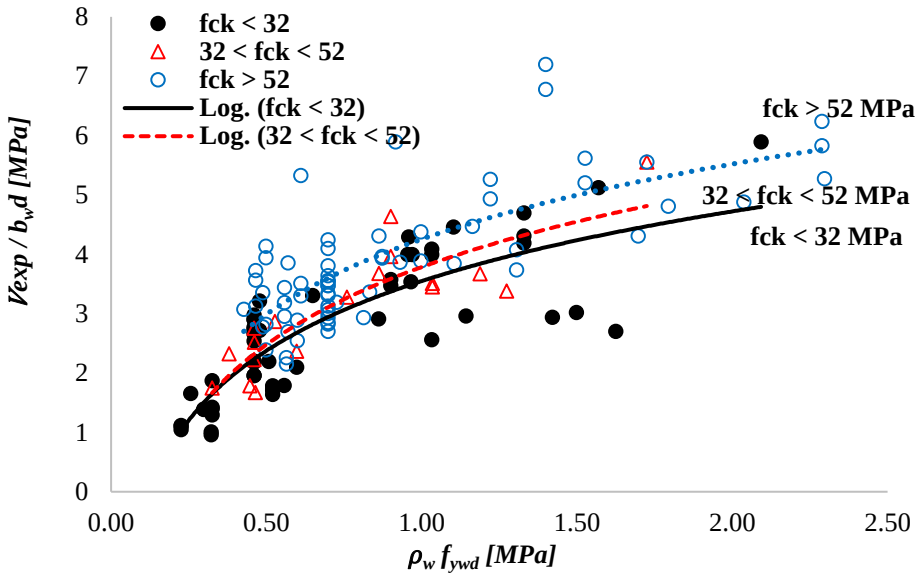

a) $\rho_w f_{ywd} < 2.5\ MPa$

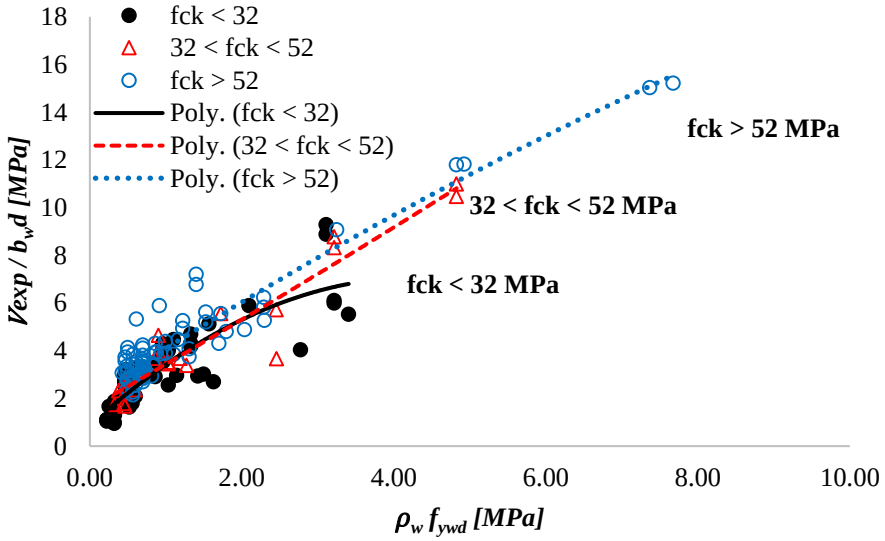

b) $\rho_w f_{ywd}$ up to 10 MPa

Figure 3.4. Trends of normalised shear resistance for experimental tests $\left(V_{exp}/b_w d\right)$ for different concrete strength bin ranges.

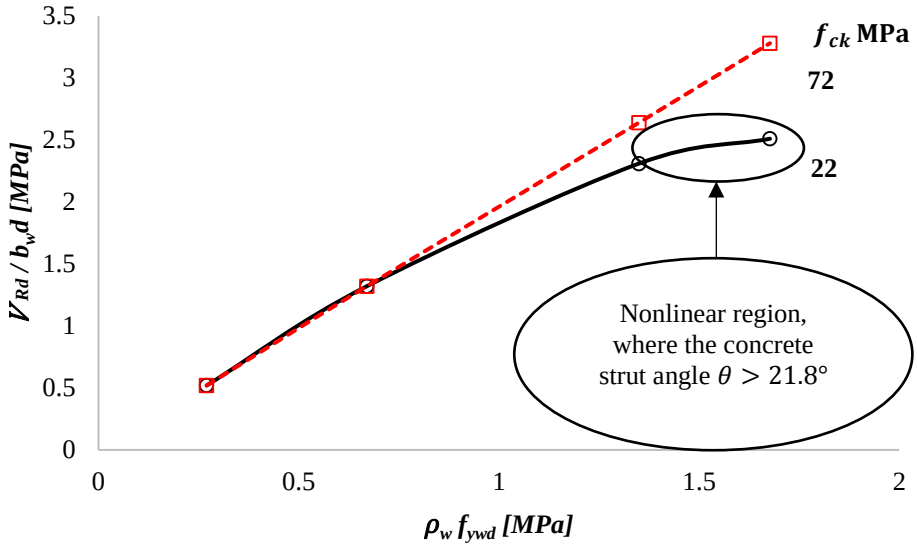

Figure 3.5. Comparison of EC2 VSIM design capacity at different f_{ck} for specific test sections.

3.3 Comparison of the shear design equations

The various shear design provisions discussed in the previous sections (SANS, Eurocode, AASHTO, CSA, ACI and Fib Model Code 2010 (III)) are compared by means of a specific example as shown in Figure 3.6 and 3.7. Test cases with $b_w = 200 \,\&\, 400$, $d = 350 \,\&\, 600$, $a/d = 2.5$ and $\rho_l = 4\%$ were chosen for the example. The test cases were varied at parametric variations of design shear reinforcement quantity $\rho_w f_{ywd}$, characteristic concrete strength f_{ck} and beam depth d. Safety factors were included for calculating the shear resistance according to the codes. AASHTO and ACI applies an overall resistance factor of 0.9 and 0.75 respectively. SANS apply a partial material factor for concrete of 1.4 and 1.15 for steel; Eurocode and Fib Model Code (III) apply a partial material factor of 1.5 for concrete and 1.15 for steel.

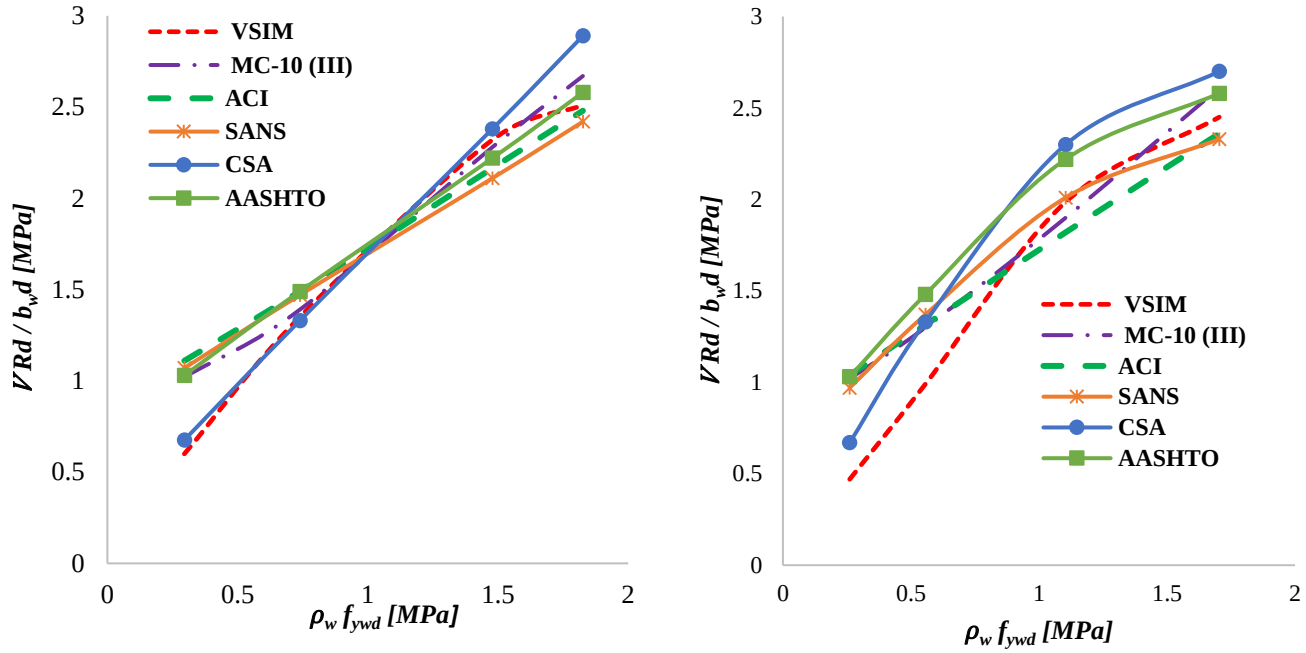

a) $d = 350\ mm$ b) $d = 600\ mm$

Figure 3.6. Comparison of SANS, Eurocode, AASHTO, CSA, ACI and Fib Model Code 2010 (III) design capacities at variations of $\rho_w f_{ywd}$ for $f_{ck} = 22\ MPa$.

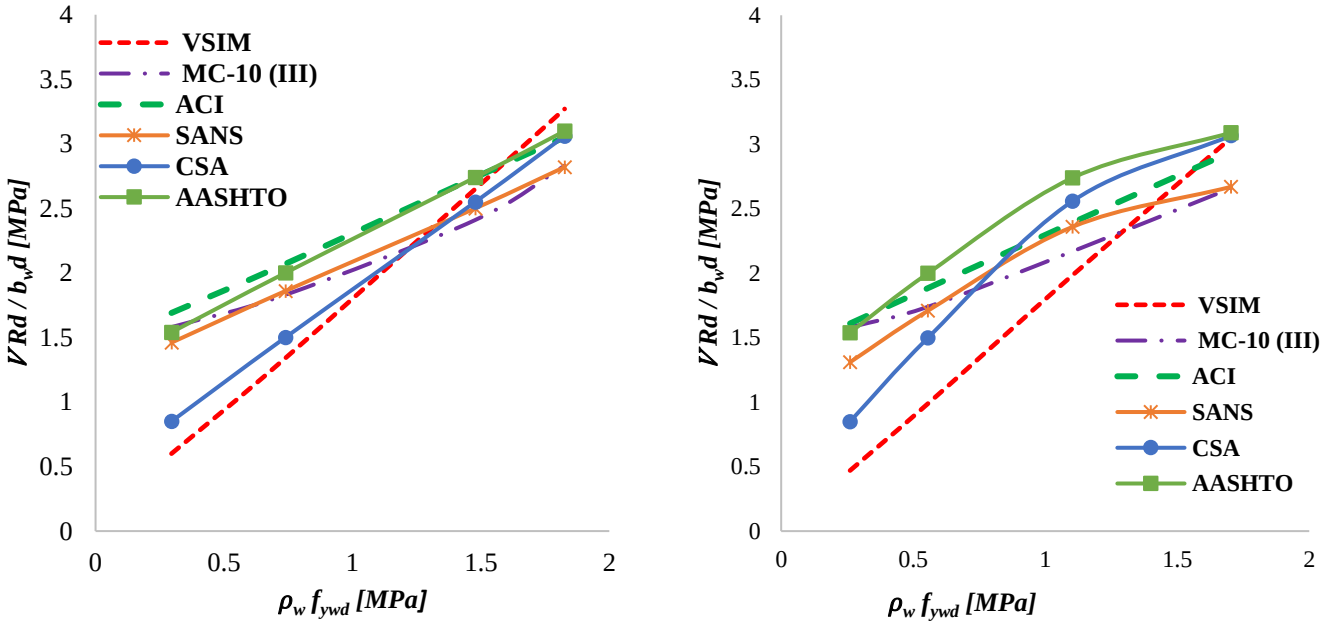

c) $d = 350\ mm$ d) $d = 600\ mm$

Figure 3.7. Comparison of SANS, Eurocode, AASHTO, CSA, ACI and Fib Model Code 2010 (III) design capacities at variations of $\rho_w f_{ywd}$ for $f_{ck} = 72\ MPa$.

The following general observations can be made from Figures 3.6 and 3.7:

- The behaviour of all the design codes are comparable in trend, albeit with substantial variation among them.
- The design values of the different formulations compare well, except at low levels of shear reinforcement where Eurocode and CSA are noticeably more conservative than the other design codes.

3.4 Summary and conclusions

This chapter has provided an overview of some of the recent shear design provisions of beams with shear reinforcement in well-established codes of practice. The SANS, Eurocode, AASHTO, CSA, ACI and Fib Model Code 2010 (III) design codes all take different approaches to shear design of reinforced concrete beams. The SANS and ACI are based on the 45° truss model with the inclusion of a concrete contribution term developed empirically. ACI 318 does not allow the use of a concrete compressive strength f_c' exceeding 69 MPa. The AASHTO LRFD and CSA shear design provisions are developed based on the MCFT. Eurocode 2 use the Variable Strut Inclination Method, a modification of the 45° truss model without concrete contribution. Fib Model code 2010 is derived from MCFT and the Generalised Stress Field Approach. AASHTO and ACI applies an overall resistance factor of 0.9 and 0.75 respectively. SANS apply a partial material factor for concrete of 1.4 and 1.15 for steel; Eurocode and Fib Model Code (III) apply a partial material factor for concrete of 1.5 and 1.15 for steel.

The design values of the different formulations compare well, except for Eurocode and CSA at low levels of shear reinforcement. The VSIM for stirrup design used in Eurocode 2 predicts a relatively high shear capacity for heavily shear reinforced concrete beams and a very low capacity for lightly shear reinforced concrete beams (Cladera & Mari, 2007). The underestimation of shear capacity at low stirrup quantities is ascribed to the neglect of concrete contribution to shear strength which is more significant in lightly shear reinforced beams and the limit on the concrete strut angle. The performance of EC2 VSIM to a certain degree depends on the limits governing the concrete compressive strut angle (θ). Investigations in this study revealed that the unbiased and unconstrained analytical formulation of VSIM (i.e. without the concrete strut angle θ limitation) naturally predicts lower than the 21.8^0 lower limit recommended by Eurocode 2. The lower limit of 21.8^0 as stated in the operational EC2 VSIM shear design function is a form of bias enforced to achieve a more

conservative estimate of shear predictions. The influence is more pronounced at lower levels of shear reinforcement.

As a result of the concrete strut angle limit enforced on EC2 VSIM capacity predictions, the influence of concrete strength on its capacity predictions is only witnessed in cases where there is combination of low concrete strength and high amount of shear reinforcement (Mensah, 2015). Considering the present state of EC2 VSIM especially the trend with shear reinforcement and the influence of concrete strength, there is need to critically assess its mean and design values parametrically against other established alternative shear approaches and experimental results. This deterministic assessment is presented in the next chapter.

Chapter 4

Deterministic comparison of selected design procedures

4.1 Introduction

The inconsistent trend of the unbiased EC2 VSIM shear resistance predictions ($V_{VSIM-L\theta}$) discussed in Chapter 1 motivated the assessment of the shear model against alternative widely used approaches and experimental results. The comparison of VSIM and the alternative shear approaches to experimental observations would provide a general overview of the performance of their unbiased capacity predictions and provide a solid basis to assess their accuracy. A good shear strength model is expected to reflect the trends depicted by the database of experimental results (Viljoen *et al*, 2018). In this context, this chapter presents a comparison of the EC2 VSIM mean and design value predictions to other alternative approaches (such as ACI 318 (2011) shear model, Fib Model Code 2010 (MC-10 (III)) shear model, best-estimate prediction by Modified Compression Field Theory (MCFT) based analysis program Response 2000 (R2k) and Compression Chord Capacity model (CCC) (Cladera *et al*., 2016)) and experimental results.

Additionally, the mean and design value analysis will be conducted using specific test sections across parametric ranges of shear reinforcement, concrete strength and beam depth. Hence, the objective of this chapter is summarised as follows:

1) To compare the trend of EC2 mean value predictions to alternative approaches and experimental observations over the parametric range of shear reinforcement, concrete strength and beam depth.
2) To compare the trend of EC2 design value predictions to other widely used design approaches at varying amounts of shear reinforcement, concrete strength and beam depth.

The assessment presented here is a rework of the investigation conducted by Viljoen *et al*. (2018) using a different database (database of beam experiments developed by Reineck *et al*. (2014)) and introducing additional shear approaches.

4.2 Mean value analysis

The mean value function for each shear method is obtained by, where applicable, expressing f_{ck}, f_c' and f_{wk} at their mean values f_{cm} (4.1) and f_{ywm} (4.2), respectively and removing all explicit partial safety factors (γ_c and γ_s) from the original formulation.

Eurocode 2 and Fib Model Code 2010 recommend the relationship presented in Equation 4.1 for obtaining the mean value for concrete strength. f_{ck} is the characteristic cylinder strength and a 5% fractile value.

$$f_{cm} = f_{ck} + 8 \text{ MPa} \tag{4.1}$$

Holicky (2009) reports the following relationship presented in Equation 4.2 for obtaining the mean value for steel yield strength.

$$f_{ywm} = f_{ywk} + 2\sigma_{fyw} \tag{4.2}$$

where $\sigma_{fywm} = 0.1 f_{yw}$ is the standard deviation of steel yield strength as observed from standard European steel production practice. The process of the EC2 mean value assessment is illustrated in Figure 4.1.

.

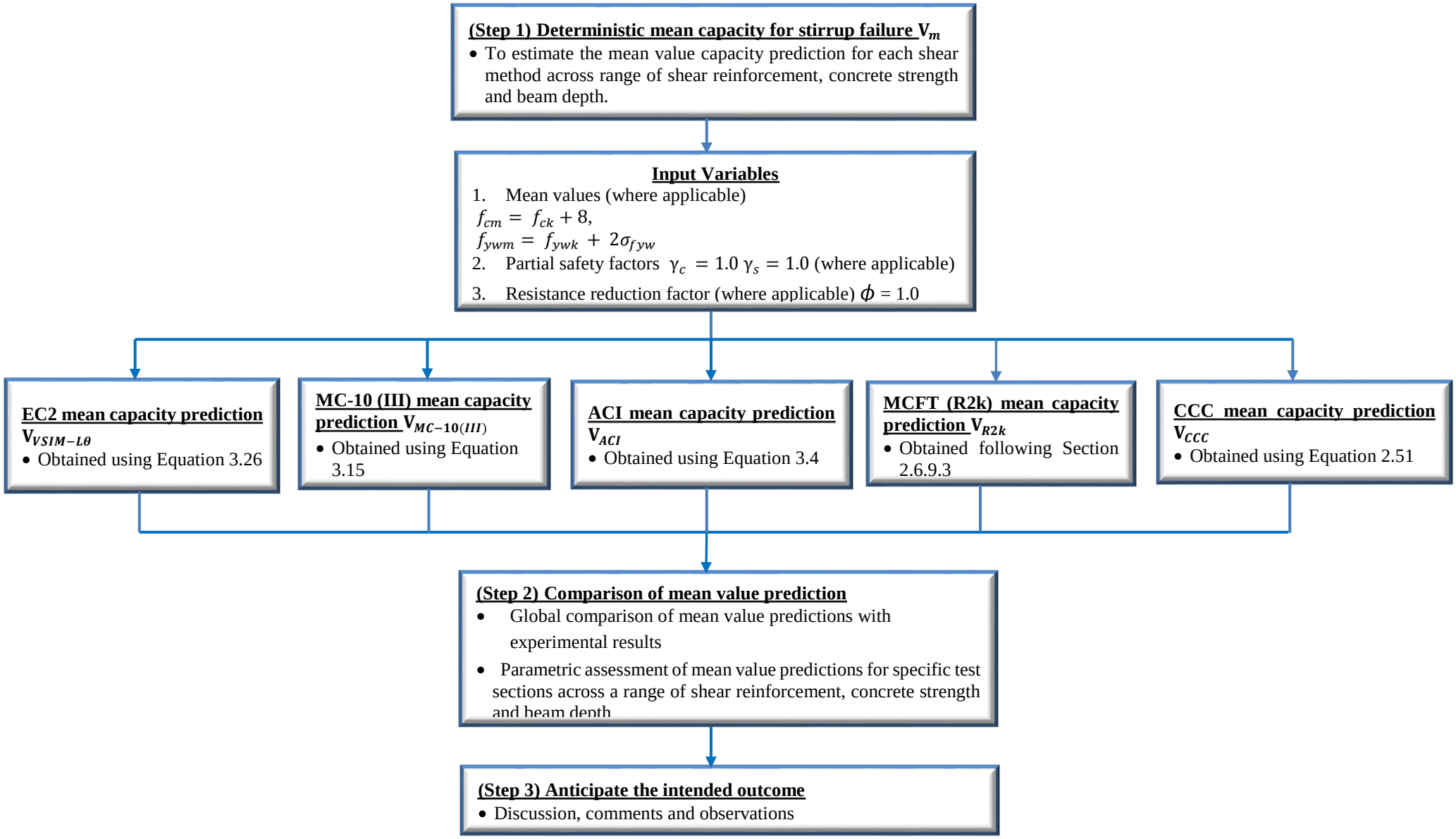

Figure 4.1. The step by step process for EC2 mean value analysis

4.3 Design value analysis

Codes of practice, for example Eurocode 2, uses the concept of the semi-probabilistic method. In this method, random variables such as the strength of the materials are treated as deterministic values after obtaining their design values from characteristic values. The transformation of a characteristic value of a random variable into a design value is performed by multiplying or dividing it by a partial factor related to this variable. The estimation of design values for shear resistance models are based on characteristic values of material properties (f_{ck}, $f_c{}'$ and f_{wk}) and partial safety factors for concrete γ_c and steel γ_s. The use of characteristic values for material properties and partial factors of safety introduces safety bias into the design formulation. The safety bias for the other basic variables such as the geometries and steel areas are conventionally assumed as 1.0. The safety bias reduces the unbiased or best estimate resistance (mean value) prediction of the model under investigation. ACI 318 does not use partial factors but resistance reduction factor (Load and Resistance Factor Design LRFD format).

The design shear resistance (V_{Rd}) of a reinforced concrete member with shear reinforcement is described as the sum of the concrete ($V_{Rd,c}$) and shear reinforcement contributions ($V_{Rd,s}$).

$$V_{Rd} = V_{Rd,c} + V_{Rd,s} \leq V_{Rd,max} \tag{4.3}$$

It is considered that the shear strength V_{Rd} in Equation 4.3 above must be lower than the shear force that produces failure in the concrete struts ($V_{Rd,\max}$). $V_{Rd,max}$ represents a check aimed at preventing the occurrence of another failure mode, namely concrete strut failure. This type of failure usually occurs with shear cracking in the web. $V_{Rd,max}$ assumes different expressions in EC2, MC-10 (III) and ACI. This was enforced and used as checks to ensure that the design inequality of $V_{Rd,s} \leq V_{Rd,max}$ was satisfied for all the test sections considered in this investigation. The contributions $V_{Rd,c}$, $V_{Rd,s}$ and $V_{Rd,max}$ according to the model in Eurocode 2, ACI 318 and Fib Model Code 2010 Level of Approximation III (LoA III) are reported earlier in Chapter 3. Figure 4.2 presents the step-by-step process for EC2 design value analysis.

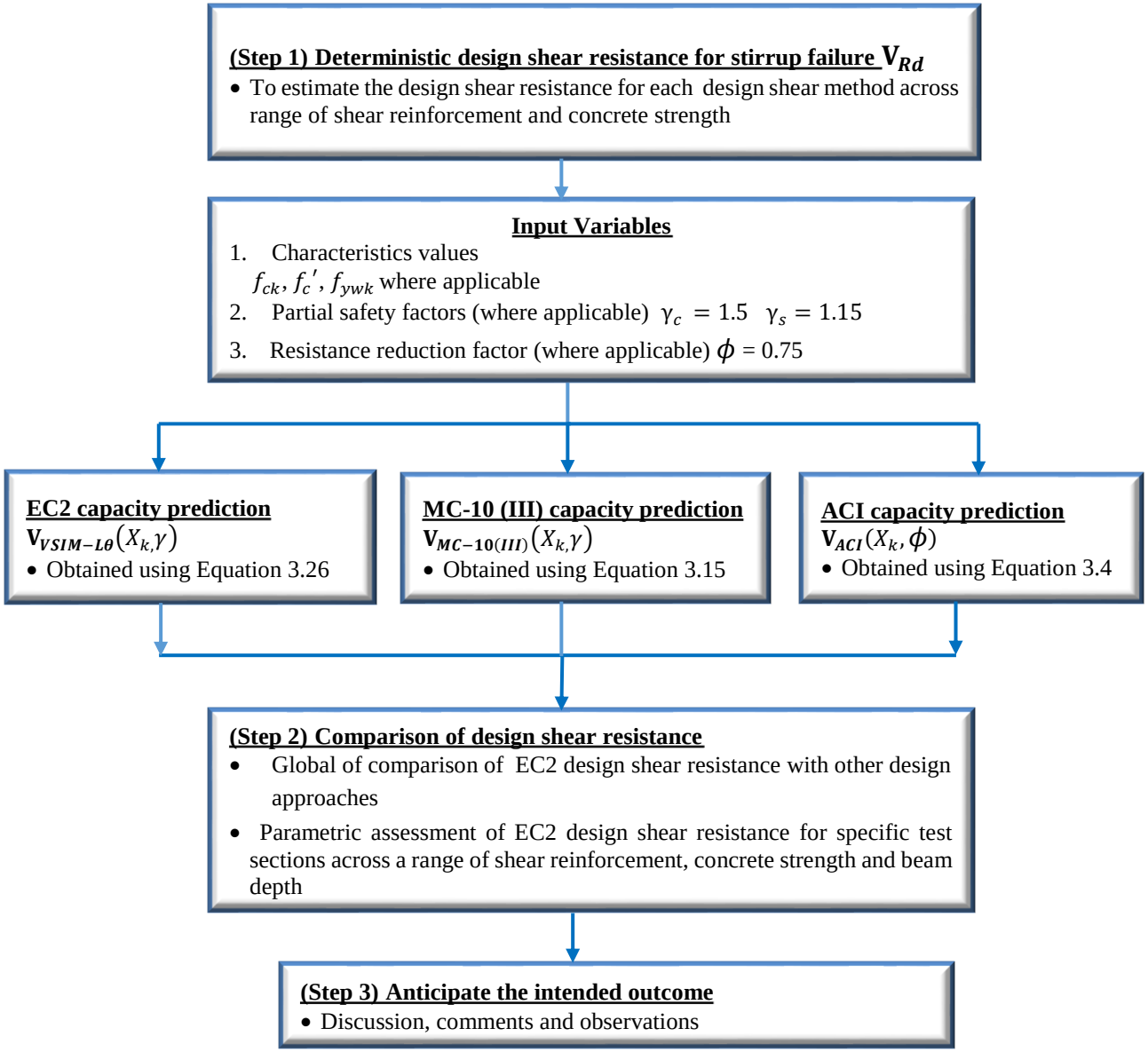

Figure 4.2. The step by step process for the EC2 design value analysis

4.4 Global comparison

4.4.1 Comparison of shear mean value predictions to experimental observation.

The plot of normalised experimental observations ($^{V_{exp}}/_{b_w\, d}$) (from the database of beam experiments developed by Reineck *et al*. (2014)) with the amount of shear reinforcement $\rho_w f_{ywm}$, for concrete strength in the range of $13.4 \leq f_{cm} < 125$ MPa is presented in Figures 4.3 and 4.4. As shown in the figures, the trend line of experimental observations is compared to the trend lines of normalised mean shear capacity ($^{V_m}/_{b_w\, d}$) predictions offered by (1) EN 1992-1-1 ($^{V_{VSIM-L\theta}}/_{b_w\, d}$), (2) MCFT (R2k) ($^{V_{R2k}}/_{b_w\, d}$), (3) Compression Chord Capacity model ($^{V_{CCC}}/_{b_w\, d}$), (4) Model Code 10 (III) ($^{V_{MC-10(III)}}/_{b_w\, d}$) and (5) ACI-318 ($^{V_{ACI}}/_{b_w\, d}$). MCFT (R2k) requires the specification of additional input parameters to predict shear resistance as compared to other procedures. Corresponding MCFT (R2k) shear capacity predictions were made for each experimental beam section for which adequate information was available to enable its prediction.

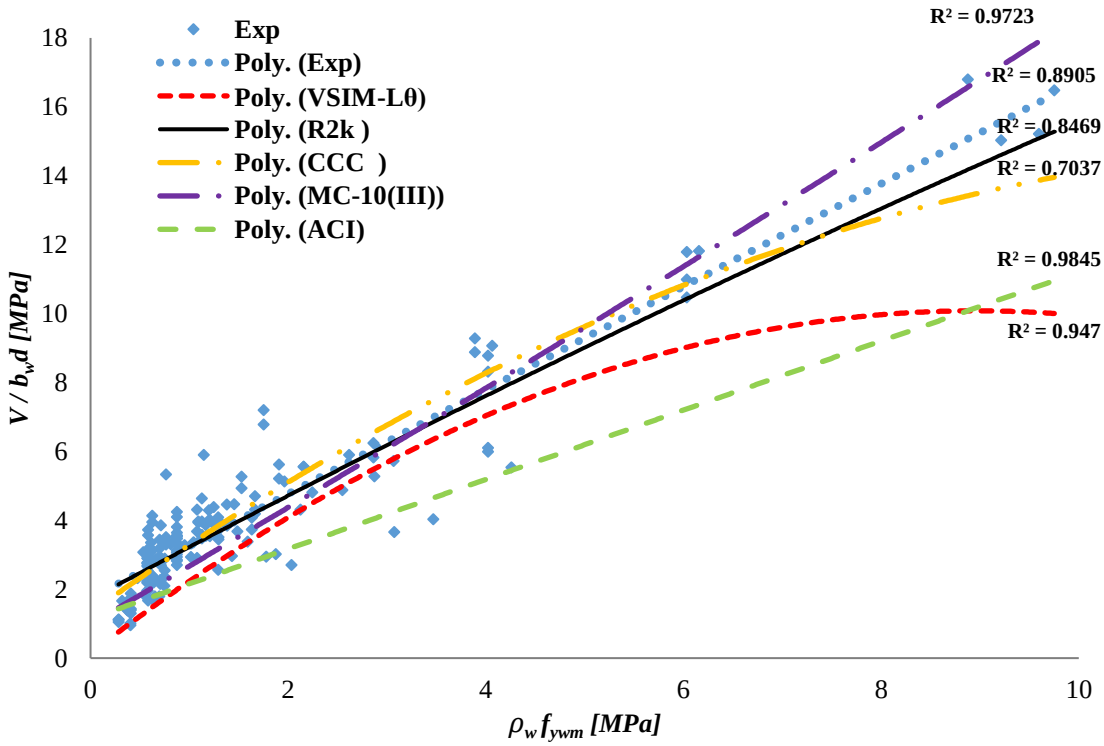

Figure 4.3. Comparison of normalised mean shear capacity to experimental observations

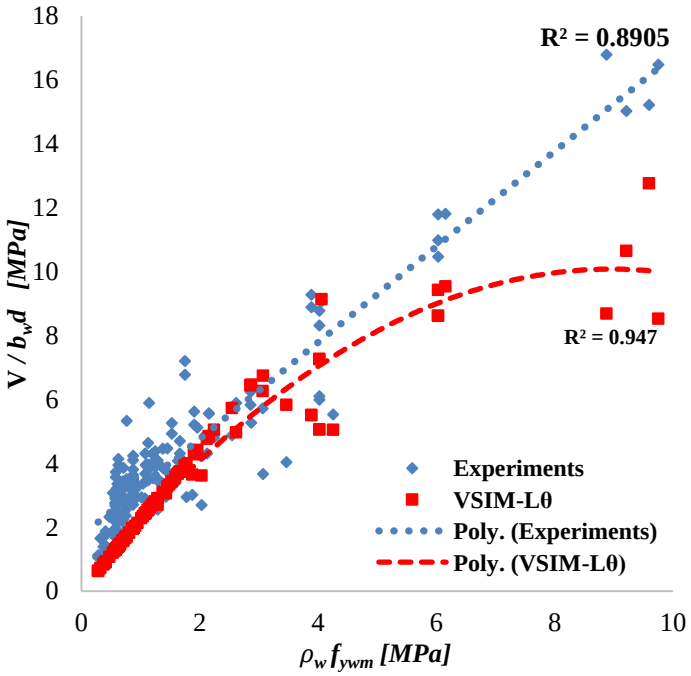

a) $V_{VSIM-L\theta}$ versus V_{exp}

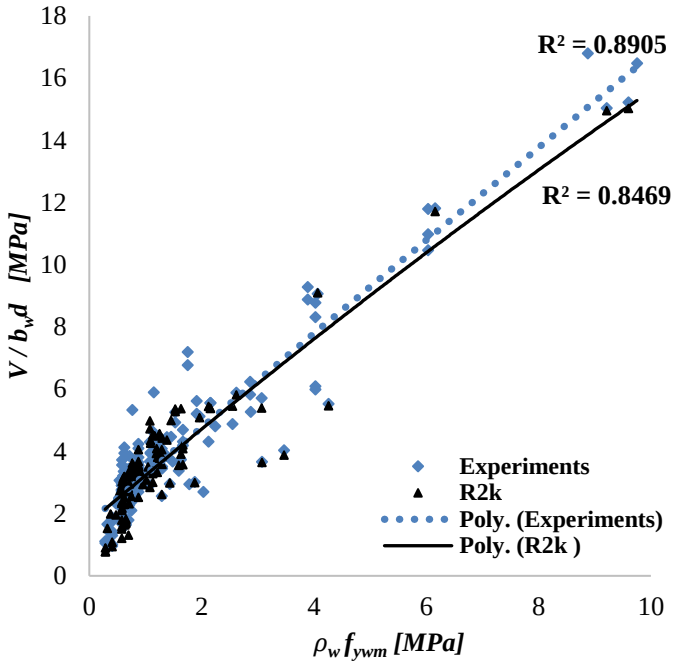

b) V_{R2k} versus V_{exp}

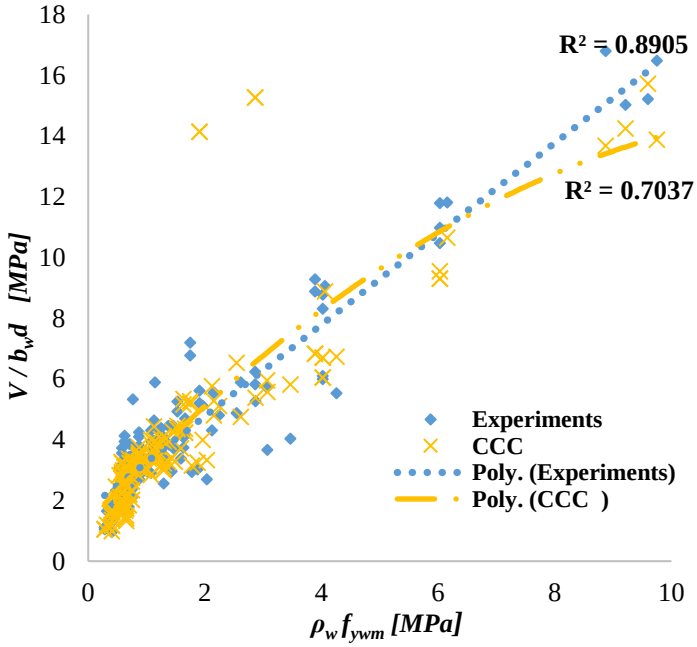

c) V_{CCC} versus V_{exp}

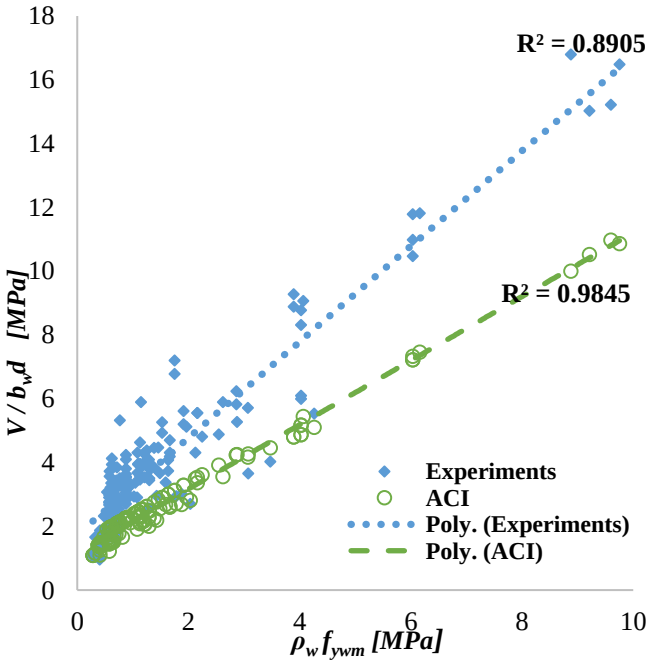

d) V_{ACI} versus V_{exp}

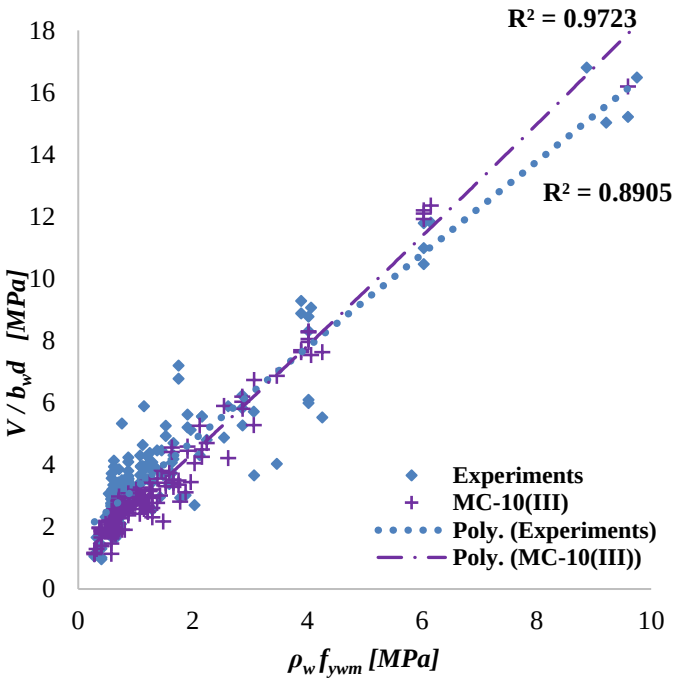

e) $V_{MC-10(III)}$ versus V_{exp}

Figure 4.4. Data points of predicted capacity for each of the prediction models together with its trend line.

The following observations were drawn from Figures 4.3 and 4.4:

- An increasing trend of normalised experimental observations ($V_{exp}/b_w d$) as $\rho_w f_{ywm}$ increases was observed.
- The trend lines of MCFT (R2k) and CCC predictions bear the closest comparison to that of the experimental observations for the range of shear reinforcement $\rho_w f_{ywm}$ considered. MC-10 (III) model provides a closer comparison to the more accurate MCFT (R2k) and CCC models.
- VSIM ($V_{VSIM-L\theta}$) and ACI (V_{ACI}) shear methods provided lower capacity predictions over the parametric range compared to other shear methods.
- The trend line of $V_{VSIM-L\theta}$ fails to capture the trend of experimental observations at higher levels of shear reinforcement $\rho_w f_{ywm}$, portraying a relatively reducing contribution of additional stirrup reinforcement. This trend of results for the VSIM model agrees with the observation reported in Figure 3.5 (Section 3.2.6).

4.4.2 Comparison of shear design value predictions to experimental observation

The comparison of the design value predictions by the various established design approaches for design ranges of shear reinforcement $\rho_w f_{ywd}$ investigated is presented in Figure 4.5(a & b). EC2 VSIM, ACI 318 and MC-10 (III) resistance were made corresponding to each experimental observation. Note that MCFT (R2k) and CCC capacity predictions are not considered in the design value analysis since they only provide best-estimate predictions.

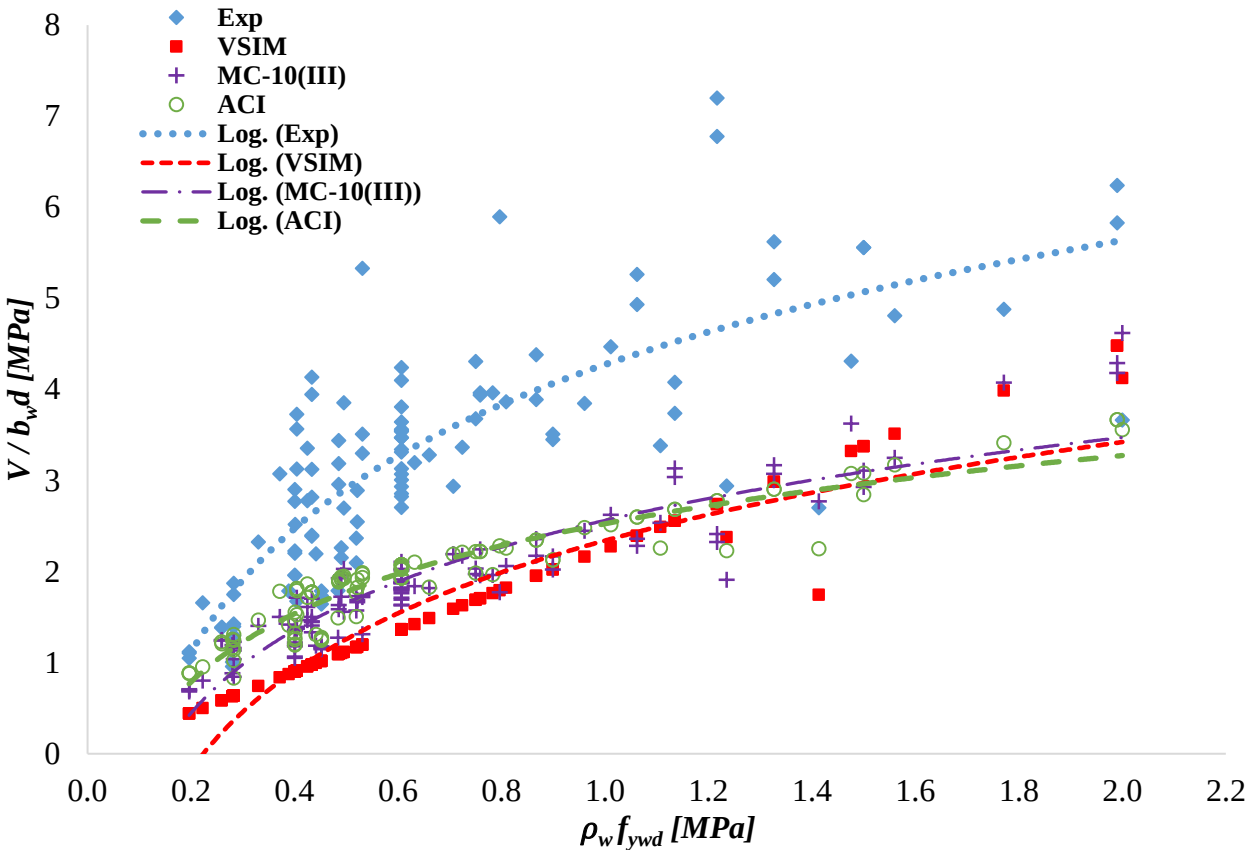

Figure 4.5(a). Comparison of normalised design value predictions to experimental observations (rectangular beams only).

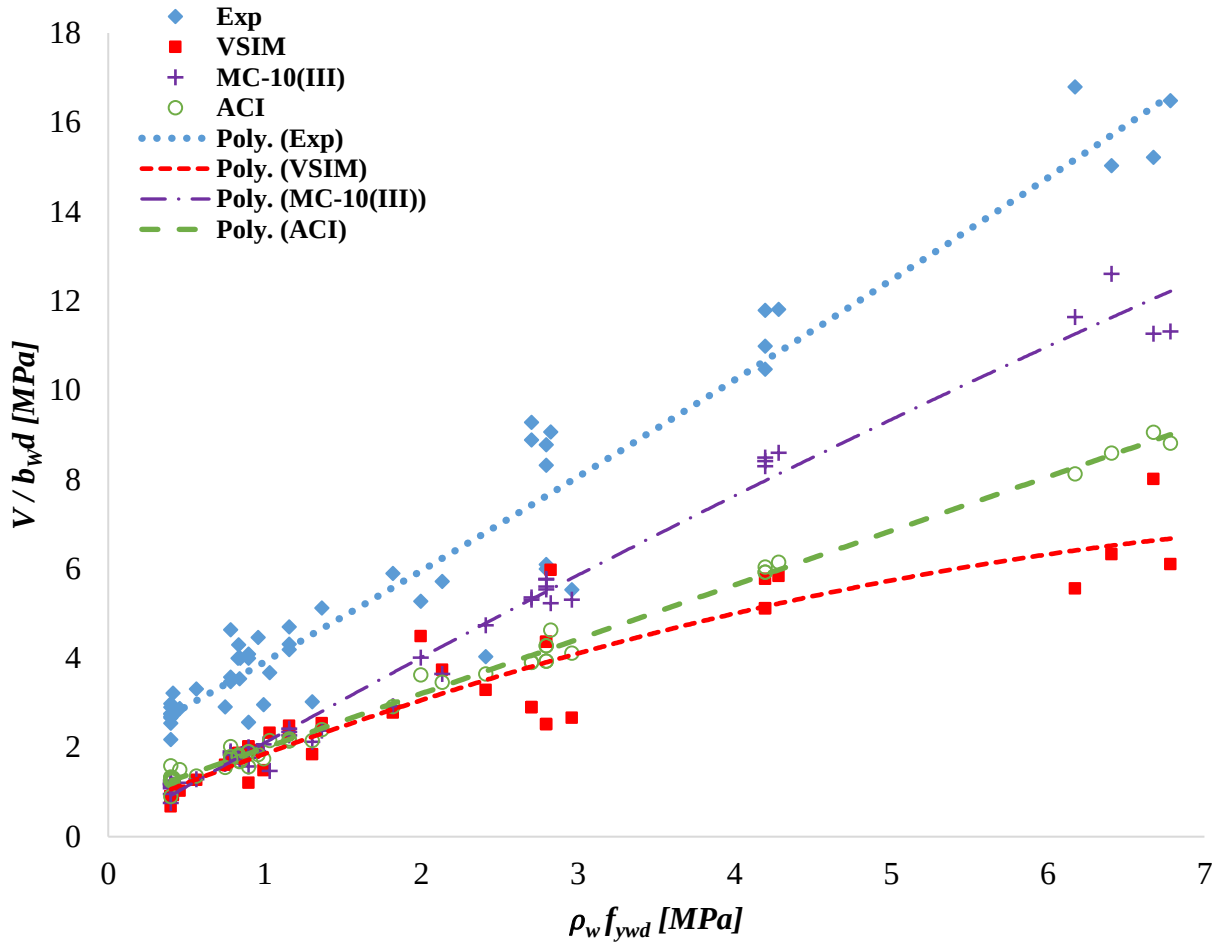

Figure 4.5(b). Comparison of normalised design value predictions to experimental observations (flanged beams only).

Close examination of the figures revealed the following:

- The trend line of EC2 design capacity is the most conservative when compared to alternative shear design provisions.
- At shear reinforcement $\rho_w f_{ywd} > 1\ MPa$ (Figure 4.5(a)), there is wider scatter of experimental observations. For a specific rectangular beam with $\rho_w f_{ywd} = 2.0\ MPa$ (from the experimental database), the observed experimental capacity is less than the corresponding EC2 and MC-10 (III) design value predictions.
- It is also worth mentioning that MC-10 (III) design approach is the least conservative out of all the design codes considered at high levels of stirrup reinforcement.

4.5 Parametric assessment of EC2 VSIM predictions

Parametric analysis of specific test sections was used to evaluate EC2 mean and design values at practical ranges of shear reinforcement, concrete strength and beam depth.

4.5.1 Parametric assessment of VSIM mean value predictions

The normalised mean value predictions ($^{V_m}/_{b_w\, d}$) provided by the different best estimate procedures versus the amount of shear reinforcement $\rho_w f_{ywm}$ are shown in Figure 4.6 and 4.7 for low concrete strength ($f_{cm} = 30$ MPa) and high concrete strength ($f_{cm} = 80$ MPa) respectively. The test sections have the following properties: $b_w = 150\ and\ 400\ mm$, $d = 350\ and\ 600\ mm$, $a/d = 2.5$, $p_l = 4\%$. Selected series of experimental tests in the region of low ($24 \leq f_{cm} < 35$ MPa) and high concrete strength ($70 \leq f_{cm} < 87$ MPa) from the experimental database were added for interest's sake. The selected series of experimental tests have a wide range of different dimensions and cannot be directly compared to the capacity predictions from the specific test sections. According to the observations from other researchers (Mensah, 2015; Bentz, 2010; Metwally, 2012; Bentz *et al.*, 2006), later confirmed in Figure 4.3, the MCFT (R2k) trend line bears the closest comparison to that of the experimental observations out of the shear methods investigated. Hence, in this analysis, MCFT (R2k) observations were assumed to best reflect the shear behaviour for the specific test sections considered.

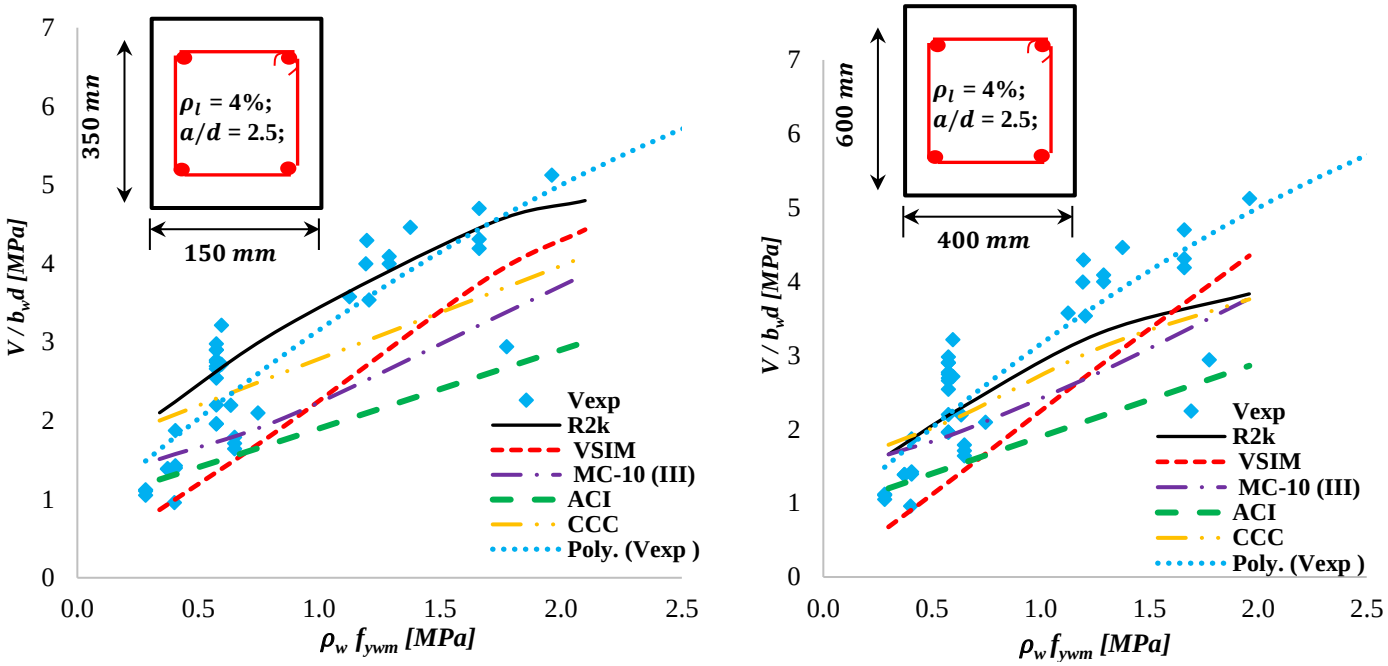

a) $d = 350mm$ b) $d = 600mm$

Figure 4.6. Normalised mean predictions of shear capacity versus the amount of shear reinforcement $\rho_w f_{ywm}$ for $f_{cm} = 30$ MPa

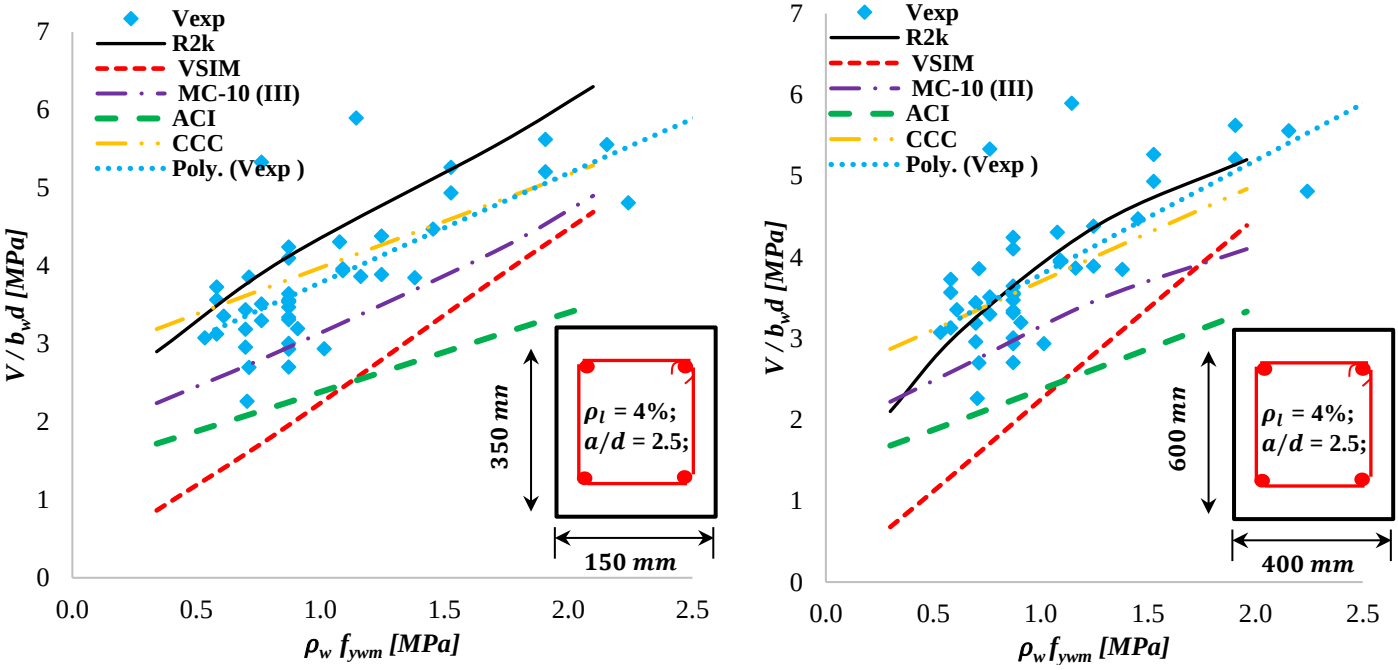

a) $d = 350mm$ b) $d = 600mm$

Figure 4.7. Normalised mean predictions of shear capacity versus the amount of shear reinforcement $\rho_w f_{ywm}$ for $f_{cm} = 80$ MPa

Scrutiny of Figures 4.6 and 4.7 leads to the following observations:

- VSIM predicts consistently more conservative values at low levels of shear reinforcement than other shear methods.
- CCC model predictions offer the best estimation of MCFT (R2k) predictions. However, CCC predictions differ substantially from MCFT (R2k) predictions for small beams (Figure 4.6(a) & Figure 4.7(a)).
- CCC predictions exceeded those of MCFT (R2k) at a very low amount of shear reinforcement
- At high levels of shear reinforcement, ACI predictions are consistently more conservative than other shear methods.

All the models considered diverge from the MCFT (R2k) predictions as shown in Figure 4.6 and 4.7. It can be observed that the shear strength prediction from the different shear models differs widely. The fundamental difference between the different shear methods is that they have been derived from different theories, analogies and assumptions, emphasising the contribution of different shear transfer mechanisms and governing parameters (Mari *et al*., 2015). The shear contributors considered in Compression Chord Capacity model includes the uncracked compression chord V_c, the dowel action of the longitudinal reinforcement V_l, the shear reinforcement V_s and the shear across web crack V_w (Figure 4.8a). Fib Model code 2010 is derived from MCFT and the Generalised Stress Field Approach. The assumed shear contribution mechanism includes the aggregate interlock and the shear reinforcement V_s (Figure 4.8b). The shear contributor in EC2 VSIM is shown in Figure 4.8c. ACI 318 is derived based on the truss model accounting for the stirrup contribution with an empirically derived concrete contribution equation. Mari *et al*. (2015) further stated that various shear strength contributors act at different stages of loading. This illustrates the difficulty in predicting shear resistance of reinforced concrete beams reliably.

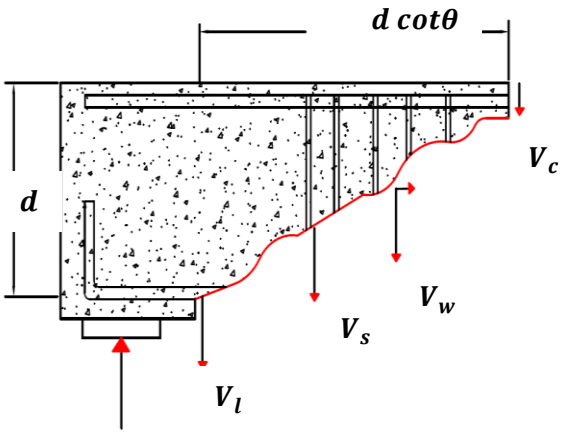

a) Compression Chord Capacity model

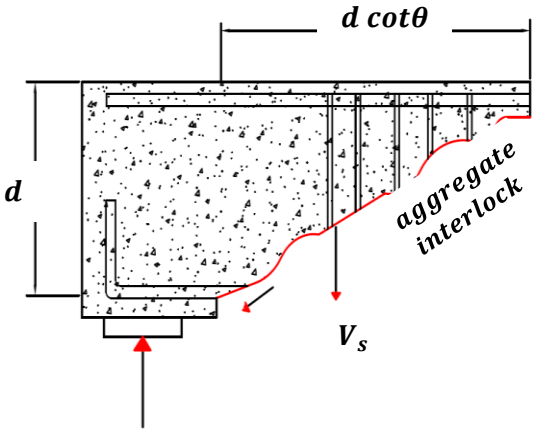

b) Fib Model code 2010

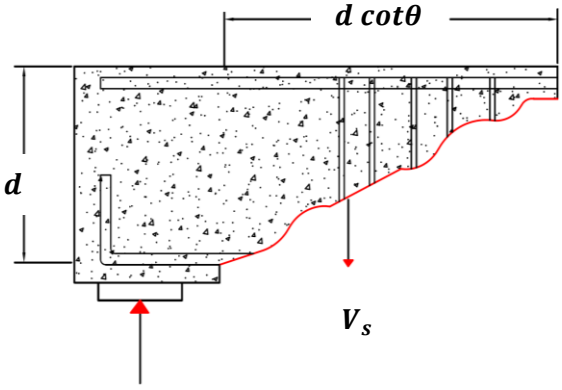

c) Variable angle truss model

V_c = Un-cracked compression chord

V_w = Shear across web crack

V_s = Shear by the stirrup

V_l = Dowel action

Figure 4.8. Shear contributing actions at failure

4.5.2 Parametric assessment of EC2 design value prediction

The normalised design value resistance predictions ($^{V_{Rd}}/_{b_w\, d}$) obtained from the different design approaches for the design range of stirrup reinforcement $\rho_w f_{ywd}$ and concrete strength f_{cd} considered are presented in Figures 4.9 and 4.10. Selected series of experimental observations are added for interest's sake. The experimental observations have a wide range of different dimensions and cannot be compared directly to design values. Note that MCFT (R2k) and CCC capacity predictions are not considered in the design value assessment since they are not design methods but rather best-estimate procedures. The test sections investigated have the following characteristics: $b_w = 150\ and\ 400\ mm$, $d = 350\ and\ 600\ mm$, $a/d = 2.5$, $\rho_l = 4\%$.

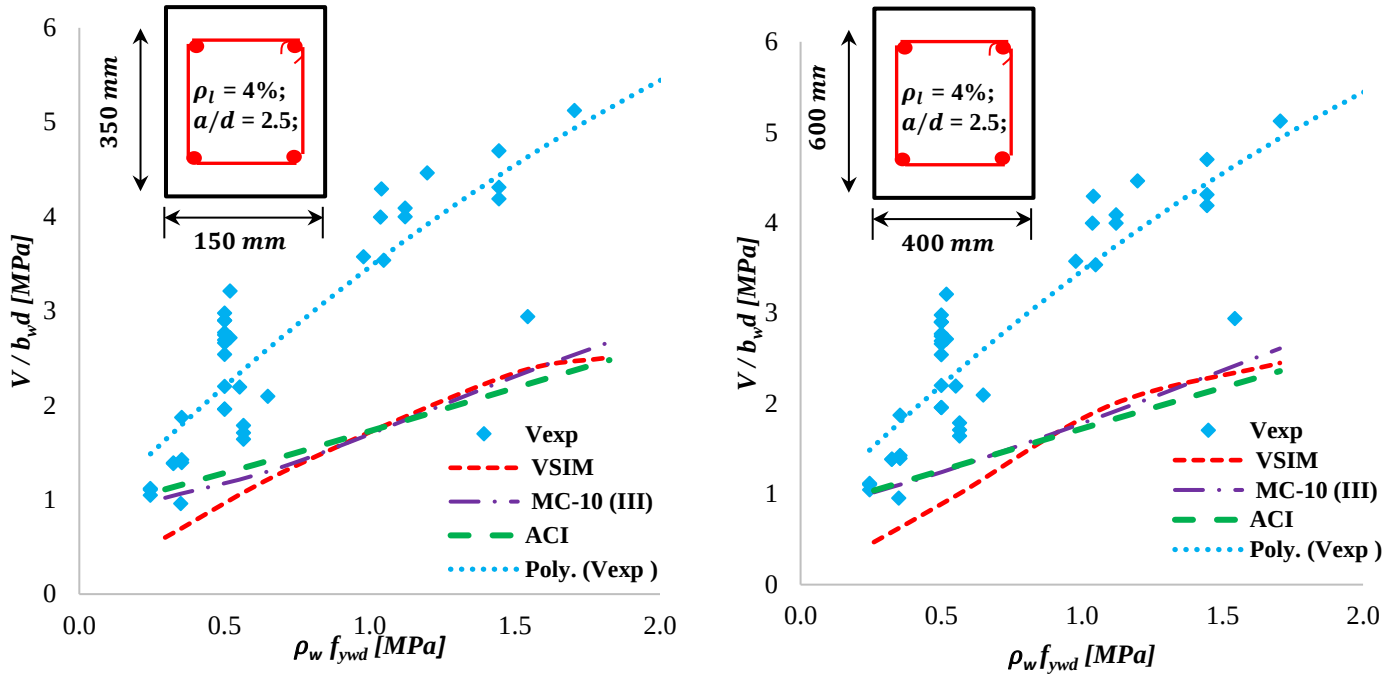

a) $d = 350mm$ b) $d = 600mm$

Figure 4.9. Normalised design value shear strength versus the amount of shear reinforcement $\rho_w f_{ywd}$ for $f_{ck} = 22$ MPa

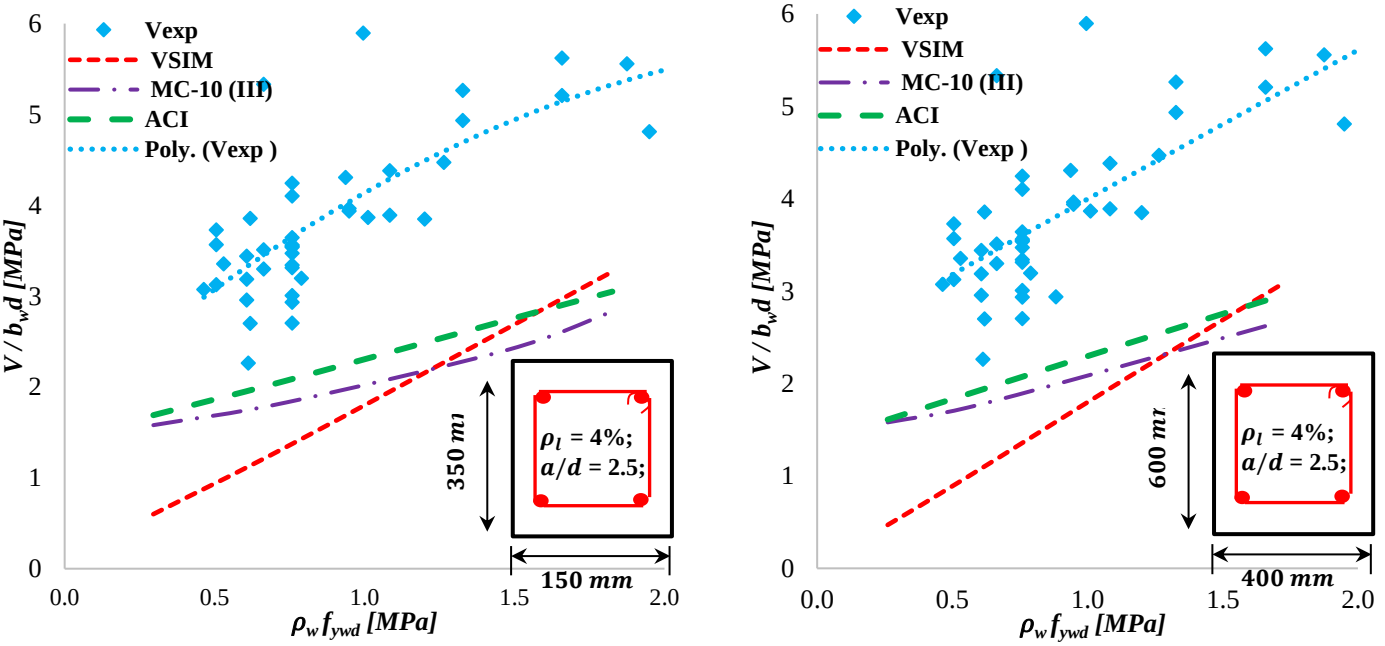

a) $d = 350mm$ b) $d = 600mm$

Figure 4.10. Normalised design value shear strength versus the amount of shear reinforcement $\rho_w f_{ywd}$ for $f_{ck} = 72$ MPa

Analysis of Figures 4.9 and 4.10 yielded the following observations:

- Generally, the design values of the different formulations compare well, except for VSIM at low levels of shear reinforcement.
- EC2 VSIM design method is the most conservative method at low levels of shear reinforcement ($\rho_w f_{ywd} < 1\ MPa$) for both low ($f_{ck} = 22$ MPa) and high ($f_{ck} = 72$ MPa) concrete strengths.

4.6 Conclusions

The assessment revealed that the mean value predictions of the different models differ considerably from one another. This reflects the difficulty of accurately and precisely predicting shear resistance in structural design. The capacity predictions from the different methods also differ from experimental observations. The extent of scatter of the various curves reveals the wide-spread uncertainty and problems associated with predicting shear resistance of beams. The uncertainty composed of the uncertainty inherent in the shear resistance model formulations and uncertainty in the prediction of the mean values of their basic variables such as concrete strength and steel yield strength

The mean value predictions of the EC2 VSIM was shown to significantly underpredict capacity for slightly shear-reinforced concrete beams. The shear method produced the most conservative mean value predictions out of all the methods investigated at $\rho_w f_{ywm} \leq 1\ MPa$. The design value analysis revealed that the design values of the various shear design methods compare well, except for EC2 VSIM at low levels of shear reinforcement ($\rho_w f_{ywd} \leq 1\ MPa$) where the design method significantly underestimates capacity for beams with both low and high concrete strengths. The trend of EC2 VSIM at low levels of stirrup reinforcement practically implies that the design method may be overly conservative at this region, and therefore uneconomic. This is an issue of concern.

Given the significant uncertainties present in shear strength predictions, reliability performance assessment and calibration of suitable partial factors for shear design procedures becomes essential. This will allow us to adequately account for the effects of these uncertainties and ensure safe and economical application of shear design procedures in practice.

Quantification of the model uncertainty and bias is an important first step, since these contribute significantly to reliability performance (Mensah, 2015). An effective reliability assessment of beams subjected to shear requires the use of a suitable general probability model for shear resistance, including provision for model uncertainty and bias that accounts for systematic differences between the model and experiment. This makes the choice of the prediction model and quantification of the model uncertainty and bias related to the model critical in assessing the reliability of the EC2 VSIM design formulation and any other shear design provision. The quantification of model uncertainty and bias for different shear strength models is presented in Chapter 6.

Chapter 5

Overview of reliability in design standards

5.1 Introduction

The objective of structural reliability investigation is to measure the probability of failure of a structure by considering the uncertainties related to the resistances and loads. Uncertainties arise owing to the lack of knowledge of the model formulation, inherent physical uncertainties, inadequate data, input parameters such as load characteristics and material properties. This chapter presents an overview of the main theoretical and practical background of structural reliability analysis and its implementation in structural design standards.

5.2 Structural reliability

Structural reliability analysis is used to assess and improve existing structural models. Holický (2009) stated that structural reliability is developed for the evaluation of the demand that the load, E is lower than the structural resistance R. This is presented in Equation 5.1.

$$E < R \tag{5.1}$$

Equation 5.1 depicts a safe or satisfactory state of the structural mechanism. A failure state occurs when the condition stated in Equation 5.1 is not satisfied. The reliability performance of any mode of failure mechanism such as shear failure in reinforced concrete beams is derived by subtracting the expected values of the applied loads from that of the resistance. The performance function $g(\mathrm{X})$ is expressed as Equation 5.2 (Holicky, 2009).

$$g(\mathrm{X}) = R(X) - E(X) \tag{5.2}$$

where E is the load effect

R is the resistance

X is a vector of basic random variables on which the resistance and loads depend.

$g(\mathrm{X})$ represents the performance function

The performance function defines three different regions (1) the limit state $g(\mathrm{X}) = 0$; (2) the safe region $g(\mathrm{X}) > 0$ and (3) the failure region $g(\mathrm{X}) < 0$. The limit state function (LSF) can be in the form of a nonlinear or a linear function of the basic variables. The probability of failure (P_f) (i.e., the probability of $g(\mathrm{X}) < 0$, shown in Figure 5.1) can be calculated mathematically using Equation 5.3. An alternative measure of the reliability of a structure is the reliability index β, which can be described as the number of standard deviations σ_{R-E}, that the safety margin is situated from the failure point (Figure 5.1). The relationship between P_f and β is defined as Equation 5.4.

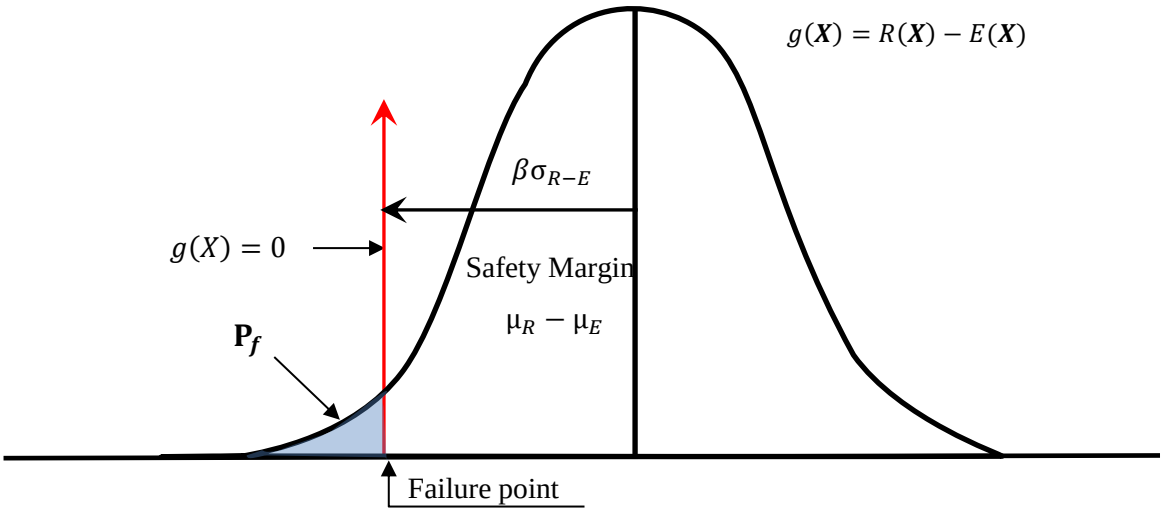

Figure 5.1 Representation of the limit state function

$$\mathrm{P}_f = P(g(\mathrm{X}) < 0) = \int_{g(X)\leq 0} f_x(X)\ dx \tag{5.3}$$

$$\mathrm{P}_f = \Phi(-\beta) \tag{5.4}$$

where $f_x(X)$ is the joint probability distribution function of the n-dimensional vector X.

Φ is the cumulative distribution function of the standardised normal distribution.

The reliability index β should be higher than the target reliability β_T (Equation 5.5) i.e. its failure probability P_f should be lower than the target failure probability $P_{f,T}$ (Equation 5.6).

$$\beta > \beta_T \tag{5.5}$$

$$P_f < P_{f,T} \tag{5.6}$$

Several reliability computational methods can be used to evaluate the probability of failure or the reliability index, some of which include the First Order Reliability Method (FORM), Advanced Second Moment (ASM) method, asymptotic Laplace expansions and computer-based Monte Carlo simulation.

The FORM was developed about 30 years ago. Today, the method is widely used and is regarded as one of the efficient approaches for the assessment of reliability index. A variety of commercial computer programs implementing the FORM are extensively used in the engineering industry for easy estimation of the nominal probability level of failure (P_f). Other reliability parameters like the direction cosine (α_{xi}) of the basic random variables can be assessed to establish the basic variable that mainly contributed to the reliability of the structural performance. The direction cosine of the i^{th} basic variable is expressed in Equation 5.7.

$$\alpha_{x_i} = (\partial g(X)/\partial X_i)/\left[\sum_i (\partial g(X)/\partial X_i)^2\right]^{1/2} \tag{5.7}$$

The direction cosines reflect the significance of each basic variable. It can be stated that as the value of the direction cosine increases, the effect of the basic variable on structural reliability performance also increases (Holicky, 2009). FORM uses only the mean value (μ_x) and the standard deviation value (σ_x) of the normal distribution of basic variables in its analysis. Non-normal distributions are transformed into normal distributions at specific points of assessment of the performance. The FORM algorithm finds the most likely failure point (design point) in this normalised design space as the point closest to the mean of the transformed variables (Holicky, 2013). The probability of failure is linearly approximated at this point. Iteration continues until the point of assessment converges to the design point. A graphical representation of FORM is illustrated in Figure 5.2. The FORM algorithm described in Holicky (2009) was used in this study.

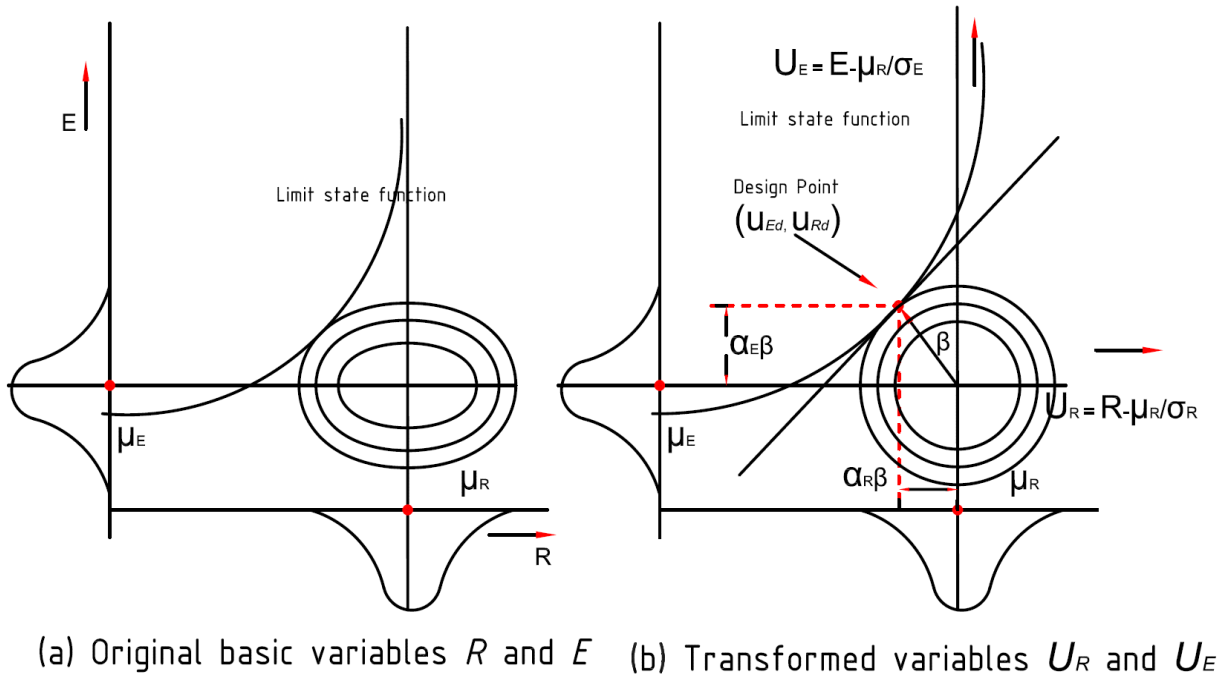

Figure 5.2. Graphical representation of FORM (Source: Holicky (2009)).

5.3 Uncertainty modelling

Models are means by which we represent and express our understanding of reality. Since it is practically impossible to understand and represent reality in its absolute intricacy, models are a partial representation of reality resulting in a state of uncertainty (Droguett & Mosheh, 2008). In using a model for prediction purposes, there are two different kinds of uncertainties involved, namely aleatory and epistemic uncertainties (Gardoni *et al*., 2002). Aleatory uncertainties emerge due to inherent variability in a physical process. They are random uncertainties that can only be controlled through efficient design practices. The epistemic uncertainties are systematic uncertainties that emerge from inadequate information and understanding of the model formulation, conservative assumptions and approximations (Droguett & Mosheh, 2008, Holicky *et al*., 2015).

Epistemic uncertainties can be estimated and calibrated to incorporate adequate conservatism into design procedure. Model uncertainty can be described as epistemic taking into account the effects forsaken in the model's formulations and simplifications of the mathematical relations (JCSS, 2001). Faber & Sorensen (2002) classified epistemic uncertainties as model uncertainty, statistical uncertainty and physical uncertainty. According to them, the physical uncertainties are uncertainties related to the modelling of loading, geometry and the material parameters.The statistical uncertainties

arise as a result of insufficient statistical data. The model uncertainty is described as the uncertainty related to the idealised mathematical formulation used to approximate the actual performance of the structure. The modern methods of structural reliability and risk analysis are used to estimate these uncertainties to meet acceptable and required levels of safety (Melchers, 1990). For several common cases model uncertainties for both load and resistance models are recommended by the Probabilistic Model Code (JCSS 2001) and are summarised in Table 5.1.

Table 5.1. Recommended probabilistic models for model uncertainties (JCSS, 2001)

Model type	Distribution	Mean	C.O.V
Load effect calculation			
Moments in frames	LN	1.0	0.1
Axial forces in frames	LN	1.0	0.05
Shear forces in frames	LN	1.0	0.1
Moments in plates	LN	1.0	0.2
Forces in plates	LN	1.0	0.1
Stresses in 2D solids	N	0.0	0.05
Stresses in 3D solids	N	0.0	0.05
Resistance models steel (static)			
Bending moment capacity	LN	1.0	0.05
Shear capacity	LN	1.0	0.05
Welded connection capacity	LN	1.15	0.15
Bolted connection capacity	LN	1.25	0.15
Resistance models concrete (static)			
Bending moment capacity	LN	1.2	0.15
Buckling	LN	1.4	0.25
Shear capacity	LN	1.0	0.1

5.4 Reliability implementation in structural design standards

National or international codes and standards form the basis on which reinforced concrete structures are designed. The principles of structural reliability are well implemented in most of the standard and design codes of practices. Guidance on the probabilistic basis of structural reliability is developed extensively by the Joint Committee on Structural Safety (JCSS) and can be found in the Probabilistic Model Code (JCSS, 2001). The code contains comprehensive information on structural reliability design. The International Standard ISO 2394 (General principles on the reliability of structures) considers the partial factor method and the full probabilistic method as the same technique for structural reliability verification. The European Standard for the Basis of Structural Design EN 1990 implements the partial factor limit state design methodology.

5.4.1 The JCSS Probabilistic Model Code 2001

The JCSS, formed in 1971, is involved in extensive research on the application of structural reliability principles. JCSS developed a Probabilistic Model Code (PMC). The JCSS PMC contains comprehensive information and proposals on various issues in structural reliability design. The code provides guidance on full probabilistic design. The PMC is divided into three parts namely (1) Basis of design; (2) Modelling of loads and (3) Modelling of structural properties. The basis of design part treats the general requirements, the basis of uncertainty modelling, principles of the limit state design, structural and reliability analysis principles, robustness requirement, durability and the target reliabilities. The second part gives comprehensive information on various loads such as live load, self-weight, ground loads, traffic loads, snow, wind, earthquake, impact and fire. The third part treats the properties of reinforcement, concrete, steel and soil and gives information on uncertainties in structural models and geometrical properties.

5.4.2 Eurocode EN 1990 (2002)

The Eurocode standards are developed based on the limit state methodology with semi-probabilistically derived characteristic values and partial factors. Partial factor limit states for standardised structural design as implemented in the EN 1990 were also adapted in SANS 10160-1 (SANS 10160-1, 2011). Partial factors can be applied to key basic random variables influencing structural performance (Holicky *et al*., 2010; Holicky *et al*., 2007). The basis of design requirements as specified in EN 1990 applies to all areas of structural design, which comprises structural resistance, serviceability, durability and fire safety of structures (Holicky *et al*., 2007; Beeby & Narayanan, 2005). These areas of structural reliability are verified by considering reliability differentiation, quality assurance, the design lifetime, design situation and limit states (Holicky & Vrouwenvelder, 2005).

5.5 Target reliability index

Several methods for setting the target reliability index (β_T) are available. Target reliability values can be derived from calibrating to existing design practice (Vrouwenvelder, 2002; Holicky *et al*., 2015). Another method for establishing the target reliability index is through cost-benefit optimization (Rackwitz, 2000). In cost-benefit analysis, target reliability is dependent on the consequences of

failure and also on the relative costs to increase safety (Vrouwenvelder, 2002). The recommended target reliability values in the PMC (JCSS, 2001) and the ISO 2394 (2015) are informed by the cost-benefit analysis. The target and acceptable reliability levels for a given structure can also be selected on the basis of human safety criteria (Fisher *et al*, 2013). Ultimate limit states and serviceability limit states have different target reliability requirements. In the following, ultimate limit states are considered.

5.5.1 ISO 2394 (ISO 2394, 1998)

The target reliability index β_T for lifetime design working life, according to the stipulations of ISO 2394, are presented in Table 5.2. The β_T values are listed as a function of the cost of safety measures and failure consequences.

Table 5.2. Target reliability index β_T for lifetime design working life (ISO 2394).

Relative cost of safety measures	**Consequences of failure**			
	Small	**Some**	**Moderate**	**Great**
High	0	1.5	2.3	3.1
Moderate	1.3	2.3	3.1	3.8
Low	2.3	3.1	3.8	4.3

5.5.2 Probabilistic Model Code (JCSS, 2001)

The PMC gives a target reliability index β_T for a one year reference period and differentiates for costs and consequences. Whether a consequence is determined as small or large is defined by the ratio of the total costs (i.e. construction costs plus direct failure costs) to construction costs. Based on the stipulations of JCSS, the β_T values for ultimate limit are presented in Table 5.3.

Table 5.3. Target reliability values β_T for one year reference period (ULS) PMC (JCSS, 2001)

Relative cost of safety measures	**Consequences of failure**		
	Minor	**Moderate**	**Large**
Large	3.1	3.3	3.7
Normal	3.7	4.2	4.4
Small	4.2	4.4	4.7

5.5.3 Eurocode (EN 1990, 2002)

The values in Eurocode reflect possible failure consequences by adapting the consequence class. They are given for the reference period of 1 and 50 years. The values are valid for component failures. Countries adopting Eurocode as the basis for the development of their national standards are required to set target reliability levels β_T based on structural risk acceptance criteria suitable for national practice. EN 1990 defines reliability classes RC1 to RC3 with the graveness of the consequences expressed as costs. Table 5.4 presents the recommended target reliability according to EN 1990.

Table 5.4. Recommended target reliability index β_T (ULS) EN 1990 (EN 1990, 2002).

Reliability class	**EN 1990 target values for reliability index**		
Reference period	Description	One year reference period	50 years reference period
RC1	Low for loss of human life, and economic, social or environmental small or negligible	4.2	3.3
RC2	Medium for loss of human life, economic, social or environmental considerable	4.7	3.8
RC3	High for loss of human life, or economic, social or environmental very great	5.2	4.3

5.5.4 American Society of Civil Engineers ASCE 7-16 (ASCE, 2017).

According to ASCE 7-16:2017, buildings and other structures are classified into four Risk Categories based on the risk to human life, health, and welfare associated with their damage or failure by nature of their occupancy or use as presented in Table 5.5. The target reliabilities according to ASCE 7-16:2017 for buildings and other structures in risk categories I–IV (Table 5.5) are presented in Table 5.6. The target reliabilities are presented for structural and non-structural components subjected to dead, live, environmental, and other loads except earthquake, tsunami, flood, and loads from extraordinary events. The target reliability indices which are provided for a 50-year reference period, have been confirmed through professional practice in AISC 360, ACI 318, and other standards and documents (ASCE, 2017). The target reliabilities provided for Risk Category II were obtained based on probabilistic analyses of structural member performance for strength design procedures as

documented in Ellingwood et al. (1982) and Galambos et al. (1982). The target reliabilities for Risk Categories I, III, and IV were obtained by reviewing the intended performance of structural members and systems, as well as target reliabilities specified by other codes and standards for similar performance criteria (ASCE, 2017).

Table 5.5. Risk Category of buildings and other structures (ASCE, 2017).

Risk Category	Use or Occupancy of buildings and structures
I	Buildings and other structures that represent low risk to human life in the event of failure
II	All buildings and other structures except those listed in Risk Categories I, III, and IV
III	Buildings and other structures, the failure of which could pose a substantial risk to human life Buildings and other structures, not included in Risk Category IV, with potential to cause a substantial economic impact and/or mass disruption of day-to-day civilian life in the event of failure Buildings and other structures not included in Risk Category IV (including, but not limited to, facilities that manufacture, process, handle, store, use, or dispose of such substances as hazardous fuels, hazardous chemicals, hazardous waste, or explosives) containing toxic or explosive substances where the quantity of the material exceeds a threshold quantity established by the authority having jurisdiction and is sufficient to pose a threat to the public if released
IV	Buildings and other structures designated as essential facilities Buildings and other structures, the failure of which could pose a substantial hazard to the community Buildings and other structures (including, but not limited to, facilities that manufacture, process, handle, store, use, or dispose of such substances as hazardous fuels, hazardous chemicals, or hazardous waste) containing sufficient quantities of highly toxic substances where the quantity of the material exceeds a threshold quantity established by the authority having jurisdiction and is sufficient to pose a threat to the public if released

Table 5.6. Target reliability values β_T for 50 years reference period and for load conditions that do not include earthquake, tsunami, or extraordinary events (ASCE, 2017).

	Risk Category			
Basis	**I**	**II**	**II**	**IV**
Failure that is not sudden and does not lead to widespread progression of damage	$\beta = 2.5$	$\beta = 3.0$	$\beta = 3.25$	$\beta = 3.5$
Failure that is either sudden or leads to widespread progression of damage	$\beta = 3.0$	$\beta = 3.5$	$\beta = 3.75$	$\beta = 4.0$
Failure that is sudden and results in widespread progression of damage	$\beta = 3.5$	$\beta = 4.0$	$\beta = 4.25$	$\beta = 4.5$

5.6 Approach to calibration of design values (EN 1990)

Design values should be based on the values of the basic variables at the FORM design point, which can be defined as the point on the failure surface closest to the average design point in the space of normalized variables (EN 1990, 2002). Through means of reliability separation for action effects and resistance, EN 1990 specifies the design value, R_d (resistance) and E_d (action effect) using the probabilistic relationship expressed in Equation 5.8 and 5.9 respectively.

$$P(R \leq R_d) = \Phi(-\propto_R \beta_T) \tag{5.8}$$

$$P(E > E_d) = \Phi(+\propto_E \beta_T) \tag{5.9}$$

where β_T is the target reliability index, and $\propto_R$ and $\propto_E$, with $|\alpha| \leq 1$, are the values of the FORM sensitivity factors. The value of α is negative for unfavourable actions and action effects, and positive for resistance. For performance function expressed in Equation 5.2, the FORM sensitivity factors are given as Equation 5.10 and 5.11.

$$\propto_R = \frac{\sigma_R}{\sqrt{{\sigma_E}^2 + {\sigma_R}^2}} \tag{5.10}$$

$$\propto_E = \frac{-\sigma_E}{\sqrt{{\sigma_E}^2 + {\sigma_R}^2}} \tag{5.11}$$

The sensitivity factors $\propto_R$ and $\propto_E$ are both functions of the resulting standard deviation σ_R and σ_E; therefore, they change in each design situation. In order to derive practical design rules for wide range

of civil engineering structures, EN 1990 recommends a fixed value of $\propto_R$ and $\propto_E$ as 0.8 and -0.7 respectively. The values have been defined by minimising the deviation from the target reliability index for different values of the ratio between the standard deviations σ_R and σ_E (König and Hosser, 1982). The Eurocode stipulations regarding this sensitivity factor state that it is applicable for typical design situations where the ratio of the standard deviations of loading and structural resistance ($^{\sigma_E}/_{\sigma_R}$) is between 0.16 and 7.6. The recommended values for partial factors in the Eurocodes correspond to the above sensitivity factors, which provides a safe approximation (Moore, 2003). Generally, it should hold that $\propto_R{}^2 + \propto_E{}^2 = 1$. The EN 1990 recommendation is on a safe side (conservative) as the sum of squares of $\propto_R$ and $\propto_E$ is greater than 1 (Gulvanessian et al., 2002).

From Equations 5.8 and 5.9, It may be assumed that the target reliability β_T of a structural member can be categorised into the resistance reliability index β_{RT} and the load part β_{ET} (EN 1990, 2002) expressed in Equation 5.12 and 5.13 respectively.

$$\beta_{RT} = \propto_R \beta_T \tag{5.12}$$

$$\beta_{ET} = -\propto_E \beta_T \tag{5.13}$$

The investigation conducted in this thesis is focused mainly on the resistance reliability index β_R. It is required that the resistance index β_R should be close to its target value β_{RT} (5.12) according to EN 1990 requirements. β_T represents the target value associated with the Reliability Class of the structure under consideration. For example, in accordance to EN 1990 β_T = 3.8 for RC2 structures. $\propto_R$ can be described as the sensitivity factor for resistance, defining the proportion of the safety ascribed to the resistance. This is taken as 0.8 in this study, as specified in EN 1990.

By FORM analysis, the resistance reliability index, β_R is determined through the assessment of the performance function expressed in Equation 5.14.

$$g(\mathrm{X}) = V(\mathrm{X}) - V_d\ (\mathrm{X}_k, \gamma, \phi) \tag{5.14}$$

where $V(\mathrm{X})$ is a general probabilistic model (GPM) for shear, in this case representing the resistance side of the limit state equation similar to $R(X)$ in Equation 5.2. The Modified Compression Field theory (MCFT) and the Compression Chord Capacity model are adopted for use as GPM in Chapter 7 and 8 of the thesis. X denotes the vector of basic variables. $\mathrm{V}_d(\mathrm{X}_k, \gamma, \phi)$ is the deterministic code design shear resistance for a specific case for which the reliability is to be determined (using EC2,

ACI 318 and Fib Model Code (III) shear provisions) and incorporating all applicable safety elements for design e.g. partials factors, characteristic values and strength reduction factor. Therefore, X_k represents the vector of their characteristic values, γ denotes the vector of relevant partial factors (where applicable) and ϕ denotes resistance reduction factor (where applicable).

5.7 Concluding remarks

The chapter summarises the fundamental concepts needed to conduct reliability analysis. Uncertainty modelling is reviewed, and the model factors related to both load and resistance models as recommended by the Probabilistic Model Code (JCSS 2001) are summarised. The implementation of reliability principles in design codes of practices is discussed. The FORM (that will be used for the performance evaluation in this study) is also discussed. The various methods for setting the target reliability (β_T), and the recommended values for β_T are provided.

Chapter 6

Characterisation of model factors for shear reliability assessment

6.1 Introduction

The inability of the different shear strength models discussed in Chapter 4 to accurately capture trends witnessed from experimental observations and also, the differences in predictions from the different models attests to the presence of significant model uncertainties. Previous studies (Mensah, 2015) have indicated that the model factor governs shear reliability performance. Overestimation of the conservative bias of the model and underestimation of its variability may lead to overestimation of the implicit safety levels. This makes the choice of the prediction model and the model factor statistics of that model critical in reliability analysis. A suitable general probabilistic model (GPM) for shear resistance and the corresponding statistics of the model factor is required to assess the reliability performance of beams in shear.

This chapter focuses on the statistical quantification and characterisation of model factors for reliability analysis of beams in shear. The required statistics are obtained from experimental test results and predictions from theoretical shear models. The shear prediction models investigated include two variations of the Variable Strut Inclination Method (VSIM) $V_{VSIM-L\theta}$ and V_{VSIM-A}. $V_{VSIM-L\theta}$ represents the unbiased behaviour of the operational EC2 VSIM design procedure with constraint applied to the strut angle θ. V_{VSIM-A} is a modification of the VSIM where the strut angle limit is ignored. The limited strut angle as stated in the operational EC2 VSIM design procedure is a form of bias enforced on the concrete compressive strut angle to ensure more conservative predictions (discussed in Section 3.2.6.7). Other prediction models investigated are ACI-318 best estimate model denoted V_{ACI}, Fib Model Code level of approximation III best estimate model denoted $V_{MC-10(III)}$, Compression Chord Capacity model denoted V_{CCC} and the Modified Compression Field Theory denoted V_{R2k}. V_{R2k} is classified as level of approximation IV (most advanced) according to the definitions of the Fib Model Code.

The chapter also elaborates on the database of compiled experimental observations to which statistical methods are applied to characterise the relevant model factors. As part of the statistical characterisation, model factors are investigated parametrically against essential shear parameters using correlation and regression assessments. Consequently, dependencies in the relevant prediction models are exposed. The derived model factor statistics will be used as input to reliability investigations conducted in Chapter 7 and 8. Finally, suitable probabilistic models were developed that can be used for reliability assessment of EC2 stirrup design procedure and other design procedures for stirrup failure.

6.2 Experimental database

6.2.1 Introduction to the experimental database

The earliest shear database was developed in 1962 by ACI-ASCE Committee 326 (Moe, 1962). The committee developed a shear database of about 194 experimental tests of reinforced concrete beams without stirrups. Through a thorough assessment of this database, the committee developed a shear design equation for reinforced concrete members without stirrups.

In the last decade, the development of shear databases attracted a great deal of attention in the shear research community. Several research groups have already developed shear databases for reinforced concrete members (Reineck, *et al*. 2003, Brown, *et al*. 2006, Collins, *et al*. 2008). These databases contain a large number of shear tests from around the world and are useful for evaluating various shear design provisions. The significant benefit of the developed database is that it enables researchers to utilise a large number of results from previous shear tests. An assessment conducted with various test results is indispensable for obtaining a better understanding of the shear behaviour of structural concrete and also for evaluating existing shear design provisions.

More recently, an extensive database of 886 experimental tests on reinforced concrete beams with vertical shear reinforcement was assembled by a joint group of ACI-DafStb consisting of ACI Subcommittee 445-D and German Committee for Structural Concrete Deutscher Ausschub fur-Stahlbeton (DafStb). From the originally collected 886 tests, 125 tests were filtered out due to missing important information such as the yield strength of the longitudinal reinforcement or the attained ultimate shear force, remaining 761 tests. The resulting 761 tests were sorted into groups of 511 tests on slender beams and 250 test on non-slender beams using the shear span to depth ratio as

criteria. In order to develop a set of slender beam tests that can be used to evaluate the accuracy and conservativeness of shear design models, the database was subjected to flexural failure check and minimum reinforcement filtering criteria as reported in Reineck *et al*. (2014). After applying the flexural failure criteria check, a subset of 180 tests remained. Of those, 20 beams had reinforcement ratios below the minimum reinforcement ratio, resulting in an evaluation database of 160 tests on slender beams used in this study. The evaluation database consists of simply supported rectangular and flanged beams subjected to point loads. The shear span to depth ratio (a/d) of the beams is greater than 2.40. The beams failed predominantly by diagonal tension and shear compression (post stirrup yield mode of failure). Experimental tests with the flexural mode of failure were excluded from the database. The evaluation database covers a wide range of design situations ranging from low to high amount of shear reinforcement, and small, ordinary and large effective depths. Beams ranging from low to high concrete strength are also included.

MCFT (R2k) requires the specification of additional input parameters to predict shear resistance as compared to VSIM procedure. Some of these parameters include maximum aggregate size, concrete cover, the percentage of longitudinal reinforcement and yield strength. Only 130 beam experiments in the evaluation database reported the maximum aggregate size. Consequently, from the evaluation database of 160 beam tests, a subset of 130 beam tests was used to derive model factor statistics for MCFT (R2k) for which adequate data were accessible to enable its prediction.

6.2.2 Range and distribution of parameter values for the full database

The range of shear parameters presented in the database corresponds to a practical range of design situations found in physical structures. In this section, the number of beams (n) in the database is plotted against main shear parameters to obtain an overview of the distribution of the shear parameters. The shear parameters studied are listed below.

i. The amount of shear reinforcement $(\rho_w f_{ywm})$
ii. Percentage of longitudinal reinforcement $(\rho_l\%)$
iii. Shear-span to depth ratio (a/d)
iv. Width of section (b_w)
v. Depth of section (d)
vi. Concrete cylinder compressive strength (f_{cm})

As shown in Figure 6.1(a), 60 (38%) of experimental test beams had a compressive cylinder strength of $f_{cm} < 40\ MPa$. 26 beams (16%) had compressive cylinder strength in the range of $40 < f_{cm} < 60\ MPa$ and 74 beams (46%) had concrete strength $f_{cm} > 60\ MPa$.

As can be observed in Figure 6.1(b), 74 beams (46%) had stirrup yield strength of $f_{ywm} < 450\ MPa$ and 56 beams (35%) had a stirrup yield strength of $f_{ywm} > 550\ MPa$. In total 119 (74%) of the beams had effective depth in the range of $150 < d < 450\ mm$ as shown in Figure 6.1(c). Only 41 beams (26%) had effective depth $d > 450\ mm$.

Figure 6.1(d) reveals that 136 of the beams (85%) had width in the range of $100 < b_w < 300\ mm$. Merely 5 beams had $b_w > 350\ mm$. The majority of the beams had a percentage of longitudinal reinforcement $\rho_l\% < 4\%$, that is, 142 beams (89%). Only 18 beams (11%) had $\rho_l > 4\%$ (see Figure 6.1(e)).

94% (106 beams) of the beams which were tested, had a slenderness ratio in the range of $2.4 < a/d < 4.4$ (Figure 6.1(f)). As presented in Figure 6.1(g), the majority of the beams (131 beams [82%]) had an amount of shear reinforcement $\rho_w f_{ywm} \leq 2.0\ MPa$. Only 29 beams had shear reinforcement in excess of $\rho_w f_{ywm} > 2\ MPa$.

In general, the highest number of data points in the database are found in the smaller size range and lower amount of shear reinforcement.

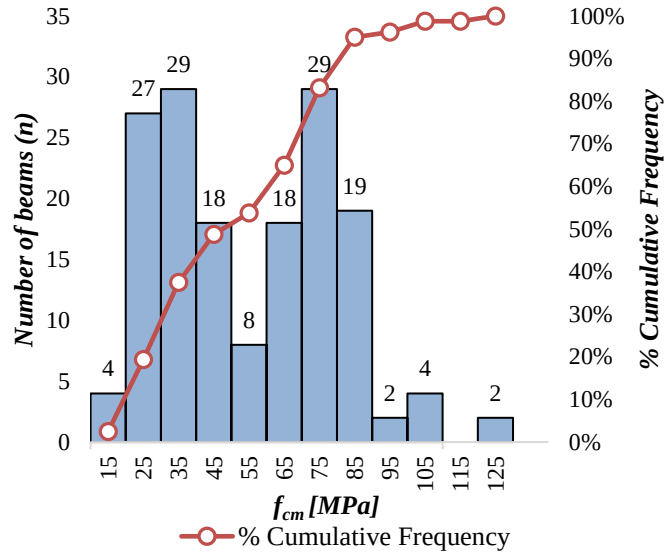

(a)

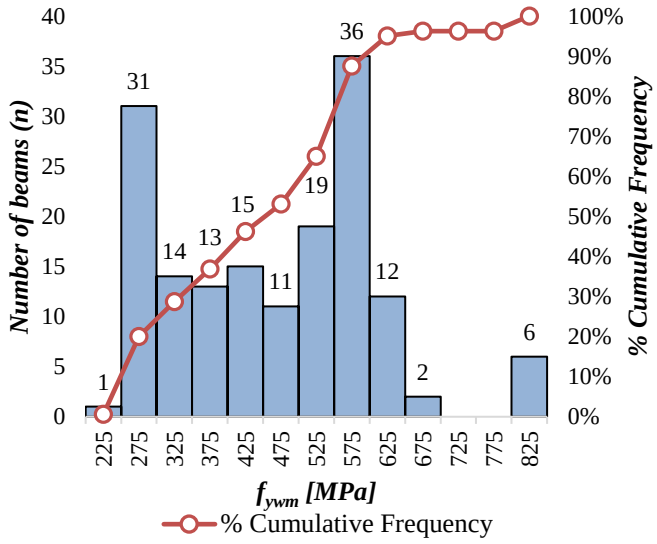

(b)

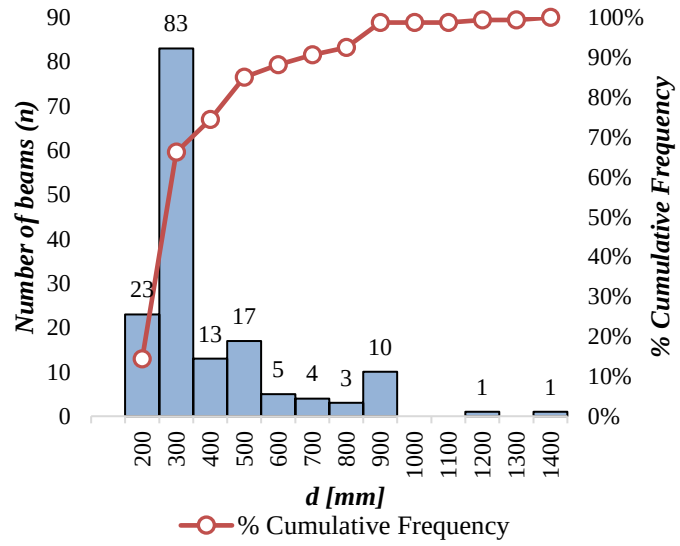

(c)

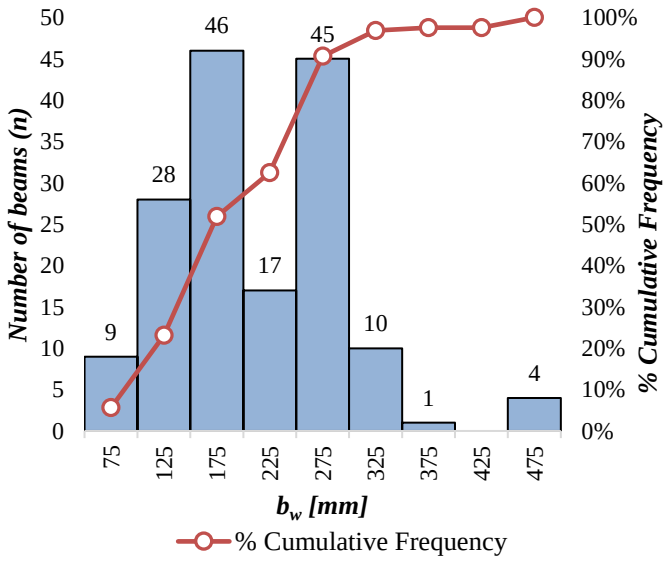

(d)

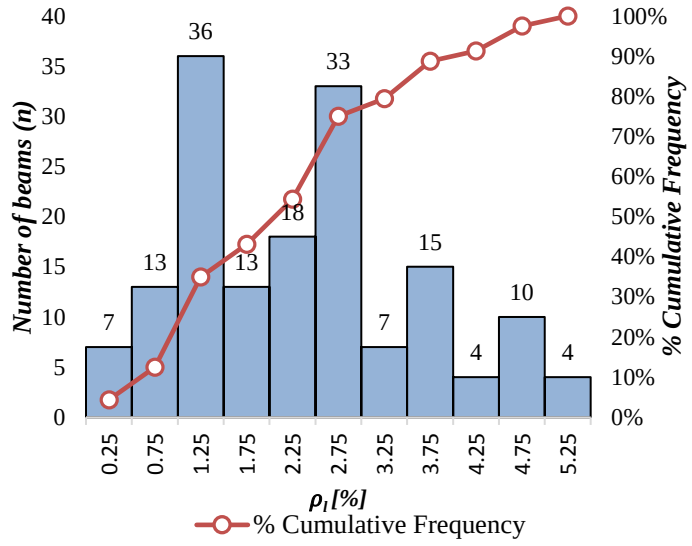

(e)

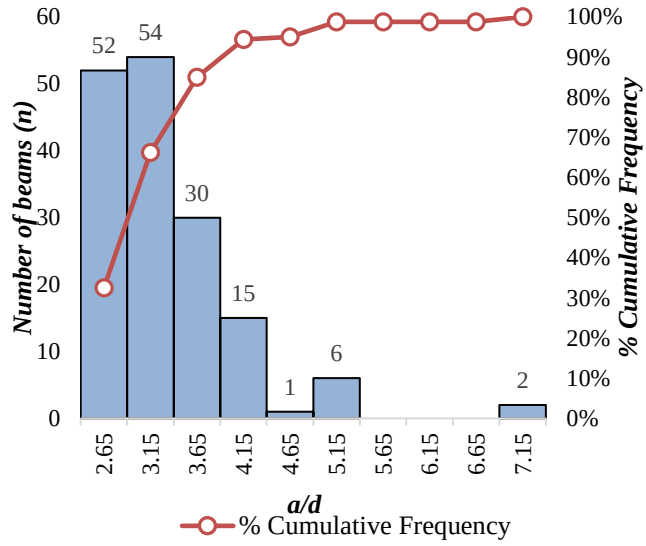

(f)

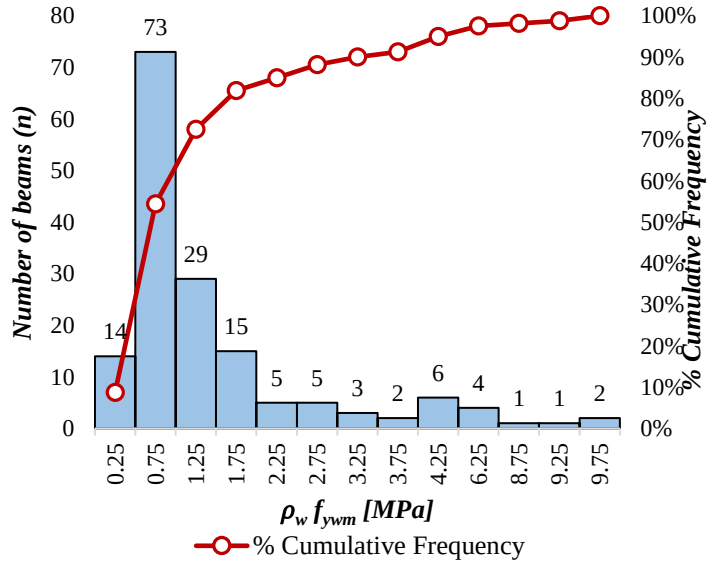

(g)

Figure 6.1. Characteristics of the experimental database: Number of beams in various parameter ranges (a) concrete strength f_{cm} (b) steel yield strength f_{ywm} (c) beam depth d (d) beam width b_w (e) longitudinal reinforcement ρ_l% (f) shear span to depth ratio a/d (g) shear reinforcement $\rho_w f_{ywm}$

6.2.3 Comparison of the statistics of the full database (160 beams) and the subset of 130 beam experiments

Table 6.1 (a & b) present the range of parameters in the database of 160 experiments (full database) and a subset of 130 beam experiments. Comparison of the statistics from the tables shows that the subset of 130 beam experiments compares well with the full database of 160 beam experiments, reflecting most of its minimum and maximum values.

Table 6.1(a) Range of parameters for the full database (160 experiments)

Parameters	Minimum Value	First Quartile (P25)	Median (P50)	Third Quartile (P75)	Maximum Value
b_w $[mm]$	75	150	180	250	457
d $[mm]$	161	263	292.50	451.40	1369
f_{cm} $[MPa]$	13.40	31.40	50.20	72.43	125.30
ρ_l [%]	0.14	1.10	2.28	3 .01	5.20
$\rho_w f_{ywm}$ $[MPa]$	0.28	0.62	0.87	1.63	9.80
a/d	2.40	2.56	3.09	3.52	7.10
V_{exp} $[kN]$	81	130.90	206.50	280.20	1330

Table 6.1(b) Range of parameters for subset database (130 experiments)

Parameters	Minimum Value	First Quartile (P25)	Median (P50)	Third Quartile (P75)	Maximum Value
b_w $[mm]$	77	152	190	250	457
d $[mm]$	198	272	292	345.50	1200
f_{cm} $[MPa]$	13.40	31.68	54.30	72.44	125.30
ρ_l [%]	0.36	1.07	2.49	2.99	4.70
$\rho_w f_{ywm}$ $[MPa]$	0.28	0.62	0.87	1.24	9.60
a/d	2.45	2.50	3.00	3.45	7.10
V_{exp} $[kN]$	81	126.22	203.42	260.20	1172.10

6.2.4 Normalised shear strength for the database

Figure 6.2 presents a 3D scatter plot of normalised experimental shear strength ($V_{exp}/b_w d$) vs amount of shear reinforcement $\rho_w f_{ywk}$ vs concrete strength f_{ck}. The graph shows the complete dataset.

Assessment of the figure reveals the followings:

- The normalised shear strength increases with increasing shear reinforcement. For ratios $\rho_w f_{ywk} > 2\ MPa$ the normalised shear strength values are high, exceeding 2 MPa in most instances.
- It was also observed that as the concrete strength increases the normalised shear strength increases. Most experimental beams with $f_{ck} > 52\ MPa$ contain $\rho_w f_{ywk} < 2\ MPa$.

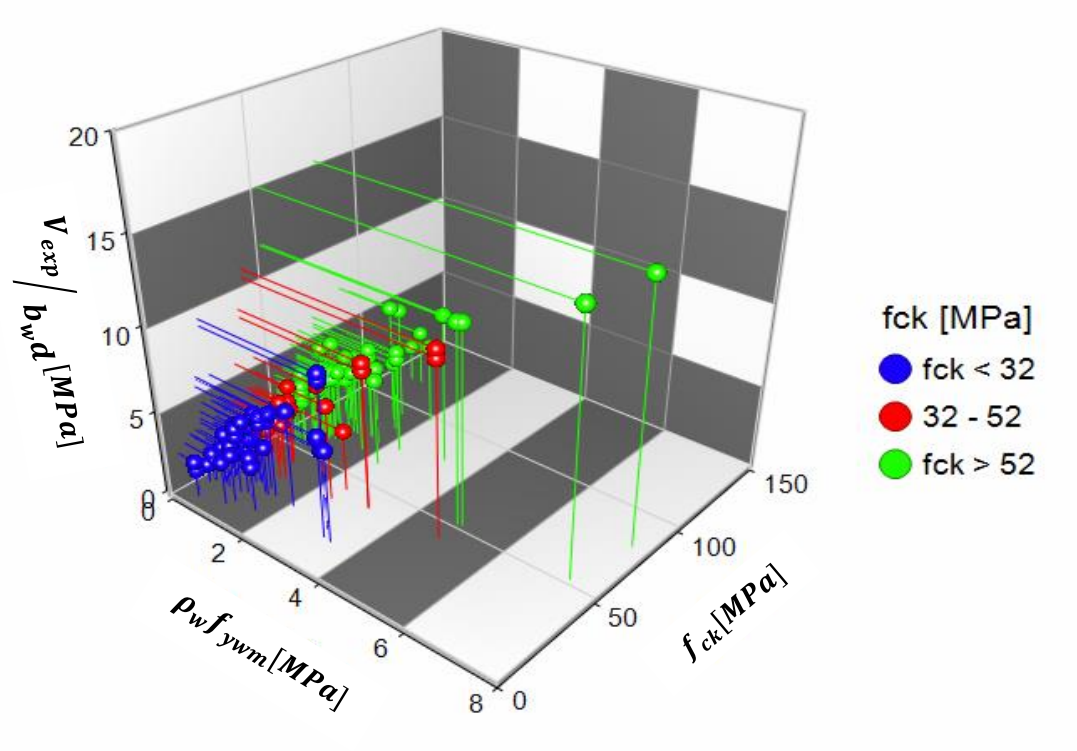

Figure 6.2. 3D scatter plots for complete dataset grouped by concrete strength

6.3 Assessment of model uncertainty and bias

Models are a partial representation of reality. The inability of models to perfectly describe reality give rise to a state of uncertainty. Model uncertainty accounts for effects neglected in the model formulations (JCSS, 2001). In view of this, it is essential to quantify the model factor accurately. Model factors are statistical quantities characterised by mean values, variances, and probability distribution functions. The performance of the derived model factors will be assessed using the following criteria:

i. The estimate of the model uncertainty and bias
ii. Trends in the model factor observations with shear parameters
iii. Probability distribution function

6.3.1 Calculation of the model factor

After experimental shear observations were compiled from the experimental tests described in Section 6.2, the predicted capacities were obtained for each equivalent test using the studied shear models. The relevant statistical properties of the model factor were obtained by comparing

experimental observations to best-estimate predictions of analytical models. In accordance with JCSS (2001) and Holicky *et al*. (2013) the description for model factor observation (MF_x) associated with a single experiment, x, as used in this study, is determined by 6.1.

$$MF_x = {V_{exp,x}}\Big/{V_{Model,x}}\,(X) \tag{6.1}$$

where, $V_{exp,x}$ represents the shear failure for a single experimental beam x which is subject to known structural conditions

X is the vector of basic/input variables some of which include depth of beam (d), concrete strength (f_{cm}) amount of longitudinal reinforcement (p_l), amount of stirrup reinforcement $\rho_w f_{ywm}$, shear-span to depth ration (a/d), width, (b_w)

$V_{Model,x}$ represents best-estimate shear resistance prediction for the same experimental beam x offered by the prediction model under consideration

The derived model factor observations are presented in the Appendix for each prediction model. The model factor observations are further assessed by using mathematical and statistical methods to derive an appropriate probability distribution for the model factor which may be used in reliability assessment. The statistical characterisation of the generated model factor observations is presented in subsequent sections. A value of $MF > 1$ implies that the prediction model underestimates shear capacity while a value of $MF < 1$ implies that the prediction model overestimates shear capacity.

6.3.1.1 Model factor based on VSIM ($V_{VSIM-L\theta}$ and V_{VSIM-A})

For comparison with experimental observations, the model factor for any single test is calculated as expressed in Equation 6.1. The model factor derived from two variations of VSIM shear predictions $V_{VSIM-L\theta}$ and V_{VSIM-A} result in model factor $MF_{VSIM-L\theta}$ and MF_{VSIM-A} respectively. For members with stirrups, the best estimate of shear resistance according to EC2 (2004) is taken to be the lesser of either 6.2 or 6.3.

$$V_{VSIM-L\theta} = \frac{A_{sw}}{s} Z f_{ywm} Cot\theta_m \tag{6.2}$$

$$V_{Rm,max} = \frac{b_w \alpha_{cw} s v_1 f_{cm}}{(Cot\theta_m + tan\theta_m)} \tag{6.3}$$

$$\theta_m = \sin^{-1} \sqrt{\frac{A_{sw} f_{ywm}}{b_w s v_1 \alpha_{cc} f_{cm}}} \tag{6.4}$$

Where A_{sw} is the cross-sectional area of the shear reinforcement

s denotes the spacing of the stirrups

f_{ywm} and f_{cm} represent the mean values of the steel yield strength and concrete compressive cylinder strength respectively

θ_m is the mean concrete strut angle

The value for v_1 may be taken to be 0.6 for $f_{ck} \leq 60$ MPa and as $0.9 - \frac{f_{ck}}{200}$ for high-strength concrete beams. The internal lever arm may be taken as $z = 0.9d$. The coefficient factor accounting for long term effects on concrete was assigned a mean value of α_{cc} = 0.85 (Holicky *et al.*, 2010). The coefficient accounting for the state of stress in the compression chord is represented by α_{cw}.

$MF_{VSIM-L\theta}$ represents the model factors derived from unbiased EC2 VISM shear resistance model $V_{VSIM-L\theta}$. Unbiased $V_{VSIM-L\theta}$ shear capacity predictions are best estimate predictions obtained based on mean values of material strength (in stead of characteristic values) thus partial material safety factors are set equal to one. The strut angle θ_d is restricted to the range of $21.8° \leq \theta_d \leq 45°$. The limit placed on the strut angle θ_d is expected to affect the derived $MF_{VSIM-L\theta}$ conservatively.

The limits imposed on the concrete compressive strut angle (θ) in the operational EC2 VSIM shear design formulation is a form of bias imposed to provide conservatism in design. (Section 3.2.6.5). Mean value predictions may be made with or without the strut angle limits. As a result, alternative function better suited for best-estimate prediction of EC2 VSIM shear resistance V_{VSIM-A} was investigated. V_{VSIM-A} is the shear resistance prediction of the unfactored EC2 VSIM shear design procedure with no constraint applied to the strut angle (VSIM-A), resulting in model factor denoted MF_{VSIM-A}.

6.3.1.2 Model factor based on Fib Model Code 10 (III) ($V_{MC-10(III)}$)

The unbiased MC-10 (III) shear resistance model is expressed as Equation 6.5. The derived model factor is denoted $MF_{MC-10(III)}$.

$$V_{MC-10(III)} = \frac{A_{sw}}{s} z f_{ywm} Cot\theta + K_v z \sqrt{f_{cm}} b_w \quad (6.5)$$

6.3.1.3 Model factor based on ACI 318 (V_{ACI})

MF_{ACI} represents the model factors derived from unbiased ACI 318 shear resistance model V_{ACI}. The best estimate prediction according to ACI 318 is calculated using the resistance model described in Equation 6.6. The concrete contribution term $V_c = \frac{1}{6}\sqrt{f_{cm}} b_w d$ is an empirical formulation obtained from the database of beam experiments (normal strength, average depth of 340mm and 2% longitudinal reinforcement) (Kuchma & Collins, 1998).

$$V_{ACI} = \frac{A_{sw}}{s} f_{ywm} d + \frac{1}{6}\sqrt{f_{cm}} b_w d \quad (6.6)$$

6.3.1.4 Model factor based on Compression Chord Capacity Model (CCC) (V_{CCC})

The unbiased predicted shear resistance V_{CCC} is obtained based on CCC resistance model expressed in Equation 6.7. The derived model factor is denoted as MF_{CCC}.

$$V_{CCC} = 1.4\frac{A_{sw}}{s} f_{ywm}(d_s - x) cot\theta + 0.3\zeta \frac{x}{d} (f_{cm})^{2/3} b_{v,eff} \quad (6.7)$$

6.3.1.5 Model factor based on MCFT-Response 2000 Predictions (V_{R2k})

The model factor statistics are derived based on the unbiased shear capacity predictions of MCFT based sectional analysis program Response-2000 (V_{R2k}). Unbiased estimates of V_{R2k} were obtained by using the mean values of shear parameters (outlined in Section 3.4.4) in the sectional analysis program. The characterised model factor is denoted MF_{R2k}. The comprehensive step by step procedure on the use of MCFT (R2k) to estimate V_{R2k} predictions is presented in Section 3.4.

6.4 Statistical analysis of the model factor observations

The statistical analysis of the derived model factors is discussed in this section. The statistical analysis comprises

- Graphical representation of the model factors using histograms
- Identification of data outliers and correction of erroneous data
- Computation of the statistical properties such as the mean value (μ_{MF}), standard deviation (σ_{MF}), coefficient of variation (Ω_{MF}) and skewness (η_{MF})
- Trends in the model factor observations with shear parameters
- Determination of appropriate distribution for the model factor

6.4.1 Graphical representation of the model factor observations using histograms

The histogram reveals the critical characteristics of a set of data in a condensed format. The observed model factor is presented in the form of a histogram to make it more useful. The histogram brings out the following characteristics, which may not be explicitly visible initially:

- An indication of whether the observed data is symmetric or asymmetric
- The range of observed data
- The most frequently occurring data
- The extent to which the observed data is scattered about the mean

The histograms are developed by plotting the number of observations within a given interval against the intervals as illustrated in Figure 6.3. Visual inspection reveals that all six histograms (representing six datasets of model factor observations) show some similar features. The following observations are made from the histograms:

- A large number of the data points are observed around the mean value
- The observations are not symmetrical about the peak frequency, indicating that the underlying distribution for the data point is not normal
- The widths of the histogram reveal the extent of variability

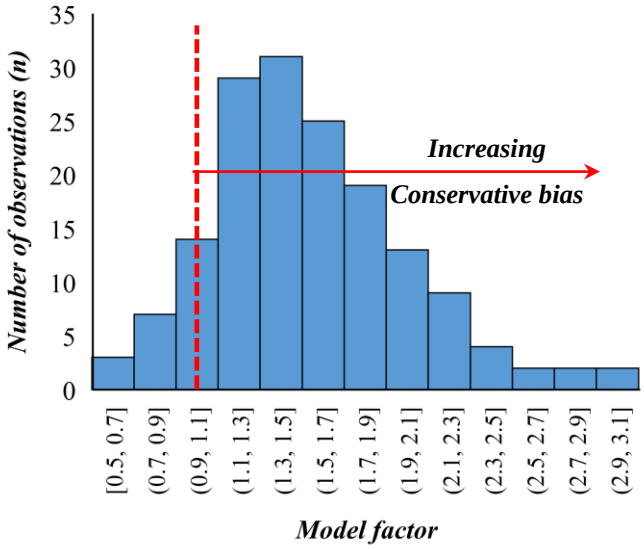

(a) $\mathbf{MF}_{VSIM-L\theta}$

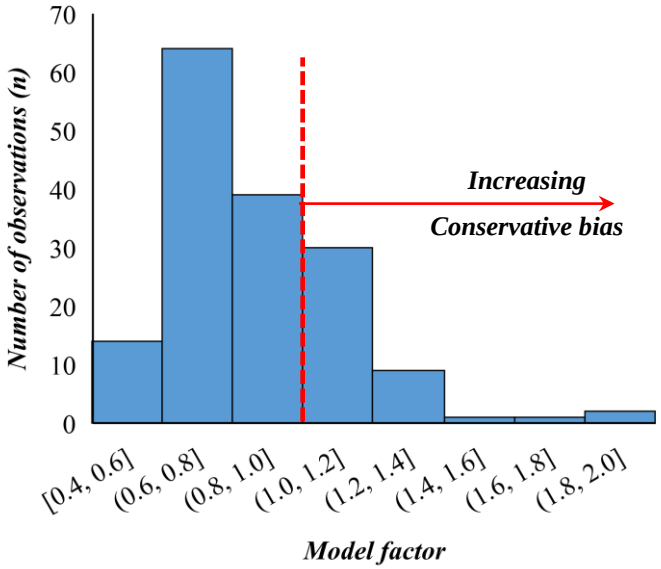

(b) $\mathbf{MF}_{VSIM-A}$

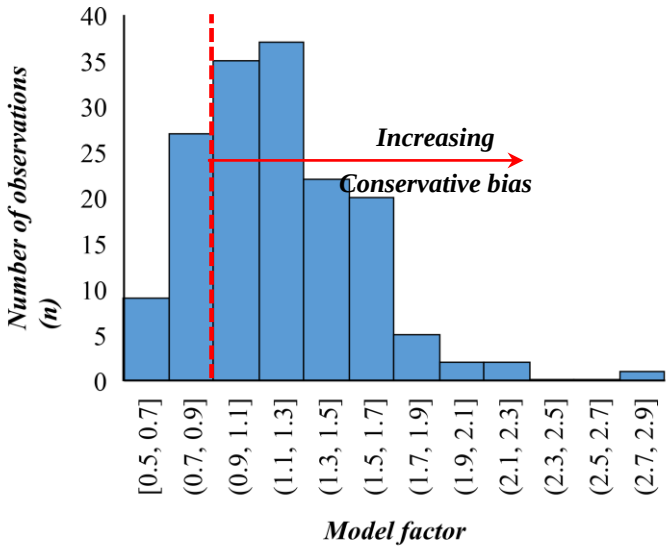

(c) $MF_{MC-10(III)}$

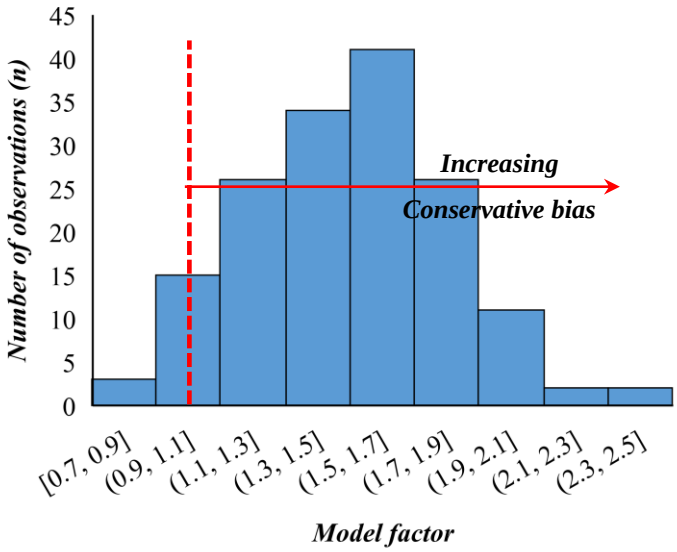

(d) MF_{ACI}

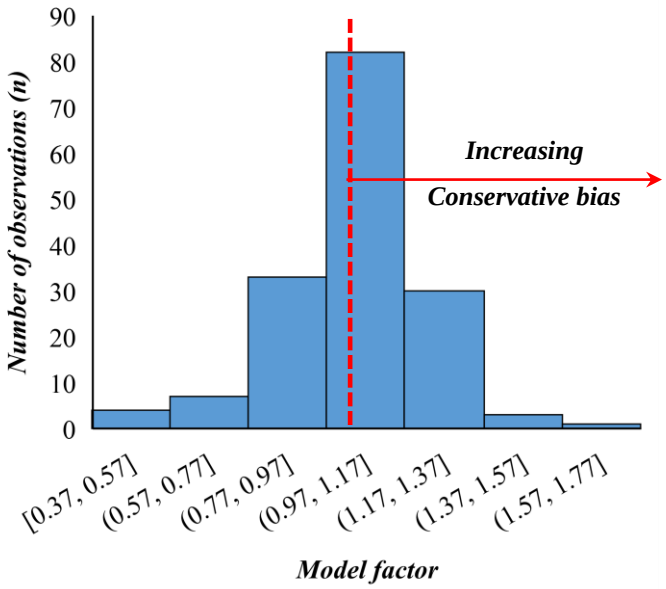

(e) MF_{CCC}

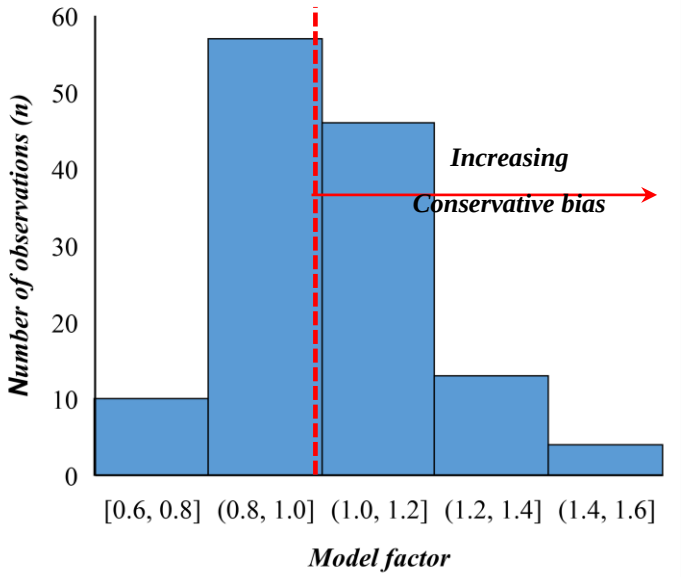

(f) MF_{R2k}

Figure 6.3. Histograms of the model factors

6.4.2 Identification of data outliers and correction of erroneous data

Although some measures seemed to indicate a few outliers for CCC model factors, closer inspection confirmed the validity of these observations. The methods used to discern potential outliers in the model factor observations include (1) the boxplot method (Figure 6.4) (2) the sample Z-score approach (McBean & Rovers, 1998) (Figure 6.5) and (3) the multivariate method (Figure 6.6). Visual examination of the figures reveal the following results:

- For model factor dataset obtained using CCC model, four data points deviate substantially from the general trend and are consequently considered as potential outliers. This outcome is the same for all three assessments.
- For all other models, no outliers are identified in the datasets. This result is similar for all three assessments.

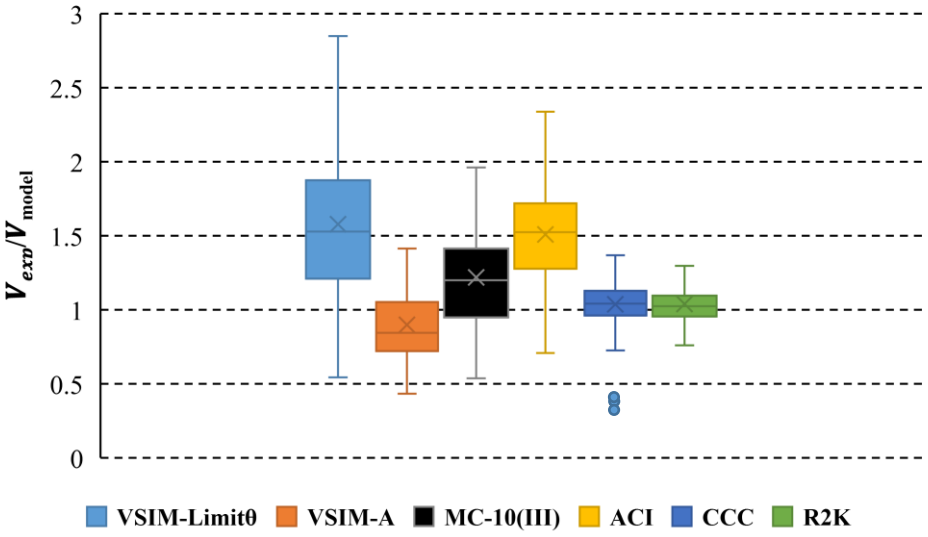

Figure 6.4. Box plot of model factors

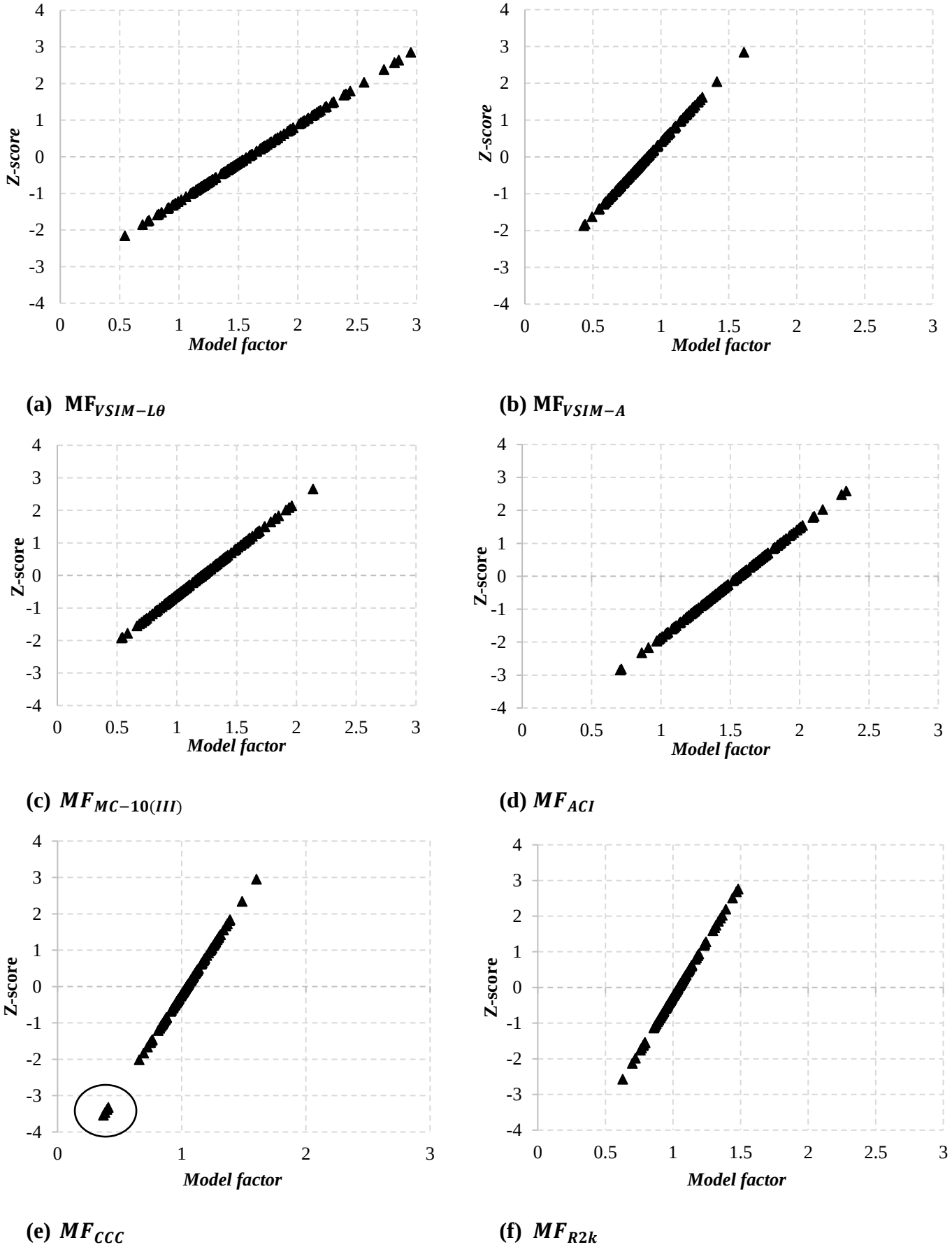

Figure 6.5. Z-scores versus model factors plots

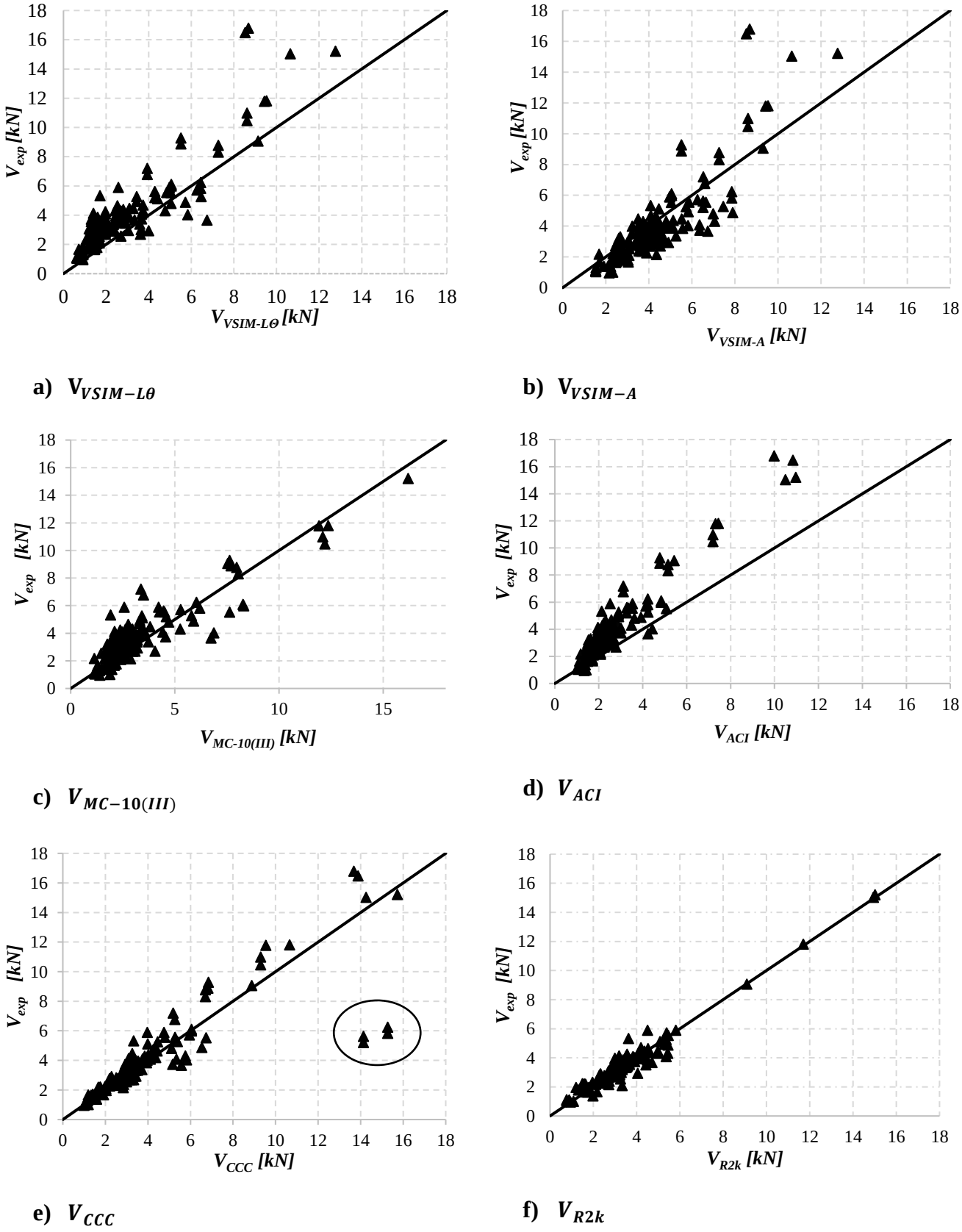

Figure 6.6. Comparison of experimental V_{exp} to predicted shear strength a) $V_{VSIM-L\theta}$, b) V_{VSIM-A}, c) $V_{MC-10(III)}$, d) V_{ACI}, e) V_{CCC}, f) V_{R2k}

6.4.2.1 Revision of potential outliers

Four data points were identified as potential outliers from the CCC based dataset of model factor observations. According to Robinson *et al*. (2005), it is erroneous to delete a data point once it is discerned as a statistical outlier without examining it carefully and meticulously. Based on this, the potential outliers were examined carefully by double checking the processes of determination and computation of their predicted shear capacity using the CCC model. This involves checking for computational errors and data entry errors. However, examination of the records for these data points showed no form of error.

Close examination of the records for these data points indicates that these are uncommon flanged beams with small section sizes ($b_w = 150\,mm$, $d = 161\,mm$ and $h_f = 200\,mm$), high concrete strength ($f_{cm} = 82\,MPa$) and high reinforcement ratios ($\rho_l = 5\%$, and average $\rho_w f_{ywm} = 2.86\,MPa$). The combination of the small section sizes, the high concrete strength and high reinforcement ratio, resulted in the higher predicted capacities by CCC model and very low model factor realisations. The other investigated models predict these same data points well. Therefore the data points are considered valid and hence they were not deleted.

6.4.3 Statistical moments

The most important statistical properties commonly used in practical applications includes, the mean μ (central measures), the standard deviation σ (dispersion measures) and the skewness η.

The sample mean describes the centre around which the observations in the dataset are distributed. The mean value μ of a dataset with n number of observations $x = (x_i \ldots\ldots, x_n)$ is given by Equation 6.9.

$$\mu = \frac{1}{n}\sum_{i=1}^{n} x_i \tag{6.9}$$

The standard deviation (variability or the dispersion or scatter) describes how far the observations are from the mean value or the centre line. It is estimated using Equation 6.10.

$$s_x = \frac{\sum(x-\mu)^2}{n-1} \tag{6.10}$$

The skewness indicates the degree of symmetry of the dataset defined in Equation 6.11.

$$\eta = \frac{\sum_{i=1}^{n}(x_i-\mu)^3}{[(n-1)*(n-1)*\sigma^3]} \tag{6.11}$$

The mean value (μ_{MF}), standard deviation (σ_{MF}), coefficient of variation (Ω_{MF}) and the skewness of each derived model factor are reported in Table 6.2.

Table 6.2. Statistical properties of model factors for the full database

Statistics of the Model Factor	**$MF_{VSIM-L\theta}$**	**MF_{VSIM-A}**	**$MF_{MC-10(III)}$**	**MF_{ACI}**	**MF_{CCC}**	**MF_{R2k}**
Number of experiments	160	160	160	160	160	Subset of 130
Mean (μ_{MF})	1.58	0.90	1.21	1.56	1.04	1.04
Standard Deviation (σ_{MF})	0.48	0.25	0.35	0.30	0.19	0.16
Coefficient of Variation	0.30	0.27	0.29	0.19	0.18	0.15
Skewness (η_{MF})	0.61	1.26	0.90	0.15	-0.74	0.74
Minimum	0.54	0.43	0.53	0.70	0.37	0.63
First Quartile (P25)	1.21	0.72	0.95	1.28	0.97	0.95
Median (P50)	1.53	0.84	1.20	1.52	1.08	1.02
Third Quartile (P75)	1.88	1.05	1.41	1.72	1.20	1.09
Maximum	3.10	1.93	2.78	2.30	1.60	1.62

From Table 6.2, $MF_{VSIM-L\theta}$ was found to have mean value of $\mu_{MF} = 1.58$, confirming that the unbiased stirrup resistance function $V_{VSIM-L\theta}$ generally underpredicts shear capacity, which is due to the conservatism provided by the lower limit on the strut angle (θ). The spread of ($\sigma_{MF} = 0.48$) suggest a large scatter of $MF_{VSIM-L\theta}$ about the mean. The model factor MF_{VSIM-A} has a mean value of $\mu_{MF} = 0.90$, indicating that V_{VSIM-A} generally overpredicts shear capacity ($\mu_{MF} < 1$) in contrast to $V_{VSIM-L\theta}$. The difference in the mean values of MF_{VSIM-A} and $MF_{VSIM-L\theta}$ reflects the conservative

influence of the limiting concrete compressive strut angle (θ). MF_{VSIM-A} shows less scatter of standard deviation of $\sigma_{MF} = 0.25$ compared to $\mathrm{MF}_{VSIM-L\theta}$ with standard deviation of $\sigma_{MF} = 0.48$. $MF_{MC-10(III)}$ was found to have a mean value of $\mu_{MF} = 1.21$, implying that the MC-10 (III) shear resistance predictions generally underestimate shear capacity (similar to $\mathrm{MF}_{VSIM-L\theta}$). Regarding model uncertainty, $MF_{MC-10(III)}$ has a standard deviation of $\sigma_{MF} = 0.35$. V_{R2k} and V_{CCC} shear capacity predictions showed closer correlation to the experimental results with their respective model factors (MF_{R2k} and MF_{CCC}) both having a mean value of $\mu_{MF} = 1.04$ (closer to the mean of one). MF_{CCC} has a relatively low standard deviation of $\sigma_{MF} = 0.19$. MF_{R2k} displayed the lowest standard deviation of all models at $\sigma_{MF} = 0.16$.

6.4.4 Trends in the model factor: correlation and regression analysis

A scatter plot of the model factor observations versus any shear parameter reveals the extent to which the shear parameter is accounted for in the model under investigation. This is shown in terms of the trend of observations and scatter around the trend (Holicky *et al*., 2015). In order to discern the sensitivity of key shear parameters influencing shear capacity (outlined in Table 6.1) on model factor, correlation and regression analysis as proposed by Tang & Ang (2007) are conducted on the presented database. Trends in the model factors are discerned by correlating the model factors with the vital shear parameters using Pearson's correlation coefficient (r).

The determined r value revealed the significance of the correlation between model factor and any shear strength parameter x. The correlation can be positive or negative. When the dependent variables tend to increase as the independent variable increases, the correlation is positive; when the dependent variables tend to increase as the independent variable decreases, the correlation is negative. The value of r lies between -1 and +1. The relationship is perfect when the absolute value of $r = 1$ and when the absolute value of $r = 0$, then the variables are independent.

The measure of the linear relationship between the model factor and any shear parameter x is called the coefficient of determination denoted R^2 (Tang & Ang., 2007). R^2 is the square of the r value for a given correlation. Table 6.3 presents the scale of the Pearson's correlation factor according to Franzblau, (1958). Cohen (1988) suggests that the scale of the correlation factor is somehow inconsistent and should not be strictly followed. A good model would not systematically under or overpredict in a way that is correllated to a shear parameter. Thus, ideal models are expected to have very weak or no correlation with parameters that influence shear capacity. If this is the case, the model

is taking adequate account of the influence of the parameter on shear capacity and systematic trends will be negligible. For this reason, we investigate anything that is not classed as very weak or no correlation.

The correlation was therefore evaluated by visual examination of the scatter plots of a model factor against shear parameters and the value of the correlation coefficient r. The outcome of the correlation assessment between the model factors and shear parameters are discussed in the subsequent section. The correlation coefficients are presented in Table 6.4. From the table, it may be concluded that CCC and MCFT (R2k) are the best performers. MC-10 (III) and ACI fail to capture size effects adequatetly. VSIM-A is overall a poor performer and should not be considered as GPM candidate.

Various parametric scatter plots for $\mathrm{MF}_{VSIM-L\theta}$, MF_{VSIM-A}, $MF_{MC-10(III)}$, MF_{ACI}, MF_{CCC} and MF_{R2k} against the main parameters affecting shear strength are presented in Figures 6.7 to 6.12. The trend lines that better fit the different MF realisations, as indicated by a stronger coefficient of determination R^2 for such fits, are shown on the figures. Generally, it was observed that there is a paucity of data points for large beams and highly shear reinforced beams.

Table 6.3. Scale of the Pearson's correlation factor (Franzblau, 1958)

Scales on Correlation Strength	
$\mathbf{0 - \pm 0.2}$	Very weak or no correlation
$\mathbf{0.2 - \pm 0.4}$	Weak correlation
$\mathbf{0.4 - \pm 0.6}$	Moderate correlation
$\mathbf{0.6 - \pm 0.8}$	Strong correlation
$\mathbf{0.8 - \pm 1}$	Very strong correlation

Table 6.4. Pearson correlation matrix between model and shear parameters

	$\mathbf{MF}_{VSIM-L\theta}$	$\mathbf{MF}_{VSIM-A}$	$\boldsymbol{MF_{R2k}}$	$\boldsymbol{MF_{MC-10(III)}}$	$\boldsymbol{MF_{ACI}}$	$\boldsymbol{MF_{CCC}}$
$\boldsymbol{b_w}$ $[\boldsymbol{mm}]$	0.11	-0.59	-0.12	-0.19	-0.40	-0.07
$\boldsymbol{d}$ $[\boldsymbol{mm}]$	-0.25	0.21	-0.20	-0.41	-0.31	0.19
$\boldsymbol{f_{cm}}$ $[\boldsymbol{MPa}]$	0.10	-0.29	-0.25	0.08	0.10	-0.21
$\boldsymbol{\rho_l}$ [%]	0.12	-0.29	-0.16	-0.13	0.24	0.09
$\boldsymbol{\rho_w f_{ywm}}$ $[\boldsymbol{MPa}]$	-0.58	0.58	-0.12	-0.26	0.01	0.004
$\boldsymbol{a/d}$	-0.02	0.18	0.06	-0.14	0.03	-0.10

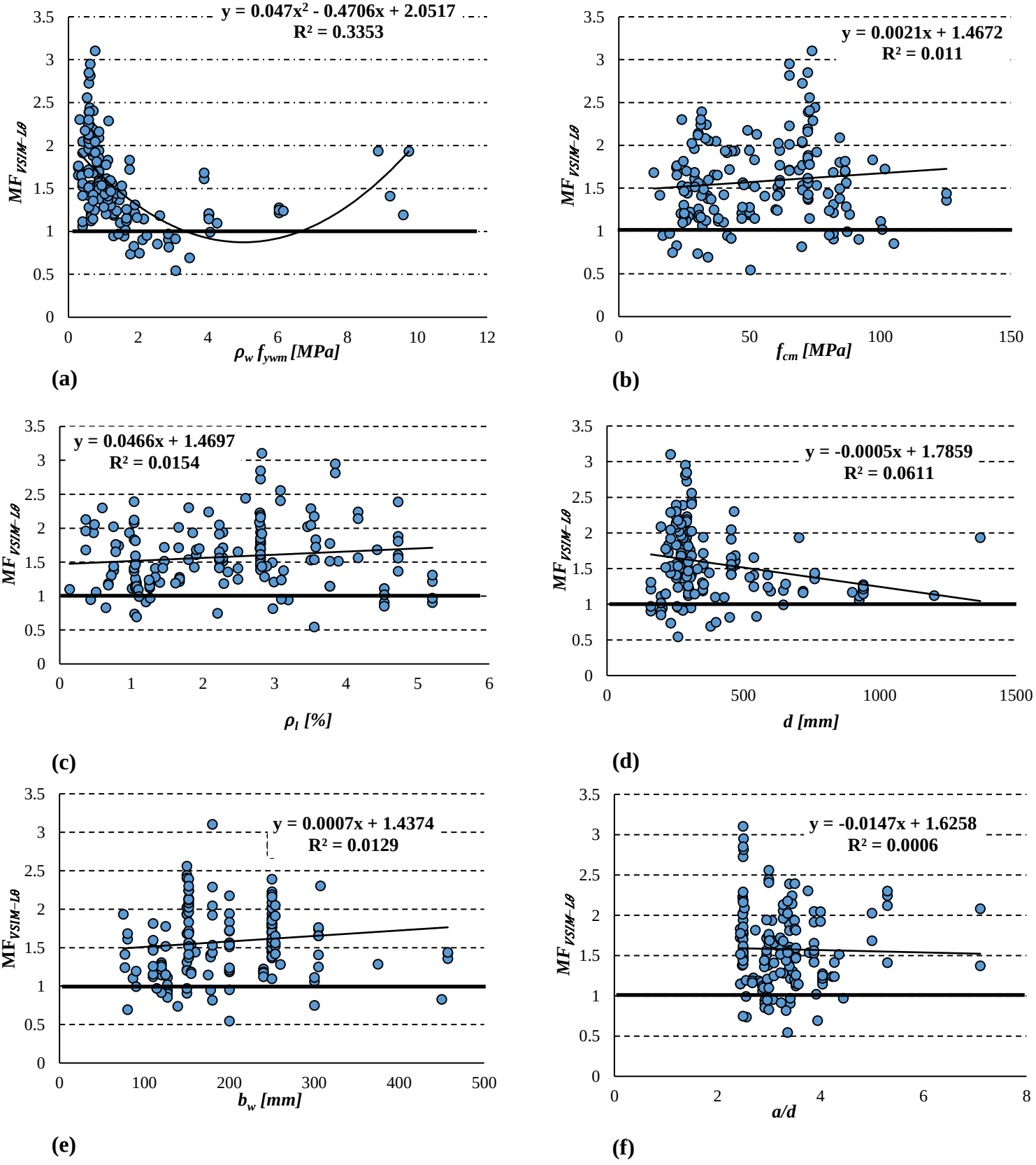

Figure 6.7. Scatter plots, with regression trend lines and correlation statistics of $MF_{VSIM-L\theta}$ versus (a) $\rho_w f_{ywm}$ (b) f_{cm} (c) ρ_l (d) d (e) b_w (f) a/d

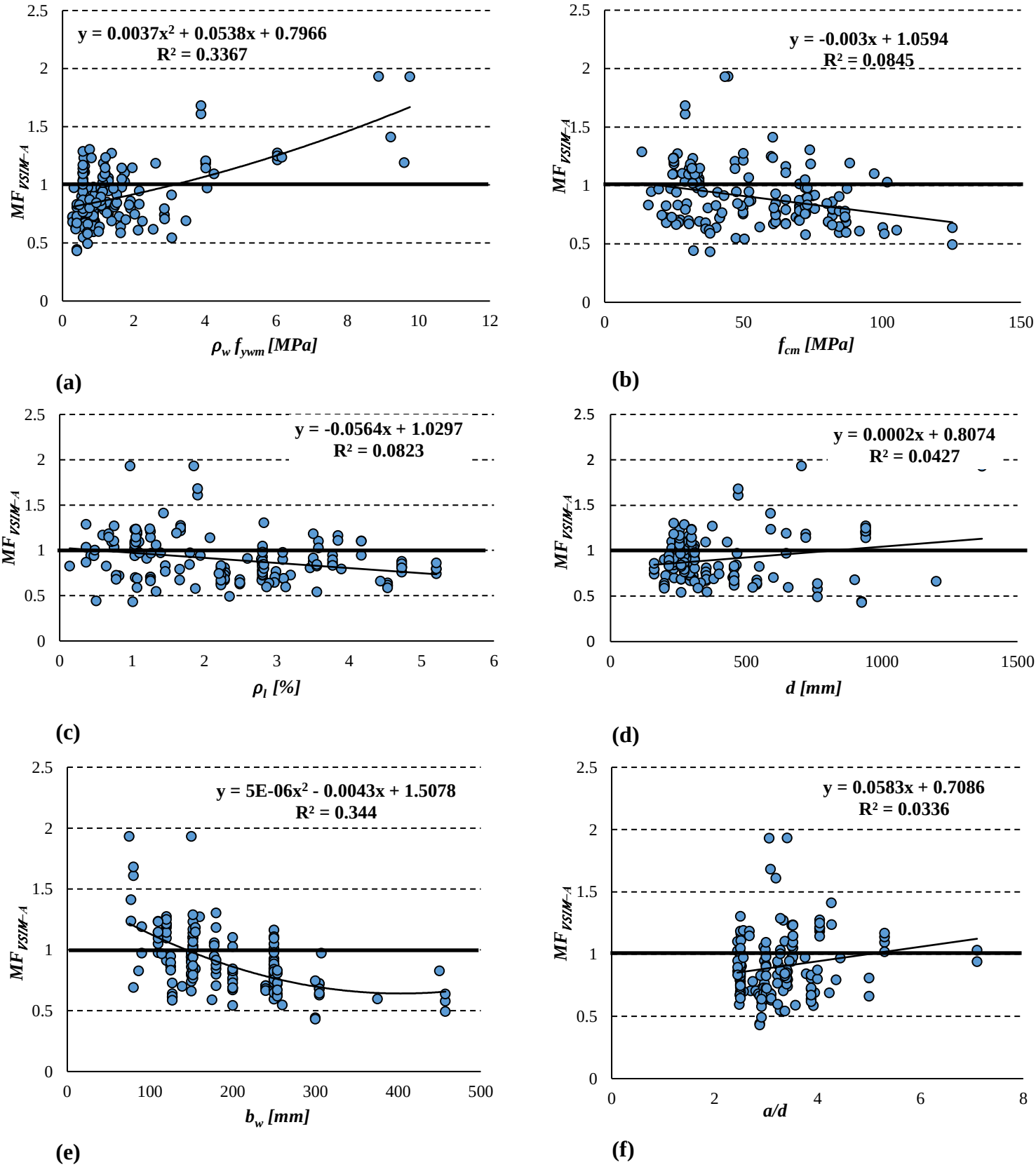

Figure 6.8. Scatter plots, with regression trend lines and correlation statistics of MF_{VSIM-A} versus (a) (a) $\rho_w f_{ywm}$ (b) f_{cm} (c) ρ_l (d) d (e) b_w (f) a/d

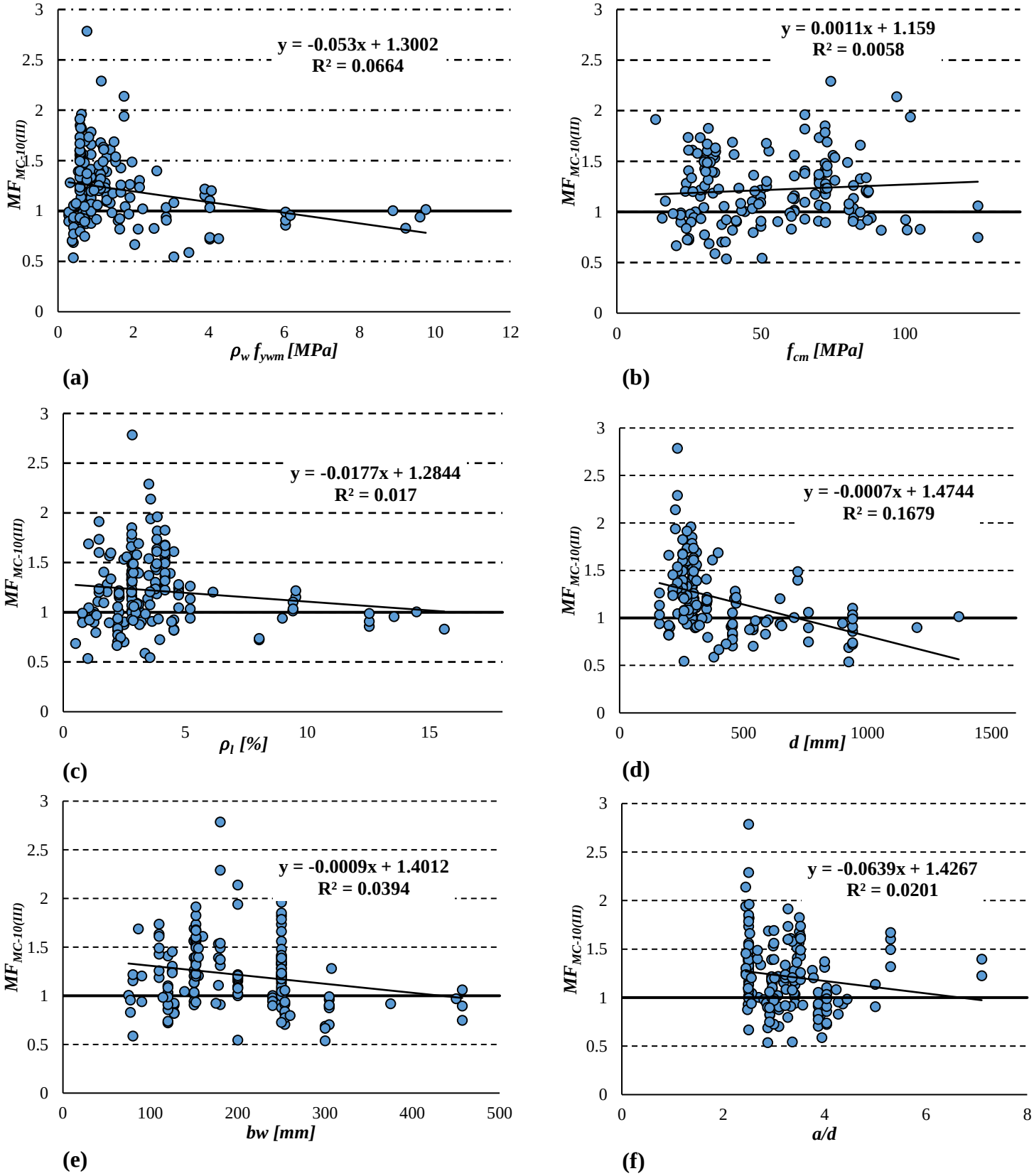

Figure 6.9. Scatter plots, with regression trend lines and correlation statistics of $MF_{MC-10(III)}$ versus (a) $\rho_w f_{ywm}$ (b) f_{cm} (c) ρ_l (d) d (e) b_w (f) a/d

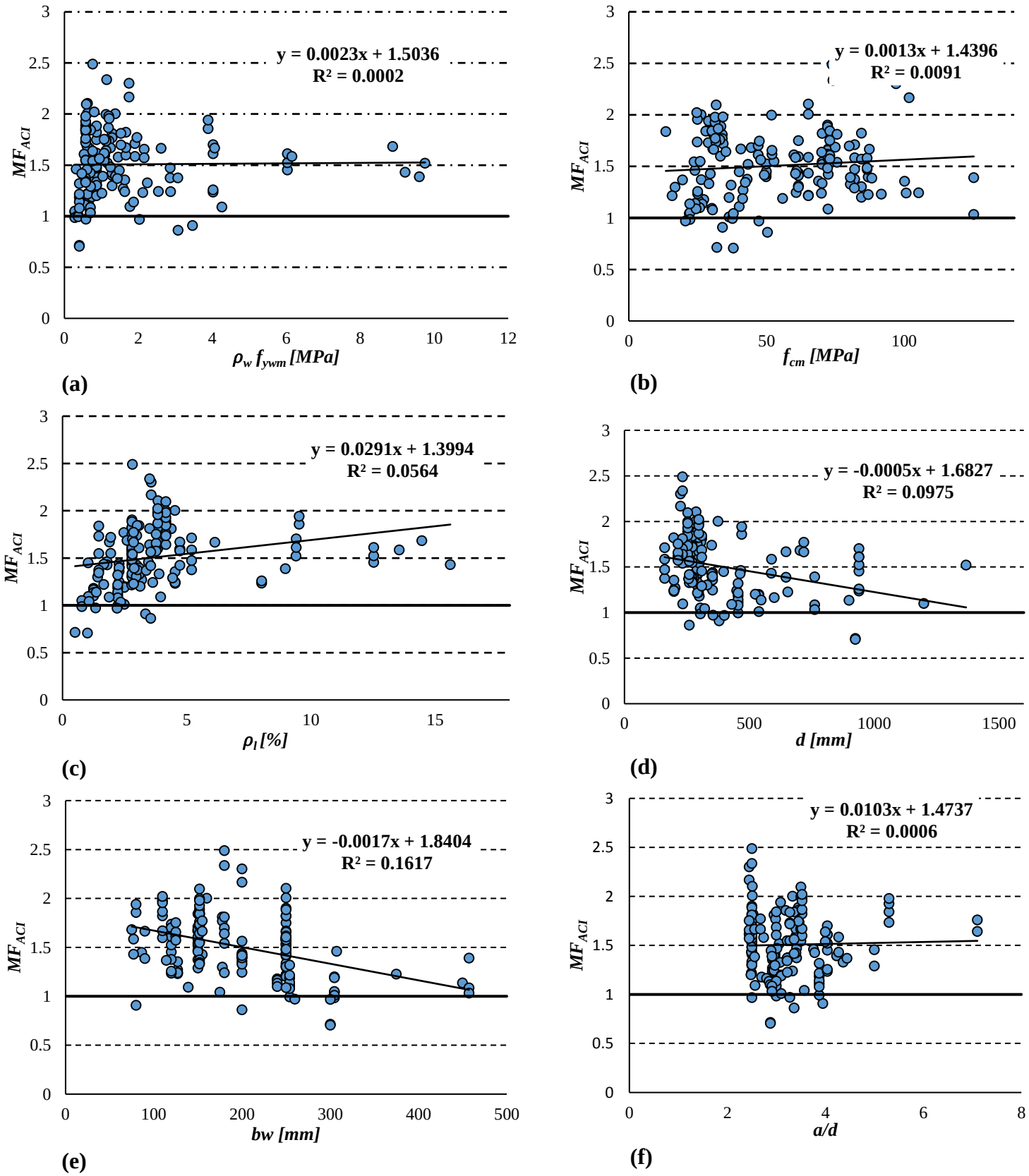

Figure 6.10. Scatter plots, with regression trend lines and correlation statistics of MF_{ACI} versus (a) (a) $\rho_w f_{ywm}$ (b) f_{cm} (c) ρ_l (d) d (e) b_w (f) a/d

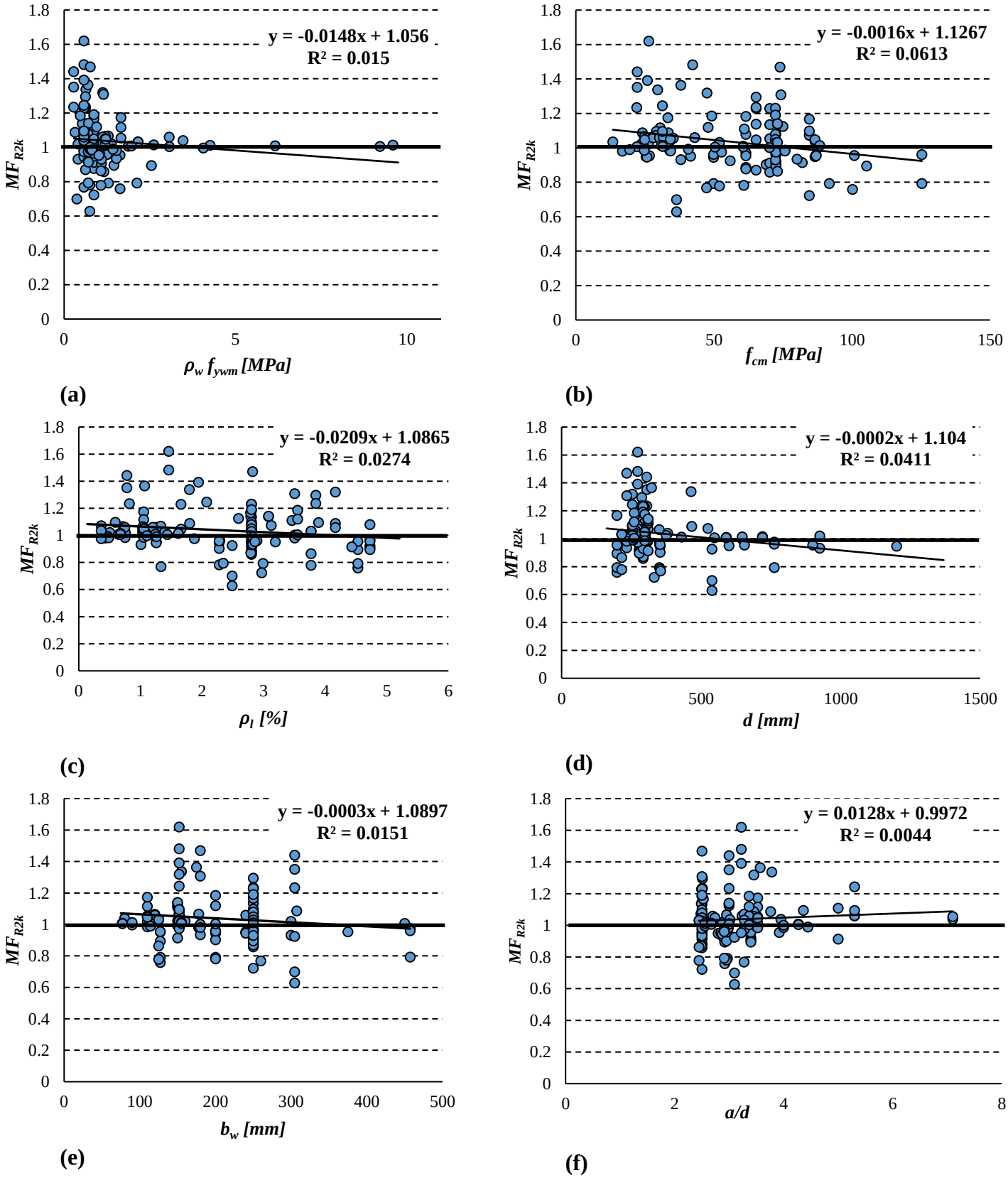

Figure 6.11 Scatter plots, with regression trend lines and correlation statistics of MF_{R2K} versus (a) $\rho_w f_{ywm}$ (b) f_{cm} (c) ρ_l (d) d (e) b_w (f) a/d

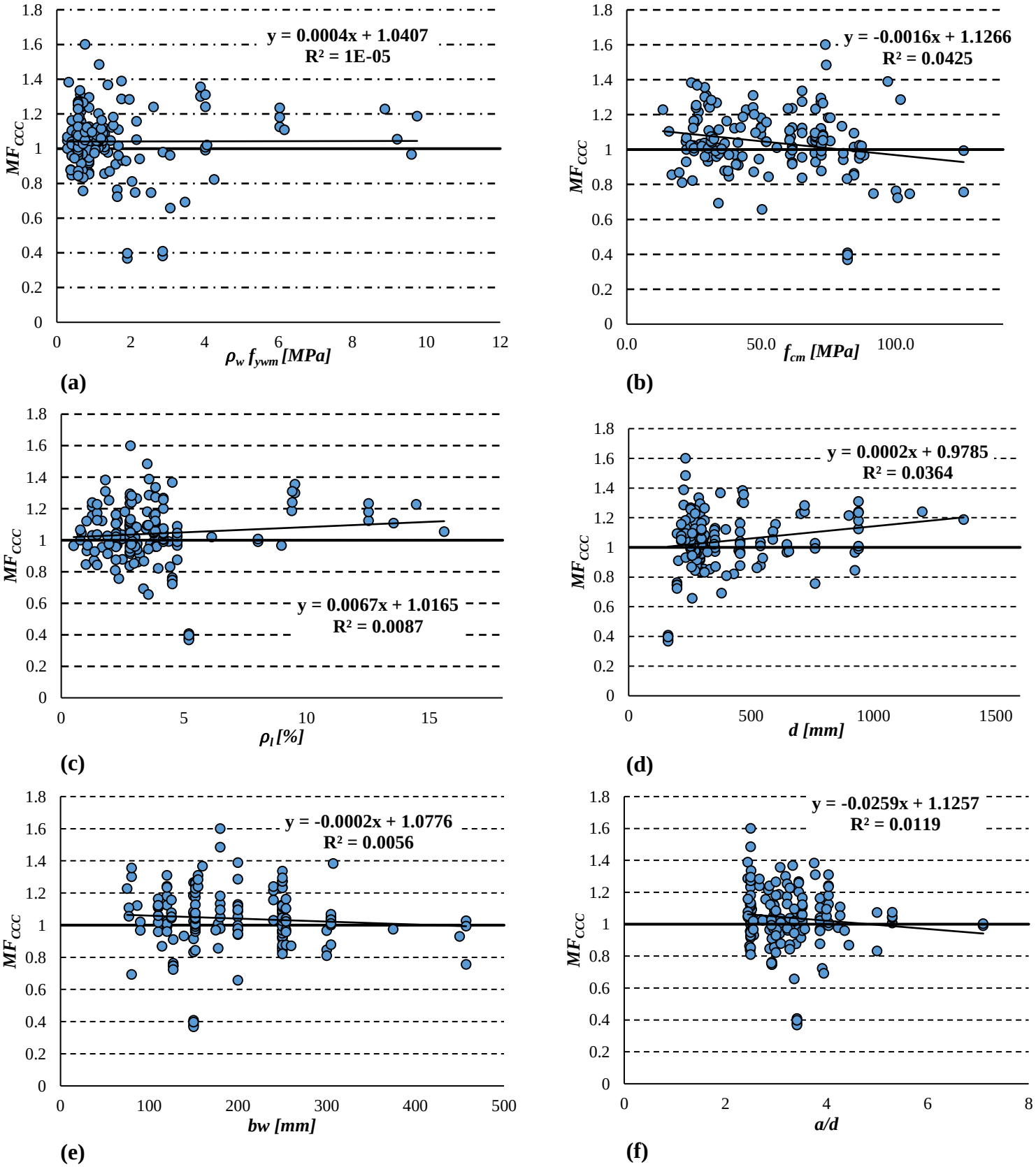

Figure 6.12. Scatter plots, with regression trend lines and correlation statistics of MF_{CCC} versus (a) (a) $\rho_w f_{ywm}$ (b) f_{cm} (c) ρ_l (d) d (e) b_w (f) a/d

6.4.4.1 $MF_{VSIM-L\theta}$ trend analysis

Figure 6.7 presents the scatter plots of model factor $MF_{VSIM-L\theta}$ against each of the parameters affecting shear strength (a) $\rho_w f_{ywm}$ (b) f_{cm} (c) ρ_l (d) d (e) b_w (f) a/d

Correlation with $\rho_w f_{ywm}$

In Figure 6.7 (a), $MF_{VSIM-L\theta}$ shows a significant trend with $\rho_w f_{ywm}$ with a negative correlation coefficient of -0.58 (Table 6.4). The plot shows that $V_{VSIM-L\theta}$ significantly underpredicts capacity at low $\rho_w f_{ywm}$ with decreasing conservative bias as $\rho_w f_{ywm}$ increases. The highest estimate of $MF_{VSIM-L\theta}$ observation is obtained at a low amount of stirrups ($\rho_w f_{ywm} < 1$ MPa) because in this range the limit on the concrete strut angle introduces a safety bias for $V_{VSIM-L\theta}$. The underprediction of shear capacity at low $\rho_w f_{ywm}$ is further caused by the neglect of the concrete contribution term in $V_{VSIM-L\theta}$ model formulation. $V_{VSIM-L\theta}$ tends to overpredict shear capacity in beams with a high amount of stirrups $\rho_w f_{ywm} > 1.8$ MPa.

Correlation with f_{cm}, ρ_l, d, a/d and b_w

$MF_{VSIM-L\theta}$ displays a slight negative trend with d (-0.25 correlation). Concrete strength f_{cm}, longitudinal reinforcement ρ_l, beam width b_w and shear span to depth ratio a/d show insignificant trends as corroborated by correlation coefficients r values below 0.12. These indicate that the most influential parameter is the amount of shear reinforcement ($\rho_w f_{ywm}$) also noted by (Mensah, 2015; Sykora *et al*., 2013).

6.4.4.2 MF_{VSIM-A} trend analysis

A comparison of MF_{VSIM-A} scatter plots (Figure 6.8[a-f]), and $MF_{VSIM-L\theta}$ scatter plots (Figure 6.7[a-f]) reflect the lower standard deviation associated with MF_{VSIM-A} about its mean**.** The comparison of the scatter plots of model factor $MF_{VSIM-L\theta}$ versus each of the (a) $\rho_w f_{ywm}$ (b) f_{cm} (c) ρ_l (d) d (e) b_w (f) a/d to that of MF_{VSIM-A}, respectively, provided an indication that the removal of the restriction on the concrete strut angle θ leads to generally unconservative MF_{VSIM-A} realisations (realisations lie predominantly below the $MF_{VSIM-A} = 1.0$ line).

Correlation with $\rho_w f_{ywm}$

A strong, increasing trend exists between MF_{VSIM-A} and increasing $\rho_w f_{ywm}$ with a strong correlation coefficient of 0.58 as indicated in Table 6.4. From Figure 6.8 it can be observed that the model factor was initially unconservative at $\rho_w f_{ywm} < 2$ and started to become conservative at $\rho_w f_{ywm} > 2$ where there is a paucity of data points. The trends, however, between $\rho_w f_{ywm}$ and the model factors MF_{VSIM-A} and $\text{MF}_{VSIM-L\theta}$ are opposite. The conservative bias increases for the MF_{VSIM-A} with increasing values of $\rho_w f_{ywm}$ and decrease for $\text{MF}_{VSIM-L\theta}$ with increasing $\rho_w f_{ywm}$.

Correlation with b_w

Figure 6.8 (d) shows that V_{VSIM-A} overestimated shear capacity as the beam width (b_w) increases. Moreover, a correlation value (r) of -0.59 particularly stated in Table 6.4 indicates a correlation between V_{VSIM-A} capacity predictions and b_w.

Correlation with f_{cm}, ρ_l, a/d

From Figure 6.8 and Table 6.4, the trends in MF_{VSIM-A} with the amount of longitudinal reinforcement (ρ_l) and concrete strength (f_{cm}) both have correlation coefficients of -0.29. MF_{VSIM-A} increases with increasing d with correlation coefficients of 0.21.

6.4.4.3 $MF_{MC-10(III)}$ trend analysis

The scatter plots of model factor $MF_{MC-10(III)}$ versus each of the (a) $\rho_w f_{ywm}$ (b) f_{cm} (c) ρ_l (d) d (e) b_w (f) a/d are presented in Figure 6.9.

Correlation with d

$MF_{MC-10(III)}$ realisations decrease with increasing depth d with a correlation coefficient of -0.41 (Figure 6.9(d)). This is an indication that MC-10 (III) method does not adequately account for the size effect on shear resistance.

Correlation with $\rho_w f_{ywm}$, f_{cm}, ρ_l, a/d, b_w

Figure 6.9 (a) displays a trend of $MF_{MC-10(III)}$ observations in the parametric range of $\rho_w f_{ywm}$ with a correlation coefficient of -0.26. The trend of decreasing conservative bias in $MF_{MC-10(III)}$ observations with increasing $\rho_w f_{ywm}$ is less severe than that of $MF_{VSIM-L\theta}$ (Figure 6.7(a)). $MF_{MC-10(III)}$ did not display any major trend with the concrete strength f_{cm}, longitudinal reinforcement ρ_l, beam width b_w and shear-span to depth ratio a/d.

6.4.4.4 MF_{ACI} trend analysis

Parametric scatter plots for model factor MF_{ACI} against the important factors affecting shear strength are illustrated in Figures 6.10 (a-f).

Correlation with d and b_w

Table 6.4 suggests a decreasing trend between the model factor MF_{ACI} with increasing member depth d and width b_w with a strong correlation coefficient of -0.40 and -0.31 respectively. The trend of MF_{ACI} is similar to the trend of $MF_{MC-10(III)}$ against d. This implies that the ACI method does not adequately account for size effect in shear resistance.

Correlation with $\rho_w f_{ywm}$, f_{cm}, ρ_l, a/d

Figure 6.10 shows a positive trend of MF_{ACI} with longitudinal reinforcement p_l with a correlation of 0.24. MF_{ACI} did not display any major trend with concrete cylinder strength f_{cm}, amount of shear reinforcement $\rho_w f_{ywm}$ and shear span to depth ratio a/d.

6.4.4.5 MF_{R2k} trend analysis

Parametric scatter plots for model factor MF_{R2k} against key parameters affecting shear strength are illustrated in Figures 6.11 (a-f). The figure portrays a scatter plot of MF_{R2k} observations with decreasing conservative bias as concrete strength f_{cm}, and depth d increases with the weak correlation values of -0.20 and -0.25 respectively. Also, MF_{R2k} did not show any major trend with shear parameters like the amount of shear reinforcement $\rho_w f_{ywm}$, longitudinal reinforcement, ρ_l, span to depth ratio, a/d and width b_w (see Table 6.4 and Figure 6.11).

6.4.4.6 MF_{CCC} trend analysis

The scatter plots for model factor MF_{CCC} against shear parameters are illustrated in Figures 6.12 (a- f). The figure presents a scatter plot of MF_{CCC} observations with decreasing conservative bias as concrete strength f_{cm} increases with a correlation coefficient of -0.21. The trend in the model factor with the depth d was also insignificant with a correlation coefficients of 0.19. Besides, MF_{CCC} did not show any major trends with other shear parameters like the amount of shear reinforcement $\rho_w f_{ywm}$, longitudinal reinforcement, ρ_l, shear-span to depth ratio, a/d and width b_w as shown in Table 6.4 and Figure 6.12.

6.4.5 Assessment of model factor statistics in different parameter ranges

The full database is subdivided based on parameter ranges as presented in Table 6.5 to assess the consistency of the model factor statistics across different parameter ranges. In general terms, it is observed that MF_{CCC} and MF_{R2k} present the lowest values of the standard deviation for most studied subsets. The comparison of results shown in Table 6.5 for the shear models revealed the changes in the model factor characteristics of each sample as the shear parameters are varied.

6.4.5.1 $\mathrm{MF}_{VSIM-L\theta}$ sample statistics

The statistics of $\mathrm{MF}_{VSIM-L\theta}$ are not consistent for the different parameter ranges as presented in Table 6.5 (a). The conservative bias μ_{MF} for $\mathrm{MF}_{VSIM-L\theta}$ is reduced for medium and highly shear reinforced members ($\rho_w f_{ywm} \geq 1$), ordinary and large members ($d > 300$), low and normal strength concrete members ($f_{cm} \leq 60$) and flanged beams relative to the conservative bias of the full database. In contrast, the conservative bias μ_{MF} increases for beams with low shear reinforcement ($\rho_w f_{ywm} < 1$), especially for small beams ($d < 300$) and high strength beams ($f_{cm} > 60$) relative to that of the full database. Standard deviation σ_{MF} is somewhat higher for high strength beams and rectangular beams.

6.4.5.2 MF_{VSIM-A} sample statistics

From Table 6.5 (b), the most conservative results are predicted for a subset of flanged beams only with $\mu_{MF} = 1.13$, while the most unconservative predictions are estimated for the subset of rectangular beams only ($\mu_{MF} = 0.79$). The standard deviation σ_{MF} and the mean value μ_{MF} of MF_{VSIM-A} for the full database (Table 6.2) are significantly higher than that of the subset of

rectangular beams only (Table 6.5 (b)) due to the inclusion of flanged beam experiments. EC2 assumes that shear force in flanged beams is carried by the web and does not consider the contribution of the compression flange to the shear resistance, thereby systematically understimating shear resistance for such members.

6.4.5.3 $MF_{MC-10(III)}$ sample statistics

The parameter range analyses (Table 6.5 (c)) carried out indicate that the mean value μ_{MF} decreased for heavily shear reinforced beams ($\rho_w f_{ywm} > 2$), large members ($d > 600$) and low strength concrete beams ($f_{cm} < 40$). The conservative bias μ_{MF} increases for small beams ($d < 300$) and low shear reinforced concrete beams ($\rho_w f_{ywm} < 1$). The standard deviation σ_{MF} associated with the different parameter ranges investigated are comparable to that of the full database.

6.4.5.4 MF_{ACI} sample statistics

The mean value μ_{MF} increases for small beams with $d < 300$ and beams with shear reinforcement in the range of $1 \leq \rho_w f_{ywm} \leq 2$. The standard deviation σ_{MF} for low strength beams ($f_{cm} < 40$) exceeded that of the full database by 0.08 (Table 6.5 (d)).

6.4.5.5 MF_{CCC} sample statistics

From Table 6.5 (e), it can be seen that the mean value μ_{MF} increases for large members ($d > 600$) and low strength concrete beams ($f_{cm} < 40$) by 0.08 and 0.07 respectively relative to the mean value of the full database (Table 6.2). The maximum reduction in mean value μ_{MF} of -0.03 was for high concrete strength $f_{cm} > 60$. The standard deviation σ_{MF} associated with the partial database exceeded that of the full database by 0.1 at high amount of shear reinforcement ($\rho_w f_{ywm} > 2$); and for four small flanged beams very low model factors were obtained which dramatically affects the skewness estimate for CCC.

6.4.5.6 MF_{R2k} sample statistics

The parameter range analyses reveal that the mean value μ_{MF} increases by at most 0.03 for $f_{cm} < 40\ MPa$ and the standard deviation σ_{MF} increases by at most 0.03 for ordinary size members ($300 \leq d \leq 600$) relative to the mean value of the full database (Table 6.2).

Table 6.5. Model factor statistics for different subsets of beams

a) $\mathbf{V_{VSIM-L\theta}}$

Parameters	$\boldsymbol{\rho_w f_{ywm}\ (MPa)}$			$\boldsymbol{f_{cm}\ (MPa)}$			$\boldsymbol{d(mm)}$			**Shape**	
	$\boldsymbol{<1}$	$\boldsymbol{1-2}$	$\boldsymbol{>2}$	$\boldsymbol{<40}$	$\boldsymbol{40-60}$	$\boldsymbol{>60}$	$\boldsymbol{<300}$	$\boldsymbol{300-600}$	$\boldsymbol{>600}$	**Rect**	**Flanged**
Mean(μ_{MF})	1.83	1.36	1.14	1.49	1.47	1.68	1.69	1.49	1.27	1.63	1.457
STD(σ_{MF})	0.43	0.29	0.33	0.43	0.42	0.51	0.51	0.42	0.23	0.48	0.43
Tests	87	44	29	56	30	74	87	44	29	109	51

b) $\mathbf{V_{VSIM-A}}$

Parameters	$\boldsymbol{\rho_w f_{ywm}\ (MPa)}$			$\boldsymbol{f_{cm}\ (MPa)}$			$\boldsymbol{d(mm)}$			**Shape**	
	$\boldsymbol{<1}$	$\boldsymbol{1-2}$	$\boldsymbol{>2}$	$\boldsymbol{<40}$	$\boldsymbol{40-60}$	$\boldsymbol{>60}$	$\boldsymbol{<300}$	$\boldsymbol{300-600}$	$\boldsymbol{>600}$	**Rect**	**Flanged**
Mean(μ_{MF})	0.83	0.91	1.08	0.95	0.95	0.84	0.90	0.85	1.00	0.79	1.13
STD(σ_{MF})	0.19	0.18	0.38	0.25	0.35	0.19	0.17	0.26	0.43	0.16	0.25
Tests	87	44	29	56	30	74	87	44	29	109	51

c) $\mathbf{V_{MC-10(III)}}$

Parameters	$\boldsymbol{\rho_w f_{ywm}\ (MPa)}$			$\boldsymbol{f_{cm}\ (MPa)}$			$\boldsymbol{d(mm)}$			**Shape**	
	$\boldsymbol{<1}$	$\boldsymbol{1-2}$	$\boldsymbol{>2}$	$\boldsymbol{<40}$	$\boldsymbol{40-60}$	$\boldsymbol{>60}$	$\boldsymbol{<300}$	$\boldsymbol{300-600}$	$\boldsymbol{>600}$	**Rect**	**Flanged**
Mean(μ_{MF})	1.25	1.33	0.96	1.19	1.13	1.28	1.36	1.06	0.95	1.19	1.27
STD(σ_{MF})	0.37	0.31	0.28	0.35	0.28	0.37	0.35	0.27	0.22	0.36	0.33
Tests	87	44	29	56	30	74	87	44	29	109	51

d) $\mathbf{V_{ACI}}$

Parameters	$\boldsymbol{\rho_w f_{ywm}\ (MPa)}$			$\boldsymbol{f_{cm}\ (MPa)}$			$\boldsymbol{d(mm)}$			**Shape**	
	$\boldsymbol{<1}$	$\boldsymbol{1-2}$	$\boldsymbol{>2}$	$\boldsymbol{<40}$	$\boldsymbol{40-60}$	$\boldsymbol{>60}$	$\boldsymbol{<300}$	$\boldsymbol{300-600}$	$\boldsymbol{>600}$	**Rect**	**Flanged**
Mean$(\boldsymbol{\mu_{MF}})$	1.47	1.64	1.43	1.47	1.45	1.55	1.63	1.34	1.35	1.44	1.64
STD$(\boldsymbol{\sigma_{MF}})$	0.33	0.29	0.27	0.38	0.25	0.28	0.28	0.29	0.31	0.32	0.27
Tests	87	44	29	56	30	74	87	44	29	109	51

e) V_{CCC}

Parameter	$\boldsymbol{\rho_w f_{ywm}\ (MPa)}$			$\boldsymbol{f_{cm}\ (MPa)}$			$\boldsymbol{d(mm)}$			**Shape**	
	$\boldsymbol{<1}$	$\boldsymbol{1-2}$	$\boldsymbol{>2}$	$\boldsymbol{<40}$	$\boldsymbol{40-60}$	$\boldsymbol{>60}$	$\boldsymbol{<300}$	$\boldsymbol{300-600}$	$\boldsymbol{>600}$	**Rect**	**Flanged**
Mean$(\boldsymbol{\mu_{MF}})$	1.06	1.06	1.03	1.11	1.09	1.01	1.04	1.04	1.12	1.01	1.15
STD$(\boldsymbol{\sigma_{MF}})$	0.15	0.22	0.29	0.17	0.16	0.23	0.22	0.17	0.18	0.20	0.16
Tests	87	44	29	56	30	74	87	44	29	109	51

f) $\boldsymbol{V_{R2k}}$

Parameters	$\boldsymbol{\rho_w f_{ywm}\ (MPa)}$			$\boldsymbol{f_{cm}\ (MPa)}$			$\boldsymbol{d(mm)}$			**Shape**	
	$\boldsymbol{<1}$	$\boldsymbol{1-2}$	$\boldsymbol{>2}$	$\boldsymbol{<40}$	$\boldsymbol{40-60}$	$\boldsymbol{>60}$	$\boldsymbol{<300}$	$\boldsymbol{300-600}$	$\boldsymbol{>600}$	**Rect**	**Flanged**
Mean$(\boldsymbol{\mu_{MF}})$	1.06	1.00	1.00	1.07	1.00	1.02	1.06	1.02	0.96	1.04	1.04
STD$(\boldsymbol{\sigma_{MF}})$	0.18	0.12	0.07	0.16	0.18	0.14	0.15	0.19	0.06	0.19	0.053
Tests	78	32	20	46	20	64	78	32	20	92	38

6.4.6 Demerit Points analysis

Collins (2001) introduced the Demerit Points analysis to assess the performance of various shear strength methods. The method measures the agreement between V_{exp} and V_{model} (with the bias included). It is based on allocating a Demerit Point value (DP) as shown in Table 6.6 for each range of model factor MF_x realisations. The V_{model} model is computed here with the bias accounted for. The Total Demerit Point score (TDP) is computed by adding the products of the percentage of each range of MF_x realisations and the DP for that range.

The TDP score shows the overall performance of the shear strength method. A smaller value of TDP indicates the shear method to be more reliable in predicting the shear strength of reinforced concrete beams. The system of analysis is applied to evaluate the performance of the investigated shear models in predicting the shear strength of experimental beams in the database. The DP score for each classification is summarised in Table 6.6. The calculated TDP score for the shear models is presented in Table 6.7 and illustrated in Figure 6.13 for visualisation.

Table 6.6. Collins (2001) Demerit Points classification

S/N	Classification	MF_x range	DP
1	Extremely dangerous	< 0.5	10
2	Dangerous	0.5-0.65	5
3	Low safety	0.65-0.85	2
4	Appropriate Safety	0.85-1.30	0
5	Conservative	1.30-2.00	1
6	Extremely conservative	>2.0	2

Table 6.7. Demerit Point analysis

Range	Classification	DP	$MF_{VSIM-L\theta}$ (%)	MF_{VSIM-A} (%)	$MF_{MC-10(III)}$ (%)	MF_{ACI} (%)	MF_{CCC} (%)	MF_{R2k} (%)
< 0.5	Extremely dangerous	10	3	1	2	1	3	0
0.5-0.65	Dangerous	5	8	3	6	4	0	0
0.65-0.85	Low safety	2	22	30	26	24	12	10
0.85-1.30	Appropriate Safety	0	52	53	50	67	81	85
1.30-2.00	Conservative	1	15	12	15	4	4	5
>2.0	Extremely conservative	2	0	1	1	0	0	0
Total Demerit Points (TDP)			**129**	**99**	**119**	**82**	**54**	**25**

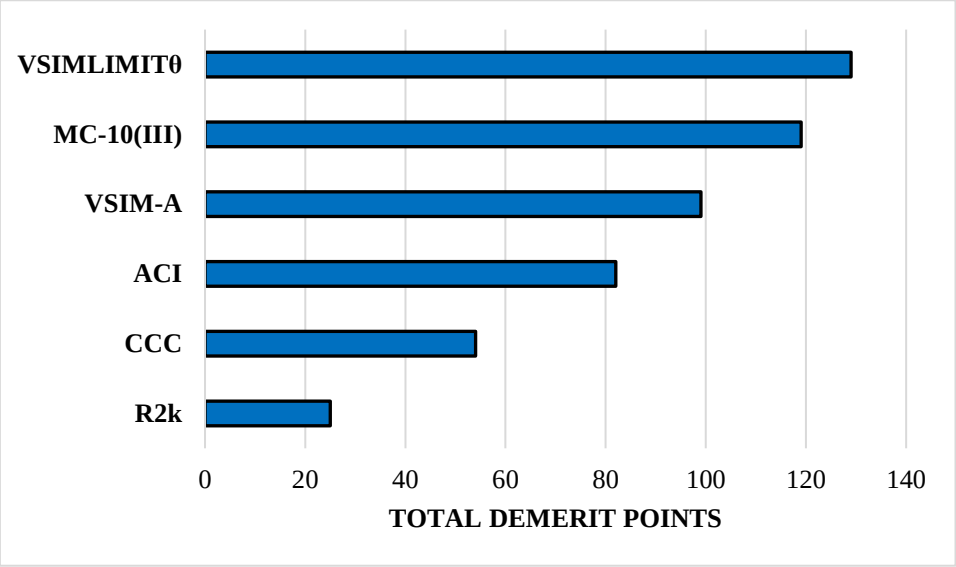

Figure 6.13. Demerit Point analysis

From Table 6.7 and Figure 6.13, the following observations were made:

- MCFT (R2k) obtained the lowest score with TDP of 25 and therefore gives the best performance, based on the analysis.
- V_{CCC} is the closest to V_{R2k} out of all the models investigated with a TDP score of 54.
- V_{ACI} and V_{VSIM-A} models earn 82 and 99 TDP score respectively.
- The worst of the procedures analysed was the operational EC2 VSIM model ($V_{VSIM-L\theta}$). The shear procedure obtained the highest TDP score of 129.

6.4.7 Choice of a probability distribution

The determination of the most suitable probability distribution function for the observed data is one of the primary goals of statistical analysis. According to the Joint Committee on Structural Safety (JCSS) Probabilistic Model Code (JCSS, 2001), the lognormal distribution is the most common distribution applied to model factors. This recommendation is also corroborated by Holicky *et al.* (2015) and Mensah (2015) specifically with regards to model factors for shear capacity predictions. Therefore, the lognormal distribution was taken as the candidate distribution for the model factors. A lognormal distribution with mean and coefficient of variation can be used to describe the characterised model factors probabilistically.

Figure 6.14 illustrates the probability density functions of the derived model factor associated with $V_{VSIM-L\theta}$, V_{VSIM-A}, $V_{MC-10(III)}$, V_{CCC} and V_{R2k} based on the evaluation database. It appears that V_{R2k} is the most appropriate model with the lowest uncertainty and bias close to unity; with V_{CCC} a close contender.

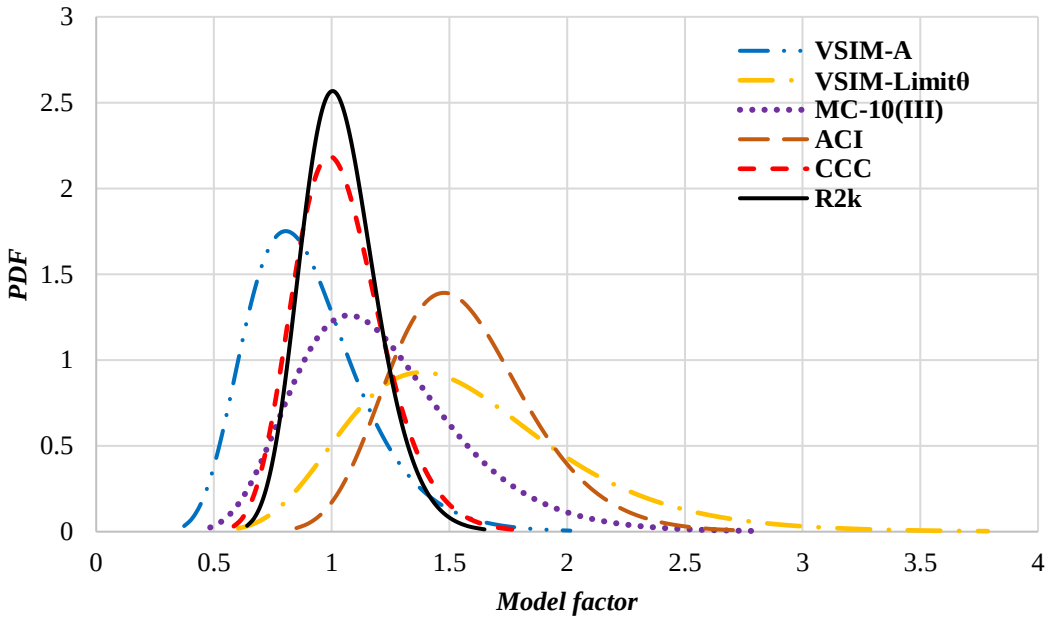

Figure 6.14. Probability density functions of the model factors

6.4.7.1 Skewness representation of the 2P-LN distribution

The skewness reported in Table 6.2, as determined according to Equation 6.11, is representative of the scatter of MF realisations and is not that associated with the 2P-LN distribution. Holický (2009), stated that the skewness is very sensitive to extreme values of a sample. The skewness of any MF represented by the 2P-LN distribution is expressed by Equation 6.12.

$$\eta_k = {\Omega_X}^3 + 3\Omega_X \tag{6.12}$$

Using the coefficient of variation (Ω_X) from Table 6.2, and according to Equation 6.12, the skewness η_k for $MF_{VSIM-L\theta}$ was determined as 0.93 (compared to 0.61 of the realisations shown in Table 6.2), whereas that for MF_{VSIM-A} was determined as 0.83 (compared to 1.26 from Table 6.2). The skewness for $MF_{MC-10(III)}$ was determined as 0.89 (compared to 0.90 of the realisations shown in Table 6.2), whereas that for MF_{ACI} was determined as 0.58 (compared to 0.15 from Table 6.2). The skewness for MF_{R2k} was determined as 0.45 (compared to 0.74 from Table 6.2), whereas that for MF_{CCC} was determined as 0.55 (compared to -0.74 in Table 6.2 for all the realisations; and 0.4 when the four

small flanged beams are omitted from the dataset). Sykora *et al.* (2018) points out that the skewness is significantly affected by extreme values. The inclusion of the four small flanged beams with very low model factor realisations (initially identified as potential outliers for CCC in Section 6.4.2) in the skewness calculation dramatically affects the skewness estimate for CCC. However, the relation between the data skewness and fitted distribution skewness improved with the omission of the four small flanged beams in the skewness calculation.

2P-Lognormal distributions had a higher ranking than Normal distribution in terms of the Kolmogorov-Smirnov and Shapiro-Wilk's W goodness of fit test, which was executed using NCSS data distribution fitting program for the model factors except for ACI. The skewness of 0.15 for ACI is closer to what is expected from a normal distribution, hence a normal distribution would appropriately represent its model factor realisations.

Holický (2009) advises that a skewness of 0.5 can be taken as a relatively high value. McBean and Rover (1998) provided a further guideline as follows; a distribution is considered highly skewed if the absolute value of skewness is greater than one; a distribution with skewness value from 0.5 to 1 is considered moderately skewed. The preceding results gave indication that the 2P-Lognormal distribution generally underestimated or overestimated the skewness of the actual data. Underestimating the skewness has the effect of underestimating the reliability β of the tail end of the resistance distribution. The assumption of 2P-Lognormal distribution for the model factors leads to some overestimation of skewness for CCC and similar underestimation of skewness for MCFT (R2k). This implies CCC as GPM will tend to overestimate reliability while R2k as GPM will tend to underestimate reliability.

6.5 Results and general discussion

6.5.1 Discussion of $MF_{VSIM-L\theta}$ results

As presented in Table 6.2, $MF_{VSIM-L\theta}$ has a mean value of $\mu_{MF} = 1.58$, confirming that the unbiased shear resistance function $V_{VSIM-L\theta}$ generally underpredicts shear capacity. The spread of $\sigma_{MF} = 0.48$ suggests a large scatter of $MF_{VSIM-L\theta}$ about the mean. In fact, this procedure yields the largest standard deviation (σ_{MF}) of all the models studied. Based on the Demerit Point analysis (Table 6.7), the $V_{VSIM-L\theta}$ approach produces "extremely dangerous" results (i.e. $MF_{VSIM-L\theta} > 2$) for 3% of the beams which is the highest number in that level of classification when compared to other models studied. Parametic correlation and regression analyses showed that $MF_{VSIM-L\theta}$ observations

are sensitive to $\rho_w f_{ywm}$ (Table 6.4). The assessment of the model factor statistics at different parameter ranges indicate inconsistency in $\mathrm{MF}_{VSIM-L\theta}$ statistics (Table 6.5(a)).

Table 6.8 presents various model factor statistics related to the studied shear strength models as provided in literature. The mean and the standard deviation of the operational EC2 VSIM model factor $\mathrm{MF}_{VSIM-L\theta}$ derived in this study is higher than that recommended by JCSS (2001) and considerably lower than those reported by other authors listed in Table 6.8. For instance, JCSS (2001) reports a standard deviation of 0.1 for the model factor related to the shear capacity of reinforced concrete beams, whereas in this study, a standard deviation of 0.48 was obtained using the EC2 shear resistance model. It is important to note that underestimation of the dispersion of the model factor may also represent an overestimation of the corresponding implicit safety levels. The large bias ($\mu_{MF} = 1.58$), high uncertainty ($\sigma_{MF} = 0.48$) and high TDP score (TDP=129) displayed by $\mathrm{MF}_{VSIM-L\theta}$ and its trend with $\rho_w f_{ywm}$ makes it evident that the $\mathrm{V}_{VSIM-L\theta}$ is not a suitable candidate for general probabilistic model representation of shear resistance.

Table 6.8. Model factor statistics from literature

	Source	Mean (μ_{MF})	S.D (σ_{MF})	Sample size #
EC2 ($\mathbf{MF}_{VSIM-L\theta}$)	Cladera & Mari (2004)	1.83	0.73	193
	Hawkins *et al*. (2005)	1.7	0.63	160
	Cladera & Mari (2007)	1.64	0.52	122
	Russo *et al*. (2013)	1.94	0.91	474
	Mensah (2015)	1.65	0.51	222
	Riberio *et al*. (2016)	1.68	0.57	103
	Mari *et al*. (2015)	1.72	0.64	239
	Olalusi and Viljoen (2017)	1.62	0.49	113
	Sykora *et al*. (2013) (Rectangular)	1.63	0.32	200
	Cladera *et al*. (2016)	1.47	0.39	170
EC2 ($\mathbf{MF}_{VSIM-A}$)	Olalusi and Viljoen (2017) (Rectangular)	0.78	0.15	113
Response 2000	Bentz (2000)	1.05	0.13	534
	Mensah (2015)	1.14	0.20	116
	Cladera (2003)	1.07	0.18	123
	Olalusi and Viljoen (2017)	1.05	0.18	98
Model Code 10 (III)	Sigrist *et al* (2013)	1.20	0.16	243
	Krejsa *et al*. (2014) (Rectangular)	1.11	0.24	199
	Mari *et al*. (2015) (Rectangular)	1.21	0.22	239
	Cladera *et al*. (2016)	1.28	0.22	170
	Sykora *et al*. (2018) (Rectangular)	1.14	0.26	450
ACI-08	Bentz (2000) (with and without stirrups)	1.20	0.38	448
	Cladera and Mari (2007) (Rectangular)	1.38	0.31	122
	Arslan (2008) $f_c \leq 41.4$	1.41	0.33	105
	$f_c > 41.4$	1.29	0.44	154
	Russo *et al*. (2013)	1.40	0.38	474
	Reineck *et al*. (2014)	1.59	0.40	157
	Ribeiro *et al*. (2016)	1.48	0.48	273
	Mari *et al*. (2017) (Rectangular)	1.25	0.26	239
	Cladera *et al*. (2016)	1.53	0.38	170
CCC	Cladera *et al*. (2016)	1.16	0.16	170

6.5.2 Discussion of MF_{VSIM-A} results

From Table 6.2 it can be seen that MF_{VSIM-A} has a mean value of $(\mu_{MF} = 0.90)$, indicating that V_{VSIM-A} generally overpredicts shear capacity. MF_{VSIM-A} shows less scatter about the mean with standard deviation of $\sigma_{MF} = 0.25$. The difference in the mean values of MF_{VSIM-A} $(\mu_{MF} = 0.90)$ and $MF_{VSIM-L\theta}$ $(\mu_{MF} = 1.58)$ quantifies the conservative influence of the limiting concrete compressive strut angle. The Demerit Point analysis (Table 6.7) indicates that VSIM-A has TDP score of 99. The analysis reveals that VSIM-A approach produces results that are in the region of "low safety" and "extremely dangerous" for about 34% of the beams. Parametric correlation and regression analyses portray MF_{VSIM-A} observations to be sensitive to $\rho_w f_{ywm}$ and beam width b_w (Table 6.2).

The performance of MF_{VSIM-A} in terms of bias $(\mu_{MF} = 0.90)$, uncertainty $(\sigma_{MF} = 0.25)$, high TDP score (TDP=99) and strong sensitivity to important shear parameters (shear reinforcement $\rho_w f_{ywm}$ and beam width b_w) makes it obvious that the V_{VSIM-A} is not a suitable candidate for general probabilistic model representation of shear resistance.

6.5.3 Discussion of $MF_{MC-10(III)}$ results

$MF_{MC-10(III)}$ was found to have a mean value $(\mu_{MF} = 1.21)$ implying that the MC-10 (III) shear resistance predictions generally underestimate shear capacity (similar to $MF_{VSIM-L\theta}$). Regarding model uncertainty, $MF_{MC-10(III)}$ has a standard deviation of $\sigma_{MF} = 0.35$. The shear method has a high Total Demerit Point score (TDP) of 119 indicating that the method does not corresponds reasonably with experimental results (Figure 6.13).

The correlation and regression analysis (Table 6.2) of $MF_{MC-10(III)}$ against shear parameters reveals that $V_{MC-10(III)}$ is significantly sensitive to the member depth d. This trend was also identified by other researchers (Krejsa *et al.*, 2014; Cladera *et al.*, 2016; Mari *et al.*, 2015). This implies that MC-10 (III) method does not adequately account for the size effect on shear resistance. This could lead to possible unsafe shear capacity prediction for beams with large depth. The parameter range analyses (Table 6.5 (c)) indicate inconsistency in $MF_{MC-10(III)}$ statistics as the shear parameters are varied.

The large bias ($\mu_{MF} = 1.21$) and high uncertainty ($\sigma_{MF} = 0.35$) displayed by $MF_{MC-10(III)}$ and its strong trend with member depth d, indicate that the $V_{MC-10(III)}$ model may not be a suitable candidate for general probabilistic model representation for shear resistance.

6.5.4 Discussion of MF_{ACI} results

MF_{ACI} has a mean value of $\mu_{MF} = 1.56$, demonstrating that V_{ACI} generally underpredicts shear capacity similar to $MF_{VSIM-L\theta}$. This procedure yields the highest mean value (μ_{MF}) of all the models investigated. MF_{ACI} has a standard deviation of $\sigma_{MF} = 0.30$ comparable to that of $MF_{MC-10(III)}$. The Demerit Point analysis shown in Table 6.7 deemed 5% of its prediction to be "dangerous" and "extremely dangerous".

Parametric correlation and regression analyses of MF_{ACI} against shear parameters indicate that V_{ACI} is significantly sensitive to the member depth d and beam width b_w, also identified by Ribeiro *et al*., (2016). The trends reveal that the ACI method does not adequately account for size effect in shear resistance. Shear resistance according to ACI-318 is the addition of the contribution from concrete and contribution from stirrups (see Section 3.2.1). The concrete contribution term in ACI-318 is expressed by an empirical equation for beams without stirrups. According to Ismail (2016), Song *et al*. (2010) and Kuchma & Collins (1998), ACI 318- 14 shear procedures yield unconservative capacity predictions for large reinforced concrete beams without stirrups as size effect is not adequately accounted for. Therefore, it could be said that size effect in ACI-318 is directly inherited from the equation for members without stirrups (empirically derived from beams with average depth of 340mm). The potential unsafe performance for large size beams is a cause for concern. The parameter range analyses (Table 6.5 (d)) indicate inconsistency in MF_{ACI} statistics at different shear parameter ranges.

The poor performance of MF_{ACI} in terms of bias ($\mu_{MF} = 1.56$), uncertainty ($\sigma_{MF} = 0.30$), high TDP score (TDP=82) and strong sensitivity to important shear parameters (member depth d and beam width b_w), is an indication that the V_{ACI} model may not be a suitable candidate for general probabilistic model representation for shear resistance.

6.5.5 Discussion of MF_{CCC} results

MF_{CCC} has a mean a value of $\mu_{MF} = 1.04$ and relatively low standard deviation of $\sigma_{MF} = 0.19$ when compared to those of the previously discussed models $MF_{VSIM-L\theta}$, MF_{VSIM-A}, $MF_{MC-10(III)}$, and

MF_{ACI}. The lower TDP score (Table 6.7) and the lower mean value and standard deviation (Table 6.2) related to V_{CCC} is an indication that the shear model agrees better with the experimental results than all the previously discussed shear methods. As stated in the DP analysis (Table 6.7), the shear strength of 81% of the experimental beam test is predicted within the appropriate safety range. However, 3% of the predicted values gave an "extremely dangerous" estimation of the shear strength (flanged beams with small section sizes [$b_w = 150\ mm$ and $d = 161\ mm$]). Generally, the trends of MF_{CCC} observations are less severe compared to the trend of all the studied models against main shear parameters. This means that the CCC model reasonably predicts the effect of the main shear parameters on shear resistance.

The better performance of MF_{CCC} in terms of bias ($\mu_{MF} = 1.04$), uncertainty ($\sigma_{MF} = 0.19$), TDP score (TDP=54) and milder sensitivity to main shear parameters makes V_{CCC} a potential candidate for general probabilistic model representation of shear resistance.

6.5.6 Discussion of MF_{R2k} results

As presented in Table 6.2, MF_{R2k} has a mean value of $\mu_{MF} = 1.04$ similar to MF_{CCC}. This confirms V_{R2k} and V_{CCC} on average as the most precise of the shear strength models applied to the experimental database in this study. MF_{R2k} displayed the lowest standard deviation of all models at $\sigma_{MF} = 0.16$. Based on the Demerit Point analysis (Table 6.7), the shear strength of 85% of the experimental beam test is predicted within the appropriate safety. None of the beams had predicted capacity equivalent to a "dangerous " or "extremely conservative" estimation of the shear strength. The parameter range analyses reflect consistency in MF_{R2k} statistics at the shear parameter ranges studied. The trends of MF_{R2k} observations are less severe compared to the trends of $MF_{VSIM-L\theta}$, MF_{ACI}, $MF_{MC-10(III)}$, and MF_{VSIM-A} against most shear parameters (see Figures 6.9 to 6.12).

The small bias ($\mu_{MF} = 1.04$), low uncertainty ($\sigma_{MF} = 0.16$) and the low TDP score (TDP=25) displayed by MF_{R2k} and its milder sensitivity to main shear parameters makes V_{R2k} the best predictor of shear resistance and the most suitable candidate for general probabilistic model representation of shear resistance of all the models considered.

6.6 Choice of general probabilistic model for shear resistance

An effective reliability assessment of a shear design procedure requires the use of a suitable general probability model (GPM) for shear resistance with corresponding model factor statistics. The general probabilistic model is a model of real shear resistance. The development of a probabilistic model for shear consists of three steps, namely the choice of shear resistance model, estimation of the model factor statistics (Section 6.4.3) and the selection of the most appropriate distribution function for the model factor (Section 6.4.7). A suitable GPM of shear should be based on shear resistance model defined by the following three criteria:

- Shear model with the minimum bias
- Shear model with the minimum uncertainty
- Shear model whose model factor has no significant sensitivity with shear parameter

The choice of GPM may influence our ability to assess safety performance adequately.

6.6.1 Suitability of MCFT (R2k) and CCC model as GPM for reliability analysis

MF_{CCC} and MF_{R2k} observations were found to have a mean value of $\mu_{MF} = 1.04$ which is the lowest of all the models investigated. In terms of standard deviation, both MF_{CCC} and MF_{R2k} have the lowest uncertainties with a standard deviation of $\sigma_{MF} = 0.19$ and 0.16. The trend analysis conducted revealed that MF_{CCC} and MF_{R2k} observations did not display any significant trends with the shear parameters investigated in this study. This implies that both models have captured the effect of shear parameters well.

The high accuracy displayed by both MF_{CCC} and MF_{R2k} observations, coupled with their relatively low uncertainty and statistical independence with major shear parameters, are features that warranted the consideration of CCC model and MCFT (R2k) calculation procedure suitable to be used as a general probabilistic model (GPM) for shear reliability and partial factor calibration. Also, the trends of normalised resistance predictions from MCFT (R2k) and CCC model bear the closest match to experimental results (see Section 4.4.1).

By considering the standard deviation ($\sigma_{MF} = 0.16$), MF_{R2k} was therefore judged to be most accurate and most suitable for the shear capacity prediction of reinforced concrete beams. Consequently, the MCFT (R2k) model was adopted to be implemented as the principal GPM for the reliability assessment of the EC2 shear design procedure and other shear design procedures. A CCC model

based GPM was subsequently implemented as an alternative GPM to validate the principal reliability investigation.

6.7 Conclusions

The key model factor statistics were derived using a database of shear reinforced experiments towards an effective reliability performance assessment of shear design procedures. Important conclusions obtained from this chapter that guided the reliability investigations presented in Chapters 7 and 8 are presented below:

- The sensitivity of $\mathrm{MF}_{VSIM-L\theta}$ to $\rho_w f_{ywm}$ (Figure 6.7(a)), especially the overestimation of shear capacity at high $\rho_w f_{ywm}$ raises concern that the design procedure may give rise to designs that are not sufficiently conservative for beams with high levels of stirrup reinforcement. The underestimation of capacity at low $\rho_w f_{ywm}$ is equally an issue of concern. Since $\mathrm{V}_{VSIM-L\theta}$ calculation procedure is an adaptation of the operational EC2 design method, reliability assessment of the EC2 design method is necessary to assess the uniformity of its performance with regard to the reliability index across range of practical application.
- $MF_{MC-10(III)}$ and MF_{ACI} portray a decreasing trend with increasing effective member depth d (Figure 6.9(d) and 6.10(d) respectively). This may lead to unsafe shear capacity predictions for beams with large depth. Reliability assessment of the design procedures should appraise the implicit reliability at variations of possible member depth d.
- Both V_{CCC} and V_{R2k} models achieved a more suitable characterisation of model factors in terms of mean and spread. MF_{CCC} has a mean value of $\mu_{MF} = 1.04$ and a spread of $\sigma_{MF} = 0.19$. MF_{R2k} is a better predictor of resistance in terms of spread with mean value of $\mu_{MF} = 1.04$ and a standard deviation of $\sigma_{MF} = 0.16$. Correlation and regression analyses show that both MF_{CCC} and MF_{R2k} did not display any major trend with the shear parameters investigated in this study.
- As discussed in Section 6.6.1, the better representation of model factor statistics displayed by both V_{CCC} and V_{R2k} prediction models (in terms of bias and uncertainty) and trend with shear paramters are pointers to their suitability as general probabilistic model (GPM) for reliability assessment. V_{CCC} and V_{R2k} model factor statistics can be used in the reliability assessment process to evaluate the inherent safety levels in any shear design procedure.

Chapter 7

Reliability assessment of EC2 VSIM shear design procedure

7.1 Introduction

The best-estimate predictions of $V_{VSIM-L\theta}$ tends from underestimating toward overestimating shear capacity with increases in the amount of shear reinforcement (Figure 6.7 (a)). This raises concern that the design procedure may not be sufficiently safe for beams with high quantities of stirrups unless adequate safety margins are introduced as part of the design provisions. Also, over conservatism at low stirrup quantities is not ideal (uneconomic performance). No evidence has been found from background documents and relevant literature that VSIM has been calibrated to account for systematic trends associated with stirrup quantities. No significant trends have been detected against other important parameters known to affect shear strength like the percentage of tension steel, shear span-to-depth ratio, beam width, effective depth etc. (Section 6.4.4.1).

This chapter, therefore, assesses the consistency and uniformity of the reliability index of EC2 shear design formulation across practical ranges of main shear design parameters (shear reinforcement $\rho_w f_{ywm}$, concrete strength f_{cm} and beam depth d). The principal reliability assessment was performed based on the probabilistic representation of MCFT (R2k) as GPM (discussed in Chapter 6). An alternative reliability analysis using CCC based GPM (discussed in Chapter 6) was also conducted to validate investigations conducted using the MCFT (R2k) based GPM. The purpose of the reliability investigation can be summarised as follows:

i. To assess the reliability performance of EC2 shear design procedure in terms of its reliability index over a practical ranges of main shear parameters: shear reinforcement $\rho_w f_{ywm}$, concrete strength f_{cm} and beam depth d. Design situations where the target reliability as specified in EN 1990 and SANS 10160 is not attained are identified.

ii. To evaluate the consistency and uniformity of the reliability index across parametric variations of shear reinforcement $\rho_w f_{ywm}$, concrete strength f_{cm} and beam depth d. The ideal shear design procedure should display a uniform level of reliability for all feasible design situations.

7.2 Methodology

The stages involved in obtaining the reliability index are presented below:

1) Selection of a suitable general probabilistic model (GPM) for the reliability analysis. The reliability conducted in this investigation is based on MCFT (R2k) implemented as the principal GPM; and CCC model implemented as an alternative GPM (Chapter 6).
2) Formulation of the Limit State Function (LSF)
3) Identification of the stochastic variables and deterministic parameters in the LSF. The model factor is considered as the only random variable in the LSF. The reliability sensitivity study conducted by Mensah (2015) identified model factor as the prominent source of uncertainties affecting the probability distribution of GPMs for shear reliability (see Section 7.2.1.1). The model factor statistics to be incorporated in the reliability assessment as derived in Chapter 6, are outlined in Table 7.2. EC2 VSIM design shear resistance $V_{VSIM-L\theta}\ (X_k, \gamma)$ is calculated using Equation 3.26 (Chapter 3).
4) The reliability indices were estimated from the exceedance probability for a Lognormal distribution. It can also be obtained from the application of First Order Reliability Method to the LSFs. The reliability indices are determined across parametric variations of shear reinforcements $\rho_w f_{ywm}$, concrete strengths f_{cm} and and beam depth d.

The flowchart outlining the step by step procedure followed in the reliability investigation is presented in Figure 7.1.

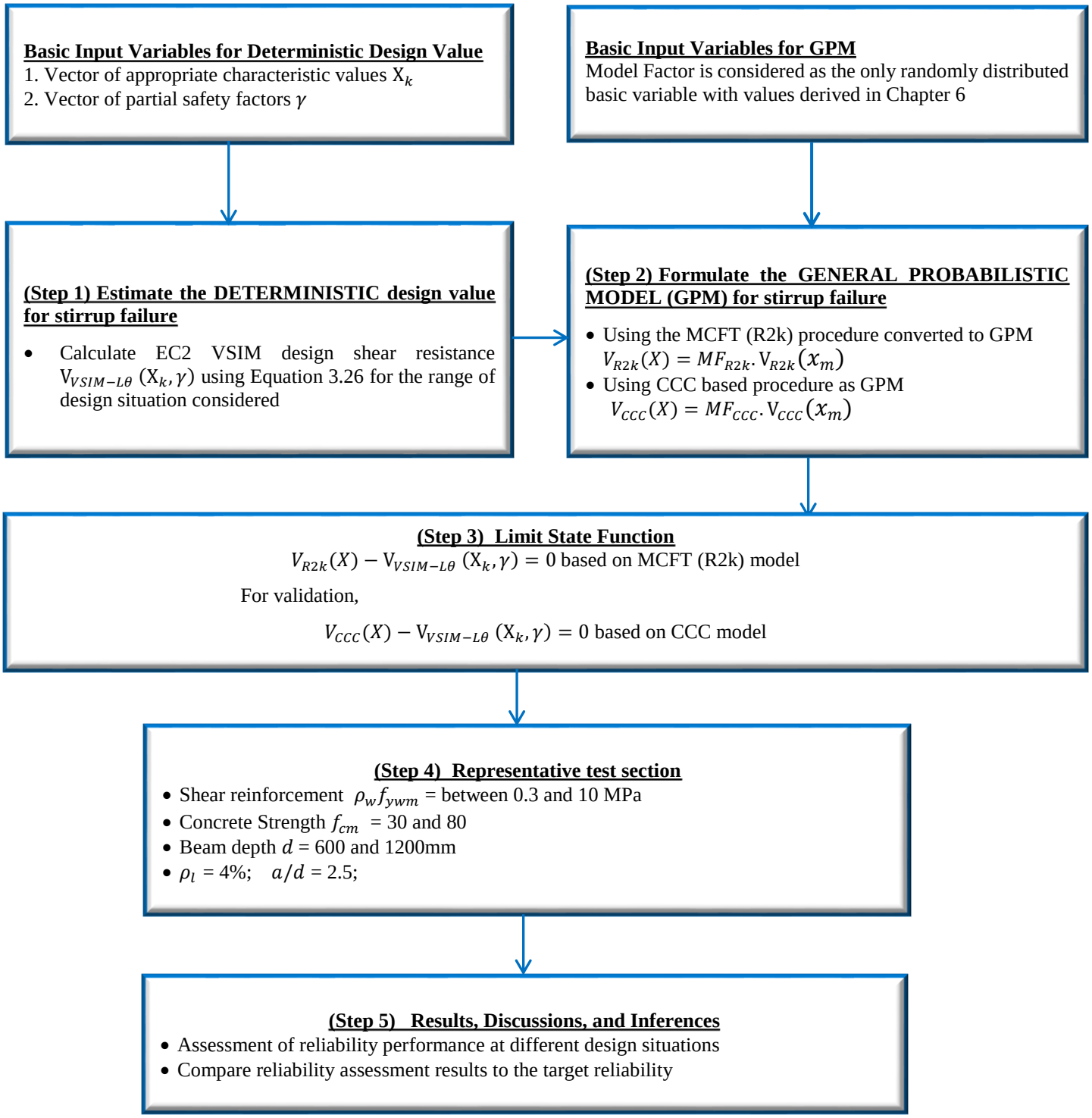

Figure. 7.1(a). Flowchart outlining the procedure for reliability assessment of EC2 VSIM shear design procedure for stirrup failure

7.2.1 Limit State Function (LSF) for reliability analysis

The Limit State Function (LSF) is established by setting the performance function equal to zero ($g(X) = 0$). For the performance function $g(X)$ (Figure 7.1(b)) presented here, the GPM is developed based on the probabilistic representation of unfactored MCFT (R2k) and CCC capacity predictions. Therefore, the LSF for the reliability analysis of EC2 shear design procedure $\mathrm{V}_{VSIM-L\theta}\ (\mathrm{X}_k, \gamma)$ can be expressed as Equation 7.1 and 7.2.

$$g(X) = \mathrm{V}_{R2k}(X) - \mathrm{V}_{VSIM-L\theta}(\mathrm{X}_k, \gamma) = 0 \tag{7.1}$$

$$g(X) = \mathrm{V}_{CCC}(X) - \mathrm{V}_{VSIM-L\theta}\ (\mathrm{X}_k, \gamma) = 0 \tag{7.2}$$

where $\mathrm{V}_{R2k}(X)$ and $\mathrm{V}_{CCC}(X)$ are the the probability distribution of true shear strength (i.e. General Probabilistic Model (GPM)) based on MCFT (R2k) and CCC model respectively (See Figure 7.1(b)). $\mathrm{V}_{VSIM-L\theta}\ (\mathrm{X}_k, \gamma)$ is the deterministic shear design value in accordance with EN 1992-1-1 design formulation. The vectors X_k and γ indicate, respectively, that the shear design value is calculated using characteristic values of basic variables and the appropriate values partial factors for concrete $\gamma_c = 1.5$ and steel $\gamma_s = 1.15$ as specified in EN 1992-1-1. The transformation of the characteristic value of a random variable into a design value is performed by dividing it by a partial factor related to this variable. The deterministic value of $\mathrm{V}_{VSIM-L\theta}\ (\mathrm{X}_k, \gamma)$ is calculated from Equation 3.26 (Section 3.2.6).

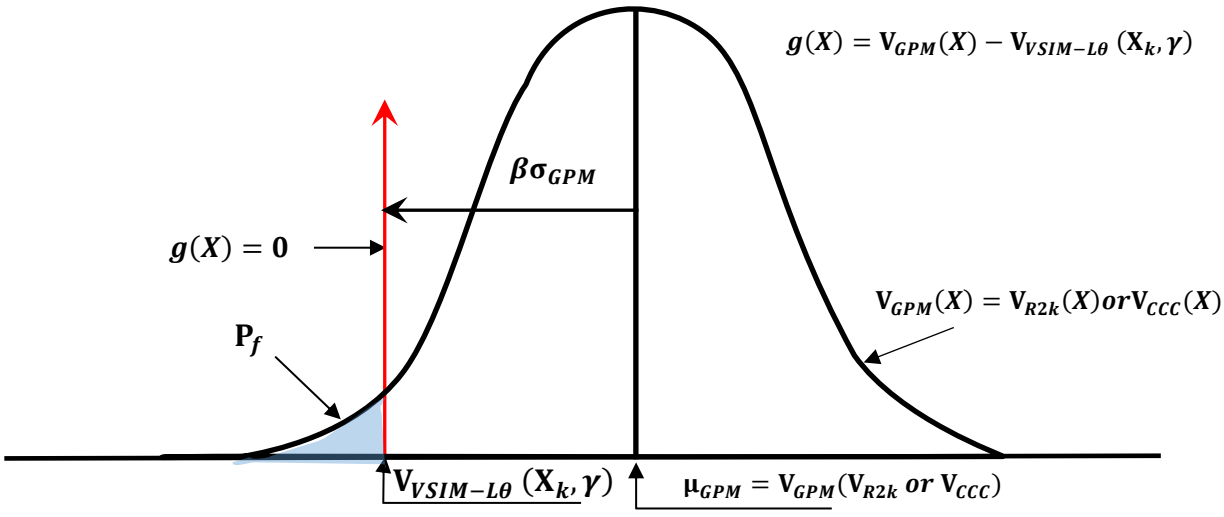

Figure 7.1(b). Probabilistic representation of the performance function $g(X)$ for shear resistance

where V_{GPM} (Figure 7.1(b)) which could alternatively be expressed as μ_{GPM}, is the GPM mean value which is obtained by inserting the mean value of the basic variable into the GPM expression in Equation 7.1 and 7.2. It is denoted V_{R2k} for MCFT (R2k) and V_{CCC} for CCC based GPM.

7.2.1.1 Motivation for a simplified probabilistic description

The reliability sensitivity study conducted by Mensah *et al.* (2013) and Mensah (2015) indicated that the model factor MF dominates EC2 shear reliability performance. The authors conducted sensitivity analysis by using two limit state functions for VSIM described in Equation 7.3 (VSIM-A based LSF) and Equation 7.4 (MCFT (R2k) based LSF). Probabilistic description of the basic variables that formed part of their reliability analysis are presented in Table 7.1.

$$g(\mathrm{X}) = MF_{VSIM-A}.\left[\frac{A_{sw}}{s}.0.9(h - C - n_l.a - e).f_{yw}.cot\theta\right] - \mathrm{V}_{VSIM-L\theta}(\mathrm{X}_k, \gamma) \tag{7.3}$$

$$g(\mathrm{X}) = MF_{R2k}.V_{R2k}(x) - \mathrm{V}_{VSIM-L\theta}(\mathrm{X}_k, \gamma) \tag{7.4}$$

Table 7.1. Probability models for the basic variables of the GPM (Mensah, 2015)

No	Description of Basic Variable	Symbol	Unit	Distribution	Mean(μ_x)	Standard Deviation (σ_x)	C.0.V	Source
1	VSIM-A	MF_{VSIM-A}	-	2P-LN	0.84	0.18	0.21	Mensah (2015)
2	MCFT(R2k)	MF_{R2k}	-	2P-LN	1.14	0.20	0.18	Mensah (2015)
3	Stirrup Area(2 legs)	A_{sw}	mm^2	N	nom.A_{sw}	-	0.02	JCSS PMC (2001)
4	Stirrup spacing	s	mm	N	nom.s	-	0.03	Huber (2005)
5	Concrete cover	C	mm	2P-LN	-	9	-	Holicky et al.(2010)
6	Beam height	h	mm	N	nom.h	-	0.01	Holicky (2009)
7	Radius of tension reinforcement	a	mm	N	nom.a	-	0.02	JCSS (PMC) (2001)
8	Diameter of stirrups	e	mm	N	nom.e	-	0.02	JCSS (PMC) (2001)
9	Beam Width	b_w	mm	N	nom.b_w	-	0.01	Holicky (2009)
10	Coefficient for scale/long-term effects	$\propto_{cc}$	-	2P-LN	0.85	-	0.1	Holicky et al.(2010)
11	Compressive cylinder strength of concrete	f_c	MPa	2P-LN	$f_{ck} + 8\ MPa$	-	-	EC2/fib MC 2010
12	Yield strength of stirrups	f_{yw}	MPa	2P-LN	$f_{ywk} + 1.645\sigma$	30	-	EN 1990

Two test cases with low stirrup quantities ($\rho_w f_{ywm} = 0.45\,MPa$) and high stirrup quantities ($\rho_w f_{ywm} = 1.8\,MPa$) were subjected to preliminary performance assessments based on a full probabilistic representation of $g(\mathrm{X})$ (i.e. all basic random variables of $g(\mathrm{X})$ having probability models contributing to overall performance uncertainty). The results of their preliminary assessment revealed that MF_{VSIM-A} dominates the uncertainty associated with the probability distribution of VSIM-A based GPM (Equation 7.3) and MF_{R2k} dominates the uncertainty associated with the probability distribution of MCFT (R2k) based GPM (Equation 7.4), achieving the value of direction cosines ($\propto_x$) of 0.95 and 0.86 respectively. Hence, they developed a simplified reliability model representing the MF as the only random variable of $g(X)$ and all other parameters were treated deterministically. Their results showed that the results of the simplified probabilistic analysis (MF treated as the only random variable) were comparable with the results of the full probabilistic analysis (all parameters treated as random variables).

The model factors MF_{CCC} and MF_{R2k} (presented in Section 7.2.3 [Table 7.2]) have comparable uncertainties to the ones used by Mensah *et al*. (2013) and Mensah (2015) in similar limit state expressions and therefore similar sensitivity factors are expected. Hence, other parameter uncertainties can be neglected. The decision to represent MF_{CCC} and MF_{R2k} as the only random variable of the performance function $g(\mathrm{X})$ as used in this study will exclude the addition of insignificant sensitivities contributing to the probability distribution of $g(\mathrm{X})$. The model factors MF can be obtained as a pure model factor if it is calculated based on a shear capacity prediction that uses the actual measured parameter values rather than the mean values. Actual measured parameter values are not available so then the model factors MF_{CCC} and MF_{R2k} obtained are not pure model factors as they included the uncertainties from other parameters taken at their mean in the model factor assessment conducted in Chapter 6. Therefore, MF already included the other uncertainties. The decision to represent MF as the only random variable (simplified reliability description) helps to avoid double accounting by excluding uncertainties from other variables. This will provide a reasonable estimate of the reliability index with reduced modelling effort. Thus, other sources of variability were not accounted for here and Equation 7.5 below can probabilistically approximate shear capacity (Figure 7.1(b)).

$$\mathrm{V}_{GPM}(X) = MF_{GPM}.V_{GPM}(x_m) \tag{7.5}$$

Therefore Equation 7.1 and 7.2 can be expressed as Equation 7.5a and 7.5b respectively

$$g(X) = MF_{R2k}.V_{R2k}(x_m) - \mathrm{V}_{VSIM-L\theta}(\mathrm{X}_k,\gamma) = 0 \quad (7.5a)$$

$$g(X) = MF_{CCC}.V_{CCC}(x_m) - \mathrm{V}_{VSIM-L\theta}(\mathrm{X}_k,\gamma) = 0 \quad (7.5b)$$

where $V_{GPM}(x_m)$ is the deterministic best-estimate prediction from the GPM under consideration using mean parameter values x_m. It is denoted $V_{R2k}(x_m)$ for MCFT (R2k) and $V_{CCC}(x_m)$ for CCC based GPM. MF_{GPM} is the model factor accounting for its bias and uncertainty relative to experimental observations, denoted MF_{R2k} for MCFT (R2k) and MF_{CCC} for CCC model

7.2.2 Probability models for the basic random variables of the GPMs

The statistical properties of the model factors MF_{R2k} and MF_{CCC} were derived in Chapter 6. Details of MF_{R2k} and MF_{CCC} statistics are presented in Table 7.2. The mean value μ_{MF} and standard deviation σ_{MF} of the model factors as derived from the entire database and detailed in Table 7.2, will be used in the reliability performance assessment of the test sections considered in this study. This was motivated by results presented in Chapter 6, where Table 6.4 clearly indicates that MF_{R2k} and MF_{CCC} derived from the subsets of the data have no significant sensitivity to the main shear parameters. The statistical properties presented in Table 7.2 are selection from Table 6.2. Assuming Lognormal for model factor leads to overestimation of skewness for CCC and underestimation of skewness for MCFT (R2k) (See Section 6.4.7.1). This implies CCC as GPM will tend to overestimate reliability while R2k as GPM will tend to underestimate reliability.

Table 7.2. Probability models for the basic random variables of the GPM

No	Description of Basic Variable	Symbol	Distr.	Mean (μ_{MF})	Standard Deviation (σ_{MF})
1	MCFT (R2k) Model Factor	MF_{R2k}	LN	1.04	0.16
2	CCC Model Factor	MF_{CCC}	LN	1.04	0.19

7.2.3 Representative beam test cases for reliability analysis

A shear design situation according to EC2 can be characterised by the following parameters: the beam cross-section (rectangular or flanged), the beam depth d, the concrete strength f_{cm} and the shear reinforcement $\rho_w f_{ywm}$. Other shear parameters did not show any major trends in comparison of VSIM

predictions to experimental results (Figure 6.7). The reliability analysis of a rectangular beam or an I-beam with varying $\rho_w f_{ywm}$, concrete strength f_{cm} and beam depth d, whilst keeping the values of all other shear parameters (b_w, b_f, h_f, ρ_l, a/d) constant, was considered adequate to provide a representative indication of the reliability performance of EC2 design procedure. The parameters which are not taken into account by EC2 design procedure (such as longitudinal reinforcement and the contribution from the flange) but accounted for by the general probabilistic models for shear used in this assessment, are expected to affect the reliability performance (Section 7.4.4).

7.2.3.1 The scope of beams covered in the reliability assessment

The reliability study is limited to the range of design situations that are allowed by the design code under investigation. By choosing representative combinations of the most vital shear parameters within the allowable limits of EC2 specifications summarised in Table 7.3, a range of feasible test sections was obtained.

Table 7.3. The allowable range of design parameters covered by the design code (EC2) for rectangular and flanged beams.

Parameter	Min	Max	EN 1992-1-1 Clause
$f_{ck}(MPa)$	12 MPa	90 MPa	3.1.2/Table 3.1
$\rho_l(\%)$	0.13%	4%	9.2.1.1
$f_{ywk}(MPa)$	Practical limit	400 to 600 MPa	3.2.2
$s\ (mm)$	Practical limit	$0.75d \leq 600mm$	9.2.2

Test sections with different beam cross-section and basic parameters as detailed in Table 7.4 and 7.5 will be used to evaluate the reliability of the design procedure. The test sections are distinguished by their $\rho_w f_{ywm}$, f_{cm}, d and cross-section type. The design parameters of the test sections are within the allowable limit of EC2 specifications presented in Table 7.3. The concrete strength f_{cm} and amount of stirrup reinforcement $\rho_w f_{ywm}$ are considered each at low and high representative values.

It is worth noting that the amount of stirrup reinforcement $\rho_w f_{ywm}$ for the rectangular test sections presented in Table 7.4 was limited to $\rho_w f_{ywm} \leq 2\ MPa$. This is because increasing the $\rho_w f_{ywm}$ to higher values will require excessive amounts of longitudinal steel ρ_l (i.e. exceeding the maximum code limit $\rho_l \leq 4\%$) in order to ensure that shear failure occurs before flexural failure. MCFT (R2k) predictions are shown in Figure 7.2 (a) for a rectangular beam with longitudinal reinforcement $\rho_l =$ 4% (at the code limit), at parametric variations of $\rho_w f_{ywm}$. The beam has $b_w = 200$, $d = 350$, $a/d =$

2.5 and $f_{cm} = 30$. As shown in the figure, at high levels of shear reinforcement, $\rho_w f_{ywm} > 2\ MPa$, yielding of longitudinal reinforcement (flexural failure) began to govern, with specimen 4 and 5 corresponding to a flexural failure. For beams with very high amounts of shear reinforcement yielding of the longitudinal steel makes it difficult to devise an experiment where shear failure governs (Collins *et al*., 2008).

Table 7.4. Basic parameters of the rectangular beams ($\rho_w f_{ywm} \leq\ 2\ MPa$)

S/N	Test section.	f_{cm} [MPa]	$\rho_w f_{ywm}$ [MPa]	s [mm]
1	**1R30A600**	30	0.30	418
2	**1R30B600**	30	0.64	196
3	**1R30C600**	30	1.27	99
4	**1R30D600**	30	2.1	63
5	**1R80A600**	80	0.30	418
6	**1R80B600**	80	0.64	196
7	**1R80C600**	80	1.27	99
8	**1R80D600**	80	2.1	63
9	**2R30A1200**	30	0.3	279.2
10	**2R30B1200**	30	0.56	149.5
11	**2R30C1200**	30	1.05	79.8
12	**2R30D1200**	30	2.1	39
13	**2R80A1200**	80	0.30	279.2
14	**2R80B1200**	80	0.56	149.5
15	**2R80C1200**	80	1.05	79.8
16	**2R80D1200**	80	2.1	39

***1R** refers to rectangular beam with $b_w = 400$, $d = 600$ and $\rho_l = 4\%$. ***2R** refers to rectangular beam with $b_w = 600$, $d = 1200$ and $\rho_l = 4\%$. All test sections have $a/d = 2.5$, aggregate size $d_{agg} = 7$, $A_{sw} = 100.5\text{mm}^2$ (Y8 stirrups) at varied spacing and $f_{ywm} = 500\ MPa$.

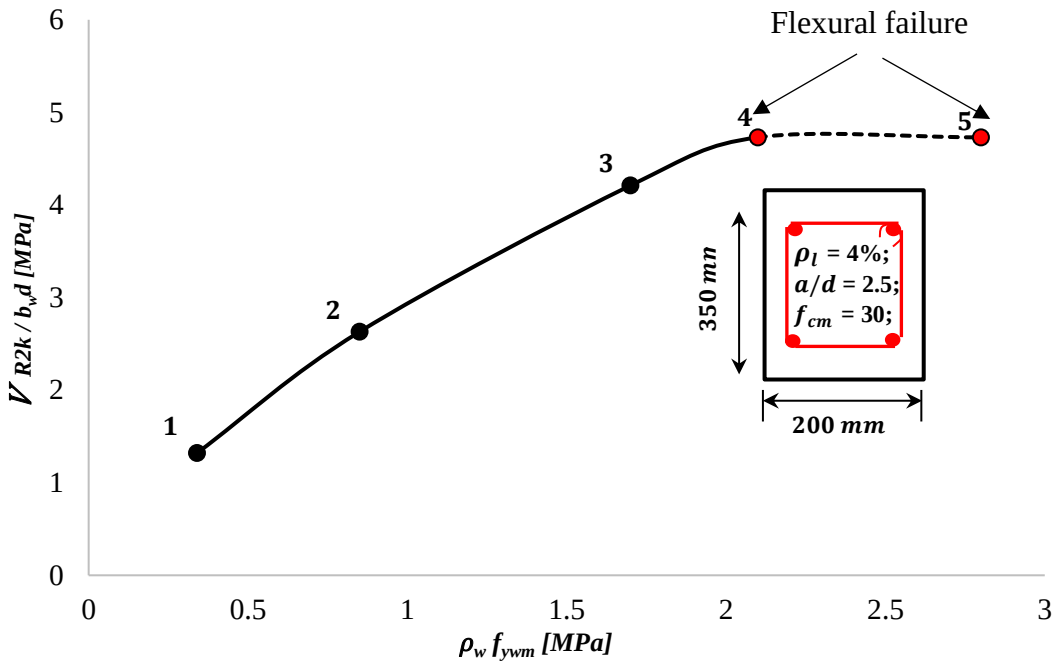

Figure 7.2(a). Normalised MCFT (R2k) capacity predictions at variations of $\rho_w f_{ywm}$

Figure 7.2 (b) presents the normalised shear strength for a subset of 142 experimental beams (rectangular and flanged beams) with longitudinal reinforcement $\rho_l \leq 4\%$ from the full database of 160 beam experiments presented in Chapter 6. The beams plotted in the figure have beam width b_w ranging from 75mm to 457mm and member depth d ranging from 198mm to 1369mm. The majority of the beams (122 beams) had an amount of shear reinforcement $\rho_w f_{ywm} \leq 2\ MPa$. The few experimental beams (20 beams) with $\rho_w f_{ywm} > 2\ MPa$ are flanged beams (I-beams). Consequently, I-beams with properties as detailed in Table 7.5 is used to assess the reliability index for beams with very high levels of shear reinforcement $\rho_w f_{ywm} > 2\ MPa$ (up to 10 MPa).

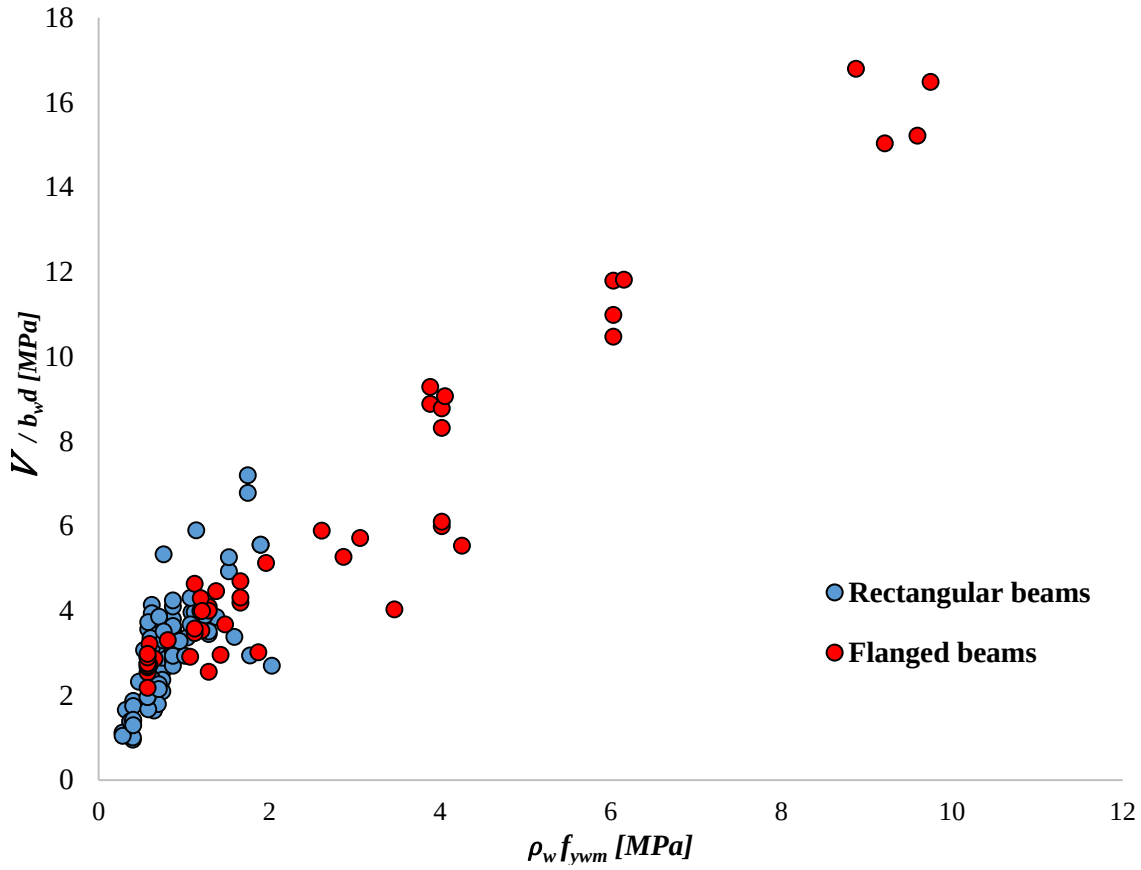

Figure 7.2(b). Subset of 142 experimental beams (rectangular and flanged) with $\rho_l \leq 4\%$ from the full database (Chapter 6)

Table 7.5. Basic parameters of the I-beams with $\rho_w f_{ywm} > 2\ MPa$ (up to 10 MPa)

S/N	Test section.	f_{cm} [MPa]	$\rho_w f_{ywm}$ [MPa]	s [mm]
1	**I30A600**	30	0.42	598
2	**I30B600**	30	2.26	133
4	**I30D600**	30	5.2	58
5	**I30E600**	30	10	30
6	**I80A600**	80	0.42	598
7	**I80B600**	80	2.26	133
9	**I80D600**	80	5.2	58
10	**I80E600**	80	10	30
11	**I30A1200**	30	0.42	598
12	**I30B1200**	30	2.26	133
14	**I30D1200**	30	5.2	58
15	**I30E1200**	30	10	30
16	**I80A1200**	80	0.42	598
17	**I80B1200**	80	2.26	133
19	**I80D1200**	80	5.2	58
20	**I80E1200**	80	10	30

***I** refers to I-beam with $b_w = 200$, $b_f = 450$, $h_f = 200$ and $d = 600$ &1200. All test sections have $\rho_l = 4\%$, $a/d = 2.5$, aggregate size $d_{agg} = 7$, $A_{sw} = 100.5\text{mm}^2$ (Y8 stirrups) at varied spacing and $f_{ywm} = 500\ MPa$

7.3 Assessment of design shear resistance and GPM mean value trends

The plot of EC2 design shear resistance $V_{VSIM-L\theta}(X_k, \gamma)$, as well as the GPM mean values V_{R2k} and V_{CCC} are presented for different concrete strengths $f_{cm} = 30$ MPa and 80 MPa in Figures 7.3 and 7.4 across the parametric range of $\rho_w f_{ywm}$ and beam depth d. It is observed from the plot that the trends of $V_{VSIM-L\theta}(X_k, \gamma)$, V_{R2k} and V_{CCC}, differ considerably with the variation of $\rho_w f_{ywm}$, f_{cm} and d. It is noticed that $V_{VSIM-L\theta}(X_k, \gamma)$ is not much influenced by increased concrete strength.

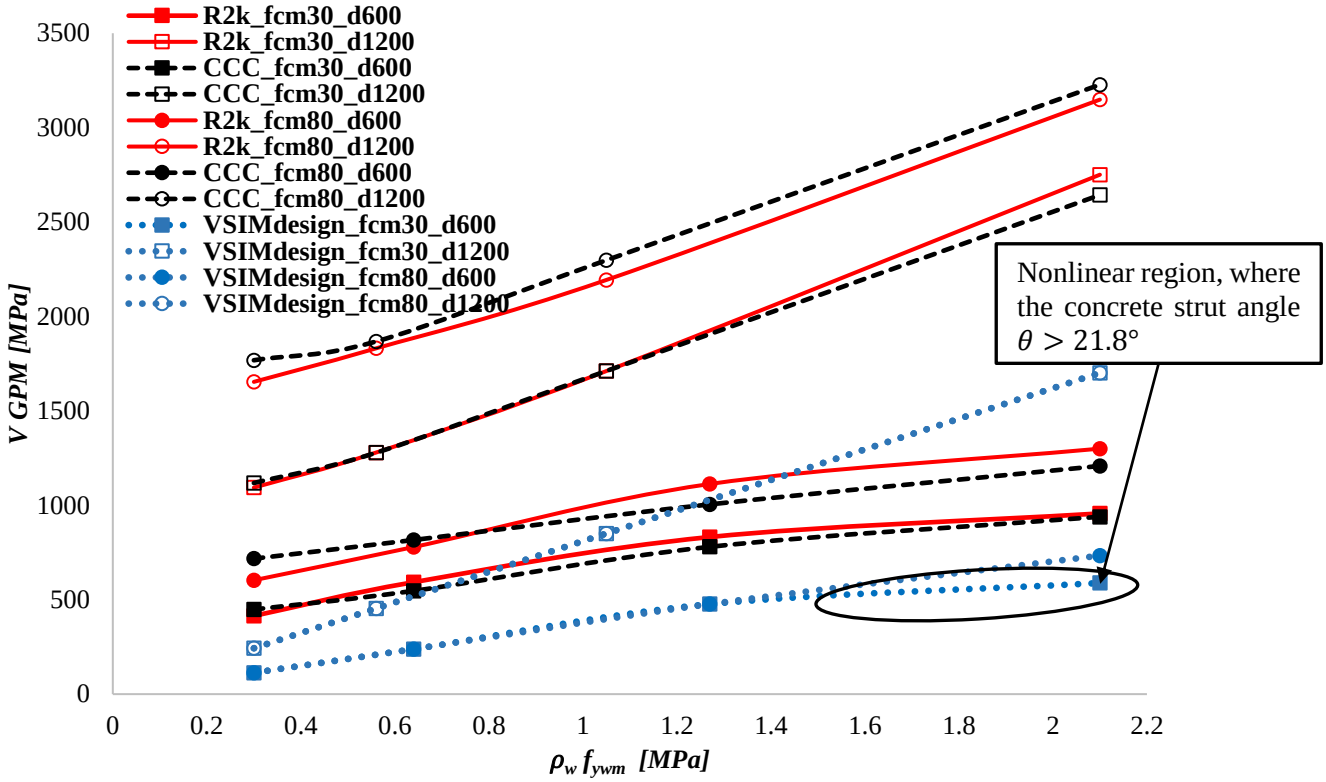

Figure 7.3. Plot of EC2 design shear resistance and GPM mean values for rectangular test sections (Table 7.4). **Note R2k_fcm30_d600 refers to V_{R2k} values for beam with $f_{cm} = 30$ MPa and $d = 600\ mm$.

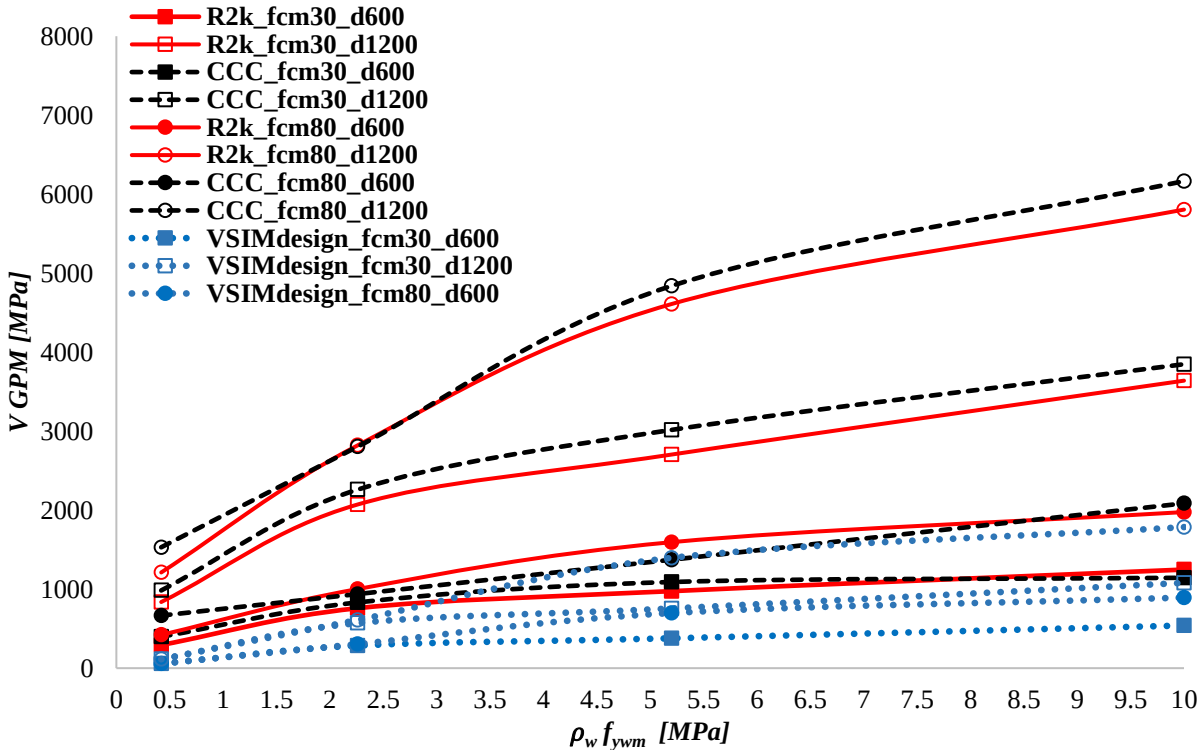

Figure 7.4. Plot of EC2 design shear resistance and GPM mean values for I-beams (Table 7.5). **Note CCC_fcm30_d600 refers to V_{CCC} values for beam with $f_{cm} = 30$ MPa and $d = 600\ mm$.

7.3.1 Effect of concrete strength f_{cm} on $V_{VSIM-L\theta}(X_k, \gamma)$ and V_{GPM}

Scrutiny of Figures 7.3 and 7.4 revealed that:

- The values of $V_{VSIM-L\theta}(X_k, \gamma)$ are not much influenced by increased concrete strength f_{cm}. The change in $V_{VSIM-L\theta}(X_k, \gamma)$ values occur at the combined situation of low concrete strength and shear reinforcement $\rho_w f_{ywm} > 1.3$ for medium sized rectangular beams ($d = 600\ mm$) and at $\rho_w f_{ywm} > 2.3$ for I-beams. At this combined situation, $V_{VSIM-L\theta}(X_k, \gamma)$ values start to become non-linear as portrayed in the figures (concrete strut angle θ exceeded 21.8°).
- V_{R2k} and V_{CCC} both account for the positive influence of increased concrete strength on shear strength.
- Thus the safety margin $V_{GPM} - V_{VSIM-L\theta}(X_k, \gamma)$ increase for higher concrete strength, which will lead to higher reliability (discussed in Section 7.3.2)

7.3.2 Safety margin and the reliability link

The safety margin $V_{GPM} - V_{VSIM-L\theta}(X_k, \gamma)$ is equivalent to $\beta . \sigma_{GPM}$ (as shown in Figure 7.1(b)). This indicates that the estimated reliability values β are dependent on the safety margin and the GPM uncertainty σ_{GPM}.

By studying Table 7.6, it can be seen that the estimated σ_{GPM} values are different at various levels of shear reinforcement, concrete strength and beam depth , with the maximum σ_{GPM} value occurring for test section **2R80D1200** as shown in Table 7.6. σ_{GPM} is dependent on the mean value prediction and the model uncertainty σ_{MF} of the respective model used as GPM ($\sigma_{GPM} = V_{GPM}(x_m) . \sigma_{MF}$). The sensitivity of σ_{GPM} values to concrete strength can be drawn from the sensitivity of the mean value prediction of the respective prediction model on which the GPM is based to concrete strength.

Table 7.6. σ_{GPM} estimates at different concrete strengths

S/N	Test section.	$\rho_w f_{ywm}$ [MPa]	f_{cm} [MPa]	V_{R2k}	V_{CCC}	$V_{VSIM-L\theta}$ (X_k, γ)	σ_{R2k} [kN]	σ_{CCC} [kN]
1	**1R30A600**	0.30	30	414.3	448.3	113.3	35.8	44.6
2	**1R30B600**	0.64	30	592.8	547.04	238.5	64.8	68.7
3	**1R30C600**	1.27	30	832	780	476.7	99.6	115.5
4	**1R30D600**	2.1	30	956.8	939.2	588.5	118.8	140.9
5	**1R80A600**	0.3	80	603.2	717.5	113.3	45.1	59.8
6	**1R80B600**	0.64	80	778.96	816.3	238.5	70.5	86.2
7	**1R80C600**	1.27	80	1112.8	1004.8	476.7	116.4	131.2
8	**1R80D600**	2.1	80	1300	1208.4	733.7	154.6	178.3
9	**2R30A1200**	0.3	30	1093.8	1118	243	80.7	81.9
10	**2R30B1200**	0.56	30	1279.4	1278.3	453.6	111.5	111.5
11	**2R30C1200**	1.05	30	1710.8	1711.3	850.6	167.2	167.3
12	**2R30D1200**	2.1	30	2750.8	2643.3	1701.1	284.1	274.5
13	**2R80A1200**	0.3	80	1653.6	1768	243	105.9	110.7
14	**2R80B1200**	0.56	80	1831	1867.5	453.6	140.5	142.3
15	**2R80C1200**	1.05	80	2193.4	2297.9	850.6	197.4	203.4
16	**2R80D1200**	2.1	80	3148.4	3227.3	1701.1	315.4	321.1

7.4 Reliability assessment and discussion

7.4.1 Overview

The reliability indices β obtained from the exceedance probability for a Lognormal distribution using the rectangular and I-beams detailed in Table 7.4 and 7.5 respectively are presented graphically in Figures 7.5 and 7.6 for parametric variations of concrete strength, stirrup reinforcement and beam depth. The resistance performance requirement ($\propto_R \beta_T$) for shear resistance recommended by basis of design standards SANS 10160 and EN 1990 are also shown on the figures assuming a typical sensitivity factor of $\propto_R = 0.8$ for resistance (EN 1990, 2002) (See Section 5.6). The figures illustrate the effect of the variation of shear reinforcement $\rho_w f_{ywm}$, concrete strength f_{cm} and beam depth d on the reliability of the EC2 shear design formulation using the representative test sections.

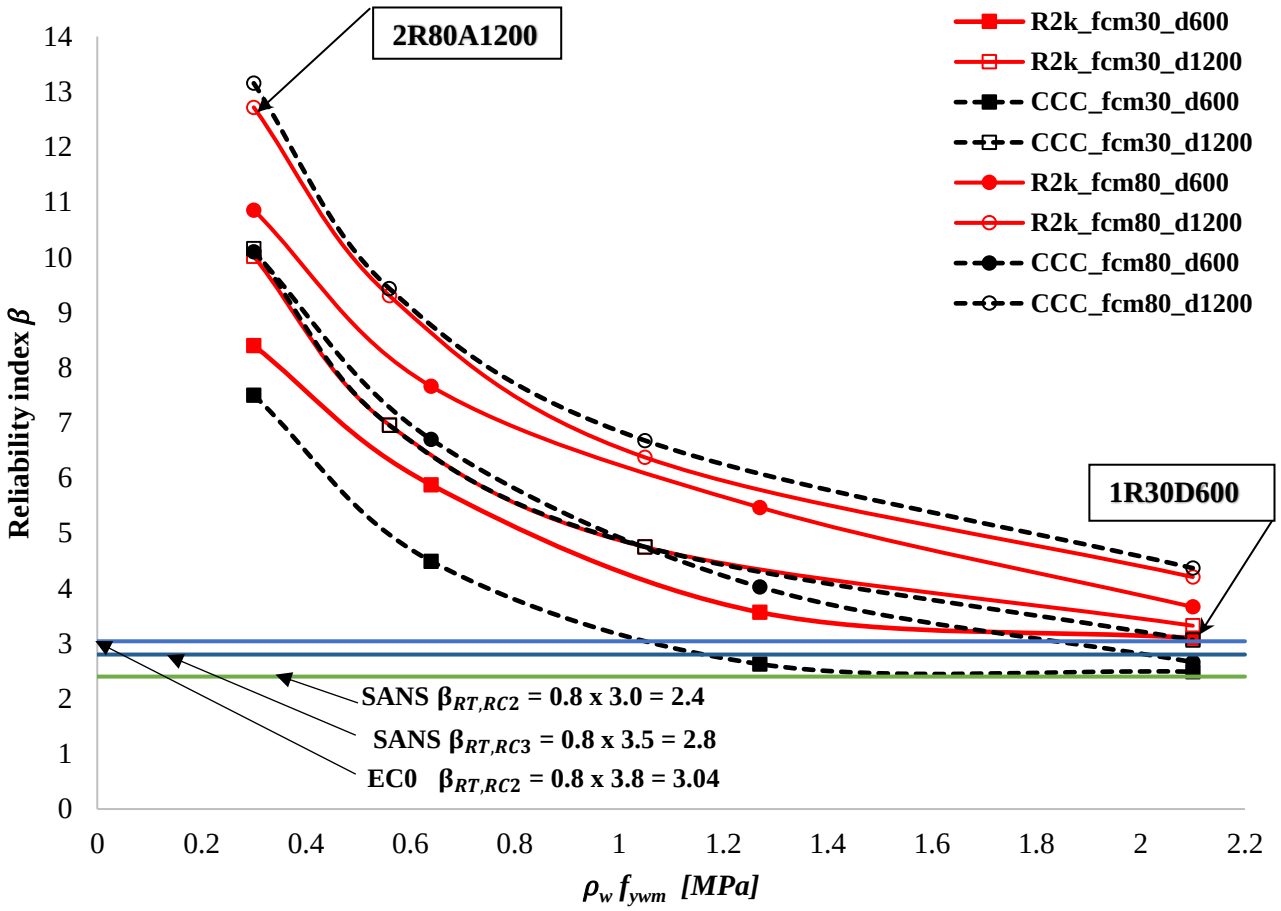

Figure 7.5. Reliability indices β obtained from the FORM evaluations of $g(\mathrm{X})$ for rectangular beams.**Note R2k_fcm30_d600 refers to β values for beam with $f_{cm} = 30$ MPa and $d = 600\ mm$ using R2k as GPM.

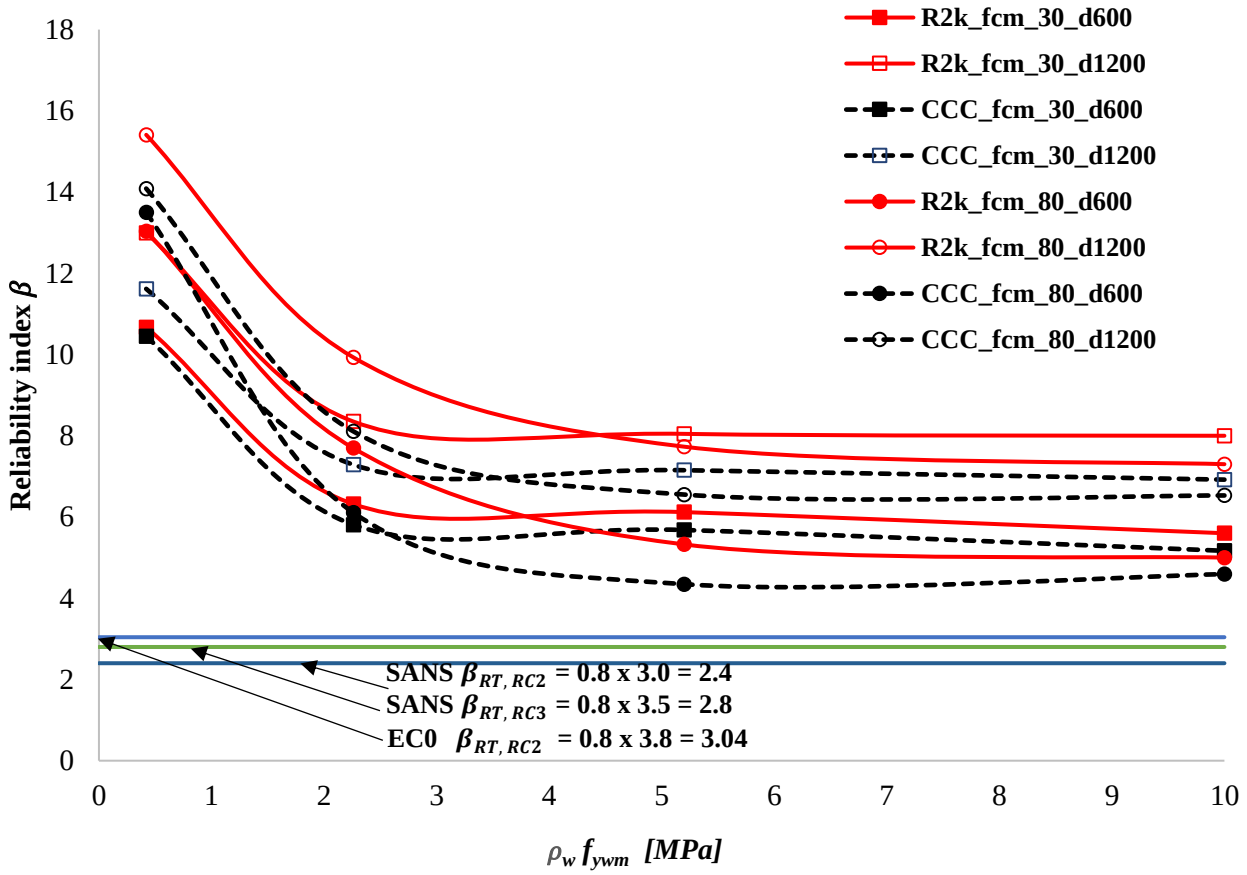

Figure 7.6. Reliability indices β obtained from the FORM evaluations of $g(\mathrm{X})$ for I-beams. Note CCC_fcm30_d600 refers to β values for beam with $f_{cm} = 30$ MPa and $d = 600\ mm$ using CCC as GPM.

7.4.2 Trends in EC2 VSIM reliability with $\rho_w f_{ywm}$

Figures 7.5 and 7.6 portray the trends in the reliability index of EC2 VSIM with amount of shear reinforcement $\rho_w f_{ywm}$ for the representative test sections detailed in Table 7.4 and 7.5. The figures show a general decrease in estimated reliability β values as $\rho_w f_{ywm}$ increases. This is due to increasing GPM uncertainty (that is σ_{GPM} increases also as shown in Table 7.6) with increases in $V_{GPM}(x_m)$.

The flattening off of the reliability index at higher levels of shear reinforcement is predominantly due to the inherent non-linearity of $V_{VSIM-L\theta}\ (\mathrm{X}_k, \gamma)$ in such situations as can be witnessed from Figure 7.3 and 7.4. The concrete strut angle is at its lower limit over the range of declining reliability. Here the reliability declines because higher capacity corresponds to higher absolute uncertainty while the absolute safety margin remains at a similar magnitude over this range (see Figures 7.3 and 7.4). For higher $\rho_w f_{ywm}$ the strut angle becomes increasingly larger than 21.8°, corresponding to relatively

reduced design shear capacity for a given amount of stirrups, thereby increasing the safety margin and halting the reliability decline with increasing $\rho_w f_{ywm}$. At low levels of stirrup reinforcement, EC2 produces overly conservative (uneconomical designs) due to the combination of ignoring the concrete contribution and the implementation of the strut angle lower limit.

7.4.3 Trends in estimated β values with concrete strength f_{cm} and beam depth d

The values of β consistently increase with increasing concrete strength f_{cm} as displayed in Figure 7.5 and 7.6 except at $\rho_w f_{ywm} > 2\ MPa$. The sensitivity of β values to f_{cm} is affected largely by the influence of concrete strength f_{cm} on V_{GPM} (see Figure 7.3 and 7.4). The GPM mean value prediction V_{GPM} increases with increasing f_{cm} contrary to $V_{VSIM-L\theta}\ (X_k, \gamma)$ which gives little credit to increasing concrete strength and only does so at high levels of shear reinforcement. In view of this, the sensitivity of β estimates to f_{cm} also stems from the failure by $V_{VSIM-L\theta}\ (X_k, \gamma)$ to capture the extra design capacity which may be achieved by increasing the concrete strength. The influence of concrete strength on V_{R2k} and V_{CCC} predictions can be drawn from the influence of concrete strength on their respective mean value predictions. The estimated β values for low strength concrete $f_{cm} = 30\ MPa$ slightly exceeds that of high strength concrete $f_{cm} = 80\ MPa$ at high stirrups (Figure 7.6).

As shown in Figures 7.5 and 7.6, the values of β increase with increasing beam depth d. Increasing beam depth implies increasing concrete contribution to the overall GPM mean value predictions V_{GPM} (i.e. higher V_{R2k} and V_{CCC} predictions). Concrete contribution is neglected in $V_{VSIM-L\theta}\ (X_k, \gamma)$ shear design formulation. Hence, the higher β estimates obtained due to increased beam depth d derive from the relatively higher V_{R2k} and V_{CCC} values acheived by increasing the beam depth d.

7.4.4 Comparison of reliability index of rectangular beams and I-beams

Examination of Figures 7.5 and 7.6 reveal that both types of beam cross sections portray a similar trend of reducing reliability index with increases in the amount of shear reinforcement $\rho_w f_{ywm}$; with reductions in concrete strength f_{cm} and with reductions in beam depth d. However, the reliability indices obtained for I-beams are higher than that of rectangular beams across range of $\rho_w f_{ywm}$, concrete strength f_{cm} and beam depth d considered.

Experimental studies (Ribas & Cladera, 2013; Sagaseta & Vollum, 2011) have shown a considerable increase in the shear strength of a flanged concrete beam compared to an equivalent rectangular cross section. According to the investigations reported by ACI-ASCE Committee 426 (1973), beams with 30cm (300mm) or wider flanges had about 25% greater ultimate shear strength than rectangular beams. This indicates that the compression flange contributes to shear strength which is being ignored in some current codes shear provisions including EC2. Other researchers (Linh Hoang, 1997; Tureyen & Frosch, 2003; Zararis *et al*., 2006; Wolf & Frosch, 2007) have also recognised that the compression flange contributes to the shear strength.

The reasons why the reliability indices of I-shaped test sections (Figure 7.6) are significantly higher than that of the rectangular test sections (Figure 7.5) can be attributed to the fact that:

- EC2 VSIM assumes shear to be carried by the web and does not consider the contribution of the flanges in I-beams to shear strength. As a result of this, design shear resistance $V_{VSIM-L\theta}\ (X_k, \gamma)$ is underestimated for such members, thereby resulting in higher reliability values.
- EC2 VSIM formulation for beams with stirrups does not take into account the extra capacity contribution from longitudinal steel (dowel action). However, this parameter is taken into account by the general probabilistic models used for the reliability assessment.

7.4.5 Comparison of the reliability index β obtained using the two GPMs

The estimated β values from MCFT (R2k) based performance function (β_{R2k}) corroborate the trends of estimated β values from the CCC based performance function (β_{CCC}). For rectangular beams, they correspond closely for high strength deep beams; less closely for low strength medium size beams. For I-beams, they correspond closely for low strength medium size beams and less closely for high strength deep beams; but still indicate clearly similar trends of reducing reliability with increasing stirrups, decreasing beam depth and decreasing concrete strength. However, the inspection of β_{CCC} and β_{R2k} revealed that for a specified combination of $\rho_w f_{ywm}$, d and f_{cm} situations, β_{R2k} are greater than β_{CCC}.

7.4.6 Reasons for the differences in the β values obtained from the two GPMs

The implementation of the two different prediction models (V_{CCC} and V_{R2k}) to establish GPM functions for shear resistance $V_{GPM}(X)$ revealed that each model is sensitive to different design parameters. Consequently, indicating that the application of the Model factors (MF_{CCC} and MF_{R2k}) to the mean value of shear resistance V_m could not equate the GPM mean values V_{GPM} for the two models. This indicates that the GPM models predict the value of true shear resistance differently. The observation that CCC predicts slightly lower mean value V_m than MCFT (R2k); and MF_{CCC} has a slightly lower standard deviation than MF_{R2k}, explains the lower reliability indices β obtained from CCC compared to MCFT (R2k). The assumption of 2P-Lognormal distribution for the model factors leads to some overestimation of skewness for CCC and similar underestimation of skewness for MCFT (R2k) (Section 6.4.7.1). This implies CCC as GPM will tend to overestimate reliability while R2k as GPM will tend to underestimate reliability.

7.4.7 Evaluation of representative β values against the performance requirements for shear resistance

In Figure 7.5 the β values of the representative rectangular test sections are plotted for $f_{cm} = 30\ and\ 80\ MPa$ and $d = 600\ and\ 1200\ mm$. It can be observed that the test sections with high concrete strength $f_{cm} = 80\ MPa$ and large size $d = 1200\ mm$ displayed the highest levels of reliability whereas the test sections with low concrete strength $f_{cm} = 30\ MPa$ and medium size $d = 600\ mm$ displayed the lowest levels of reliability.

It is required that the resistance index β_R should be close to its target value $\beta_{RT} = 0.8\ x\ \beta_T$ for Reliability Class 2 and 3 structures according to SANS 101601 and Reliability Class 2 structures according to EN 1990 requirements. Reliability indices of all the test sections investigated are higher than the target reliabilities for all f_{cm}, $\rho_w f_{ywm}$ and d design situations considered.

7.4.8 Consistency of EC2 VSIM reliability

The reliability indices presented in Figure 7.5 and 7.6 indicate the highly non-uniformity of the reliability of EC2 VSIM shear design formulation. The reliability level decreases as shear reinforcement increases and concrete strength reduces. However, when the shear reinforcement

decreases and the concrete strength increases, the reliability level rises rapidly. The reliability level also increases with increasing beam depth d. For a deep beam ($d = 1200\,mm$) with high concrete strength ($f_{cm} = 80\,MPa$) and low stirrup ($\rho_w f_{ywm} = 0.30\,MPa$) designed according to EC2 shear design formulation, the reliability is as high as $\beta = 12.7$. This is substantially greater than the target reliabilities of SANS 10160 and EN 1990, implying uneconomical designs. VSIM is shown in Figures 4.6, 4.7, 4.9, 4.10 and 6.7(a) to significantly underestimate shear capacity predictions. This can be ascribed to the neglect of concrete contribution to shear strength which is more significant in lightly shear reinforced beams and also the limit on the concrete strut angle. Other researchers (Cladera, 2002; Cladera & Mari, 2007; Todisco *et al.*, 2016; Ismail, 2016; Russo et al., 2013; Sykora et al., 2013; Sagaseta &Vollum, 2011; Collins *et al.*, 2007; Mensah, 2015) have also confirmed the overly conservative performance of VSIM at low levels of shear reinforcements.

7.5 Summary and conclusions

The reliability of EC2 shear procedure can be summarised as follows:

- EC2 shear design formulation was assessed for two types of beams (rectangular beams and I-beams) using two different GPM functions (MCFT (R2k) based GPM and CCC based GPM). Based on the assessment conducted in Chapter 6, MCFT (R2k) based GPM is described to better capture true shear performance. Therefore, the main conclusions in this study are drawn from the reliability assessment using the MCFT (R2k) based GPM, and CCC based assessment used as validation. Both GPMs captured similar trends.
- The design formulation is assessed to have high reliability for low levels of shear reinforcement, high concrete strength and large beam size, and an actively reduced reliability (but still adequate) with increased levels of shear reinforcement, reduced concrete strength and reduced beam depth.
- For beams with a low amount of shear reinforcement, the estimated reliability index is substantially greater than the target reliabilities of SANS 10160 and EN 1990, implying uneconomical designs.
- VSIM is uneconomical with reliability index as high as 12.7 for lightly shear reinforced beams. This is attributed to the neglect of concrete contribution to shear strength which is more significant in lightly shear reinforced beams and the limit on the concrete strut angle. Other researchers (Cladera, 2002; Cladera & Mari, 2007; Todisco *et al.*, 2016; Ismail, 2016; Russo

et al., 2013; Sykora et al., 2013) have also confirmed the conservative predictions of VSIM at low shear reinforcement. The overly conservative reliability estimates imply uneconomical design which could result in inefficient allocation of societal resources.

- It may be noted in many beam systems, restraints of shrinkage may result in axial tension and corresponding shrinkage cracks, especially in lightly reinforced beams. The influence of this on shear capacity should be investigated.
- Reliability indices of all the rectangular test sections are in accordance with the target reliability requirement for Reliability Class 2 structures prescribed by basis of design standards SANS 10160 and EN 1990, for the practical design range considered.
- EC2 underestimates design shear resistance for I-beams due to the neglect of shear contributions from compression flanges and longitudinal reinforcements (dowel action), thereby resulting in higher reliability values for such beams.
- For I-beams with shear reinforcement in excess of 2 MPa (i.e. $\rho_w f_{ywm} > 2\ MPa$), the obtained reliability indices meet the target reliabilities for the design range considered.
- The reliability trend is highly inconsistent and non-uniform, directly portraying the sensitivity of the design formulation to $\rho_w f_{ywm}$. This confirms the poor performance of the EC2 design code with respect to $\rho_w f_{ywm}$.

Chapter 8

Reliability analysis of ACI and Fib Model Code shear design procedure

8.1 Introduction

The reliability performance assessment conducted in Chapter 7 revealed the inconsistency of EC2 VSIM shear reliability across practical ranges of main shear design parameters. In this chapter, alternative approaches are assessed in order to find design formulations that perform better in terms of achieving the target reliability index consistently. The reliability of ACI and Fib Model Code 10 (III) design procedures are assessed at variations of shear reinforcement $\rho_w f_{ywm}$, concrete strength f_{cm} and beam depth d; and compared to that of the EC2 shear design formulation to appraise the impact of the safety bias incorporated in the various shear design procedures across a range of practical design situations. ACI 318 does not use partial factors but resistance reduction factor.

Importantly, a decrease in the model factor was observed with increased beam depth d for MC-10 (III) and ACI 318 as shown in Figure 6.9(d) and 6.10(d) respectively. Adequate reliability performance of ACI and MC-10 (III) for deep beams should be confirmed. This model factor trend was also noted by other researchers (Ismail, 2016; Cladera *et al*., 2016; Sykora *et al*., 2018). Therefore, this chapter presents the reliability performance of ACI and Fib model Code 10 (III) at parametric variations of amount of shear reinforcement $\rho_w f_{ywm}$, concrete strength f_{cm} and beam depth d.

8.2 Methodology

This chapter is organised similarly as Chapter 7, following the same methodology illustrated in Figure 7.1 (Chapter 7). Similar limit state functions, with design values of MC-10 or ACI assessed respectively; and using R2k based GPM, with CCC based GPM as validation.

8.2.1 Limit state function (LSF) for shear assessment

To assess the reliability performance of MC-10 (III) and ACI 318 shear design procedures, a different limit state function was set up for each design procedure similar to that presented in Chapter 7 for EC2 VSIM (expressed in Equation 8.1). The FORM is applied to the LSF to estimate the reliability index.

$$g(X) = MF_{GPM}.\mathrm{V}_{GPM}(x_m) - \mathrm{V}_{Rd}(\mathrm{X}_k, \gamma, \phi) \tag{8.1}$$

The design resistance $\mathrm{V}_{Rd}(\mathrm{X}_k, \gamma, \phi)$ is the deterministic design value obtained from MC-10 (III) $\mathrm{V}_{MC-10(III)}(\mathrm{X}_k, \gamma)$ (Equation 3.15) or ACI-318 $\mathrm{V}_{ACI}(\mathrm{X}_k, \phi)$ (Equation 3.4) with the application of appropriate partial safety factors γ (where applicable), shear strength reduction factor ϕ (where applicable) and characteristic values. The GPM is based on MCFT (R2k); or CCC for validation. The statistical properties of the model factors MF_{GPM} are the same as presented in Chapter 7.

8.2.2 Representative beam test cases for the reliability analysis

The parameters for the test sections established to obtain the reliability index at parametric variations of concrete strength, amount of shear reinforcement and beam depth are presented in Table 8.1. The shear reinforcement $\rho_w f_{ywm}$, concrete strength f_{cm} and beam depth d are considered each at low and high representative values.

Table 8.1. Basic parameters of the test sections

S/N	Test section.	f_{cm} [MPa]	$\rho_w f_{ywm}$ [MPa]	s [mm]
1	**1R30A350**	30	0.34	887
2	**1R30B350**	30	0.85	355
3	**1R30C350**	30	1.7	177
4	**1R30D350**	30	2.1	144
5	**1R80A350**	80	0.34	887
6	**1R80B350**	80	0.85	355
7	**1R80C350**	80	1.7	177
8	**1R80D350**	80	2.1	144
9	**2R30A1200**	30	0.3	251
10	**2R30B1200**	30	0.56	134
11	**2R30C1200**	30	1.05	71.8
12	**2R30D1200**	30	2.1	36
13	**2R80A1200**	80	0.3	251
14	**2R80B1200**	80	0.56	134
15	**2R80C1200**	80	1.05	71.8
16	**2R80D1200**	80	2.1	36

***1R** refers to rectangular beam with $b_w = 150$ and $d = 350$. ***2R** refers to rectangular beam with $b_w = 600$ and $d = 1200$. All test sections have $\rho_l = 4\%$, $^{a}/_{d} = 2.5$, aggregate size $d_{agg} = 19$, $A_{sw} = 100.5\text{mm}^2$ (Y8 stirrups) at varied spacing and $f_{ywm} = 450\ MPa$.

8.3 Analysis of the trend of design shear resistance and the GPM mean value

The plot of MC-10 (III) $V_{MC-10(III)}$ (X_k, γ) and ACI $V_{ACI}(X_k, \phi)$ design shear resistances with GPM mean values (V_{R2k} and V_{CCC}) are shown in Figures 8.1 and 8.2, at variation of $\rho_w f_{ywm}$, concrete strength ($f_{cm} = 30$ MPa and $f_{cm} = 80$ Mpa) and effective beam depth ($d = 350\ mm$ and $d = 1200\ mm$).

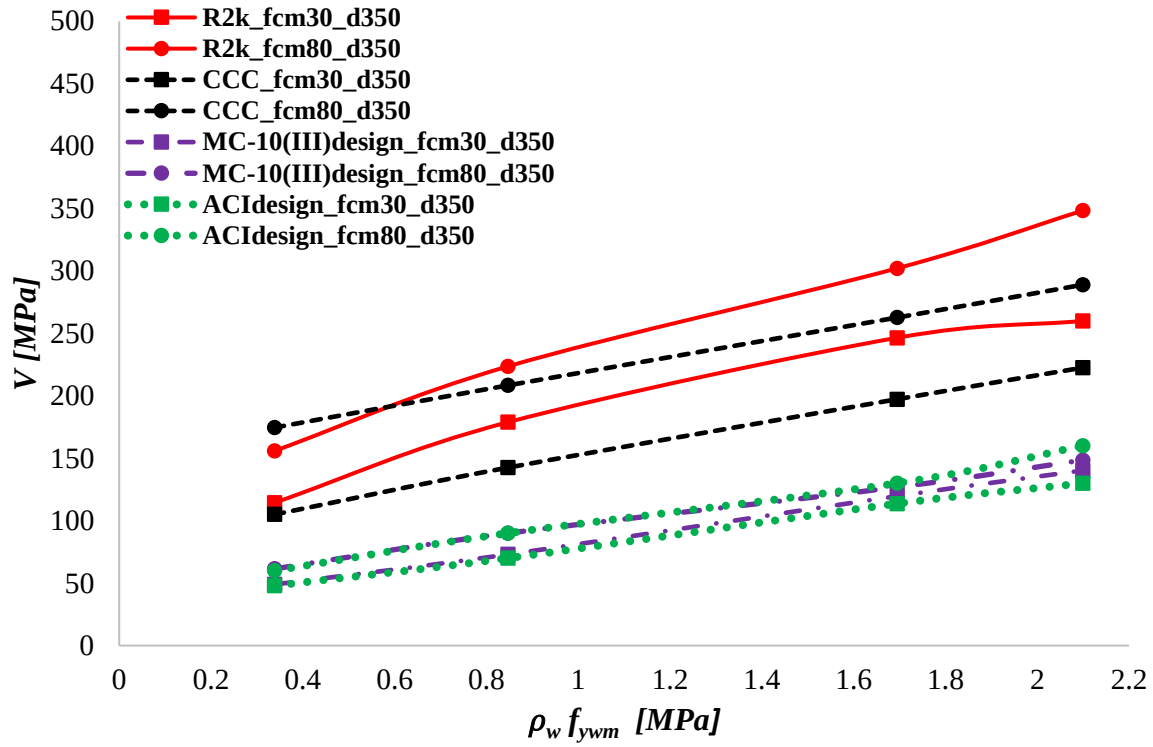

Figure 8.1. Plot of MC-10 (III), ACI 318 design shear resistance and GPM mean values for effective member depth $d = 350\ mm$

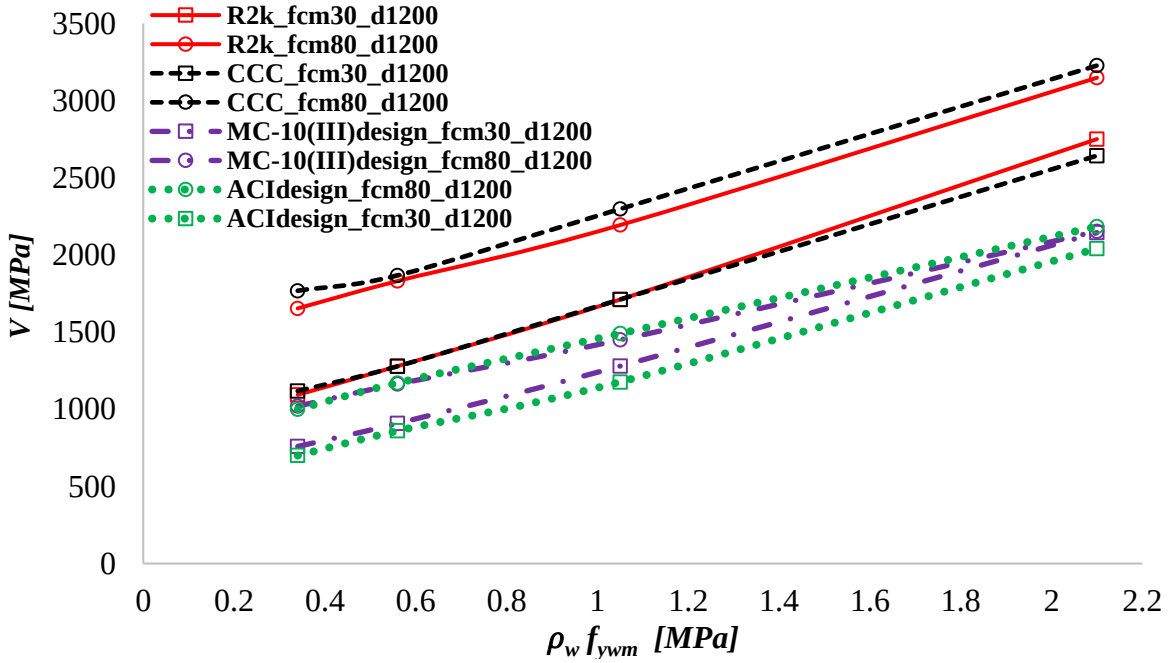

Figure 8.2. Plot of MC-10 (III), ACI 318 design shear resistance and GPM mean values for effective member depth $d = 1200\ mm$

Generally, a significant $V_{GPM} - V_{Rd}\ (X_k, \gamma, \phi)$ margin is observed from the figures over the considered range of shear reinforcement $\rho_w f_{ywm}$, effective beam depth d and concrete strength f_{cm}. As expected, the GPM mean values V_{GPM} and the design shear resistance ($V_{MC-10(III)}\ (X_k, \gamma)$ and $V_{ACI}(X_k, \phi)$) generally increase as the amount of shear reinforcement $\rho_w f_{ywm}$, effective beam depth d and concrete strength f_{cm} increase.

V_{R2k} predictions differ substantially from V_{CCC} predictions for small beams (Figure 8.1). For this specific case, the CCC model may not be good. The model overestimated capacity compared to experiments for a few cases of small beams discussed in Chapter 6 (Section 6.4.2.1). In general MCFT (R2k) V_{R2k} was evaluated to better capture true shear performance (discussed in Section 7.2.1.1).

8.3.1 Influence of concrete strength and shear reinforcement on $V_{Rd}\ (X_k, \gamma)$ and V_{GPM}

Close examination of Figure 8.1 and 8.2 reveal the following:

- The $V_{GPM} - V_{Rd}\ (X_k, \gamma, \phi)$ margin as illustrated in Figure 8.1 and 8.2 is predominantly caused by the sensitivity of V_{GPM} to concrete strength. Mean shear capacity is positively influenced by increased concrete strength as illustrated by its significant increase for both GPMs. V_{GPM} predictions are shown in the figures to be more sensitive to concrete strength than the design shear resistance $V_{Rd}\ (X_k, \gamma, \phi)$.
- Increased concrete strength f_{cm} increases the design shear resistance $V_{Rd}(X_k, \gamma, \phi)$. This can be attributed to the relative magnitude of the concrete contribution term to the overall shear resistance. In both the MC-10 (III) and ACI formulation the design shear resistance is based on a stirrup contribution and a concrete contribution. The sensitivity of MC-10 (III) and ACI design shear resistance to concrete strength can be explained by the inclusion of these concrete contribution terms in their respective design formulations.
- The influence of increased concrete strength slightly reduces in MC-10 (III) as $\rho_w f_{ywm}$ increases, particularly for deep beams (Figure 8.2) due to the reduced relative concrete contribution to the overall design shear resistance.

8.3.2 Influence of effective member depth on $V_{Rd}\ (X_k, \gamma, \phi)$ and V_{GPM}

A relatively larger safety margin $V_{GPM} - V_{Rd}\ (X_k, \gamma, \phi)$ is observed in the case of shallow beams (Figure 8.1) compared to deep beams (Figure 8.2) at all $\rho_w f_{ywm}$ situations. This is because the design values $V_{MC-10(III)}\ (X_k, \gamma)$ and $V_{ACI}(X_k, \phi)$ seem to overestimate the positive influence of increased beam depth, compared to V_{GPM} predictions.

8.4 Reliability investigation and discussion

8.4.1 Reliability of individual test sections

The reliability of two test sections IR80A and 2R30D from Table 8.1 is presented here. The parameters of the beams are illustrated in Figure 8.3. Test section IR80A (small beam with high concrete strength and little shear reinforcement) was assessed to have the highest reliability index of β = 6.6 and 6.2 for MC-10 (III) and ACI shear design formulation respectively whereas test section 2R30D (large beam with low concrete strength and heavily shear reinforced) was assessed to have the lowest reliability index of β = 1.6 and 1.9 for MC-10 (III) and ACI shear design formulation respectively. MC-10(III) and ACI 318 provide conservative predictions for small beams and unconservative predictions for large beams as shown in Figure 6.10(d) and 6.9(d). This is also confirmed by investigations conducted by (Mari *et al*., 2015; Cladera *et al*., 2016; Ismail, 2016)

Combinations of low amounts of shear reinforcement $\rho_w f_{ywm}$, small beam depth d and high concrete strength f_{cm}

Beam IR80A is a lightly shear reinforced ($\rho_w f_{ywm} = 0.34\ MPa$) small beam with a high concrete strength of $f_{cm} = 80$ MPa. The high concrete strength increases the obtained GPM mean values V_{GPM} (best estimate of true shear capacity). The small effective member depth of beam IR80A results in reduced concrete contribution to the overall design shear resistance, resulting in smaller $V_{Rd}\ (X_k, \gamma, \phi)$ values compared to a large beam. The combination of high concrete strength and small member depth increased the safety margin ($V_{GPM} - V_{MC-10(III)}\ (X_k, \gamma)$). Beam IR80A has a relatively low GPM uncertainty due to lower $V_{GPM}(x_m)$ as a result of the low amount of shear reinforcement (Section 8.4.2.2). The combined effect of the high safety margin with low GPM uncertainty resulted in relatively higher reliability for both MC-10 (III) and ACI shear design formulation.

Combinations of high amounts of shear reinforcement $\rho_w f_{ywm}$, large depth d and low concrete strength f_{cm}

Beam 2R30D had the lowest reliability index in the parametric assessment at $\beta = 1.6$ and 1.9 respectively for MC-10 (III) and ACI shear design formulation. Beam 2R30D is heavily shear reinforced with $\rho_w f_{ywm} = 2.1$ and low concrete strength of $f_{cm} = 30$ MPa. The large effective member depth of beam 2R30D directly indicates a relatively high concrete contribution to the total design shear resistance, resulting in large $V_{MC-10(III)}(X_k, \gamma)$ and $V_{ACI}(X_k, \phi)$ values when compared to a small beam. High $V_{Rd}(X_k, \gamma, \phi)$ values together with comparatively low V_{GPM} values imply low safety margins. Beam 2R30D has a high GPM uncertainty (that is σ_{GPM} increases) due to the relatively increased $V_{GPM}(x_m)$ as a result of the high amount of shear reinforcement (Section 8.4.2.2). The combined effect of the low safety margin with high GPM uncertainty resulted in relatively lower levels of reliability for this case, for both MC-10 (III) and ACI shear design formulation.

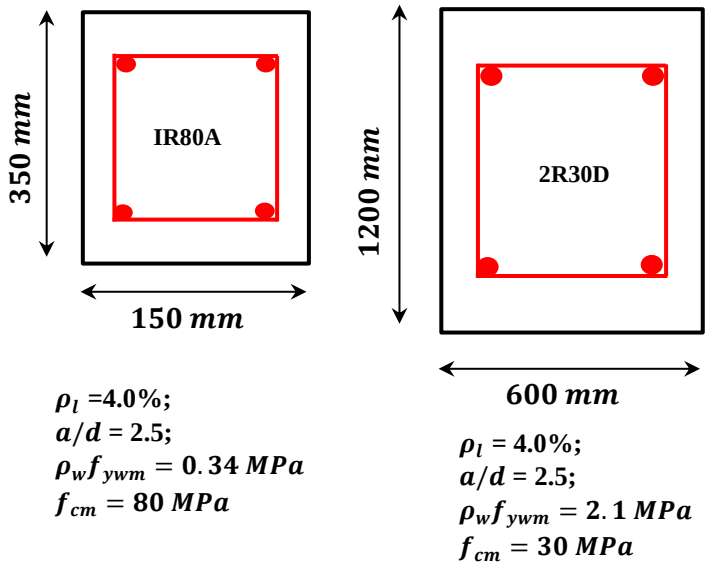

Figure 8.3. Parameters of individual test section

8.4.2 Assessment of estimated β values with $\rho_w f_{ywm}$, d and f_{cm}

This section presents the influence of the amount of shear reinforcement $\rho_w f_{ywm}$, beam depth d and concrete strength f_{cm} on the reliability of the ACI and MC-10 (III) shear design formulation using the test sections presented in Table 8.1. The obtained reliability indices from a number of test sections are

presented graphically in Figures 8.4 and 8.5 to portray the trends in reliability with respect to the investigated shear parameters. The reliability levels of both MC-10 (III) and ACI, as presented in Figures 8.4 and 8.5 respectively, decline with increasing stirrups $\rho_w f_{ywm}$ and beam size. The estimated reliability index increases with increasing concrete strength.

For small beams, the reliability index obtained using MCFT (R2k) based GPM (β_{R2k}) are substantially greater than that of CCC based GPM (β_{CCC}). This is explained by the observation that CCC predicts mostly lower GPM mean values V_{GPM} than MCFT (R2k) (Figure 8.1); and MF_{CCC} has a slightly higher standard deviation than MF_{R2k} (Table 7.2). The reliability indices obtained using both MCFT (R2k) and CCC based GPMs meet the target reliabilities in the case of small beams.

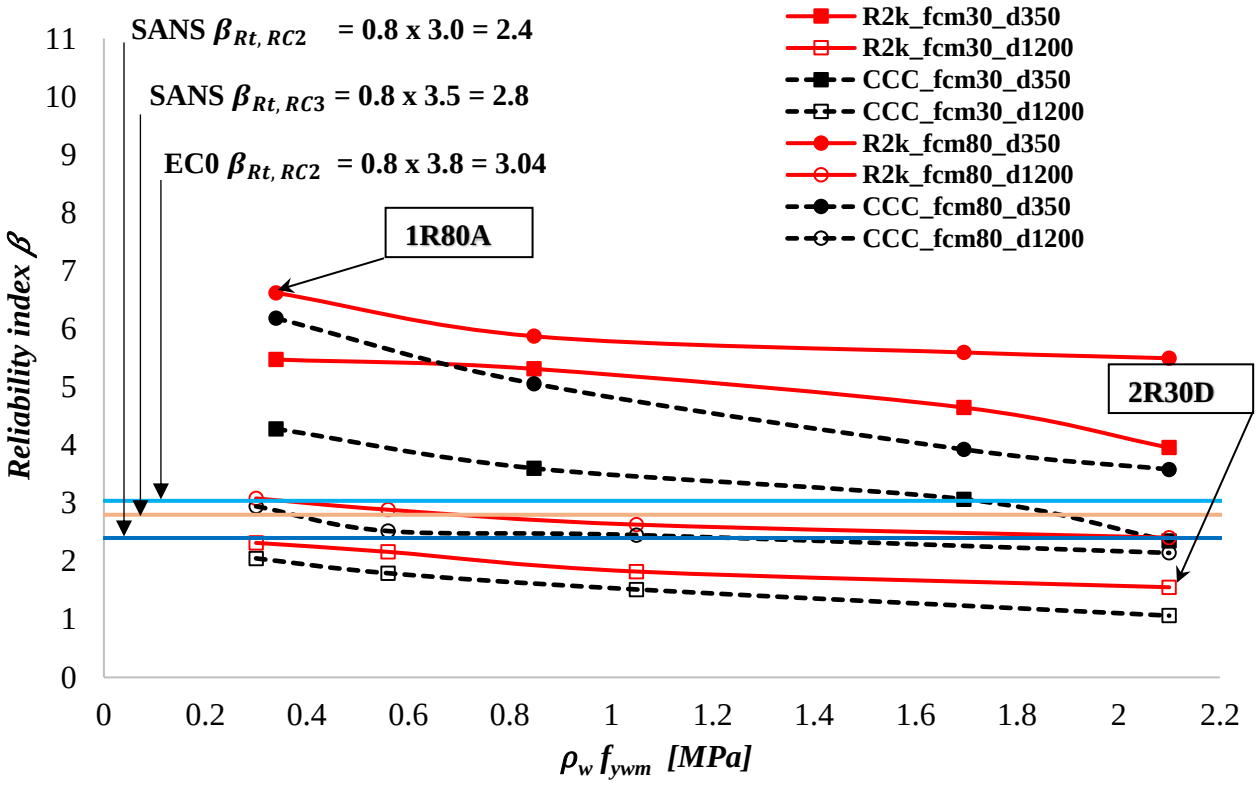

Figure 8.4. MC -10 (III) reliability indices β obtained from the FORM evaluations of $g(X)$

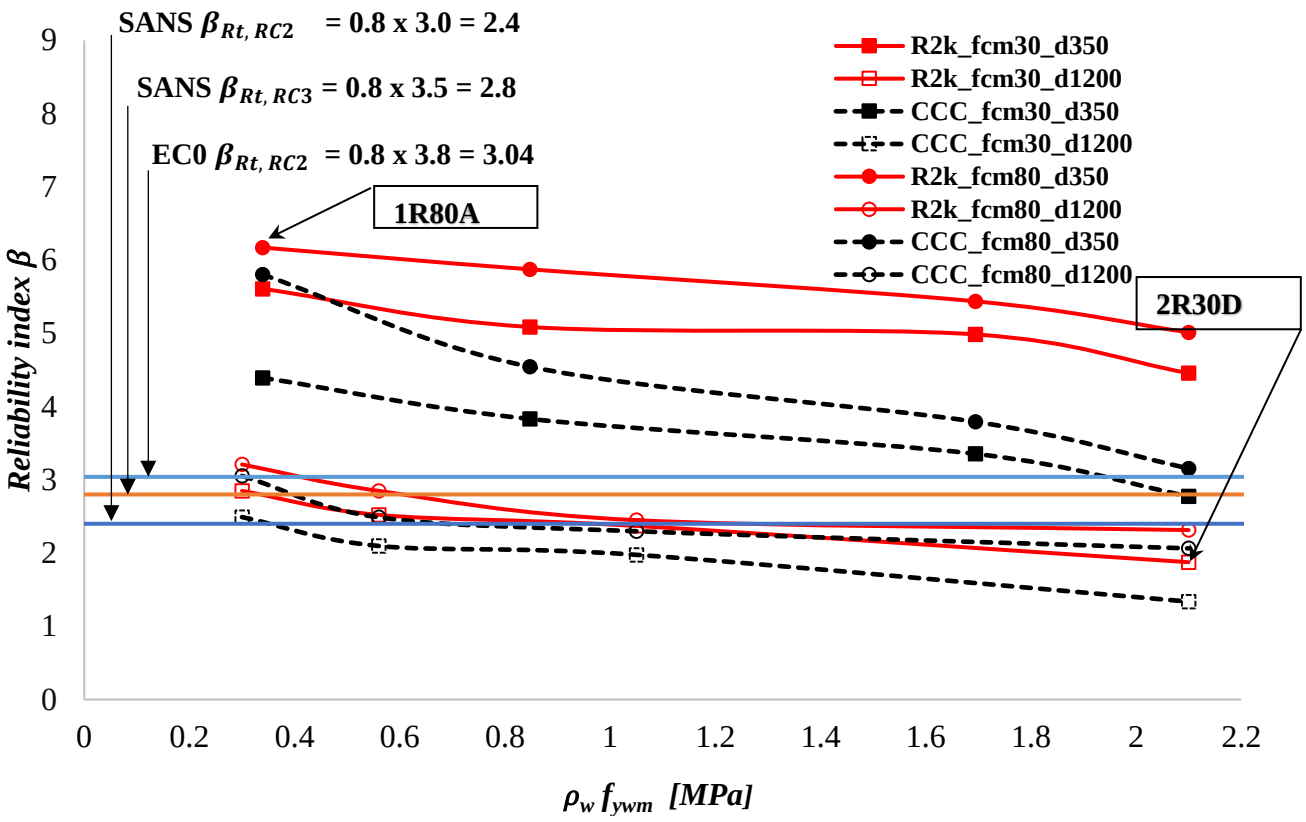

Figure 8.5. ACI reliability indices β using the strength reduction factor in ACI 318-11

8.4.2.1 Trends in estimated β values with beam member d

Figures 8.4 and 8.5 show a significant decrease in β values with increasing beam depth d for both MC-10 (III) and ACI design formulations. This is because the design values $V_{MC-10(III)}(X_k, \gamma)$ and $V_{ACI}(X_k, \phi)$ over-accounts for the contribution of increased beam depth as captured by the V_{R2k} and V_{CCC} predictions.

8.4.2.2 Trends in β values with increasing $\rho_w f_{ywm}$ and concrete strength f_{cm}

A decreasing trend in ACI and MC-10 (III) reliability as $\rho_w f_{ywm}$ increases is observed from Figure 8.4 and 8.5. This is due to increasing GPM uncertainty with increases in $V_{GPM}(X_m)$, thereby resulting in a decreasing level of reliability for both the ACI and MC-10 (III) shear design formulations. The figures also show an increase in estimated reliability β values as the concrete strength f_{cm} increases. The sensitivity of β values to f_{cm} is mainly governed by the sensitivity of V_{R2k} and V_{CCC} to f_{cm} (see Figures 8.1 and 8.2)

8.4.3 Evaluation of representative β values against the performance requirements for shear resistance

The target reliability requirement prescribed by basis of design standards SANS 10160 and EN 1990 (Reliability Class 2 structures) are shown on Figures 8.4 and 8.5. Deep beams ($d = 1200mm$) with low concrete strength ($f_{cm} = 30\ MPa$), designed according to MC-10 (III) shear design formulation falls quite significantly below the target reliabilities. Investigations conducted by Ismail (2016), Cladera *et al*. (2016) and Sykora *et al*. (2018) initially pointed to the possible inadequate reliability of MC-10 (III) for deep beams. The reliability indices presented in Figure 8.4 confirm indequate reliability of the design code for low strength deep beams.

However, small beams ($d = 350\ mm$) designed according to both MC-10 (III) and ACI shear design formulations are in accordance with the target reliabilities for the range of shear reinforcement $\rho_w f_{ywm}$ and concrete strength f_{cm} investigated.

8.4.4 Consistency of ACI and MC-10 (III) reliability

A reasonable consistency in the reliability of ACI and MC-10 (III) shear design formulation across range of $\rho_w f_{ywm}$ is observed from Figures 8.4 and 8.5. For small beams ($d = 350mm$), the reliability level slightly decreases with increasing stirrups $\rho_w f_{ywm}$ from a value of 6.6 to a value of 5.5 for MC-10 (III) design formulation and from a value of 6.2 to a value of 5.0 for ACI design formulation. However, the reliability level drastically decreases with increasing member depth d. The ACI and MC-10 (III) design formulations do not correctly account for size effect, resulting in the rapid decrease in reliability as the effective member depth increases (i.e. reliability is not consistent).

8.5 Comparison of reliability index of EC2 VSIM to ACI and MC-10 (III)

In this section, the Eurocode 2 VSIM reliability trend is compared to the corresponding Fib Model Code Level of Approximation three (MC-10 (III)) and American Concrete Institute building standard ACI 318 reliability index for rectangular test sections with $d = 600mm$ (detailed in Table 7.3 [Section 7.2.4]) and $d = 1200\ mm$ (Table 8.1). The MC-10 (III) and ACI 318 design formulations were chosen for comparison because they represent established design procedures suitable for routine

design. EC2 VSIM assumes that the shear reinforcement carries all the shear force, neglecting the concrete contribution. ACI 318 building standard adopts the 45^0 truss analogy in the estimation of shear reinforcement contribution to shear resistance. It assumes that the total design shear resistance is the summation of the concrete contribution and the contribution from shear reinforcement. The Fib Model Code (III) shear design formulation is based on the Modified Compression Field theory and the General stress field theory. The MC-10 (III) design provisions establish in general that the total shear resistance is constituted of the sum of the concrete contribution and the stirrup contribution. Figure 8.6 (a & b) below presents the comparison of the reliability index obtained from EC2, MC-10 (III) and ACI design formulation.

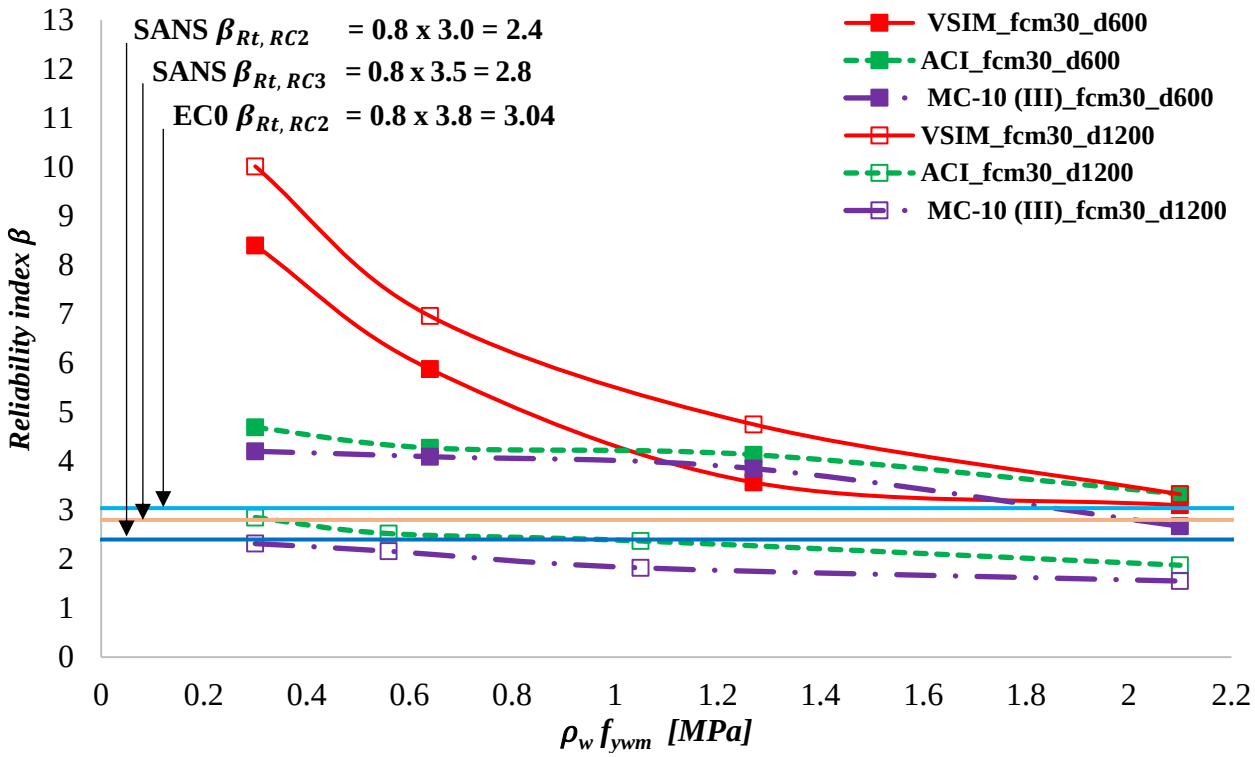

a) $f_{cm} = 30\ MPa$

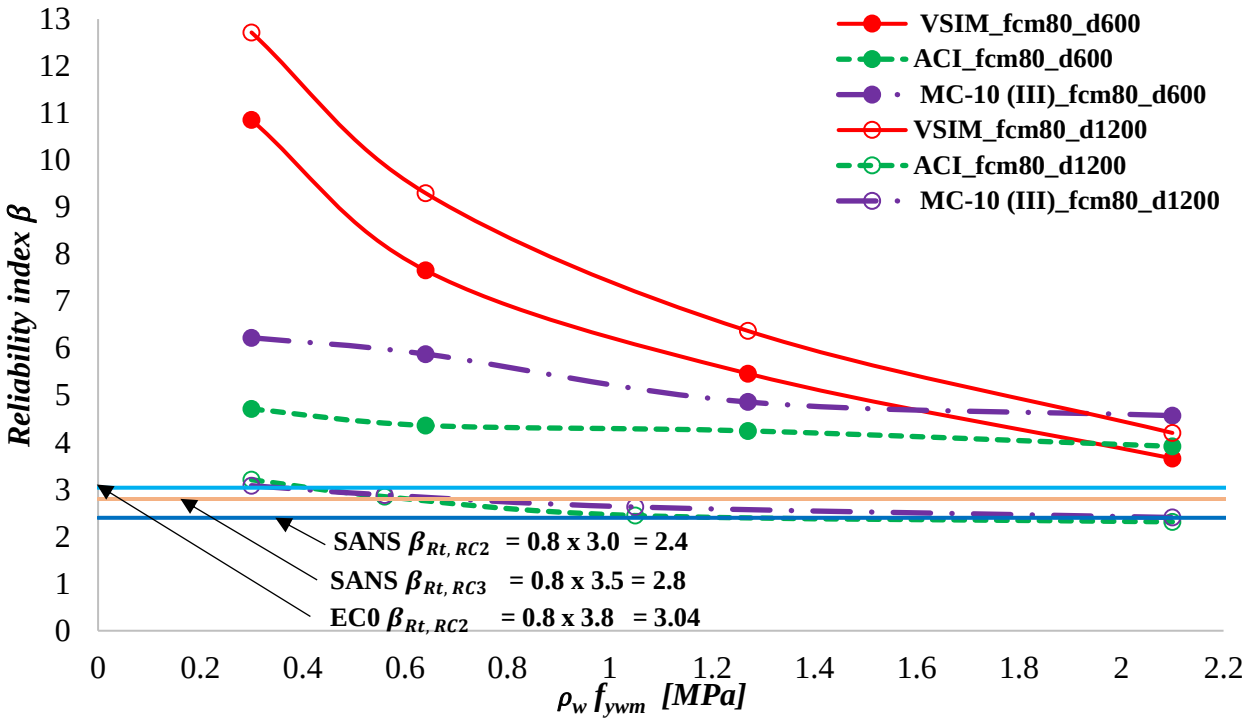

b) $f_{cm} = 80\ MPa$

Figure 8.6. Comparison of the reliability index of a range of possible design situations

Critical examination of Figure 8.6 (a & b) reveals that:

- Generally, the reliability level decreases with increasing shear reinforcement ($\rho_w f_{ywm}$) and increases with increasing concrete strength (f_{cm}) for all the design codes.
- The reliability indices obtained for MC-10 (III) and ACI shear design formulations at low levels of shear reinforcement ($\rho_w f_{ywm} < 1\ MPa$) are closer to the resistance target reliability values than that of EC2 VSIM. It has previously been shown that EC2 VSIM provides excessively conservative predictions at low amounts of shear reinforcement.
- EC2 shear reliability increases with increasing beam depth d, whereas MC-10 (III) and ACI shear reliability decreases with increasing beam depth d.
- The reliability of deep beam ($d = 1200mm$) with low concrete strength ($f_{cm} = 30\ MPa$) designed according to MC-10 (III) shear design formulation falls quite significantly below the target reliability values.

- For medium size beams ($d = 600mm$), the reliability indices of all the design codes exceeded the target reliability requirement for Reliability Class 2 structures prescribed by basis of design standards SANS 10160 and EN 1990.

8.6 Summary and conclusions

The reliability of ACI and MC-10 (III) can be summarised as follows:

- The lowest levels of reliability for ACI and MC-10 (III) can be expected for highly shear reinforced members with low concrete strength and large member depth.
- For deep beams ($d = 1200mm$) with low concrete strength ($f_{cm} = 30\ MPa$), the estimated reliability index for MC-10 (III) falls quite significantly below the target reliabilities (as low as $\beta = 1.6$ at $\rho_w f_{ywm} = 2.1\ MPa$). The work of Ismail (2016), Cladera *et al*. (2016) and Sykora *et al*. (2018) initially pointed to the possible inadequate reliability for deep beams designed according to MC-10 (III) shear design provisions.
- The highest levels of reliability for ACI and MC-10 (III) can be expected for low shear reinforced members with high concrete strength and small member depth.
- The reliability indicies of small (shallow) beams designed according to ACI and MC-10 (III) substantially exceed target reliabilities.
- For small beams ($d = 350mm$), the reliability level slightly decreases with increasing stirrups $\rho_w f_{ywm}$ from a value of 6.6 to a value of 5.5 for MC-10 (III) design formulation and from a value of 6.2 to a value of 5.0 for ACI design formulation.

Conclusions

9.1 Overview

The Eurocode 2 (EC2) stirrup design procedure is based on the Variable Strut Inclination Method (VSIM) for shear. South Africa is on the advent of adopting the EC2 as the equivalent standard for local use, hence the VSIM-based stirrup design procedure will be adopted as well.

Investigations conducted by Cladera & Mari (2007) provided an initial indication that the best-estimate predictions of VSIM are systematically sensitive to the amount of shear reinforcement. VSIM capacity predictions underestimate shear capacity at low stirrup quantities but, conversely, overestimate shear capacity at high stirrup quantities. Investigations presented in Chapters 4 and 6 of this thesis confirmed findings by Cladera & Mari (2007).

The failure of VSIM to accurately capture trends witnessed from experimental observations attests to the presence of significant model uncertainties in the shear strength model. No evidence has been found from background documents and relevant literature that VSIM has been calibrated to account for systematic trends associated with stirrup quantities. This raised concern that the EC2 VSIM design procedure may be potentially unsafe at high stirrup quantities even though conventional partial factors and characteristic values are enforced. Also, over conservatism at low stirrup reinforcement would not be ideal (uneconomic performance). The evaluation of the general performance of EC2 VSIM design formulation, therefore, became one of the crucial tasks of South Africa's adoption process.

Although the primary goal of this investigation stemmed from the appraisal of the reliability performance of EC2 VSIM design procedures across practical ranges of main design parameters (concrete strength, shear reinforcement and beam depth), other established alternative shear design formulations from across the globe were also investigated in an attempt to understand the behaviour of shear in beams fully and to efficiently assess shear reliability performance. The insights gained from these reliability-based investigations are not only applicable to the South African environment but have contributed to worldwide research efforts on shear in reinforced concrete beams and practical application of reliability methods in deriving structural design guidelines.

9.2 Achievement of research objectives

Four critical questions were posed in the introductory chapter of this dissertation to define the problem statement of this investigation clearly. These questions were:

1. What are the model uncertainties in shear resistance models?
2. Which of these models is most suitable as a general probabilistic model (GPM) for shear resistance?
3. Over the range of practical design situations, does the EC2 shear design formulation consistently meet reliability targets?
4. What is the reliability performance of alternative shear design provisions (Fib Model Code 2010 and ACI-318) compared to EC2?

This investigation has directly addressed the issues raised in these questions. The objectives of this research introduced in Chapter 1 have been accomplished and presented in the previous chapters which can shortly be summarised as follows:

a) An outline of the current understanding of shear failure in beams has been provided, discussing and illustrating the underlying shear transfer mechanisms and the effect of critical shear parameters on the behaviour of RC beams with stirrups. Salient features of the different models that have been developed for predicting shear strength of beams with stirrups were presented and discussed extensively. Shear design provisions of beams with shear reinforcement in well-established codes of practices were reviewed and presented.

b) The VSIM model and alternative widely used shear models like ACI-318 shear model, Fib Model Code 2010 (MC-10 (III)) model, Modified Compression Field Theory (MCFT) based analysis program Response 2000 (R2k), and Compression Chord Capacity Model CCC (Cladera *et al*., 2016) were compared to experimental results in Chapter 4. Parametric mean and design value analysis were conducted for the various shear strength models. The mean value analysis provided an overview of the performance of their unbiased capacity predictions and provided basis to assess their accuracy. The design value analysis provided a comparison of the trend of EC2 design value predictions to other established design provisions like ACI 318 and Fib Model Code 10.

c) Quantification of model uncertainty and bias is an essential first step towards effective shear reliability assessment since these contribute significantly to reliability performance. Quantification and statistical assessment of model factors related to shear capacity predictions were presented in Chapter 6. The derived model factors were investigated parametrically against important shear design parameters. The model factors related to the operational EC2 VSIM shear capacity predictions were found to be sensitive to the amount of shear reinforcement with model factors significantly above one (underpredicting capacity) at low levels of stirrup reinforcement. Correlation and regression assessments uncovered milder sensitivities to other vital parameters affecting shear strength. The model factor statistics derived herein were used in reliability assessment of the EC2 VSIM shear design provisions and alternative shear design procedures.

d) Based on the results obtained from the model factor characterisation (Chapter 6), two shear resistance models were considered suitable as general probabilistic models GPMs for the reliability assessment of EC2 shear design procedure and alternative shear design procedures. The principal GPM was established based on the probabilistic representation of the MCFT. MCFT capacity predictions were obtained from the implementation sectional analysis program Response-2000 (R2k). As a validation procedure, an alternative GPM based on the Compression Chord Capacity Model (CCC) was implemented.

e) Reliability performance of EC2 VSIM design procedure was conducted at parametric variations of stirrup reinforcement, concrete strength and beam depth using the principally derived GPM function MCFT (R2k) and the alternate GPM function CCC (as validation) as presented in Chapter 7. The First Order Reliability Method (FORM) was used to compute the reliability index for specific test sections. The results from the reliability performance investigations showed a general decreasing trend of reliability levels as shear reinforcement increases and increasing reliability levels as concrete strength and beam depth increases.

f) The reliability performance assessment of the alternative shear design provisions was presented in Chapter 8. The alternative design provisions investigated include shear design provisions in ACI and Fib Model Code 2010 (MC-10 (III)). The assessment revealed that the reliability levels generally decrease with increasing shear reinforcement and increase with increasing concrete strength for all the design codes investigated. MC-10 (III) and ACI shear reliability decreases with increasing beam depth d.

g) It was concluded from the reliability investigations that deep beams with low concrete strengths designed according to MC-10 (III) have inadequate reliabilities for the design range considered. However, small (shallow) beams designed according to ACI and MC-10 (III) have adequate reliabilities. The reliability of EC2 for all the beams investigated meets the target reliabilities. However, EC2 VSIM reliability indices at low levels of shear reinforcement substantially exceed the target reliabilities, implying uneconomical designs in this range. Generally, the reliability trends of the different design provisions directly portray inconsistent reliability performance across range of practical applications. The reliability trend of EC2 is inconsistent over the range of shear reinforcement; ACI and MC-10 (III) reliability is inconsistent over the range of beam depths.

The different analyses undertaken to appraise the performance of EC2 VSIM design procedure are summarised in Section 9.3 below.

9.3 Reliability performance of EC2 VSIM

9.3.1 EC2 VSIM design function for shear resistance

For members with stirrups, the primary EC2 VSIM design function for shear resistance $V_{Rd,s}$ considers only the shear strength contribution from stirrup reinforcement, neglecting the contribution from concrete. The EC2 VSIM design shear resistance is taken to be the lesser of either $V_{Rd,s}$ or $V_{Rd,max}$. $V_{Rd,max}$ represents the upper limit of design shear resistance set to avoid web-crushing failures. The VSIM for shear is basically a truss model allowing for the variable inclination of concrete struts θ within the confines of $1 \leq \cot\theta \leq 2.5$.

The performance of EC2 VSIM to a certain degree depends on the limits governing the concrete compressive strut angle (θ). Investigations in this study revealed that the unbiased and unconstrained analytical formulation of VSIM (i.e. without the concrete strut angle θ limitation) naturally predicts lower than the 21.8^0 lower limit recommended by Eurocode 2. The lower limit of 21.8^0 as stated in the operational EC2 VSIM shear design function is a form of bias enforced to achieve a more conservative estimate of shear predictions. The influence is more pronounced at lower levels of shear reinforcement. Generally, safety bias is introduced into the design procedure through the use of partial factors, characteristic values and a lower limit on the strut angle.

It was concluded that the unbiased VSIM predictions underestimate shear capacity at low stirrup quantities. This is ascribed to the neglect of concrete contribution to shear strength which is more significant in lightly shear reinforced beams. Conversely, the model overestimates shear capacity at high stirrup quantities (Section 6.4.4). Concrete strength only affects EC2 VSIM predictions at a combination of low concrete strength and high amount of shear reinforcement when the design concrete strut angle θ predicted by VSIM exceeds 21.8° (Section 3.2.6.6).

9.3.2 Deterministic assessment of VSIM stirrup design procedure

The sensitivity of VSIM procedure to the amount of shear reinforcement $\rho_w f_{ywm}$ motivated the assessment of the shear model against alternative widely used approaches (MCFT (R2k), MC-10 (III), ACI and CCC) and experimental results. The comparative assessment was performed to gain some insight in the performance of EC2 VSIM to other available alternative methods and assess the accuracy of the various shear methods. The following observations were made from the assessment:

- The trend lines of the MCFT (R2k) and CCC capture the experimental observations reasonably well.
- VSIM and ACI mean values are consistently conservative over the parametric range compared to other shear methods.
- The trend line of $V_{VSIM-L\theta}$ fails to capture the trend of experimental observations at higher levels of shear reinforcement $\rho_w f_{ywm}$, portraying a relatively reducing contribution of additional stirrup reinforcement.

Normalised EC2 VSIM mean value predictions were compared with MCFT (R2k), MC-10 (III), ACI and CCC for specific test sections. MCFT (R2k) observations were assumed to reflect the best shear behaviour for the test sections considered due to its better performance. The following observations were made from the analysis:

- The various shear methods are not only theoretically different but also provide different mean value trends as the amount of shear reinforcement $\rho_w f_{ywm}$, concrete strength and beam depth varies.
- VSIM predicts consistently more conservative values at low levels of shear reinforcement than other shear methods.

- CCC model offers the best estimation of MCFT (R2k) predictions. However, CCC predictions differ substantially from MCFT (R2k) predictions for small beams.

The trend line of normalised EC2 design shear strength for specific test sections was compared to the trend line of other design provisions (ACI 318 and MC-10(III)) at parametric variations of design shear reinforcement $\rho_w f_{ywd}$, characteristic concrete strength f_{ck} and beam depth. The following observations were made from the investigation:

- The design values of the various shear design methods compare well except at low levels of shear reinforcements ($\rho_w f_{ywd} < 1\ MPa$).
- EC2 VSIM design method is the most conservative method at low levels of shear reinforcement for both low and high concrete strengths.

The mean and design value analysis have shown a clear indication of inconsistency across the range of shear reinforcement $\rho_w f_{ywm}$, concrete strength f_{cm} and beam depth which is of some concern. The inability of the different shear strength models to accurately capture trends witnessed from experimental observations and also, the differences in predictions from the different models attests to the presence of significant model uncertainties.

For these reasons, quantification of the model factors for the various models and subsequent reliability assessment of EC2 VSIM shear design formulation and the alternative shear design procedures were conducted.

9.3.3 Characterisation of model uncertainty and bias for shear reliability assessment

Some key model factor statistics were derived using a database of shear reinforced experiments towards an effective reliability performance assessment of shear design procedures. The models investigated include two forms of the Variable Strut Inclination Method (VSIM) ($V_{VSIM-L\theta}$) and (V_{VSIM-A}), the best-estimate predictions from MCFT (R2k), Fib Model Code 10 (III), ACI 318 model and CCC model.

Each model factor distribution was evaluated using correlation and regression analyses against main parameters affecting shear capacity prediction which includes shear span to depth ratio a/d, amount

of longitudinal tension reinforcement ρ_l, amount of shear-reinforcement $\rho_w f_{ywm}$, effective depth d, concrete strength f_{cm} and beam width b_w.

The key outcomes of the statistical assessment were as follows:

- The model factor $\text{MF}_{VSIM-L\theta}$ (associated with the $\text{V}_{VSIM-L\theta}$ calculation procedure) has a mean value of $\mu_{MF} = 1.58$ and a standard deviation of $\sigma_{MF} = 0.48$, confirming that the unbiased shear resistance function $\text{V}_{VSIM-L\theta}$ generally underpredicts shear capacity.
- The spread of $\sigma_{MF} = 0.48$ suggests a large scatter of $\text{MF}_{VSIM-L\theta}$ about the mean. Parametric correlation and regression analyses showed that $\text{V}_{VSIM-L\theta}$ predictions are sensitive to $\rho_w f_{ywm}$, significantly underpredicting shear capacity initially and later overpredicting shear capacity as $\rho_w f_{ywm}$ increases.
- The model factor MF_{VSIM-A} has a mean value of $(\mu_{MF} = 0.90)$, indicating that V_{VSIM-A} generally overpredicts shear capacity. MF_{VSIM-A} shows less scatter about the mean with standard deviation of $\sigma_{MF} = 0.25$. Correlation and regression analyses of MF_{VSIM-A} against important shear parameters revealed that V_{VSIM-A} is significantly sensitive to $\rho_w f_{ywm}$ and beam width b_w.
- The model factor $MF_{MC-10(III)}$ was found to have a mean value of $\mu_{MF} = 1.21$ and a standard deviation of $\sigma_{MF} = 0.35$. Parametric correlation and regression analyses of $MF_{MC-10(III)}$ against main shear parameters show that $V_{MC-10(III)}$ has a strong correlation with the member depth d, indicating that the MC-10 (III) method does not adequately account for the size effect on shear resistance.
- MF_{ACI} has a mean value of $\mu_{MF} = 1.56$ with a standard deviation of $\sigma_{MF} = 0.30$, implying that V_{ACI} generally underpredicts shear capacity. MF_{ACI} was shown to have a strong correlation with the effective member depth d and beam width b_w, implying that the ACI method does not adequately take into account the size effect on shear resistance.
- Both V_{CCC} and V_{R2k} models achieved a more suitable characterisation of the model factor in terms of mean and spread. MF_{CCC} has a mean value of $\mu_{MF} = 1.04$ and a spread of $\sigma_{MF} = 0.19$. However, the CCC model significantly overpredicts capacity for some specific small beams (see Section 6.4.2).

- MF_{R2k} is a better predictor of resistance in terms of spread with a standard deviation of $\sigma_{MF} = 0.16$ and a mean value of $\mu_{MF} = 1.04$.
- Correlation and regression analyses show that both MF_{CCC} and MF_{R2k} did not display any major trend with the shear parameters investigated in this study. This implies that MCFT (R2k) and CCC model have captured the effect of shear parameters well.

The model factor is expected to have a significant footprint on the assessed reliability of design procedures for reinforced concrete beams subjected to shear. Overestimation of the conservative bias of the model factor and underestimation of its variability may lead to overestimation of the implicit safety levels. The GPM for shear capacity prediction should be chosen carefully to correspond to minimum model bias and uncertainty. The significant uncertainties and bias displayed by $V_{VSIM-L\theta}$, V_{VSIM-A}, $V_{MC-10(III)}$, V_{ACI} and their trend with shear parameters makes it evident that the shear models may not provide a suitable GPM representation for reliability performance assessment. The better description of model factor statistics displayed by both V_{CCC} and V_{R2k} prediction models in terms of bias and uncertainty and their insignificant trend with shear parameters are pointers to their suitability as general probabilistic models (GPM) for reliability assessment. V_{CCC} and V_{R2k} models and their model factor statistics can be used in the reliability assessment process to evaluate the inherent safety levels in any shear design procedure.

9.3.4 Reliability analysis of EC2 VSIM design shear resistance $V_{VSIM-L\theta}$

The systematic sensitivity of $V_{VSIM-L\theta}$ predictions to the amount of stirrup reinforcement motivated the need for the reliability assessment of the design procedure to appraise the consistency and uniformity of its performance with regards to reliability index over the range of practical application (shear reinforcements $\rho_w f_{ywm}$, concrete strengths f_{cm} and beam depths d). The FORM method was implemented for the performance evaluation of VSIM procedure.

The principal reliability assessment from which main conclusions were drawn, was performed based on the probabilistic representation of MCFT (R2k) as GPM. MCFT (R2k) mean value predictions were admitted as the principal model for developing the GPM for shear resistance due to its more precise capacity predictions and milder sensitivity to the main shear parameters (discussed in Section 7.2.1.1). Alternative reliability assessment using CCC based GPM was also conducted to validate investigations done using the principal GPM. The implementation of the two GPMs, however, provided the following powerful and useful insights:

- The estimated β values from MCFT (R2k) based performance function (β_{R2k}) corroborate the trends of estimated β values from the CCC based performance function (β_{CCC}).
- They both indicate uneconomically high reliability of the EC2 design formulation at low levels of shear reinforcement and strongly reduced (but still adequate) reliability with increased shear reinforcement.
- Also, the estimated β values increase with increasing concrete strengths and beam depth using both GPMs.
- The inspection of β_{CCC} and β_{R2k} revealed that for a specified combination of $\rho_w f_{ywm}$, d and f_{cm} situations, β_{R2k} are greater than β_{CCC}. The observation that CCC predicts slightly lower mean value V_m than MCFT (R2k); and MF_{CCC} has a slightly higher standard deviation than MF_{R2k}, explains the lower reliability indices β obtained from CCC compared to MCFT (R2k).

9.3.4.1 Comparison of the reliability index of rectangular beams and I-beams

The reliability investigation of rectangular and I-shaped beams reveals that both shapes of beams portray a similar trend of reliability index with the amount of shear reinforcement $\rho_w f_{ywm}$, concrete strength f_{cm} and beam depth d. However, the reliability index obtained for I-shaped beams are significantly higher than that of rectangular beams. The difference in the reliability indices can be ascribed to the fact that EC2 underestimates design shear resistance for I-beams due to the neglect of shear contributions from compression flanges and longitudinal reinforcements (dowel action), thereby resulting in higher reliability values for such beams.

The rectangular beams were therefore considered the most critical representative test sections for reliability assessment of EC2 VSIM. Consequently, main conclusions were drawn from the reliability assessment using rectangular beam test sections.

9.3.4.2 Main conclusions from the reliability performance of VSIM

The main conclusions from the reliability assessment of EC2 shear procedure can be summarised as follows:

- EC2 shear design formulation is assessed to have high reliability for low levels of shear reinforcement, high concrete strength and large beam depth, and an actively reduced reliability (but still adequate) with increased levels of shear reinforcement, reduced concrete strength and beam depth.
- For beams with low amount of shear reinforcement, the estimated reliability index is substantially greater than the target reliability requirement for Reliability Class 2 structures prescribed by basis of design standards SANS 10160 and EN 1990, implying uneconomical designs.
- Reliability indices of all the rectangular test sections investigated meet the target reliabilities for the design range considered.
- EC2 underestimates design shear resistance for I-beams due to the neglect of shear contributions from compression flanges and longitudinal reinforcements (dowel action), thereby resulting in higher reliability values for such beams.
- For I-beams with shear reinforcements in excess of 2 MPa (i.e $\rho_w f_{ywm} > 2\,MPa$), the obtained reliability indices meet the target reliabilities for the design range considered.

9.3.5 Reliability analysis of alternative shear design procedures ACI 318 and Fib Model Code 10 (MC-10(III))

The reliability assessment conducted in Chapter 7 revealed the inconsistent reliability performance of EC2 shear design formulation across practical ranges of main shear design parameters. This motivated the evaluation of alternative approaches (ACI and MC-10(III)) in order to find design formulation that performs better in terms of achieving the target reliability index consistently. A decreasing trend in the model factor was observed with increased beam depth d for MC-10 (III) and ACI 318 as presented in Chapter 6. This motivated the need to confirm the adequacy of the reliability of deep beams designed according to ACI and MC-10 (III).

The reliability performance of ACI and MC-10 (III) shear design provisions was assessed at parametric variations of shear reinforcement $\rho_w f_{ywm}$, concrete strength f_{cm} and beam depth d; and

compared to that of the EC2 shear design formulation. The FORM was used to estimate the reliability index for specific beam configurations.

9.3.5.1 Main conclusions from the reliability investigation of ACI 318 and MC-10 (III)

The main conclusions from the reliability analysis of ACI and MC-10 (III) can be summarised as follows:

- The reliability levels of ACI and MC-10 (III) slightly decreases as the amount of shear reinforcement increases $\rho_w f_{ywm}$ and increases as the concrete strength increases.
- The reliability level drastically decreases with increasing beam effective member depth. It is possible for low strength deep beams that are heavily shear reinforced to exhibit levels of reliability that are consistently low.
- The reliability index of deep beam ($d = 1200\,mm$) with low concrete strength ($f_{cm} = 30\,MPa$) designed according to MC-10 (III) shear design formulation falls quite significantly below the target reliabilities. The work of Ismail (2016), Cladera *et al*. (2016) and Sykora *et al*. (2018) initially pointed to the possible inadequate reliability for deep beams designed according to MC-10 (III) shear design provisions. The reliability of MC-10 (III) as presented in this study confirms indequate reliability of the design provision for low strength deep beams.
- Reliability indices of MC-10 (III) and ACI design formulation for small beams ($d = 350\,mm$) substantially exceeded the target reliabilities for the design range considered.

9.3.5.2 Comparison of reliability trend of EC2 VSIM to ACI and MC-10(III)

The trend of the reliability of EC2 VSIM was compared to that of MC-10 (III) and ACI 318 design formulation for medium size ($d = 600mm$) and large ($d = 1200mm$) rectangular beams. ACI and MC-10 (III) were chosen for comparison because they represent an established design procedure suitable for routine design. The comparative assessment reveals the following:

- For the three design procedures, the reliability level decreases with increasing shear reinforcement ($\rho_w f_{ywm}$) and increases with increasing concrete strength (f_{cm}).

- MC-10 (III) and ACI predict less conservative reliability estimates at low amount of shear reinforcement compared to EC2 VSIM, indicating that MC-10 (III) and ACI are more economical at this design situation.
- EC2 shear reliability increases with increasing beam depth d, whereas MC-10 (III) and ACI shear reliability decreases with increasing beam depth d.
- For deep beams ($d = 1200\ mm$) with low concrete strengths ($f_{cm} = 30\ MPa$), the reliability of MC-10 (III) shear design formulation falls quite significantly below the target reliability values.
- For medium size beams ($d = 600mm$), all the design codes achieved the target reliability requirement for Reliability Class 2 structures prescribed by basis of design standards SANS 10160.
- The reliability trends of the different design provisions portray inconsistent reliability performance across the range of practical applications.

9.4 Recommendations for future research

The following recommendations are made on the basis of the research findings of this study:

- Experimental database of beams with stirrup failure: Refinement of the model factor statistics can be achieved through an increment of the database for stirrup failure investigated in this study. Therefore there is a need to expand the current database with more effort directed to deep and highly shear reinforced beams. The majority of the available tests so far have concentrated mostly in the regions of small and ordinary beams, low and moderate shear reinforcement.
- Improvement of the EC2 VSIM shear provisions for beams with stirrups: This could be accomplished by introducing a concrete contribution term (to account for contributions from compression flange and longitudinal reinforcement) to reduce overconservatism at low levels of shear reinforcement. Such improvement should address improving the consistency and uniformity of the design procedure across the range of application and alleviate the trend with shear reinforcement.
- Web-crushing failure: The assessment of Prinsloo (2012) confirmed the possibility of the occurrence of web-crushing failures at high levels of shear reinforcement. High amount of shear reinforcement increases the chances of the ultimate web-crushing strength being

attained before shear link yielding occurs. Reliability analysis of the web-crushing strength is a critical issue that requires attention in order to have full reliability calibration of the EN 1992-1-1 (EC2) shear design procedure. The steps followed in treating model uncertainty and bias for stirrup failure as implemented in this study can also be adopted in characterising model uncertainties associated with web-crushing failure.

- Experimental database on beams with web-crushing failure: Inferences from the preliminary investigations conducted by Prinsloo (2012) was drawn from limited data. Most of the available tests so far, in literature, have been conducted on stirrup failure. To validate the preliminary findings concerning web- crushing failure, additional tests are required on beams failing through web-crushing.
- Pre-stressed concrete beams: The performance assessment conducted in this study is also recommended to be further extended to shear in pre-stressed concrete beams. The shear database on pre-stressed concrete members compiled by Reineck *et al*. (2014) can be adopted for this investigation.
- Development of safe and economical shear design procedures: This study identifies the need for a more extensive study on recently published authorial models (such as Compression Chord Capacity model (Cladera *et al*., 2016)) towards developing shear design procedures that consistently achieve adequate safety and economical designs. The CCC model was shown to overpredict capacity for some specific small beams. This area deserves more investigation.

List of References

ACI-ASCE Committee 426 (1973). The shear strength of reinforced concrete members. *ACI Structural Journal,* Proc.,70:1091–187.

ACI Committee, American Concrete Institute, and International Organization for Standardization. (2008). Building code requirements for structural concrete (ACI 318-08) and commentary. American Concrete Institute.

ACI-ASCE Committee 445. Report on Shear and Torsion. (2009). Recent Approaches to Shear Design of Structural Concrete. *ACI Structural Journal*, vol. 124, pp. 1375-1416.

ACI Committee 318. (2011). Building Code Requirements for Structural Concrete (ACI 318-11M) and Commentary. American Concrete Institute.

AISC. (2016). Specification for structural steel buildings. AISC 360, Chicago.

American Society of Civil Engineers ASCE 7-16:2017. Minimum design loads and associated criteria for buildings and other structures. Reston, VA: ASCE.

Aguilar, G., Matamoros, A., Parra-Montesinos, G., Ramírez, J. and Wight, J. (2002). Experimental evaluation of design procedures for shear strength of deep reinforced concrete beams. *ACI Structural Journal*, vol. 99, no. 4, pp.539-548.

AASHTO LRFD (2002). AASHTO LRFD Bridge Design Specifications, American Association of State Highway and Transportation Officials.

Amani, J. and Moeini, R. (2012). Prediction of shear strength of reinforced concrete beams using adaptive neuro-fuzzy inference system and artificial neural network. *Scientia Iranica*, vol. 19, no. 2, pp.242-248.

Andermatt, M. and Lubell, A (2013). Behavior of concrete deep beams reinforced with internal fiber-reinforced polymer-experimental study. *ACI Structural Journal*, vol. 110, no. 4, p.585.

Angelakos, D., Bentz, E. and Collins, M. (2001). Effect of Concrete Strength and Minimum Stirrups on Shear Strength of Large Members. *ACI Structural Journal*, vol. 98, no. 3, pp. 290-300

Arafa, M., Alqedra, M. and An-Najjar, H. (2011). Neural network models for predicting shear strength of reinforced normal and high strength concrete deep beams. *Journal of Applied Science*, vol. 11, no. 2, pp.266-274.

Arun, M. and Ramakrishnan, S. (2014). Size Effect on Shear Behavior of High Strength RC Slender Beams. *Int. J. Res. Eng. Technol*, vol. 3, no. 8, pp.113-118.

Arslan, G. (2008). Shear strength of reinforced concrete beams with stirrups. *Materials and Structures*, *41*(1), 113-122.

Ashour A., Alvarez L. and Toropov V. (2003) Empirical modelling of shear strength of RC deep beams by genetic programming. *Comput Struct* vol. 81, no. 5, pp. 331–338

Attard, M. and Mendis, P. (1993). Ductility of High-Strength Concrete Columns. *Australian Civil Engineering Transactions*, vol. 35, no. 4, pp. 295-306.

Bazant, Z. and Sun, H. (1987). Size effect in diagonal shear failure: influence of aggregate size and stirrups. *ACI Material Journal*, vol. 84, no. 4, pp. 259–71.

Belarbi, A. and Hsu, T. T. (1995). Constitutive laws of softened concrete in biaxial tension compression. *Structural Journal*, vol. 92, no. 5, pp. 562-573.

Beeby, A. and Narayanan, S. (1995). Designers' Handbook to Eurocode 2: Part 1.1: Design of Concrete Structures (Eurocode Design Handbooks) (Pt. 1) . *American Society of Civil Engineers* ISBN 10: 0727716689.

Bentz, E. (2000). Sectional Analysis of Reinforced Concrete Members, PhD thesis, Department of Civil Engineering, University of Toronto, Toronto, ON, Canada, pp. 184.

Bentz, E. (2010). MC2010: Shear strength of beams and implications of the new approaches. Technical report, fib bulletin 57: Shear and punching shear in RC and FRC elements. fédération international du béton (fib), Switzerland.

Bentz, E., Vecchio, F. and Collins, M. (2006). Simplified modified compression field theory for calculating shear strength of reinforced concrete elements. *ACI Structural Journal*, vol. 103, no. 4, pp. 614.

Braestrup, M., Nielsen, M. and Bach, F. (1976). Rational Analysis and Design of Stirrups in Reinforced Concrete Beams. Report No. R79, Structural Research Laboratory, Technical University of Denmark.

Brown, M. D., Bayrak, O., and Jirsa, J. O. (2006). Design for shear based on loading conditions. *ACI Structural Journal*, *103*(4), 541.

Carino, N. Woodward, K. Leyendecker, E. and Fattal, S. (1983). A review of the Skyline Plaza collapse. *Concr. Int.*

Cladera, A. (2003). *Shear design of reinforced high-strength concrete beams*. Universitat Politècnica de Catalunya.

Cladera, A. and Marı, A. (2004). Shear design procedure for reinforced normal and high strength concrete beams using artificial neural networks. Part II: Beams with stirrups. *Engineering Structures*, vol. 26, No. 7, pp. 927–936.

Cladera, A. and Marí, A. (2007). Shear strength in the new Eurocode 2. A step forward? *Structural concrete*, vol. 8, no. 2, pp.57-66.

Cladera, A., Marí, A., Bairán, J. M., Ribas, C., Oller, E., and Duarte, N. (2016). The compression chord capacity model for the shear design and assessment of reinforced and prestressed concrete beams. *Structural Concrete*, *17*(6), 1017-1032.

Cohen, J. (1988). Statistical power analysis for the behavioral sciences. Hilsdale. *NJ: Lawrence Earlbaum Associates*, *2*.

Collins, M., Mitchell, D., Adebar, P. and Vecchio, F. (1996). A General Shear Design Method, *ACI Structural Journal*, vol 93, pp. 36 – 45.

Collins, M. and Kuchma, D. (1999). How safe are our large, lightly reinforced concrete beams, slabs and footings? *ACI Structural Journal*, vol. 96, no.4, pp. 482-490.

Collins, M. (2001). Evaluation of shear design procedures for concrete structures. *A Report prepared for the CSA technical committee on reinforced concrete design*.

Collins, M., Bentz, E., Sherwood, E. and Xie, L. (2007). *An Adequate Theory for the Shear Strength of Reinforced Concrete Structures*. University of Cambridge. Retrieved February 18, 2016, from http://www-civ.eng.cam.ac.uk/cjb/concplas/07collins.pdf

Collins, M., Bentz, E. and Sherwood, E. (2008). Where is Shear Reinforcement Required? Review of Research Results and Design Procedures. *ACI Structural Journal*, vol. 105, no. 5, pp. 590–600.

CSA Standard A23.3-04 (2004). Design of Concrete Structures for Buildings, Canadian Standards Association, Rexdale, Ontario, Canada.

Desai, S. B. (2004). Influence of constituents of concrete on its tensile strength and shear strength. *Structural Journal*, *101*(1), 29-38.

Dei Poli, S., Prisco, M. and Gambarova, P. (1990). Stress field in Web RCC Thin Web Beams Failing in Shear. *Journal of Structure Eng ASCE*, vol. 9, pp. 2496–2515.

Droguett, E. and Mosleh, A. (2008). Bayesian Methodology for Model Uncertainty Using Model Performance Data. *Risk Analysis*, vol. 28, no. 5, pp. 1457–1476.

Ellingwood, B., MacGregor, J. G., Galambos, T. V., and Cornell, C. A. (1982). Probability based load criteria: Load factors and load combinations. J. Struct. Div. 108(5), 978–997.

Ellingwood, B. (1994). Probability-based codified design: past accomplishments and future challenges. *Structural safety*, vol. 13, pp. 159-176.

EN 1992-1-1: Eurocode 2 (EC2) (2004). Design of concrete structures – Part 1-1: General rules and rules for buildings. European Committee for Standardisation (CEN), Brussels.

EN 1990 (2002). Eurocode – Basis of structural design. European Standard, European Committee for Standardization, Brussels.

Faber, M. and Sorensen, J. (2002). Reliability based code calibration. *The Joint Committee on Structural Safety, Zurich, Switzerland*.

Farooq, U. and Bedi, K. (2014). Study of Shear Bahavior of RC Beams: Non Linear Analysis. In Conference, *Structural Engineering Convention*, pp. 3477-3488.

Fédération Internationale du Béton (fib) (2010). Shear and punching shear in RC and FRC elements, *fib Bulletin*, vol 57.

Fédération Internationale du Béton (*fib*) (2010). Fib Model Code for Concrete Structures. First complete draft. *Bulletin, 55*.

Fédération Internationale du Béton (*fib*) (2013). Fib Model Code for Concrete Structures 2010.

Fischer, K., Barnardo-Viljoen, C. and Faber, M. H. (2013). Deriving target reliabilities from the LQI. *Small (C), 5*(4.2), 10.

Frosch, R. and Wolf, T. (2003). Simplified Shear Design of Prestressed Concrete Members. *Joint Transportation Research Program*, pp.192.

Franzblau, A. N. (1958). A primer of statistics for non-statisticians.

Grebović, R. and Radovanović, Ž. (2015). Shear Strength of High Strength Concrete Beams Loaded Close to the Support. *Procedia Engineering, 117*, pp.487-494.

Gandomi, A., Yun, G. and Alavi, A. (2013). An evolutionary approach for modeling of shear strength of RC deep beams. *Materials and structures*, vol. 46, no. 12, 2109-2119.

Gardoni, P., Armen, D. and Khalid, M. (2002). Probabilistic capacity models and fragility estimates for reinforced concrete columns based on experimental observations. Journal of Engineering Mechanics, vol. 128, no. 10, pp. 1024-1038.

Gambaorva P. (1988). On Aggregate Interlocking Mechanism in Reinforced Concrete Plates with Excessive Cracking, *IASBE colloquium Zurich*, vol. 25, no. 12, pp. 105–134.

Galambos, T. V., Ellingwood, B., MacGregor, J. G., and Cornell, C. A. (1982). Probability based load criteria: Assessment of current design practice. J. Struct. Div., 108(5), 959–977.

Gulvanessian, H., Calgaro, J. A., and Holický, M. (2002). *Designer's guide to EN 1990: eurocode: basis of structural design*. Thomas Telford.

Ghafar, A., Javed, A., Rehman, H., Ahmed, K. and Ilyas, M. (2016). Development of Shear Capacity Equations for Rectangular Reinforced Concrete Beams. *Pakistan journal of engineering and applied sciences*.

Hassan A., Hossain K., Lachemi M. (2008). Behaviour of Full-Scale Self-Consolidating Concrete Beams in Shear. *Cement and Concrete Composites*, vol. 30, pp. 588-596.

Hawkins, N. M. (2005). *Simplified shear design of structural concrete members* (Vol. 549). Transportation Research Board.

Holicky, M. and Vrouwenvelder, T. (2005). *Implementation of Eurocodes Handbook 2 Reliability Backgrounds*: Basic Concept of Structural Reliability. Leonardo da Vinci Pilot Project CZ/02/B/F/PP-134007, Prague.

Holicky, M., Retief, J. and Dunaiski, P. (2007). The reliability basis of design for structural resistance.

Holický, M. (2009). Reliability analysis for structural design. ISBN 978-1-920338-11-4, SUN MeDIA, Stellenbosch, South Africa.

Holický, M. and Sýkora, M. (2010). Stochastic models in analysis of structural reliability. In *Proceedings of the international symposium on stochastic models in reliability engineering, life sciences and operation management, Beer Sheva, Israel*.

Holický, M., Retief, J.V. and Wium, J.A. (2010). Partial factors for selected reinforced concrete members: Background to a revision of SANS 10100-1. *SAICE Journal*, 52 (1), 36-44.

Holický, M. (2013). *Introduction to probability and statistics for engineers*. Springer Science and Business Media.

Holický, M., Retief, J. and Sýkora, M. (2015). Assessment of model uncertainties for structural resistance. *Probabilistic Engineering Mechanics*.

Holický, M., Retief, J. V., Diamantidis, D. and Viljoen, C. (2015). On standardization of the reliability basis of structural design. In *Proceedings of the 12th International Conference on Applications of Statistics and Probability in Civil Engineering*.

Hsu, T. (1992). Unified theory of reinforced concrete (Vol. 5). *CRC press*.

Idris, A., Olasehinde, A. and Jowunlo, O. (2014). Reliability-Based Design of Reinforced Concrete Raft Footings Using Finite Element Method, Jordan Journal of Civil Engineering, vol 8, no. 4.

Ismail, K. S. (2016). *Shear behaviour of reinforced concrete deep beams* (Doctoral dissertation, University of Sheffield).

ISO, S. (1998). 2394. General Principles on Reliability for Structures. *Zurich: ISO*.

JCSS. JCSS Probabilistic Model Code. (2001). *Joint Committee on Structural Safety*, Zurich. ISBN 978-3-909386-79-6.

Jensen, B. and Lapko, A. (2009). On Shear Reinforcement Design of Structural Concrete Beams on the Basis of the Theory of Plasticity. *Journal of Civil Engineering and Management*, vol. 15, no. 4, pp. 395-403.

Johnson, M. and Ramirez, J. (1989). Minimum Shear Reinforcement in Beams with Higher Strength Concrete, *ACI Structural Journal*, vol. 86, no. 4, pp. 376-382.

Kassem, W. (2015). Shear strength of deep beams: a mathematical model and design formula. *Structural Concrete*, vol. 16, no. 2, 184-194.

Karihaloo, B., Abdalla, H. and Xiao, Q. (2003). Size effect in concrete beams. *Engineering fracture mechanics*, vol *70, no.* 7, pp. 979-993.

Kani, G. (1967). How Safe Are Our Large Concrete Beams? *ACI Journal Proceedings*, vol. 64, no. 3, pp. 128-141.

Kim, J. and Park, Y. (1994). Shear Strength of Reinforced High Strength Concrete Beams without Web Reinforcement, *Magazine of Concrete Research*, vol. 46.

Kim, J. and Park, Y. (1996). Prediction of shear strength of reinforced concrete beams without web reinforcement. *American Concrete Institute*.

Kong, P. and Rangan, B. (1998). Shear strength of high-performance concrete beams, *ACI Structural Journal*, vol. 95, no. 6, pp. 677-688.

König G, Hosser D. (1982). The Simplified Level II Method and its Application on the Derivation of Safety Elements for level I. *CEB Bulletin No 147. International Federation for Structural Concrete*: Lausanne.

Kuchma, D., Végh, P., Simionopoulos, K., Stanik, B. and Collins, M. (1997). The Influence of Concrete Strength, Distribution of Longitudinal Reinforcement and Member Size of the Shear Strength of Reinforced Concrete Beams, *CEB Bulletin*, no. 237, 21 pp.

Kuchma, D. and Collins, M. (1998). Advances in understanding shear performance of concrete structures. *Progress in Structural Engineering and Materials*, vol. 1, no. 4, pp. 360-369.

Kuchma, D., Kim, K., Kim, S., Sun, S., Akamat, A. and Hawkins, N. (2004). Simplified Shear Design of Structural Concrete Members. *Concrete Bridge Conference*.

Kuchma, D., Hawkins, N., Sang-Ho, K., Shaoyun, S. and Kang, S. (2008). Simplified shear provisions of the AASHTO LRFD Bridge Design specifications. *PCI Journal.*

Krejsa, J., Holicky, M. and Sykora, M. (2014). Uncertainty in shear resistance of reinforced concrete beams with stirrups–comparison of EN 1992-1-1 and fib MC 2010 approaches. *Transactions of the VŠB–Technical University of Ostrava, Civil Engineering Series.*, vol. 14, no. 1, pp. 48-56.

Lee, J. and Kim, U. (2008). Effect of longitudinal tensile reinforcement ratio and shear span-depth ratio on minimum shear reinforcement in beams. ACI Structural Journal, vol. 105, no. 2, pp. 134–44.

Linh Hoang, C. (1997). Shear strength of non-shear reinforced concrete elements: Part 2. T-beams.

Madsen, H. O., Krenk, S. and Lind, N. C. (2006). *Methods of structural safety*. Courier Corporation.

Marí, A., Bairán, J., Cladera, A., Oller, E. and Ribas, C. (2015). Shear-flexural strength mechanical model for the design and assessment of reinforced concrete beams. *Structure and Infrastructure Engineering*, vol. *11, no.* 11,pp. 1399-1419.

Mansour, M., Dicleli, M., Lee, J. and Zhang, J. (2004). Predicting the shear strength of reinforced concrete beams using artificial neural networks. *Engineering Structures*, vol. *26, no.* 6, pp.781-799.

McBean, E. A. and Rovers, F. A. (1998). Statistical procedures for analysis of environmental monitory data and risk assessment. Prentice-Hall

Melchers, R. E. (1990). Structural Reliability Analysis and Prediction, Wiley.

Metwally, I. (2012). Evaluate the capability and accuracy of response-2000 program in prediction of the shear capacities of reinforced and prestressed concrete members. *HBRC Journal*, vol. 8, no. 2, pp.99-106.

Mensah, K. K., Retief, J. V. and Barnardo-Viljoen, C. (2013). Eurocode 2's Variable Strut Inclination Method for shear, its modelling uncertainty and reliability calibration. In *Proceedings of fib Symposium on Engineering a Concrete Future: Technology Modeling & Construction*.

Mensah, K.K. (2015). Reliability Assessment of Structural Concrete with Special Reference to Stirrup Design. PhD dissertation, Dept. of Civil Eng., Univ. of Stellenbosch, Stellenbosch, South Africa.

Mitchell, D. and Collins, M. (1974). Diagonal Compression Field Theory—A Rational Model for Structural Concrete in Pure Torsion, ACI Journal, Proceedings vol. 71, pp. 396-408.

Moody, K.G., Viest, I.M., Elstner, R.C. and Hognestad, E. (1954). Shear strength of reinforced concrete beams Part 1-Tests of simple beams. *Journal Proceedings*, vol. 51, no. 12.

Mosley, B., Bungey, J. and Hulse, R. (2007). *Reinforced Concrete Design to Eurocode 2 (6th ed.).* Palgrave Macmillan, New York, USA.

Mörsch, E. (1909). Concrete-Steel Construction. McGraw-Hill, New York, (English translation by E. P. Goodrich).

Moe, J. (1962). Discussion of shear and diagonal tension by joint ACI-ASCE Committee 326. In *ACI Journal, Proceedings* (Vol. 59, No. 9, pp. 1334-1339).

Moore, J (2003). Safety of structures" An independent technical expert review of partial factors for actions and load combinations in EN 1990 "Basis of Structural Design, Building Research Establishment Ltd.

Mphonde, A. and Frantz, G. (1984). Shear Tests of High- and Low-Strength Concrete Beams Without Stirrups, ACI Journal, vol.81. no.4, pp.350-357.

Muttoni, A. and Ruiz, M. F. (2008). Shear strength of members without transverse reinforcement as function of critical shear crack width. *ACI Structural Journal*, *105*(2), 163.

Nilson, A. and Winter, G. (1991). *Design of Concrete Structures*, McGraw-Hill

Ožbolt J. and Eligehausen R. (1996). Size Effect in Concrete and RC Structures; Diagonal Shear and Torsion, *Studi E Ricerche*, vol. 17, pp 37-68.

Olalusi, O. and Vijoen, C.(2017). Towards Effective General Probabilistic Representation for Shear Resistance: *12th International Conference on Structural Safety and Reliability (ICOSSAR)*. TU Wien Vienna, Austria

Pang, X. and Hsu, T. (1996). Fixed angle softened truss model for reinforced concrete. *ACI Structural Journal*, vol. *93*, *no.* 2, pp 197-207.

Perera, R. and Vique, J. (2009). Strut-and-tie modelling of reinforced concrete beams using genetic algorithms optimization. *Construction and Building Materials*, vol. 23, no. 8, 2914-2925.

Pillai, S. and Kirk, D. (1983). *Reinforced Concrete Design in Canada*, McGraw-Hill Ryerson Limited.

Prinsloo, J.P. (2012). Assessment and Reliability Implications of Web-Crushing of Beams According to Eurocode 2. BEng(Civil) final year project, Dept. of Civ. Eng., Univ. of Stellenbosch, Stellenbosch, South Africa.

Rahal, K. and Al-Shaleh, K. (2004). Minimum transverse reinforcement in 65 MPa concrete beams. *ACI Structural Journal*, vol. 101, no. (6), 872-878.

Rackwitz, R. (2000). Optimization—the basis of code-making and reliability verification. *Structural safety*, *22*(1), 27-60.

Rajagopalan, K. and Ferguson, P. (1968) Exploratory shear tests emphasizing percentage of longitudinal steel. *ACI Structural Journal*,1968, vol. 65, no. 8, pp. 634–8.

Ramirez, J., French, C., Adebar, P., Bonacci, J. and Collins, M. (1998). Recent approaches to shear design of structural concrete, *Journal of Structural Engineering*, vol. 124, no. 12, pp.1374.

Rao, G. and Sundaresan, R (2014). Size-Dependent Shear Strength of Reinforced Concrete Deep Beams Based on Refined Strut-And-Tie Model. *Journal of Frontiers in Construction Engineering*, vol. 3, no. 1, pp. 9-19.

Rao, G. and Injaganeri, S (2011). Evaluation of size-dependent design shear strength of reinforced concrete beams without web reinforcement, *Sadhana*, vol. 36, no. 3, pp. 393-410.

Rahal, K. and Al-Shaleh, K. (2004). Minimum transverse reinforcement in 65 MPa concrete beams. *ACI Structural Journal*, vol. *101, no.* 6, pp. 872-878.

Retief, J.V. (2015). Contributions to the implementation of the principles of reliability to the standardized basis of structural design. Diss. Stellenbosch: Stellenbosch University.

Reineck, K. (1991). Ultimate shear force of structural concrete members without transverse reinforcement derived from a mechanical model (SP-885). *Structural Journal*, vol. *88,* no. 5, pp.592-602.

Reineck, K. H., Kuchma, D. A., Kim, K. S. and Marx, S. (2003). Shear database for reinforced concrete members without shear reinforcement. *Structural Journal*, *100*(2), 240-249.

Reineck, K. H., Bentz, E., Fitik, B., Kuchma, D. A. and Bayrak, O. (2014). ACI-DAfStb databases for shear tests on slender reinforced concrete beams with stirrups. *ACI Structural Journal*, *111*(5), 1147.

Ribas, C. and Cladera, A. (2013). Experimental study on shear strength of beam-and-block floors. *Engineering Structures*, *57*, 428-442

Ribeiro, A. B., Calixto, J. M. F. and Diniz, S. M. C. (2016). Assessment of epistemic uncertainties in the shear strength of slender reinforced concrete beams. *Engineering Structures*, *116*, 140-147.

Roller, J. and Russel, H. (1990). Shear strength of high-strength concrete beams with web reinforcement. *Structural Journal*, vol. *87, no.* 2, pp 191-198.

Robinson, R. B., Cox, C. D. and Odom, K. (2005). Identifying outliers in correlated water quality data. *Journal of environmental engineering*, *131*(4), 651-657.

Ritter, W. (1899). Die bauweise hennebique. *Schweizerische Bauzeitung*, vol. 33, no. 7, pp 59–61.

Russo, G., Somma, G., and Angeli, P. (2004). Design shear strength formula for high strength concrete beams. *Materials and structures*, vol. *37, no.* 10, pp 680-688.

Russo, G., Mitri, D. and Pauletta, M. (2013). Shear strength design formula for RC beams with stirrups. *Engineering Structures*, vol. 51, pp. 226-235.

SANS 10100-1. (2000). *The structural use of concrete – Part 1: Design.* South African Bureau of Standards, Pretoria.

SANS (2011a). SANS 10160-1 - *Basis of structural design and actions for buildings and industrial structures, Part 1: Basis of structural design*. South African Bureau of Standards, Pretoria.

Sagaseta, J. and Vollum, R. (2011). Influence of beam cross-section, loading arrangement and aggregate type on shear strength. *Magazine of Concrete Research*, vol. 63, no. 2, pp.139-155.

Shah, A. and Ahmad, S. (2009). Statistical model for the prediction of shear strength of high strength reinforced concrete beams. *Arabian Journal for Science and Engineering*, vol. *34, no.* 2B, p.400.

Sherwood E., Bentz E. and Collins M. (2007). Effect of Aggregate Size on Beam-Shear Strength of Thick Slabs, *ACI Structural Journal*, vol. 104, no. 2, pp. 180-190.

Shin, S, Lee, K, Moon, J. and Ghosh, S. (1999). Shear strength of reinforced high-strength concrete beams with shear span-to-depth ratios between 1.5 and 2.5. *Structural Journal*, vol. *96, no.* 4, pp 549-556.

Sigrist, V. (2013). Assessment of Structural Concrete Members using the fib ModelCode 2010 Shear Provisions. In *IABSE Symposium Report*, vol. 99, no. 7, pp. 1687-1693). International Association for Bridge and Structural Engineering.

Słowik, M. and Nowicki, T. (2012). The analysis of diagonal crack propagation in concrete beams. *Computational Materials Science*, vol. 52, no. 1, pp. 261-267.

Słowik, M. (2014). Shear Failure Mechanism in Concrete Beams. *Procedia Materials Science*, *3*, pp.1977-1982.

Smith, K. and Vantsiotis, A. (1982). Shear strength of deep beams. *ACI Journal Proceedings, ACI*.

Song, J., Kang, W. H., Kim, K. S. and Jung, S. (2010). Probabilistic shear strength models for reinforced concrete beams without shear reinforcement. *Structural engineering & mechanics*, *11*(1), 15.

Sun, S. and Kuchma, D. (2007). Shear Behavior and Capacity of Large Scale Prestressed High Strength Concrete Bulb-Tee Girders. *ProQuest*.

Sýkora, M., Holický, M. and Krejsa, J. (2013). Model uncertainty for shear resistance of reinforced concrete beams with shear reinforcement according to EN 1992-1-1. *Transactions of the VŠB–Technical University of Ostrava, Civil Engineering Series*, *13*(2), 150-159.

Sykora, M., Krejsa, J., Mlcoch, J., Prieto, M. and Tanner, P. (2018). Uncertainty in shear resistance models of reinforced concrete beams according to fib MC2010. *Structural Concrete*, *19*(1), 284-295.

Tan, K. and Cheng, G. (2006). Size effect on shear strength of deep beams: Investigating with strut-and-tie model, *Journal of structural engineering*, vol. 132, no. 5, pp 673-685.

Tan, K., Kong, F., Teng, S. and Weng, L. (1997). Effect of web reinforcement on high-strength concrete deep beams. *ACI structural journal*, vol. *94, no.* 5, pp. 572-582.

Tan, K., Kong, F., Teng, S. and Guan, L. (1995). High-strength concrete deep beams with effective span and shear span variations. *ACI Structural Journal*, vol. *92, no.* 4, pp 395-405.

Tang, C. and K. Tan (2004). Interactive mechanical model for shear strength of deep beams. *Journal of Structural Engineering*, vol. 130, no. 10, pp. 1534-1544.

Tang, W. H. and Ang, A. (2007). *Probability concepts in engineering: Emphasis on applications to civil and environmental engineering*. Hoboken, NJ: Wiley.

Todisco, L., Reineck, K. and Bayrak, O. (2015). Database with Shear Tests on Non-Slender Reinforced Concrete Beams with Vertical Stirrups. *ACI Structural Journal*, vol. *112*, *no.* 6, p.761.

Todisco, L., Reineck, K.H. and Bayrak, O. (2016). European design rules for point loads near supports evaluated with data from shear tests on non-slender beams with vertical stirrups. *Structural Concrete*, vol. 17, no. 2, pp.135-144.

Tureyen, A. and Frosch, R. (2003). Concrete shear strength: another perspective. *Structural Journal*, vol. *100, no.* 5, pp.609-615.

Vecchio, F. and Collins, M. (1986). The modified compression field theory for reinforced concrete elements subjected to shear. *ACI Structural Journal*, vol. 86, No. 2,pp. 219–231.

Vecchio, F. J., and Collins, M. P. (1993). Compression response of cracked reinforced concrete. *Journal of Structural Engineering*, *119*(12), pp 3590-3610.

Vecchio, F. (2000). Disturbed stress field model for reinforced concrete: formulation. *Journal of structural engineering*, vol. 126, no. 9, pp. 1070-1077.

Viktor, S., Bentz, E., Ruiz, M., Foster, S. and Muttoni, A. (2013). Background to the fib Model Code 2010 shear provisions-part 1; beams and slabs. *Structural Concrete*, vol. 14, no. 3, pp. 195–203.

Viljoen, C., Retief, J.V. and Mensah, K.K. (2018). A deterministic performance assessment of the EN 1992-1-1 stirrup design procedure against available alternatives. (Submitted to SAICE Journal)

Vollum, R. L., and Fang, L. (2014). Shear enhancement in RC beams with multiple point loads. *Engineering Structures*, *80*, 389-405.

Vrouwenvelder, A. C. W. M. (2002). Reliability Based Code calibration. The use of the JCSS Probabilistic Model Code. In *Joint Committee of Structural Safety (JCSS) Workshop on Code Calibration, Zurich, Switzerland, 21-22 March, 1-8*.

Walraven, J. and Bigaj-van Vliet, A. (2011). The 2010 fib model code for structural concrete: a new approach to structural engineering. *Structural Concrete*, vol. *12, no.* 3, pp.139-147.

Wang, H. (2002). *Reinforced concrete beam design for shear*. University of Calgary

Walraven, J. and Lehwalter, N. (1994). Size Effects in Short Beams Loaded in Shear. *ACI Structural Journal*, vol. 91, no. 5, pp. 583-593.

Wang W., Xing F. and Cao Z. (2006). Experimental Study on Shear Failure Modes for Ultrahigh Strength Concrete RC Beams without Stirrups, *Journal of Shenzhen University Science and Engineering*, vol. 23, no. 3, pp. 189-194.

Wolf, T. S. and Frosch, R. J. (2007). Shear design of prestressed concrete: A unified approach. *Journal of Structural Engineering*, *133*(11), 1512-1519.

Wium, J. A., Retief, J.V. and Viljoen, C. (2014). Lessons from development of design standards in South Africa. IABSE Symposium Report, vol. 102, no. 3, pp.3198–3205. Available at: http://www.ingentaconnect.com/content/iabse/report/2014/00000102/00000003/art00005\nhttp://openurl.ingenta.com/content/xref?genre=articleandissn=2221-3783andvolume=102andissue=3andspage=3198.

Yousif, J. and Kun, Y. (2016). Specification of deep beams affects the shear strength capacity, *Civil and Environmental Research*, vol. 8, no. 2, pp.56-68.

Yoon, Y., Cook, W. and Mitchell, D. (1996). Minimum shear reinforcement in normal, medium, and high-strength concrete beams. *ACI Structural Journal*, vol. 93, no. 5, pp. 576–84.

Zararis, P. (2003). Shear Strength and Minimum Shear Reinforcement of Reinforced Concrete Slender Beams, *ACI Structural Journal*, vol. 100, no. 2, pp. 203–215.

Zararis, I. P., Karaveziroglou, M. K. and Zararis, P. D. (2006). Shear strength of reinforced concrete T-beams. *ACI structural journal*, *103*(5), 693.

Zhang, N. and Tan, K. (2007). Size effect in RC deep beams: Experimental investigation and STM verification. *Engineering Structures*, vol. 29, no. 12, pp. 3241-3254.

Test No.	Author[Source]	Beam name	b_w [mm]	d [mm]	f_{cm} [MPa]	ρ_l [%]	ρ_w [%]	f_{ywm} [MPa]	$\rho_w f_{ywm}$ [MPa]	a/d	V_{exp} [kN]	$V_{VSIM-L0}$ [kN]	$MF_{VSIM-L0}$	V_{VSIM-A} [kN]	MF_{VSIM-A}
1	Ahmad_1996_003_NNW-3	NNW-3	127	203	41.5	3.19	0.49	324.14	1.59	2.92	87.27	106.78	0.82	119.83	0.73
2	Ahmad_1996_006_NHW-3	NHW-3	127	198	100.2	4.53	0.50	324.14	1.63	2.92	102.61	99.12	1.04	160.08	0.64
3	Ahmad_1996_007_NHW-3a	NHW-3a	127	198	91.8	4.53	0.65	324.14	2.12	2.92	108.46	129.49	0.84	177.61	0.61
4	Ahmad_1996_008_NHW-3b	NHW-3b	127	198	105.3	4.53	0.79	324.14	2.55	2.92	122.78	154.38	0.80	198.73	0.62
5	Ahmad_1996_009_NHW-4	NHW-4	127	198	100.8	4.53	0.50	324.14	1.63	3.92	94.03	99.09	0.95	160.26	0.59
6	Angelakos_1999_001_DB0.530M	DB0.530M	300	925	32.0	0.50	0.08	508.00	0.40	2.88	265.86	301.12	0.88	600.02	0.44
7	Angelakos_1999_004_DB140M	DB140M	300	925	38.0	1.01	0.08	508.00	0.40	2.88	279.50	292.76	0.95	646.34	0.43
8	Aparicio_1997_001_VHA	VHA	75	704	44.5	1.86	1.77	500.31	8.88	3.41	886.82	458.65	1.93	458.65	1.93
9	Aparicio_1997_002_HA-45	HA-45	150	1369	43.3	0.97	1.68	582.03	9.75	3.06	3384.45	1751.79	1.93	1751.79	1.93
10	Bernhardt_1986_002_S7 A	S7 A	150	161	82.1	5.20	0.67	427.00	2.86	3.42	140.72	168.83	0.83	189.61	0.74
11	Bernhardt_1986_003_S7 B	S7 B	150	161	82.1	5.20	0.67	427.00	2.86	3.42	150.72	168.83	0.89	189.61	0.79
12	Bernhardt_1986_004_S8 A	S8 A	150	161	82.1	5.20	0.45	427.00	1.91	3.42	125.72	112.44	1.12	157.56	0.80
13	Bernhardt_1986_005_S8 B	S8 B	150	161	82.1	5.20	0.45	427.00	1.91	3.42	135.72	112.44	1.21	157.56	0.86
14	Bhal_1968_001_B1S	B1S	240	300	27.2	1.26	0.15	441.45	0.65	2.70	128.70	130.73	0.98	182.30	0.71
15	Bhal_1968_002_B2S	B2S	240	600	25.5	1.26	0.15	441.45	0.65	2.80	249.57	265.84	0.94	353.19	0.71
16	Bhal_1968_003_B3S	B3S	240	900	26.7	1.26	0.15	441.45	0.65	2.85	369.39	394.16	0.94	541.54	0.68
17	Bhal_1968_004_B4S	B4S	240	1200	25.8	1.26	0.15	441.45	0.65	2.88	472.61	529.96	0.89	710.62	0.67
18	Bresler_1963_001_A-1	A-1	307	466	24.1	1.80	0.10	325.52	0.32	3.76	237.46	131.78	1.80	243.75	0.97
19	Bresler_1963_007_C-1	C-1	155	464	29.6	1.80	0.20	325.52	0.64	3.78	157.66	125.10	1.26	186.80	0.84
20	Caldera_2002_001_H 50/2	H 50/2	200	353	49.9	2.28	0.11	530.00	0.58	2.95	177.64	103.22	1.72	218.98	0.81
21	Caldera_2002_002_H 50/3	H 50/3	200	351	49.9	2.29	0.24	540.00	1.29	2.97	242.07	230.55	1.05	320.36	0.76
22	Caldera_2002_003_H 50/4	H 50/4	200	351	49.9	2.99	0.24	540.00	1.29	2.97	246.34	230.55	1.07	320.36	0.77
23	Caldera_2002_004_H 60/2	H 60/2	200	353	60.8	2.28	0.14	530.00	0.75	2.95	179.74	131.76	1.36	267.81	0.67
24	Caldera_2002_007_H 75/2	H 75/2	200	353	68.9	2.28	0.14	530.00	0.75	2.95	203.94	130.47	1.56	279.53	0.73
25	Caldera_2002_010_H 100/2	H 100/2	200	353	87.0	2.28	0.17	530.00	0.91	2.95	225.55	155.83	1.45	328.56	0.69
26	Cederwall_1974_003_734-46	734-46	139	234	30.2	1.04	0.41	436.55	1.78	2.56	95.65	136.60	0.70	136.60	0.70
27	Gabrielsson_1993_006_HS1	HS1	200	260	80.5	3.09	0.43	522.00	2.24	3.08	250.00	285.11	0.88	363.57	0.69
28	Gabrielsson_1993_007_HS2	HS2	200	260	80.5	3.09	0.26	522.00	1.38	4.23	200.00	175.40	1.14	289.84	0.69
29	Gabrielsson_1993_008_HPS1	HPS1	200	225	97.1	3.57	0.34	522.00	1.75	2.44	324.00	190.33	1.70	293.99	1.10
30	Gabrielsson_1993_009_HPS2	HPS2	200	225	101.8	3.57	0.34	522.00	1.75	2.44	305.00	189.88	1.61	296.76	1.03
31	Guidi_1963_001_V	V	80	380	34.1	1.07	0.71	490.50	3.47	3.95	122.63	177.21	0.69	177.21	0.69
32	Guralnik_1960_004_IB-2R	IB-2R	178	308	16.8	0.43	0.24	528.97	1.29	2.97	140.11	147.93	0.95	147.93	0.95
33	Guralnik_1960_006_IC-2R	IC-2R	178	310	34.0	1.33	0.24	528.97	1.29	2.95	225.07	190.38	1.18	212.42	1.06
34	Guralnik_1960_008_ID-2R	ID-2R	178	306	34.0	0.75	0.24	528.97	1.29	2.99	217.51	188.19	1.16	209.98	1.04
35	Hamadi_1976_002_GT-2	GT-2	120	350	24.9	0.72	0.38	320.00	1.21	3.46	148.50	135.30	1.10	135.30	1.10
36	Hegger_2001_001_SVB 3b	SVB 3b	180	450	70.0	2.97	0.56	514.00	2.87	3.33	427.00	574.52	0.74	604.80	0.71
37	Hegger_2003_001_NSC 3L	NSC 3L	80	470	29.0	1.91	0.71	550.00	3.89	3.19	334.00	207.38	1.61	207.38	1.61
38	Hegger_2003_002_NSC 3R	NSC 3R	80	470	29.0	1.91	0.71	550.00	3.89	3.09	349.00	207.38	1.68	207.38	1.68
39	Johnston_1939_002_B2-II	B2-II	305	305	22.0	0.82	0.10	275.86	0.28	3.00	102.68	77.28	1.33	142.59	0.72
40	Johnston_1939_009_T3-I	T3-I	305	305	22.2	0.78	0.10	275.86	0.28	3.00	103.89	77.05	1.35	143.22	0.73
41	Johnston_1939_010_T3-II	T3-II	305	305	22.2	0.78	0.10	275.86	0.28	3.00	97.44	77.05	1.26	143.22	0.68
42	Johnson_1989_001_1	1.00	305	539	36.4	2.49	0.16	479.31	0.75	3.10	344.26	324.22	1.06	506.30	0.68

Test No.	Author[Source]	Beam name	b_w [mm]	d [mm]	f_{cm} [MPa]	ρ_l [%]	ρ_w [%]	f_{ywm} [MPa]	$\rho_w f_{ywm}$ [MPa]	a/d	V_{exp} [kN]	$V_{VSIM-L0}$ [kN]	$MF_{VSIM-L0}$	V_{VSIM-A} [kN]	MF_{VSIM-A}
43	Johnson_1989_002_2	2.00	305	539	36.4	2.49	0.08	479.31	0.37	3.10	228.16	161.88	1.41	362.24	0.63
44	Johnson_1989_005_5	5.00	305	539	55.9	2.49	0.16	479.31	0.75	3.10	388.29	307.78	1.26	602.99	0.64
45	Kong_1997_001_S1-1	S1-1	250	292	61.6	2.80	0.15	569.00	0.87	2.50	228.30	158.50	1.44	299.42	0.76
46	Kong_1997_002_S1-2	S1-2	250	292	61.6	2.80	0.15	569.00	0.87	2.50	208.30	158.50	1.31	299.42	0.70
47	Kong_1997_003_S1-3	S1-3	250	292	61.6	2.80	0.15	569.00	0.87	2.50	206.10	158.50	1.30	299.42	0.69
48	Kong_1997_004_S1-4	S1-4	250	292	61.6	2.80	0.15	569.00	0.87	2.50	277.90	158.50	1.75	299.42	0.93
49	Kong_1997_005_S1-5	S1-5	250	292	61.6	2.80	0.15	569.00	0.87	2.50	253.30	158.50	1.60	299.42	0.85
50	Kong_1997_006_S1-6	S1-6	250	292	61.6	2.80	0.15	569.00	0.87	2.50	224.10	158.50	1.41	299.42	0.75
51	Kong_1997_007_S2-1	S2-1	250	292	70.2	2.80	0.10	569.00	0.58	2.50	260.30	104.56	2.49	257.04	1.01
52	Kong_1997_008_S2-2	S2-2	250	292	70.2	2.80	0.12	569.00	0.70	2.50	232.50	125.49	1.85	280.95	0.83
53	Kong_1997_009_S2-3	S2-3	250	292	70.2	2.80	0.15	569.00	0.87	2.50	253.30	156.90	1.61	313.06	0.81
54	Kong_1997_010_S2-4	S2-4	250	292	70.2	2.80	0.15	569.00	0.87	2.50	219.40	156.90	1.40	313.06	0.70
55	Kong_1997_011_S2-5	S2-5	250	292	70.2	2.80	0.20	569.00	1.16	2.50	282.10	209.28	1.35	359.47	0.78
56	Kong_1997_013_S3-1	S3-1	250	297	65.3	1.66	0.10	632.00	0.62	2.49	209.20	114.49	1.83	263.88	0.79
57	Kong_1997_014_S3-2	S3-2	250	297	65.3	1.66	0.10	632.00	0.62	2.49	178.00	114.49	1.55	263.88	0.67
58	Kong_1997_015_S3-3	S3-3	250	293	65.3	2.79	0.10	632.00	0.62	2.49	228.60	112.94	2.02	260.32	0.88
59	Kong_1997_016_S3-4	S3-4	250	293	65.3	2.79	0.10	632.00	0.62	2.49	174.90	112.94	1.55	260.32	0.67
60	Kong_1997_017_S3-5	S3-5	250	287	65.3	3.85	0.10	632.00	0.62	2.51	296.60	110.63	2.68	254.99	1.16
61	Kong_1997_018_S3-6	S3-6	250	287	65.3	3.85	0.10	632.00	0.62	2.51	282.90	110.63	2.56	254.99	1.11
62	Kong_1997_019_S4-1	S4-1	250	524	84.5	3.12	0.15	569.00	0.87	2.48	354.00	278.21	1.27	593.49	0.60
63	Kong_1997_021_S4-3	S4-3	250	332	84.5	2.97	0.15	569.00	0.87	2.50	243.40	176.27	1.38	376.02	0.65
64	Kong_1997_022_S4-4	S4-4	250	292	84.5	2.80	0.15	569.00	0.87	2.50	258.10	155.03	1.66	330.72	0.78
65	Kong_1997_024_S4-6	S4-6	250	198	84.5	2.79	0.15	569.00	0.87	2.53	202.90	105.13	1.93	224.26	0.90
66	Kong_1997_025_S5-1	S5-1	250	292	86.6	2.80	0.15	569.00	0.87	3.01	241.70	154.82	1.56	332.77	0.73
67	Kong_1997_026_S5-2	S5-2	250	292	86.6	2.80	0.15	569.00	0.87	2.74	259.90	154.82	1.68	332.77	0.78
68	Kong_1997_027_S5-3	S5-3	250	292	86.6	2.80	0.15	569.00	0.87	2.50	243.80	154.82	1.57	332.77	0.73
69	Kong_1997_031_S7-1	S7-1	250	278	72.4	4.73	0.10	569.00	0.58	3.40	217.20	99.33	2.19	247.14	0.88
70	Kong_1997_032_S7-2	S7-2	250	278	72.4	4.73	0.12	569.00	0.70	3.40	205.40	119.22	1.72	270.14	0.76
71	Kong_1997_033_S7-3	S7-3	250	278	72.4	4.73	0.15	569.00	0.87	3.40	246.50	149.05	1.65	301.04	0.82
72	Kong_1997_034_S7-4	S7-4	250	278	72.4	4.73	0.19	569.00	1.09	3.40	273.60	186.36	1.47	335.19	0.82
73	Kong_1997_035_S7-5	S7-5	250	278	72.4	4.73	0.22	569.00	1.25	3.40	304.40	213.03	1.43	357.27	0.85
74	Kong_1997_036_S7-6	S7-6	250	278	72.4	4.73	0.26	569.00	1.45	3.40	310.60	248.60	1.25	384.36	0.81
75	Kong_1997_037_S8-1	S8-1	250	292	72.2	2.80	0.10	569.00	0.58	2.50	272.10	104.36	2.61	259.37	1.05
76	Kong_1997_038_S8-2	S8-2	250	292	72.2	2.80	0.12	569.00	0.70	2.50	251.00	125.24	2.00	283.51	0.89
77	Kong_1997_039_S8-3	S8-3	250	292	72.2	2.80	0.15	569.00	0.87	2.50	309.60	156.59	1.98	315.93	0.98
78	Kong_1997_040_S8-4	S8-4	250	292	72.2	2.80	0.15	569.00	0.87	2.50	265.80	156.59	1.70	315.93	0.84
79	Kong_1997_041_S8-5	S8-5	250	292	72.2	2.80	0.19	569.00	1.09	2.50	289.20	195.79	1.48	351.77	0.82
80	Kong_1997_042_S8-6	S8-6	250	292	72.2	2.80	0.22	569.00	1.25	2.50	283.90	223.80	1.27	374.94	0.76
81	Krefeld_1966_010_26-1	26-1	254	456	40.1	2.23	0.16	341.38	0.56	3.87	206.83	168.36	1.23	323.63	0.64
82	Krefeld_1966_012_29b-1	29b-1	254	456	37.7	2.23	0.11	341.38	0.37	3.87	160.13	113.20	1.41	258.63	0.62
83	Krefeld_1966_015_29a-2	29a-2	254	456	37.2	2.23	0.11	372.41	0.41	3.87	216.62	123.74	1.75	268.38	0.81
84	Krefeld_1966_016_29b-2	29b-2	254	456	41.4	2.23	0.11	372.41	0.41	3.87	202.38	121.89	1.66	280.74	0.72

Test No.	Author[Source]	Beam name	b_w [mm]	d [mm]	f_{cm} [MPa]	ρ_l [%]	ρ_w [%]	f_{ywm} [MPa]	$\rho_w f_{ywm}$ [MPa]	a/d	V_{exp} [kN]	$V_{VSIM-L0}$ [kN]	$MF_{VSIM-L0}$	V_{VSIM-A} [kN]	MF_{VSIM-A}
85	Krefeld_1966_017_29c-2	29c-2	254	456	24.1	2.23	0.11	372.41	0.41	3.87	161.46	135.11	1.20	221.29	0.73
86	Krefeld_1966_018_29d-2	29d-2	254	456	30.4	2.23	0.11	372.41	0.41	3.87	165.02	128.08	1.29	245.87	0.67
87	Krefeld_1966_021_29g-2	29g-2	254	456	15.7	2.23	0.11	372.41	0.41	3.87	149.90	160.14	0.94	180.19	0.83
88	Leonhardt_1962_002_ET2	ET2	150	300	23.8	1.40	0.34	313.92	1.08	3.50	130.94	134.65	0.97	134.65	0.97
89	Leonhardt_1963_010_TA12	TA12	160	375	26.2	0.75	0.31	440.47	1.38	3.33	267.69	210.44	1.27	210.44	1.27
90	Levi_1989/1993_001_RC 30 A1	RC 30 A1	120	940	25.0	1.07	0.84	480.00	4.02	4.04	676.00	570.81	1.18	570.81	1.18
91	Levi_1989/1993_002_RC 30 A2	RC 30 A2	120	940	25.0	1.07	0.84	480.00	4.02	4.04	688.00	570.81	1.21	570.81	1.21
92	Levi_1989/1993_003_RC 60 A1	RC 60 A1	120	940	47.0	1.26	0.84	480.00	4.02	4.04	990.00	819.63	1.21	819.63	1.21
93	Levi_1989/1993_004_RC 60 A2	RC 60 A2	120	940	47.0	1.26	0.84	480.00	4.02	4.04	938.00	819.63	1.14	819.63	1.14
94	Levi_1989/1993_005_RC 60 B1	RC 60 B1	120	940	50.0	1.67	1.26	480.00	6.03	4.04	1181.00	971.57	1.22	971.57	1.22
95	Levi_1989/1993_006_RC 60 B2	RC 60 B2	120	940	50.0	1.67	1.26	480.00	6.03	4.04	1239.00	971.57	1.28	971.57	1.28
96	Levi_1989/1993_007_RC 70 B1	RC 70 B1	120	940	60.0	1.67	1.26	480.00	6.03	4.04	1330.00	1063.78	1.25	1063.78	1.25
97	Maruyama_1988_001_RS2-WD	RS2-WD	86	398	40.1	0.14	0.23	645.00	1.48	2.89	126.00	133.06	0.95	152.07	0.83
98	Moayer_1974_002_P20	P20	150	279	40.7	0.47	0.21	310.34	0.66	3.50	120.10	71.74	1.67	127.53	0.94
99	Özden_1967_002_T6	T6	110	298	33.4	1.05	0.61	272.72	1.66	3.52	137.34	140.37	0.98	140.37	0.98
100	Özden_1967_003_T7	T7	110	298	30.5	1.05	0.61	272.72	1.66	3.52	141.26	134.44	1.05	134.44	1.05
101	Özden_1967_004_T9	T9	110	298	30.5	1.05	0.61	272.72	1.66	3.52	154.02	134.44	1.15	134.44	1.15
102	Ozcebe_1999_003_TS56	TS56	150	310	61.0	3.46	0.24	255.00	0.61	5.00	129.20	70.66	1.83	159.86	0.81
103	Ozcebe_1999_006_TS59	TS59	150	310	82.0	4.43	0.28	255.00	0.71	5.00	125.40	80.74	1.55	189.29	0.66
104	Ozcebe_1999_009_TS36	TS36	150	310	75.0	2.59	0.24	255.00	0.61	3.00	155.90	69.58	2.24	171.11	0.91
105	Ozcebe_1999_011_TH39	TH39	150	310	73.0	3.08	0.21	255.00	0.53	3.00	142.90	60.99	2.34	158.97	0.90
106	Ozcebe_1999_012_TS39	TS39	150	310	73.0	3.08	0.28	255.00	0.71	3.00	179.20	81.34	2.20	182.95	0.98
107	Petersson_1972_001_V1	V1	175	322	38.0	1.07	0.22	323.00	0.70	3.57	100.93	102.96	0.98	171.10	0.59
108	Petersson_1972_002_VL1	VL1	120	278	43.0	1.20	0.84	366.00	3.07	3.24	190.73	208.93	0.91	208.93	0.91
109	Quast_1999_001_1/1	1/1	260	355	47.3	1.33	0.09	641.00	0.58	3.27	154.37	136.81	1.13	281.37	0.55
110	Regan_1971_001_R8	R8	152	272	26.4	1.46	0.21	270.00	0.58	3.22	81.00	66.95	1.21	97.33	0.83
111	Regan_1971_004_R11	R11	152	272	25.9	1.95	0.21	270.00	0.58	3.22	91.00	67.25	1.35	96.51	0.94
112	Regan_1971_005_R12	R12	152	254	33.5	4.17	0.21	270.00	0.58	3.45	112.00	59.53	1.88	101.27	1.11
113	Regan_1971_011_R20	R20	152	272	42.3	1.46	0.21	270.00	0.58	3.22	92.00	61.55	1.49	119.92	0.77
114	Regan_1971_012_R21	R21	152	254	47.4	4.17	0.40	280.00	1.13	3.45	153.00	111.03	1.38	161.78	0.95
115	Regan_1971_013_R22	R22	152	272	29.1	3.89	0.21	270.00	0.58	4.36	81.00	65.47	1.24	101.89	0.79
116	Regan_1971_016_R25	R25	152	254	30.4	4.17	0.21	270.00	0.58	3.45	107.00	60.61	1.77	97.00	1.10
117	Regan_1971_021_T3	T3	152	272	28.9	0.36	0.21	270.00	0.58	3.28	105.00	65.58	1.60	101.51	1.03
118	Regan_1971_022_T4	T4	152	272	34.3	0.48	0.21	270.00	0.58	3.28	110.00	63.50	1.73	109.57	1.00
119	Regan_1971_025_T7	T7	152	264	27.9	0.75	0.21	280.00	0.60	3.37	109.00	66.50	1.64	98.73	1.10
120	Regan_1971_026_T8	T8	152	254	31.7	1.04	0.21	280.00	0.60	3.50	124.00	62.34	1.99	100.64	1.23
121	Regan_1971_029_T13	T13	152	272	13.4	0.36	0.21	270.00	0.58	3.28	90.00	69.85	1.29	69.85	1.29
122	Regan_1971_030_T15	T15	152	254	33.1	1.04	0.21	270.00	0.58	7.10	104.00	59.66	1.74	100.74	1.03
123	Regan_1971_032_T17	T17	152	254	35.3	1.04	0.40	280.00	1.13	7.10	134.00	115.68	1.16	142.36	0.94
124	Regan_1971_033_T19	T19	152	254	30.2	1.04	0.21	270.00	0.58	5.30	106.00	60.67	1.75	96.77	1.10
125	Regan_1971_034_T20	T20	152	254	31.7	1.04	0.40	280.00	1.13	5.30	138.00	117.97	1.17	135.43	1.02
126	Regan_1971_038_T25	T25	152	272	52.7	0.36	0.21	270.00	0.58	3.28	114.00	60.04	1.90	130.93	0.87

Test No.	Author[Source]	Beam name	b_w [mm]	d [mm]	f_{cm} [MPa]	ρ_l [%]	ρ_w [%]	f_{ywm} [MPa]	$\rho_w f_{ywm}$ [MPa]	a/d	V_{exp} [kN]	$V_{VSIM-L0}$ [kN]	$MF_{VSIM-L0}$	V_{VSIM-A} [kN]	MF_{VSIM-A}
127	Regan_1971_039_T26	T26	152	254	51.9	1.04	0.40	280.00	1.13	3.50	179.00	109.96	1.63	167.69	1.07
128	Regan_1971_046_T34	T34	152	254	31.3	2.08	0.21	270.00	0.58	5.30	112.00	60.25	1.86	98.35	1.14
129	Regan_1971_047_T35	T35	152	254	31.3	0.59	0.21	270.00	0.58	5.30	115.00	60.25	1.91	98.35	1.17
130	Rehm_1978_001_RsIS / BQ II 0	RsIS / BQ II 0	250	430	24.5	1.10	0.76	560.00	4.26	3.00	594.78	542.81	1.10	542.81	1.10
131	Rehm_1978_004_RnIIS	RnIIS	450	548	22.1	0.64	0.34	557.00	1.87	3.00	744.73	899.85	0.83	899.85	0.83
132	Reineck_1991_001_Stb III	Stb III	77	590	60.6	1.25	1.20	515.00	6.16	4.27	536.67	433.33	1.24	433.33	1.24
133	Reineck_1991_002_Stb I	Stb I	77	589	60.6	1.44	1.68	549.00	9.21	4.27	681.73	482.85	1.41	482.85	1.41
134	Roller_1990_007_7	7.00	457	762	72.4	1.88	0.16	445.17	0.70	2.91	787.83	603.57	1.31	1360.55	0.58
135	Roller_1990_009_9	9.00	457	762	125.3	2.35	0.16	445.17	0.70	2.91	749.40	586.77	1.28	1517.19	0.49
136	Roller_1990_010_10	10.00	457	762	125.3	2.89	0.23	445.17	1.04	2.91	1172.14	866.38	1.35	1834.02	0.64
137	Sarsam_1992_007_BL2-H	BL2-H	180	233	75.7	2.82	0.09	820.00	0.76	4.00	138.30	78.45	1.76	172.59	0.80
138	Sarsam_1992_008_BS2-H	BS2-H	180	233	73.9	2.82	0.09	820.00	0.76	2.50	223.50	78.57	2.84	171.33	1.30
139	Sarsam_1992_010_BS4-H	BS4-H	180	233	80.1	2.82	0.19	820.00	1.53	2.50	206.90	156.46	1.32	244.76	0.85
140	Sarsam_1992_011_CL2-H	CL2-H	180	233	70.1	3.51	0.09	820.00	0.76	4.00	147.20	78.86	1.87	168.50	0.87
141	Sarsam_1992_013_CS3-H	CS3-H	180	233	74.2	3.51	0.14	820.00	1.14	2.50	247.20	117.88	2.10	208.61	1.19
142	Sarsam_1992_014_CS4-H	CS4-H	180	233	75.7	3.51	0.19	820.00	1.53	2.50	220.70	157.03	1.41	240.65	0.92
143	Shin_1999_009_MHB 2.5-25	MHB 2.5-25	125	215	52.0	3.77	0.29	365.91	1.08	2.45	98.80	73.26	1.35	114.46	0.86
144	Shin_1999_010_MHB 2.5-50	MHB 2.5-50	125	215	52.0	3.77	0.59	365.91	2.16	2.45	149.32	146.86	1.02	157.62	0.95
145	Shin_1999_021_HB 2.5-25	HB 2.5-25	125	215	73.0	3.77	0.29	365.91	1.08	2.45	115.72	71.19	1.63	129.21	0.90
146	Shin_1999_022_HB 2.5-50	HB 2.5-50	125	215	73.0	3.77	0.59	365.91	2.16	2.45	149.32	142.58	1.05	178.97	0.83
147	Soerensen_1974_001_T-21	T-21	110	298	32.5	1.05	0.52	228.57	1.19	3.52	130.95	105.71	1.24	119.50	1.10
148	Soerensen_1974_003_T-23	T-23	110	298	34.2	1.05	0.34	349.24	1.20	3.52	140.76	104.99	1.34	122.61	1.15
149	Soerensen_1974_007_T-2-B	T-2-B	110	298	24.9	1.05	0.31	397.31	1.21	3.52	130.95	105.93	1.24	105.93	1.24
150	Soerensen_1974_009_T-4-B	T-4-B	110	298	24.7	1.05	0.20	397.31	0.81	3.52	108.39	76.14	1.42	87.91	1.23
151	Stroband_1997_002_2	2.00	90	647	87.4	1.10	0.68	600.00	4.06	2.56	528.00	542.28	0.97	542.28	0.97
152	Stroband_1997_003_3	3.00	90	647	88.3	1.62	1.52	630.00	9.60	2.56	886.27	743.65	1.19	743.65	1.19
153	Taylor_1966_004_HSS-1-B	HSS-1-B	114	257	19.5	1.26	0.33	437.93	1.43	4.44	86.98	89.77	0.97	89.77	0.97
154	Yoon_1996_009_H2-N	H2-N	375	655	87.0	2.86	0.24	430.00	1.02	3.23	721.00	606.55	1.19	1206.80	0.60
155	Rosenbusch_2003_001_1.3-1	1.3/1	200	260	49.2	3.55	0.07	680.00	0.47	3.37	120.80	62.70	1.93	145.94	0.83
156	Rosenbusch_2003_002_1.4-1	1.4/1	200	260	47.9	3.55	0.14	680.00	0.95	3.37	170.61	125.91	1.36	201.78	0.85
157	Rosenbusch_2003_004_1.7-1	1.7/1	200	260	50.4	3.55	0.56	550.00	3.07	3.37	190.46	350.53	0.54	350.53	0.54
158	Kautsch_2010_001_A2	A2	155	719	30.8	0.68	0.43	605.00	2.62	2.68	657.10	554.59	1.18	554.59	1.18
159	Kautsch_2010_002_B2	B2	155	719	31.4	0.68	0.32	605.00	1.96	2.68	571.22	498.01	1.15	498.01	1.15
160	Tanimura_2005_031_41	41.00	300	400	20.6	2.20	0.52	388.00	2.03	2.50	324.00	433.89	0.75	433.89	0.75

	$MF_{VSIM-L0}$		MF_{VSIM-A}
Mean μ_{MF}	1.41		0.90
Std. Dev σ_{MF}	0.42		0.25

Test No.	Author[Source]	Beam name	b_w [mm]	d [mm]	f_{cm} [MPa]	ρ_l [%]	ρ_w [%]	f_{ywm} [MPa]	$\rho_w f_{ywm}$ [MPa]	a/d	V_{exp} [kN]	$V_{MC\text{-}10(III)}$ [kN]	$MF_{MC\text{-}10(III)}$	V_{ACI} [kN]	MF_{ACI}
1	Ahmad_1996_003_NNW-3	NNW-3	127	203	41.5	3.19	0.49	324.14	1.59	2.92	87.27	96.47	0.90	68.64	1.27
2	Ahmad_1996_006_NHW-3	NHW-3	127	198	100.2	4.53	0.50	324.14	1.63	2.92	102.61	111.12	0.92	75.73	1.35
3	Ahmad_1996_007_NHW-3a	NHW-3a	127	198	91.8	4.53	0.65	324.14	2.12	2.92	108.46	132.27	0.82	88.05	1.23
4	Ahmad_1996_008_NHW-3b	NHW-3b	127	198	105.3	4.53	0.79	324.14	2.55	2.92	122.78	148.45	0.83	98.72	1.24
5	Ahmad_1996_009_NHW-4	NHW-4	127	198	100.8	4.53	0.50	324.14	1.63	3.92	94.03	114.60	0.82	75.73	1.24
6	Angelakos_1999_001_DB0.530M	DB0.530M	300	925	32.0	0.50	0.08	508.00	0.40	2.88	265.86	386.77	0.69	372.19	0.71
7	Angelakos_1999_004_DB140M	DB140M	300	925	38.0	1.01	0.08	508.00	0.40	2.88	279.50	521.16	0.54	395.57	0.71
8	Aparicio_1997_001_VHA	VHA	75	704	44.5	1.86	1.77	500.31	8.88	3.41	886.82	883.20	1.00	527.10	1.68
9	Aparicio_1997_002_HA-45	HA-45	150	1369	43.3	0.97	1.68	582.03	9.75	3.06	3384.45	3340.31	1.01	2226.87	1.52
10	Bernhardt_1986_002_S7 A	S7 A	150	161	82.1	5.20	0.67	427.00	2.86	3.42	140.72	149.66	0.94	102.36	1.37
11	Bernhardt_1986_003_S7 B	S7 B	150	161	82.1	5.20	0.67	427.00	2.86	3.42	150.72	145.82	1.03	102.36	1.47
12	Bernhardt_1986_004_S8 A	S8 A	150	161	82.1	5.20	0.45	427.00	1.91	3.42	125.72	110.88	1.13	79.33	1.58
13	Bernhardt_1986_005_S8 B	S8 B	150	161	82.1	5.20	0.45	427.00	1.91	3.42	135.72	107.50	1.26	79.33	1.71
14	Bhal_1968_001_B1S	B1S	240	300	27.2	1.26	0.15	441.45	0.65	2.70	128.70	128.51	1.00	109.19	1.18
15	Bhal_1968_002_B2S	B2S	240	600	25.5	1.26	0.15	441.45	0.65	2.80	249.57	254.87	0.98	214.21	1.17
16	Bhal_1968_003_B3S	B3S	240	900	26.7	1.26	0.15	441.45	0.65	2.85	369.39	391.09	0.94	325.60	1.13
17	Bhal_1968_004_B4S	B4S	240	1200	25.8	1.26	0.15	441.45	0.65	2.88	472.61	525.64	0.90	429.96	1.10
18	Bresler_1963_001_A-1	A-1	307	466	24.1	1.80	0.10	325.52	0.32	3.76	237.46	185.38	1.28	162.52	1.46
19	Bresler_1963_007_C-1	C-1	155	464	29.6	1.80	0.20	325.52	0.64	3.78	157.66	130.88	1.20	110.46	1.43
20	Caldera_2002_001_H 50/2	H 50/2	200	353	49.9	2.28	0.11	530.00	0.58	2.95	177.64	146.05	1.22	123.48	1.44
21	Caldera_2002_002_H 50/3	H 50/3	200	351	49.9	2.29	0.24	540.00	1.29	2.97	242.07	210.41	1.15	173.05	1.40
22	Caldera_2002_003_H 50/4	H 50/4	200	351	49.9	2.99	0.24	540.00	1.29	2.97	246.34	225.16	1.09	173.05	1.42
23	Caldera_2002_004_H 60/2	H 60/2	200	353	60.8	2.28	0.14	530.00	0.75	2.95	179.74	179.83	1.00	144.28	1.25
24	Caldera_2002_007_H 75/2	H 75/2	200	353	68.9	2.28	0.14	530.00	0.75	2.95	203.94	173.75	1.17	150.17	1.36
25	Caldera_2002_010_H 100/2	H 100/2	200	353	87.0	2.28	0.17	530.00	0.91	2.95	225.55	189.75	1.19	161.39	1.40
26	Cederwall_1974_003_734-46	734-46	139	234	30.2	1.04	0.41	436.55	1.78	2.56	95.65	91.59	1.04	87.44	1.09
27	Gabrielsson_1993_006_HS1	HS1	200	260	80.5	3.09	0.43	522.00	2.24	3.08	250.00	244.68	1.02	188.26	1.33
28	Gabrielsson_1993_007_HS2	HS2	200	260	80.5	3.09	0.26	522.00	1.38	4.23	200.00	185.06	1.08	143.46	1.39
29	Gabrielsson_1993_008_HPS1	HPS1	200	225	97.1	3.57	0.34	522.00	1.75	2.44	324.00	151.49	2.14	140.72	2.30
30	Gabrielsson_1993_009_HPS2	HPS2	200	225	101.8	3.57	0.34	522.00	1.75	2.44	305.00	157.31	1.94	140.72	2.17
31	Guidi_1963_001_V	V	80	380	34.1	1.07	0.71	490.50	3.47	3.95	122.63	208.96	0.59	134.86	0.91
32	Guralnik_1960_004_IB-2R	IB-2R	178	308	16.8	0.43	0.24	528.97	1.29	2.97	140.11	126.66	1.11	107.89	1.30
33	Guralnik_1960_006_IC-2R	IC-2R	178	310	34.0	1.33	0.24	528.97	1.29	2.95	225.07	161.90	1.39	124.31	1.81
34	Guralnik_1960_008_ID-2R	ID-2R	178	306	34.0	0.75	0.24	528.97	1.29	2.99	217.51	141.92	1.53	122.89	1.77
35	Hamadi_1976_002_GT-2	GT-2	120	350	24.9	0.72	0.38	320.00	1.21	3.46	148.50	105.41	1.41	85.44	1.74
36	Hegger_2001_001_SVB 3b	SVB 3b	180	450	70.0	2.97	0.56	514.00	2.87	3.33	427.00	470.06	0.91	344.13	1.24
37	Hegger_2003_001_NSC 3L	NSC 3L	80	470	29.0	1.91	0.71	550.00	3.89	3.19	334.00	289.47	1.15	179.79	1.86
38	Hegger_2003_002_NSC 3R	NSC 3R	80	470	29.0	1.91	0.71	550.00	3.89	3.09	349.00	286.82	1.22	179.79	1.94
39	Johnston_1939_002_B2-II	B2-II	305	305	22.0	0.82	0.10	275.86	0.28	3.00	102.68	107.08	0.96	98.54	1.04
40	Johnston_1939_009_T3-I	T3-I	305	305	22.2	0.78	0.10	275.86	0.28	3.00	103.89	104.94	0.99	98.88	1.05
41	Johnston_1939_010_T3-II	T3-II	305	305	22.2	0.78	0.10	275.86	0.28	3.00	97.44	108.64	0.90	98.88	0.99
42	Johnson_1989_001_1	1.00	305	539	36.4	2.49	0.16	479.31	0.75	3.10	344.26	393.37	0.88	287.14	1.20

Test No.	Author[Source]	Beam name	b_w [mm]	d [mm]	f_{cm} [MPa]	ρ_l [%]	ρ_w [%]	f_{ywm} [MPa]	$\rho_w f_{ywm}$ [MPa]	a/d	V_{exp} [kN]	$V_{MC\text{-}10(III)}$ [kN]	$MF_{MC\text{-}10(III)}$	V_{ACI} [kN]	MF_{ACI}
43	Johnson_1989_002_2	2.00	305	539	36.4	2.49	0.08	479.31	0.37	3.10	228.16	324.66	0.70	225.81	1.01
44	Johnson_1989_005_5	5.00	305	539	55.9	2.49	0.16	479.31	0.75	3.10	388.29	429.76	0.90	326.38	1.19
45	Kong_1997_001_S1-1	S1-1	250	292	61.6	2.80	0.15	569.00	0.87	2.50	228.30	196.63	1.16	158.79	1.44
46	Kong_1997_002_S1-2	S1-2	250	292	61.6	2.80	0.15	569.00	0.87	2.50	208.30	205.09	1.02	158.79	1.31
47	Kong_1997_003_S1-3	S1-3	250	292	61.6	2.80	0.15	569.00	0.87	2.50	206.10	206.07	1.00	158.79	1.30
48	Kong_1997_004_S1-4	S1-4	250	292	61.6	2.80	0.15	569.00	0.87	2.50	277.90	178.17	1.56	158.79	1.75
49	Kong_1997_005_S1-5	S1-5	250	292	61.6	2.80	0.15	569.00	0.87	2.50	253.30	186.91	1.36	158.79	1.60
50	Kong_1997_006_S1-6	S1-6	250	292	61.6	2.80	0.15	569.00	0.87	2.50	224.10	198.35	1.13	158.79	1.41
51	Kong_1997_007_S2-1	S2-1	250	292	70.2	2.80	0.10	569.00	0.58	2.50	260.30	150.08	1.73	143.04	1.82
52	Kong_1997_008_S2-2	S2-2	250	292	70.2	2.80	0.12	569.00	0.70	2.50	232.50	175.63	1.32	151.53	1.53
53	Kong_1997_009_S2-3	S2-3	250	292	70.2	2.80	0.15	569.00	0.87	2.50	253.30	191.72	1.32	164.27	1.54
54	Kong_1997_010_S2-4	S2-4	250	292	70.2	2.80	0.15	569.00	0.87	2.50	219.40	205.15	1.07	164.27	1.34
55	Kong_1997_011_S2-5	S2-5	250	292	70.2	2.80	0.20	569.00	1.16	2.50	282.10	219.74	1.28	185.50	1.52
56	Kong_1997_013_S3-1	S3-1	250	297	65.3	1.66	0.10	632.00	0.62	2.49	209.20	148.84	1.41	145.82	1.43
57	Kong_1997_014_S3-2	S3-2	250	297	65.3	1.66	0.10	632.00	0.62	2.49	178.00	162.37	1.10	145.82	1.22
58	Kong_1997_015_S3-3	S3-3	250	293	65.3	2.79	0.10	632.00	0.62	2.49	228.60	165.51	1.38	143.85	1.59
59	Kong_1997_016_S3-4	S3-4	250	293	65.3	2.79	0.10	632.00	0.62	2.49	174.90	188.04	0.93	143.85	1.22
60	Kong_1997_017_S3-5	S3-5	250	287	65.3	3.85	0.10	632.00	0.62	2.51	296.60	151.32	1.96	140.91	2.10
61	Kong_1997_018_S3-6	S3-6	250	287	65.3	3.85	0.10	632.00	0.62	2.51	282.90	155.49	1.82	140.91	2.01
62	Kong_1997_019_S4-1	S4-1	250	524	84.5	3.12	0.15	569.00	0.87	2.48	354.00	404.03	0.88	294.78	1.20
63	Kong_1997_021_S4-3	S4-3	250	332	84.5	2.97	0.15	569.00	0.87	2.50	243.40	244.42	1.00	186.77	1.30
64	Kong_1997_022_S4-4	S4-4	250	292	84.5	2.80	0.15	569.00	0.87	2.50	258.10	194.42	1.33	164.27	1.57
65	Kong_1997_024_S4-6	S4-6	250	198	84.5	2.79	0.15	569.00	0.87	2.53	202.90	122.21	1.66	111.39	1.82
66	Kong_1997_025_S5-1	S5-1	250	292	86.6	2.80	0.15	569.00	0.87	3.01	241.70	201.03	1.20	164.27	1.47
67	Kong_1997_026_S5-2	S5-2	250	292	86.6	2.80	0.15	569.00	0.87	2.74	259.90	194.30	1.34	164.27	1.58
68	Kong_1997_027_S5-3	S5-3	250	292	86.6	2.80	0.15	569.00	0.87	2.50	243.80	200.23	1.22	164.27	1.48
69	Kong_1997_031_S7-1	S7-1	250	278	72.4	4.73	0.10	569.00	0.58	3.40	217.20	174.88	1.24	136.18	1.59
70	Kong_1997_032_S7-2	S7-2	250	278	72.4	4.73	0.12	569.00	0.70	3.40	205.40	196.51	1.05	144.27	1.42
71	Kong_1997_033_S7-3	S7-3	250	278	72.4	4.73	0.15	569.00	0.87	3.40	246.50	206.20	1.20	156.39	1.58
72	Kong_1997_034_S7-4	S7-4	250	278	72.4	4.73	0.19	569.00	1.09	3.40	273.60	227.36	1.20	171.55	1.59
73	Kong_1997_035_S7-5	S7-5	250	278	72.4	4.73	0.22	569.00	1.25	3.40	304.40	238.24	1.28	182.38	1.67
74	Kong_1997_036_S7-6	S7-6	250	278	72.4	4.73	0.26	569.00	1.45	3.40	310.60	264.63	1.17	196.82	1.58
75	Kong_1997_037_S8-1	S8-1	250	292	72.2	2.80	0.10	569.00	0.58	2.50	272.10	147.08	1.85	143.04	1.90
76	Kong_1997_038_S8-2	S8-2	250	292	72.2	2.80	0.12	569.00	0.70	2.50	251.00	169.63	1.48	151.53	1.66
77	Kong_1997_039_S8-3	S8-3	250	292	72.2	2.80	0.15	569.00	0.87	2.50	309.60	173.42	1.79	164.27	1.88
78	Kong_1997_040_S8-4	S8-4	250	292	72.2	2.80	0.15	569.00	0.87	2.50	265.80	187.90	1.41	164.27	1.62
79	Kong_1997_041_S8-5	S8-5	250	292	72.2	2.80	0.19	569.00	1.09	2.50	289.20	208.36	1.39	180.19	1.60
80	Kong_1997_042_S8-6	S8-6	250	292	72.2	2.80	0.22	569.00	1.25	2.50	283.90	230.71	1.23	191.56	1.48
81	Krefeld_1966_010_26-1	26-1	254	456	40.1	2.23	0.16	341.38	0.56	3.87	206.83	252.80	0.82	186.37	1.11
82	Krefeld_1966_012_29b-1	29b-1	254	456	37.7	2.23	0.11	341.38	0.37	3.87	160.13	227.04	0.71	161.00	0.99
83	Krefeld_1966_015_29a-2	29a-2	254	456	37.2	2.23	0.11	372.41	0.41	3.87	216.62	205.39	1.05	164.16	1.32
84	Krefeld_1966_016_29b-2	29b-2	254	456	41.4	2.23	0.11	372.41	0.41	3.87	202.38	221.85	0.91	170.61	1.19

Test No.	Author[Source]	Beam name	b_w [mm]	d [mm]	f_{cm} [MPa]	ρ_l [%]	ρ_w [%]	f_{ywm} [MPa]	$\rho_w f_{ywm}$ [MPa]	a/d	V_{exp} [kN]	$V_{MC\text{-}10(III)}$ [kN]	$MF_{MC\text{-}10(III)}$	V_{ACI} [kN]	MF_{ACI}
85	Krefeld_1966_017_29c-2	29c-2	254	456	24.1	2.23	0.11	372.41	0.41	3.87	161.46	192.74	0.84	141.41	1.14
86	Krefeld_1966_018_29d-2	29d-2	254	456	30.4	2.23	0.11	372.41	0.41	3.87	165.02	213.26	0.77	152.98	1.08
87	Krefeld_1966_021_29g-2	29g-2	254	456	15.7	2.23	0.11	372.41	0.41	3.87	149.90	159.91	0.94	123.21	1.22
88	Leonhardt_1962_002_ET2	ET2	150	300	23.8	1.40	0.34	313.92	1.08	3.50	130.94	108.90	1.20	84.82	1.54
89	Leonhardt_1963_010_TA12	TA12	160	375	26.2	0.75	0.31	440.47	1.38	3.33	267.69	166.30	1.61	133.67	2.00
90	Levi_1989/1993_001_RC 30 A1	RC 30 A1	120	940	25.0	1.07	0.84	480.00	4.02	4.04	676.00	936.29	0.72	547.22	1.24
91	Levi_1989/1993_002_RC 30 A2	RC 30 A2	120	940	25.0	1.07	0.84	480.00	4.02	4.04	688.00	933.48	0.74	547.22	1.26
92	Levi_1989/1993_003_RC 60 A1	RC 60 A1	120	940	47.0	1.26	0.84	480.00	4.02	4.04	990.00	898.30	1.10	581.97	1.70
93	Levi_1989/1993_004_RC 60 A2	RC 60 A2	120	940	47.0	1.26	0.84	480.00	4.02	4.04	938.00	908.09	1.03	581.97	1.61
94	Levi_1989/1993_005_RC 60 B1	RC 60 B1	120	940	50.0	1.67	1.26	480.00	6.03	4.04	1181.00	1376.79	0.86	812.80	1.45
95	Levi_1989/1993_006_RC 60 B2	RC 60 B2	120	940	50.0	1.67	1.26	480.00	6.03	4.04	1239.00	1364.24	0.91	812.80	1.52
96	Levi_1989/1993_007_RC 70 B1	RC 70 B1	120	940	60.0	1.67	1.26	480.00	6.03	4.04	1330.00	1344.94	0.99	825.44	1.61
97	Maruyama_1988_001_RS2-WD	RS2-WD	86	398	40.1	0.14	0.23	645.00	1.48	2.89	126.00	74.67	1.69	86.99	1.45
98	Moayer_1974_002_P20	P20	150	279	40.7	0.47	0.21	310.34	0.66	3.50	120.10	76.68	1.57	71.93	1.67
99	Özden_1967_002_T6	T6	110	298	33.4	1.05	0.61	272.72	1.66	3.52	137.34	115.80	1.19	85.89	1.60
100	Özden_1967_003_T7	T7	110	298	30.5	1.05	0.61	272.72	1.66	3.52	141.26	112.32	1.26	84.52	1.67
101	Özden_1967_004_T9	T9	110	298	30.5	1.05	0.61	272.72	1.66	3.52	154.02	107.97	1.43	84.52	1.82
102	Ozcebe_1999_003_TS56	TS56	150	310	61.0	3.46	0.24	255.00	0.61	5.00	129.20	113.70	1.14	88.67	1.46
103	Ozcebe_1999_006_TS59	TS59	150	310	82.0	4.43	0.28	255.00	0.71	5.00	125.40	138.42	0.91	97.18	1.29
104	Ozcebe_1999_009_TS36	TS36	150	310	75.0	2.59	0.24	255.00	0.61	3.00	155.90	100.00	1.56	92.45	1.69
105	Ozcebe_1999_011_TH39	TH39	150	310	73.0	3.08	0.21	255.00	0.53	3.00	142.90	102.60	1.39	88.90	1.61
106	Ozcebe_1999_012_TS39	TS39	150	310	73.0	3.08	0.28	255.00	0.71	3.00	179.20	106.00	1.69	97.18	1.84
107	Petersson_1972_001_V1	V1	175	322	38.0	1.07	0.22	323.00	0.70	3.57	100.93	109.49	0.92	96.87	1.04
108	Petersson_1972_002_VL1	VL1	120	278	43.0	1.20	0.84	366.00	3.07	3.24	190.73	176.11	1.08	138.60	1.38
109	Quast_1999_001_1/1	1/1	260	355	47.3	1.33	0.09	641.00	0.58	3.27	154.37	193.99	0.80	158.99	0.97
110	Regan_1971_001_R8	R8	152	272	26.4	1.46	0.21	270.00	0.58	3.22	81.00	67.42	1.20	59.04	1.37
111	Regan_1971_004_R11	R11	152	272	25.9	1.95	0.21	270.00	0.58	3.22	91.00	68.13	1.34	58.72	1.55
112	Regan_1971_005_R12	R12	152	254	33.5	4.17	0.21	270.00	0.58	3.45	112.00	71.96	1.56	59.31	1.89
113	Regan_1971_011_R20	R20	152	272	42.3	1.46	0.21	270.00	0.58	3.22	92.00	74.46	1.24	68.45	1.34
114	Regan_1971_012_R21	R21	152	254	47.4	4.17	0.40	280.00	1.13	3.45	153.00	112.22	1.36	87.62	1.75
115	Regan_1971_013_R22	R22	152	272	29.1	3.89	0.21	270.00	0.58	4.36	81.00	86.76	0.93	60.84	1.33
116	Regan_1971_016_R25	R25	152	254	30.4	4.17	0.21	270.00	0.58	3.45	107.00	70.73	1.51	57.56	1.86
117	Regan_1971_021_T3	T3	152	272	28.9	0.36	0.21	270.00	0.58	3.28	105.00	60.58	1.73	60.69	1.73
118	Regan_1971_022_T4	T4	152	272	34.3	0.48	0.21	270.00	0.58	3.28	110.00	68.89	1.60	63.97	1.72
119	Regan_1971_025_T7	T7	152	264	27.9	0.75	0.21	280.00	0.60	3.37	109.00	69.05	1.58	59.17	1.84
120	Regan_1971_026_T8	T8	152	254	31.7	1.04	0.21	280.00	0.60	3.50	124.00	67.96	1.82	59.15	2.10
121	Regan_1971_029_T13	T13	152	272	13.4	0.36	0.21	270.00	0.58	3.28	90.00	47.04	1.91	48.94	1.84
122	Regan_1971_030_T15	T15	152	254	33.1	1.04	0.21	270.00	0.58	7.10	104.00	74.48	1.40	59.09	1.76
123	Regan_1971_032_T17	T17	152	254	35.3	1.04	0.40	280.00	1.13	7.10	134.00	109.40	1.22	81.54	1.64
124	Regan_1971_033_T19	T19	152	254	30.2	1.04	0.21	270.00	0.58	5.30	106.00	70.93	1.49	57.47	1.84
125	Regan_1971_034_T20	T20	152	254	31.7	1.04	0.40	280.00	1.13	5.30	138.00	104.67	1.32	79.53	1.74
126	Regan_1971_038_T25	T25	152	272	52.7	0.36	0.21	270.00	0.58	3.28	114.00	71.21	1.60	73.64	1.55

Test No.	Author[Source]	Beam name	b_w [mm]	d [mm]	f_{cm} [MPa]	ρ_l [%]	ρ_w [%]	f_{ywm} [MPa]	$\rho_w f_{ywm}$ [MPa]	a/d	V_{exp} [kN]	$V_{MC\text{-}10(III)}$ [kN]	$MF_{MC\text{-}10(III)}$	V_{ACI} [kN]	MF_{ACI}
127	Regan_1971_039_T26	T26	152	254	51.9	1.04	0.40	280.00	1.13	3.50	179.00	106.73	1.68	89.63	2.00
128	Regan_1971_046_T34	T34	152	254	31.3	2.08	0.21	270.00	0.58	5.30	112.00	69.91	1.60	58.11	1.93
129	Regan_1971_047_T35	T35	152	254	31.3	0.59	0.21	270.00	0.58	5.30	115.00	68.87	1.67	58.11	1.98
130	Rehm_1978_001_RsIS / BQ II 0	RsIS / BQ II 0	250	430	24.5	1.10	0.76	560.00	4.26	3.00	594.78	820.13	0.73	545.92	1.09
131	Rehm_1978_004_RnIIS	RnIIS	450	548	22.1	0.64	0.34	557.00	1.87	3.00	744.73	767.98	0.97	654.47	1.14
132	Reineck_1991_001_Stb III	Stb III	77	590	60.6	1.25	1.20	515.00	6.16	4.27	536.67	561.34	0.96	338.36	1.59
133	Reineck_1991_002_Stb I	Stb I	77	589	60.6	1.44	1.68	549.00	9.21	4.27	681.73	821.89	0.83	476.41	1.43
134	Roller_1990_007_7	7.00	457	762	72.4	1.88	0.16	445.17	0.70	2.91	787.83	879.96	0.90	725.59	1.09
135	Roller_1990_009_9	9.00	457	762	125.3	2.35	0.16	445.17	0.70	2.91	749.40	1001.69	0.75	725.59	1.03
136	Roller_1990_010_10	10.00	457	762	125.3	2.89	0.23	445.17	1.04	2.91	1172.14	1106.44	1.06	842.53	1.39
137	Sarsam_1992_007_BL2-H	BL2-H	180	233	75.7	2.82	0.09	820.00	0.76	4.00	138.30	105.55	1.31	89.80	1.54
138	Sarsam_1992_008_BS2-H	BS2-H	180	233	73.9	2.82	0.09	820.00	0.76	2.50	223.50	80.25	2.78	89.80	2.49
139	Sarsam_1992_010_BS4-H	BS4-H	180	233	80.1	2.82	0.19	820.00	1.53	2.50	206.90	138.90	1.49	121.81	1.70
140	Sarsam_1992_011_CL2-H	CL2-H	180	233	70.1	3.51	0.09	820.00	0.76	4.00	147.20	107.43	1.37	89.80	1.64
141	Sarsam_1992_013_CS3-H	CS3-H	180	233	74.2	3.51	0.14	820.00	1.14	2.50	247.20	107.96	2.29	105.80	2.34
142	Sarsam_1992_014_CS4-H	CS4-H	180	233	75.7	3.51	0.19	820.00	1.53	2.50	220.70	143.46	1.54	121.81	1.81
143	Shin_1999_009_MHB 2.5-25	MHB 2.5-25	125	215	52.0	3.77	0.29	365.91	1.08	2.45	98.80	78.86	1.25	61.14	1.62
144	Shin_1999_010_MHB 2.5-50	MHB 2.5-50	125	215	52.0	3.77	0.59	365.91	2.16	2.45	149.32	114.62	1.30	90.11	1.66
145	Shin_1999_021_HB 2.5-25	HB 2.5-25	125	215	73.0	3.77	0.29	365.91	1.08	2.45	115.72	79.59	1.45	66.00	1.75
146	Shin_1999_022_HB 2.5-50	HB 2.5-50	125	215	73.0	3.77	0.59	365.91	2.16	2.45	149.32	120.85	1.24	94.97	1.57
147	Soerensen_1974_001_T-21	T-21	110	298	32.5	1.05	0.52	228.57	1.19	3.52	130.95	87.89	1.49	70.14	1.87
148	Soerensen_1974_003_T-23	T-23	110	298	34.2	1.05	0.34	349.24	1.20	3.52	140.76	86.22	1.63	71.07	1.98
149	Soerensen_1974_007_T-2-B	T-2-B	110	298	24.9	1.05	0.31	397.31	1.21	3.52	130.95	81.34	1.61	66.90	1.96
150	Soerensen_1974_009_T-4-B	T-4-B	110	298	24.7	1.05	0.20	397.31	0.81	3.52	108.39	62.47	1.74	53.62	2.02
151	Stroband_1997_002_2	2.00	90	647	87.4	1.10	0.68	600.00	4.06	2.56	528.00	438.98	1.20	316.81	1.67
152	Stroband_1997_003_3	3.00	90	647	88.3	1.62	1.52	630.00	9.60	2.56	886.27	943.09	0.94	639.13	1.39
153	Taylor_1966_004_HSS-1-B	HSS-1-B	114	257	19.5	1.26	0.33	437.93	1.43	4.44	86.98	88.49	0.98	63.54	1.37
154	Yoon_1996_009_H2-N	H2-N	375	655	87.0	2.86	0.24	430.00	1.02	3.23	721.00	786.09	0.92	587.97	1.23
155	Rosenbusch_2003_001_1.3-1	1.3/1	200	260	49.2	3.55	0.07	680.00	0.47	3.37	120.80	112.24	1.08	85.24	1.42
156	Rosenbusch_2003_002_1.4-1	1.4/1	200	260	47.9	3.55	0.14	680.00	0.95	3.37	170.61	141.44	1.21	109.11	1.56
157	Rosenbusch_2003_004_1.7-1	1.7/1	200	260	50.4	3.55	0.56	550.00	3.07	3.37	190.46	350.32	0.54	220.99	0.86
158	Kautsch_2010_001_A2	A2	155	719	30.8	0.68	0.43	605.00	2.62	2.68	657.10	470.10	1.40	394.47	1.67
159	Kautsch_2010_002_B2	B2	155	719	31.4	0.68	0.32	605.00	1.96	2.68	571.22	384.13	1.49	322.48	1.77
160	Tanimura_2005_031_41	41.00	300	400	20.6	2.20	0.52	388.00	2.03	2.50	324.00	486.27	0.67	334.20	0.97

	$MF_{MC\text{-}10(III)}$		MF_{ACI}
Mean μ_{MF}	1.22		1.51
Std. Dev σ_{MF}	0.35		0.32

Test No.	Author[Source]	Beam name	b_w [mm]	d [mm]	f_{cm} [MPa]	ρ_l [%]	ρ_w [%]	f_{ywm} [MPa]	$\rho_w f_{ywm}$ [MPa]	a/d	V_{exp} [kN]	V_{CCC} [kN]	MF_{CCC}	V_{R2k} [kN]	MF_{R2k}
1	Ahmad_1996_003_NNW-3	NNW-3	127	203	41.5	3.19	0.49	324.14	1.59	2.92	87.27	95.85	0.91	91.70	0.95
2	Ahmad_1996_006_NHW-3	NHW-3	127	198	100.2	4.53	0.50	324.14	1.63	2.92	102.61	134.51	0.76	135.20	0.76
3	Ahmad_1996_007_NHW-3a	NHW-3a	127	198	91.8	4.53	0.65	324.14	2.12	2.92	108.46	144.98	0.75	136.90	0.79
4	Ahmad_1996_008_NHW-3b	NHW-3b	127	198	105.3	4.53	0.79	324.14	2.55	2.92	122.78	164.32	0.75	137.30	0.89
5	Ahmad_1996_009_NHW-4	NHW-4	127	198	100.8	4.53	0.50	324.14	1.63	3.92	94.03	129.89	0.72	98.50	0.95
6	Angelakos_1999_001_DB0.530M	DB0.530M	300	925	32.0	0.50	0.08	508.00	0.40	2.88	265.86	275.15	0.97	260.70	1.02
7	Angelakos_1999_004_DB140M	DB140M	300	925	38.0	1.01	0.08	508.00	0.40	2.88	279.50	330.18	0.85	300.00	0.93
8	Aparicio_1997_001_VHA	VHA	75	704	44.5	1.86	1.77	500.31	8.88	3.41	886.82	722.21	1.23		
9	Aparicio_1997_002_HA-45	HA-45	150	1369	43.3	0.97	1.68	582.03	9.75	3.06	3384.45	2849.63	1.19		
10	Bernhardt_1986_002_S7 A	S7 A	150	161	82.1	5.20	0.67	427.00	2.86	3.42	140.72	368.81	0.38		
11	Bernhardt_1986_003_S7 B	S7 B	150	161	82.1	5.20	0.67	427.00	2.86	3.42	150.72	368.81	0.41		
12	Bernhardt_1986_004_S8 A	S8 A	150	161	82.1	5.20	0.45	427.00	1.91	3.42	125.72	341.41	0.37		
13	Bernhardt_1986_005_S8 B	S8 B	150	161	82.1	5.20	0.45	427.00	1.91	3.42	135.72	341.41	0.40		
14	Bhal_1968_001_B1S	B1S	240	300	27.2	1.26	0.15	441.45	0.65	2.70	128.70	124.87	1.03	121.50	1.06
15	Bhal_1968_002_B2S	B2S	240	600	25.5	1.26	0.15	441.45	0.65	2.80	249.57	215.84	1.16	263.00	0.95
16	Bhal_1968_003_B3S	B3S	240	900	26.7	1.26	0.15	441.45	0.65	2.85	369.39	303.83	1.22	387.50	0.95
17	Bhal_1968_004_B4S	B4S	240	1200	25.8	1.26	0.15	441.45	0.65	2.88	472.61	381.01	1.24	500.00	0.95
18	Bresler_1963_001_A-1	A-1	307	466	24.1	1.80	0.10	325.52	0.32	3.76	237.46	171.63	1.38	218.50	1.09
19	Bresler_1963_007_C-1	C-1	155	464	29.6	1.80	0.20	325.52	0.64	3.78	157.66	120.30	1.31	117.90	1.34
20	Caldera_2002_001_H 50/2	H 50/2	200	353	49.9	2.28	0.11	530.00	0.58	2.95	177.64	157.33	1.13	188.00	0.94
21	Caldera_2002_002_H 50/3	H 50/3	200	351	49.9	2.29	0.24	540.00	1.29	2.97	242.07	216.55	1.12	251.80	0.96
22	Caldera_2002_003_H 50/4	H 50/4	200	351	49.9	2.99	0.24	540.00	1.29	2.97	246.34	226.52	1.09	311.00	0.79
23	Caldera_2002_004_H 60/2	H 60/2	200	353	60.8	2.28	0.14	530.00	0.75	2.95	179.74	184.87	0.97	229.90	0.78
24	Caldera_2002_007_H 75/2	H 75/2	200	353	68.9	2.28	0.14	530.00	0.75	2.95	203.94	193.89	1.05	226.00	0.90
25	Caldera_2002_010_H 100/2	H 100/2	200	353	87.0	2.28	0.17	530.00	0.91	2.95	225.55	225.90	1.00	235.50	0.96
26	Cederwall_1974_003_734-46	734-46	139	234	30.2	1.04	0.41	436.55	1.78	2.56	95.65	102.54	0.93		
27	Gabrielsson_1993_006_HS1	HS1	200	260	80.5	3.09	0.43	522.00	2.24	3.08	250.00	265.59	0.94		
28	Gabrielsson_1993_007_HS2	HS2	200	260	80.5	3.09	0.26	522.00	1.38	4.23	200.00	204.45	0.98		
29	Gabrielsson_1993_008_HPS1	HPS1	200	225	97.1	3.57	0.34	522.00	1.75	2.44	324.00	233.22	1.39		
30	Gabrielsson_1993_009_HPS2	HPS2	200	225	101.8	3.57	0.34	522.00	1.75	2.44	305.00	237.06	1.29		
31	Guidi_1963_001_V	V	80	380	34.1	1.07	0.71	490.50	3.47	3.95	122.63	176.95	0.69	118.00	1.04
32	Guralnik_1960_004_IB-2R	IB-2R	178	308	16.8	0.43	0.24	528.97	1.29	2.97	140.11	163.74	0.86	143.00	0.98
33	Guralnik_1960_006_IC-2R	IC-2R	178	310	34.0	1.33	0.24	528.97	1.29	2.95	225.07	226.53	0.99	211.00	1.07
34	Guralnik_1960_008_ID-2R	ID-2R	178	306	34.0	0.75	0.24	528.97	1.29	2.99	217.51	215.40	1.01	221.00	0.98
35	Hamadi_1976_002_GT-2	GT-2	120	350	24.9	0.72	0.38	320.00	1.21	3.46	148.50	145.14	1.02	139.50	1.06
36	Hegger_2001_001_SVB 3b	SVB 3b	180	450	70.0	2.97	0.56	514.00	2.87	3.33	427.00	435.96	0.98		
37	Hegger_2003_001_NSC 3L	NSC 3L	80	470	29.0	1.91	0.71	550.00	3.89	3.19	334.00	256.72	1.30		
38	Hegger_2003_002_NSC 3R	NSC 3R	80	470	29.0	1.91	0.71	550.00	3.89	3.09	349.00	257.28	1.36		
39	Johnston_1939_002_B2-II	B2-II	305	305	22.0	0.82	0.10	275.86	0.28	3.00	102.68	98.11	1.05	83.20	1.23
40	Johnston_1939_009_T3-I	T3-I	305	305	22.2	0.78	0.10	275.86	0.28	3.00	103.89	97.35	1.07	72.10	1.44
41	Johnston_1939_010_T3-II	T3-II	305	305	22.2	0.78	0.10	275.86	0.28	3.00	97.44	97.35	1.00	72.10	1.35
42	Johnson_1989_001_1	1.00	305	539	36.4	2.49	0.16	479.31	0.75	3.10	344.26	332.62	1.03	548.00	0.63

Test No.	Author[Source]	Beam name	b_w [mm]	d [mm]	f_{cm} [MPa]	ρ_l [%]	ρ_w [%]	f_{ywm} [MPa]	$\rho_w f_{ywm}$ [MPa]	a/d	V_{exp} [kN]	V_{CCC} [kN]	MF_{CCC}	V_{R2k} [kN]	MF_{R2k}
43	Johnson_1989_002_2	2.00	305	539	36.4	2.49	0.08	479.31	0.37	3.10	228.16	259.65	0.88	326.20	0.70
44	Johnson_1989_005_5	5.00	305	539	55.9	2.49	0.16	479.31	0.75	3.10	388.29	384.29	1.01	420.00	0.92
45	Kong_1997_001_S1-1	S1-1	250	292	61.6	2.80	0.15	569.00	0.87	2.50	228.30	224.84	1.02	235.00	0.97
46	Kong_1997_002_S1-2	S1-2	250	292	61.6	2.80	0.15	569.00	0.87	2.50	208.30	224.84	0.93	235.00	0.89
47	Kong_1997_003_S1-3	S1-3	250	292	61.6	2.80	0.15	569.00	0.87	2.50	206.10	224.84	0.92	235.00	0.88
48	Kong_1997_004_S1-4	S1-4	250	292	61.6	2.80	0.15	569.00	0.87	2.50	277.90	224.84	1.24	235.00	1.18
49	Kong_1997_005_S1-5	S1-5	250	292	61.6	2.80	0.15	569.00	0.87	2.50	253.30	224.84	1.13	235.00	1.08
50	Kong_1997_006_S1-6	S1-6	250	292	61.6	2.80	0.15	569.00	0.87	2.50	224.10	224.84	1.00	235.00	0.95
51	Kong_1997_007_S2-1	S2-1	250	292	70.2	2.80	0.10	569.00	0.58	2.50	260.30	211.15	1.23	211.90	1.23
52	Kong_1997_008_S2-2	S2-2	250	292	70.2	2.80	0.12	569.00	0.70	2.50	232.50	221.26	1.05	205.00	1.13
53	Kong_1997_009_S2-3	S2-3	250	292	70.2	2.80	0.15	569.00	0.87	2.50	253.30	236.41	1.07	240.60	1.05
54	Kong_1997_010_S2-4	S2-4	250	292	70.2	2.80	0.15	569.00	0.87	2.50	219.40	236.41	0.93	240.60	0.91
55	Kong_1997_011_S2-5	S2-5	250	292	70.2	2.80	0.20	569.00	1.16	2.50	282.10	261.68	1.08	328.60	0.86
56	Kong_1997_013_S3-1	S3-1	250	297	65.3	1.66	0.10	632.00	0.62	2.49	209.20	186.26	1.12	170.20	1.23
57	Kong_1997_014_S3-2	S3-2	250	297	65.3	1.66	0.10	632.00	0.62	2.49	178.00	186.26	0.96	170.20	1.05
58	Kong_1997_015_S3-3	S3-3	250	293	65.3	2.79	0.10	632.00	0.62	2.49	228.60	208.65	1.10	201.00	1.14
59	Kong_1997_016_S3-4	S3-4	250	293	65.3	2.79	0.10	632.00	0.62	2.49	174.90	208.65	0.84	201.00	0.87
60	Kong_1997_017_S3-5	S3-5	250	287	65.3	3.85	0.10	632.00	0.62	2.51	296.60	222.02	1.34	229.00	1.30
61	Kong_1997_018_S3-6	S3-6	250	287	65.3	3.85	0.10	632.00	0.62	2.51	282.90	222.02	1.27	229.00	1.24
62	Kong_1997_019_S4-1	S4-1	250	524	84.5	3.12	0.15	569.00	0.87	2.48	354.00	410.25	0.86	330.00	1.07
63	Kong_1997_021_S4-3	S4-3	250	332	84.5	2.97	0.15	569.00	0.87	2.50	243.40	285.20	0.85	336.80	0.72
64	Kong_1997_022_S4-4	S4-4	250	292	84.5	2.80	0.15	569.00	0.87	2.50	258.10	254.39	1.01	235.00	1.10
65	Kong_1997_024_S4-6	S4-6	250	198	84.5	2.79	0.15	569.00	0.87	2.53	202.90	185.53	1.09	174.00	1.17
66	Kong_1997_025_S5-1	S5-1	250	292	86.6	2.80	0.15	569.00	0.87	3.01	241.70	250.19	0.97	233.00	1.04
67	Kong_1997_026_S5-2	S5-2	250	292	86.6	2.80	0.15	569.00	0.87	2.74	259.90	253.54	1.03	248.00	1.05
68	Kong_1997_027_S5-3	S5-3	250	292	86.6	2.80	0.15	569.00	0.87	2.50	243.80	256.83	0.95	257.00	0.95
69	Kong_1997_031_S7-1	S7-1	250	278	72.4	4.73	0.10	569.00	0.58	3.40	217.20	224.57	0.97	201.20	1.08
70	Kong_1997_032_S7-2	S7-2	250	278	72.4	4.73	0.12	569.00	0.70	3.40	205.40	234.19	0.88	223.10	0.92
71	Kong_1997_033_S7-3	S7-3	250	278	72.4	4.73	0.15	569.00	0.87	3.40	246.50	248.62	0.99	255.40	0.97
72	Kong_1997_034_S7-4	S7-4	250	278	72.4	4.73	0.19	569.00	1.09	3.40	273.60	266.66	1.03	302.00	0.91
73	Kong_1997_035_S7-5	S7-5	250	278	72.4	4.73	0.22	569.00	1.25	3.40	304.40	279.54	1.09	318.00	0.96
74	Kong_1997_036_S7-6	S7-6	250	278	72.4	4.73	0.26	569.00	1.45	3.40	310.60	296.72	1.05	347.00	0.90
75	Kong_1997_037_S8-1	S8-1	250	292	72.2	2.80	0.10	569.00	0.58	2.50	272.10	213.79	1.27	221.30	1.23
76	Kong_1997_038_S8-2	S8-2	250	292	72.2	2.80	0.12	569.00	0.70	2.50	251.00	223.90	1.12	232.60	1.08
77	Kong_1997_039_S8-3	S8-3	250	292	72.2	2.80	0.15	569.00	0.87	2.50	309.60	239.06	1.30	260.10	1.19
78	Kong_1997_040_S8-4	S8-4	250	292	72.2	2.80	0.15	569.00	0.87	2.50	265.80	239.06	1.11	253.50	1.05
79	Kong_1997_041_S8-5	S8-5	250	292	72.2	2.80	0.19	569.00	1.09	2.50	289.20	258.00	1.12	311.00	0.93
80	Kong_1997_042_S8-6	S8-6	250	292	72.2	2.80	0.22	569.00	1.25	2.50	283.90	271.54	1.05	276.00	1.03
81	Krefeld_1966_010_26-1	26-1	254	456	40.1	2.23	0.16	341.38	0.56	3.87	206.83	213.09	0.97		
82	Krefeld_1966_012_29b-1	29b-1	254	456	37.7	2.23	0.11	341.38	0.37	3.87	160.13	182.57	0.88		
83	Krefeld_1966_015_29a-2	29a-2	254	456	37.2	2.23	0.11	372.41	0.41	3.87	216.62	186.27	1.16		
84	Krefeld_1966_016_29b-2	29b-2	254	456	41.4	2.23	0.11	372.41	0.41	3.87	202.38	194.49	1.04		

Test No.	Author[Source]	Beam name	b_w [mm]	d [mm]	f_{cm} [MPa]	ρ_l [%]	ρ_w [%]	f_{ywm} [MPa]	$\rho_w f_{ywm}$ [MPa]	a/d	V_{exp} [kN]	V_{CCC} [kN]	MF_{CCC}	V_{R2k} [kN]	MF_{R2k}
85	Krefeld_1966_017_29c-2	29c-2	254	456	24.1	2.23	0.11	372.41	0.41	3.87	161.46	157.79	1.02		
86	Krefeld_1966_018_29d-2	29d-2	254	456	30.4	2.23	0.11	372.41	0.41	3.87	165.02	172.16	0.96		
87	Krefeld_1966_021_29g-2	29g-2	254	456	15.7	2.23	0.11	372.41	0.41	3.87	149.90	135.68	1.10		
88	Leonhardt_1962_002_ET2	ET2	150	300	23.8	1.40	0.34	313.92	1.08	3.50	130.94	127.80	1.02	128.00	1.02
89	Leonhardt_1963_010_TA12	TA12	160	375	26.2	0.75	0.31	440.47	1.38	3.33	267.69	195.74	1.37	262.00	1.02
90	Levi_1989/1993_001_RC 30 A1	RC 30 A1	120	940	25.0	1.07	0.84	480.00	4.02	4.04	676.00	682.05	0.99		
91	Levi_1989/1993_002_RC 30 A2	RC 30 A2	120	940	25.0	1.07	0.84	480.00	4.02	4.04	688.00	682.05	1.01		
92	Levi_1989/1993_003_RC 60 A1	RC 60 A1	120	940	47.0	1.26	0.84	480.00	4.02	4.04	990.00	755.43	1.31		
93	Levi_1989/1993_004_RC 60 A2	RC 60 A2	120	940	47.0	1.26	0.84	480.00	4.02	4.04	938.00	755.43	1.24		
94	Levi_1989/1993_005_RC 60 B1	RC 60 B1	120	940	50.0	1.67	1.26	480.00	6.03	4.04	1181.00	1049.56	1.13		
95	Levi_1989/1993_006_RC 60 B2	RC 60 B2	120	940	50.0	1.67	1.26	480.00	6.03	4.04	1239.00	1049.56	1.18		
96	Levi_1989/1993_007_RC 70 B1	RC 70 B1	120	940	60.0	1.67	1.26	480.00	6.03	4.04	1330.00	1077.09	1.23		
97	Maruyama_1988_001_RS2-WD	RS2-WD	86	398	40.1	0.14	0.23	645.00	1.48	2.89	126.00	112.26	1.12		
98	Moayer_1974_002_P20	P20	150	279	40.7	0.47	0.21	310.34	0.66	3.50	120.10	131.27	0.91	121.00	0.99
99	Özden_1967_002_T6	T6	110	298	33.4	1.05	0.61	272.72	1.66	3.52	137.34	143.07	0.96	117.00	1.17
100	Özden_1967_003_T7	T7	110	298	30.5	1.05	0.61	272.72	1.66	3.52	141.26	138.82	1.02	134.00	1.05
101	Özden_1967_004_T9	T9	110	298	30.5	1.05	0.61	272.72	1.66	3.52	154.02	138.82	1.11	138.00	1.12
102	Ozcebe_1999_003_TS56	TS56	150	310	61.0	3.46	0.24	255.00	0.61	5.00	129.20	120.31	1.07	116.50	1.11
103	Ozcebe_1999_006_TS59	TS59	150	310	82.0	4.43	0.28	255.00	0.71	5.00	125.40	150.60	0.83	137.20	0.91
104	Ozcebe_1999_009_TS36	TS36	150	310	75.0	2.59	0.24	255.00	0.61	3.00	155.90	131.86	1.18	138.60	1.12
105	Ozcebe_1999_011_TH39	TH39	150	310	73.0	3.08	0.21	255.00	0.53	3.00	142.90	131.77	1.08	125.60	1.14
106	Ozcebe_1999_012_TS39	TS39	150	310	73.0	3.08	0.28	255.00	0.71	3.00	179.20	141.62	1.27	157.10	1.14
107	Petersson_1972_001_V1	V1	175	322	38.0	1.07	0.22	323.00	0.70	3.57	100.93	104.12	0.97	74.00	1.36
108	Petersson_1972_002_VL1	VL1	120	278	43.0	1.20	0.84	366.00	3.07	3.24	190.73	198.44	0.96	180.00	1.06
109	Quast_1999_001_1/1	1/1	260	355	47.3	1.33	0.09	641.00	0.58	3.27	154.37	176.98	0.87	201.00	0.77
110	Regan_1971_001_R8	R8	152	272	26.4	1.46	0.21	270.00	0.58	3.22	81.00	69.01	1.17	50.00	1.62
111	Regan_1971_004_R11	R11	152	272	25.9	1.95	0.21	270.00	0.58	3.22	91.00	72.60	1.25	65.40	1.39
112	Regan_1971_005_R12	R12	152	254	33.5	4.17	0.21	270.00	0.58	3.45	112.00	88.35	1.27	103.00	1.09
113	Regan_1971_011_R20	R20	152	272	42.3	1.46	0.21	270.00	0.58	3.22	92.00	81.62	1.13	62.10	1.48
114	Regan_1971_012_R21	R21	152	254	47.4	4.17	0.40	280.00	1.13	3.45	153.00	127.28	1.20	116.00	1.32
115	Regan_1971_013_R22	R22	152	272	29.1	3.89	0.21	270.00	0.58	4.36	81.00	84.35	0.96	74.00	1.09
116	Regan_1971_016_R25	R25	152	254	30.4	4.17	0.21	270.00	0.58	3.45	107.00	85.03	1.26	101.20	1.06
117	Regan_1971_021_T3	T3	152	272	28.9	0.36	0.21	270.00	0.58	3.28	105.00	101.22	1.04	98.00	1.07
118	Regan_1971_022_T4	T4	152	272	34.3	0.48	0.21	270.00	0.58	3.28	110.00	112.63	0.98	112.00	0.98
119	Regan_1971_025_T7	T7	152	264	27.9	0.75	0.21	280.00	0.60	3.37	109.00	106.95	1.02	103.00	1.06
120	Regan_1971_026_T8	T8	152	254	31.7	1.04	0.21	280.00	0.60	3.50	124.00	115.58	1.07	121.00	1.02
121	Regan_1971_029_T13	T13	152	272	13.4	0.36	0.21	270.00	0.58	3.28	90.00	73.27	1.23	87.00	1.03
122	Regan_1971_030_T15	T15	152	254	33.1	1.04	0.21	270.00	0.58	7.10	104.00	104.96	0.99	100.00	1.04
123	Regan_1971_032_T17	T17	152	254	35.3	1.04	0.40	280.00	1.13	7.10	134.00	133.45	1.00	127.00	1.06
124	Regan_1971_033_T19	T19	152	254	30.2	1.04	0.21	270.00	0.58	5.30	106.00	105.19	1.01	100.00	1.06
125	Regan_1971_034_T20	T20	152	254	31.7	1.04	0.40	280.00	1.13	5.30	138.00	132.74	1.04	130.00	1.06
126	Regan_1971_038_T25	T25	152	272	52.7	0.36	0.21	270.00	0.58	3.28	114.00	135.08	0.84	117.00	0.97

Test No.	Author[Source]	Beam name	b_w [mm]	d [mm]	f_{cm} [MPa]	ρ_l [%]	ρ_w [%]	f_{ywm} [MPa]	$\rho_w f_{ywm}$ [MPa]	a/d	V_{exp} [kN]	V_{CCC} [kN]	MF_{CCC}	V_{R2k} [kN]	MF_{R2k}
127	Regan_1971_039_T26	T26	152	254	51.9	1.04	0.40	280.00	1.13	3.50	179.00	171.25	1.05	175.00	1.02
128	Regan_1971_046_T34	T34	152	254	31.3	2.08	0.21	270.00	0.58	5.30	112.00	106.95	1.05	90.00	1.24
129	Regan_1971_047_T35	T35	152	254	31.3	0.59	0.21	270.00	0.58	5.30	115.00	106.95	1.08	105.00	1.10
130	Rehm_1978_001_RsIS / BQ II 0	RsIS / BQ II 0	250	430	24.5	1.10	0.76	560.00	4.26	3.00	594.78	723.44	0.82	588.00	1.01
131	Rehm_1978_004_RnIIS	RnIIS	450	548	22.1	0.64	0.34	557.00	1.87	3.00	744.73	801.10	0.93	740.00	1.01
132	Reineck_1991_001_Stb III	Stb III	77	590	60.6	1.25	1.20	515.00	6.16	4.27	536.67	484.06	1.11	532.00	1.01
133	Reineck_1991_002_Stb I	Stb I	77	589	60.6	1.44	1.68	549.00	9.21	4.27	681.73	646.34	1.05	678.00	1.01
134	Roller_1990_007_7	7.00	457	762	72.4	1.88	0.16	445.17	0.70	2.91	787.83	766.33	1.03	808.00	0.98
135	Roller_1990_009_9	9.00	457	762	125.3	2.35	0.16	445.17	0.70	2.91	749.40	990.20	0.76	945.00	0.79
136	Roller_1990_010_10	10.00	457	762	125.3	2.89	0.23	445.17	1.04	2.91	1172.14	1179.24	0.99	1220.00	0.96
137	Sarsam_1992_007_BL2-H	BL2-H	180	233	75.7	2.82	0.09	820.00	0.76	4.00	138.30	131.76	1.05	140.10	0.99
138	Sarsam_1992_008_BS2-H	BS2-H	180	233	73.9	2.82	0.09	820.00	0.76	2.50	223.50	139.59	1.60	152.10	1.47
139	Sarsam_1992_010_BS4-H	BS4-H	180	233	80.1	2.82	0.19	820.00	1.53	2.50	206.90	182.46	1.13	221.40	0.93
140	Sarsam_1992_011_CL2-H	CL2-H	180	233	70.1	3.51	0.09	820.00	0.76	4.00	147.20	134.41	1.10	147.00	1.00
141	Sarsam_1992_013_CS3-H	CS3-H	180	233	74.2	3.51	0.14	820.00	1.14	2.50	247.20	166.44	1.49	189.00	1.31
142	Sarsam_1992_014_CS4-H	CS4-H	180	233	75.7	3.51	0.19	820.00	1.53	2.50	220.70	186.74	1.18	225.00	0.98
143	Shin_1999_009_MHB 2.5-25	MHB 2.5-25	125	215	52.0	3.77	0.29	365.91	1.08	2.45	98.80	94.55	1.04	126.90	0.78
144	Shin_1999_010_MHB 2.5-50	MHB 2.5-50	125	215	52.0	3.77	0.59	365.91	2.16	2.45	149.32	129.03	1.16	144.80	1.03
145	Shin_1999_021_HB 2.5-25	HB 2.5-25	125	215	73.0	3.77	0.29	365.91	1.08	2.45	115.72	107.39	1.08	134.00	0.86
146	Shin_1999_022_HB 2.5-50	HB 2.5-50	125	215	73.0	3.77	0.59	365.91	2.16	2.45	149.32	141.86	1.05	144.80	1.03
147	Soerensen_1974_001_T-21	T-21	110	298	32.5	1.05	0.52	228.57	1.19	3.52	130.95	123.51	1.06	129.00	1.02
148	Soerensen_1974_003_T-23	T-23	110	298	34.2	1.05	0.34	349.24	1.20	3.52	140.76	126.24	1.12	134.00	1.05
149	Soerensen_1974_007_T-2-B	T-2-B	110	298	24.9	1.05	0.31	397.31	1.21	3.52	130.95	112.48	1.16	125.00	1.05
150	Soerensen_1974_009_T-4-B	T-4-B	110	298	24.7	1.05	0.20	397.31	0.81	3.52	108.39	96.48	1.12	110.00	0.99
151	Stroband_1997_002_2	2.00	90	647	87.4	1.10	0.68	600.00	4.06	2.56	528.00	517.30	1.02	530.00	1.00
152	Stroband_1997_003_3	3.00	90	647	88.3	1.62	1.52	630.00	9.60	2.56	886.27	915.96	0.97	875.00	1.01
153	Taylor_1966_004_HSS-1-B	HSS-1-B	114	257	19.5	1.26	0.33	437.93	1.43	4.44	86.98	100.15	0.87	87.90	0.99
154	Yoon_1996_009_H2-N	H2-N	375	655	87.0	2.86	0.24	430.00	1.02	3.23	721.00	740.20	0.97	756.00	0.95
155	Rosenbusch_2003_001_1.3-1	1.3/1	200	260	49.2	3.55	0.07	680.00	0.47	3.37	120.80	127.80	0.95	102.00	1.18
156	Rosenbusch_2003_002_1.4-1	1.4/1	200	260	47.9	3.55	0.14	680.00	0.95	3.37	170.61	155.67	1.10	152.40	1.12
157	Rosenbusch_2003_004_1.7-1	1.7/1	200	260	50.4	3.55	0.56	550.00	3.07	3.37	190.46	289.82	0.66	189.80	1.00
158	Kautsch_2010_001_A2	A2	155	719	30.8	0.68	0.43	605.00	2.62	2.68	657.10	529.63	1.24	648.00	1.01
159	Kautsch_2010_002_B2	B2	155	719	31.4	0.68	0.32	605.00	1.96	2.68	571.22	444.94	1.28	567.00	1.01
160	Tanimura_2005_031_41	41.00	300	400	20.6	2.20	0.52	388.00	2.03	2.50	324.00	399.73196	0.8105431		

	MF_{CCC}		MF_{R2k}
	1.04		1.04
	0.19		0.16

Test No.	Author/Beam name	Beam name	b_w [mm]	d [mm]	f_{ck} [MPa]	ρ_l [%]	f_{ywk} [MPa]	$\rho_w f_{ywk}$ [MPa]	a/d	V_{exp} [kN]	$V_{VSIM\text{-}L\theta}$ (X_k, γ) [kN]	V_{ACI} (X_k, γ) [kN]	$V_{MC\text{-}10(III)}$ (X_k, γ) [kN]
1	Ahmad_1996_003_NNW-3	NNW-3	127	203	33.5	3.19	259.31	1.27	2.92	87.27	64.27	58.24	65.47
2	Ahmad_1996_006_NHW-3	NHW-3	127	198	92.2	4.53	259.31	1.31	2.92	102.61	64.27	67.52	76.45
3	Ahmad_1996_007_NHW-3a	NHW-3a	127	198	83.8	4.53	259.31	1.70	2.92	108.46	83.56	77.37	91.23
4	Ahmad_1996_008_NHW-3b	NHW-3b	127	198	97.3	4.53	259.31	2.04	2.92	122.78	100.27	85.91	102.53
5	Ahmad_1996_009_NHW-4	NHW-4	127	198	92.8	4.53	259.31	1.31	3.92	94.03	64.27	67.52	78.81
6	Angelakos_1999_001_DB0.530M	DB0.530M	300	925	24.0	0.50	406.40	0.32	2.88	265.86	174.71	322.36	244.70
7	Angelakos_1999_004_DB140M	DB140M	300	925	30.0	1.01	406.40	0.32	2.88	279.50	174.71	348.24	331.22
8	Aparicio_1997_001_VHA	VHA	75	704	36.5	1.86	400.25	7.10	3.41	886.82	293.41	429.00	614.40
9	Aparicio_1997_002_HA-45	HA-45	150	1369	35.3	0.97	465.62	7.80	3.06	3384.45	1253.78	1809.12	2323.70
10	Bernhardt_1986_002_S7 A	S7 A	150	161	74.1	5.20	341.60	2.29	3.42	140.72	108.15	88.55	103.58
11	Bernhardt_1986_003_S7 B	S7 B	150	161	74.1	5.20	341.60	2.29	3.42	150.72	108.15	88.55	100.96
12	Bernhardt_1986_004_S8 A	S8 A	150	161	74.1	5.20	341.60	1.53	3.42	125.72	72.10	70.12	76.53
13	Bernhardt_1986_005_S8 B	S8 B	150	161	74.1	5.20	341.60	1.53	3.42	135.72	72.10	70.12	74.23
14	Bhal_1968_001_B1S	B1S	240	300	19.2	1.26	353.16	0.52	2.70	128.70	73.27	92.01	83.30
15	Bhal_1968_002_B2S	B2S	240	600	17.5	1.26	353.16	0.52	2.80	249.57	146.53	179.23	164.90
16	Bhal_1968_003_B3S	B3S	240	900	18.7	1.26	353.16	0.52	2.85	369.39	219.80	273.78	253.12
17	Bhal_1968_004_B4S	B4S	240	1200	17.8	1.26	353.16	0.52	2.88	472.61	293.07	360.24	339.60
18	Bresler_1963_001_A-1	A-1	307	466	16.1	1.80	260.41	0.26	3.76	237.46	71.78	136.64	114.72
19	Bresler_1963_007_C-1	C-1	155	464	21.6	1.80	260.41	0.51	3.78	157.66	71.39	93.90	85.24
20	Caldera_2002_001_H 50/2	H 50/2	200	353	41.9	2.28	424.00	0.46	2.95	177.64	63.69	109.85	95.80
21	Caldera_2002_002_H 50/3	H 50/3	200	351	41.9	2.29	432.00	1.03	2.97	242.07	142.03	149.45	142.03
22	Caldera_2002_003_H 50/4	H 50/4	200	351	41.9	2.99	432.00	1.03	2.97	246.34	142.03	149.45	152.00
23	Caldera_2002_004_H 60/2	H 60/2	200	353	52.8	2.28	424.00	0.60	2.95	179.74	82.80	128.76	119.21
24	Caldera_2002_007_H 75/2	H 75/2	200	353	60.9	2.28	424.00	0.60	2.95	203.94	82.80	134.97	117.41
25	Caldera_2002_010_H 100/2	H 100/2	200	353	79.0	2.28	424.00	0.73	2.95	225.55	100.37	148.57	129.83
26	Cederwall_1974_003_734-46	734-46	139	234	22.2	1.04	349.24	1.42	2.56	95.65	77.30	72.56	62.12
27	Gabrielsson_1993_006_HS1	HS1	200	260	72.5	3.09	417.60	1.79	3.08	250.00	182.54	164.94	168.99
28	Gabrielsson_1993_007_HS2	HS2	200	260	72.5	3.09	417.60	1.10	4.23	200.00	112.41	129.09	127.23
29	Gabrielsson_1993_008_HPS1	HPS1	200	225	89.1	3.57	417.60	1.40	2.44	324.00	123.22	124.97	104.61
30	Gabrielsson_1993_009_HPS2	HPS2	200	225	93.8	3.57	417.60	1.40	2.44	305.00	123.22	124.97	108.57
31	Guidi_1963_001_V	V	80	380	26.1	1.07	392.40	2.77	3.95	122.63	99.92	110.87	143.99
32	Guralnik_1960_004_IB-2R	IB-2R	178	308	8.8	0.43	423.17	1.03	2.97	140.11	65.97	85.84	85.97
33	Guralnik_1960_006_IC-2R	IC-2R	178	310	26.0	1.33	423.17	1.03	2.95	225.07	111.18	104.83	110.23
34	Guralnik_1960_008_ID-2R	ID-2R	178	306	26.0	0.75	423.17	1.03	2.99	217.51	109.91	103.63	96.30
35	Hamadi_1976_002_GT-2	GT-2	120	350	16.9	0.72	256.00	0.97	3.46	148.50	73.53	70.50	71.81
36	Hegger_2001_001_SVB 3b	SVB 3b	180	450	62.0	2.97	411.20	2.30	3.33	427.00	363.98	293.25	324.73
37	Hegger_2003_001_NSC 3L	NSC 3L	80	470	21.0	1.91	440.00	3.11	3.19	334.00	108.99	146.61	201.37
38	Hegger_2003_002_NSC 3R	NSC 3R	80	470	21.0	1.91	440.00	3.11	3.09	349.00	108.99	146.61	199.53
39	Johnston_1939_002_B2-II	B2-II	305	305	14.0	0.82	220.69	0.23	3.00	102.68	41.03	81.88	64.73
40	Johnston_1939_009_T3-I	T3-I	305	305	14.2	0.78	220.69	0.23	3.00	103.89	41.03	82.28	63.54
41	Johnston_1939_010_T3-II	T3-II	305	305	14.2	0.78	220.69	0.23	3.00	97.44	41.03	82.28	65.65

Test No.	Author/Beam name	Beam name	b_w [mm]	d [mm]	f_{ck} [MPa]	ρ_l [%]	f_{ywk} [MPa]	$\rho_w f_{ywk}$ [MPa]	a/d	V_{exp} [kN]	$V_{VSIM\text{-}L\theta}$ (X_k, γ) [kN]	V_{ACI} (X_k, γ) [kN]	$V_{MC\text{-}10(III)}$ (X_k, γ) [kN]
42	Johnson_1989_001_1	1.00	305	539	28.4	2.49	383.45	0.60	3.10	344.26	191.99	247.45	258.11
43	Johnson_1989_002_2	2.00	305	539	28.4	2.49	383.45	0.30	3.10	228.16	95.99	198.39	205.30
44	Johnson_1989_005_5	5.00	305	539	47.9	2.49	383.45	0.60	3.10	388.29	191.99	289.82	284.21
45	Kong_1997_001_S1-1	S1-1	250	292	53.6	2.80	455.20	0.70	2.50	228.30	99.70	140.98	131.22
46	Kong_1997_002_S1-2	S1-2	250	292	53.6	2.80	455.20	0.70	2.50	208.30	99.70	140.98	136.67
47	Kong_1997_003_S1-3	S1-3	250	292	53.6	2.80	455.20	0.70	2.50	206.10	99.70	140.98	137.30
48	Kong_1997_004_S1-4	S1-4	250	292	53.6	2.80	455.20	0.70	2.50	277.90	99.70	140.98	119.29
49	Kong_1997_005_S1-5	S1-5	250	292	53.6	2.80	455.20	0.70	2.50	253.30	99.70	140.98	124.95
50	Kong_1997_006_S1-6	S1-6	250	292	53.6	2.80	455.20	0.70	2.50	224.10	99.70	140.98	132.33
51	Kong_1997_007_S2-1	S2-1	250	292	62.2	2.80	455.20	0.47	2.50	260.30	66.46	130.77	101.64
52	Kong_1997_008_S2-2	S2-2	250	292	62.2	2.80	455.20	0.56	2.50	232.50	79.76	137.56	119.14
53	Kong_1997_009_S2-3	S2-3	250	292	62.2	2.80	455.20	0.70	2.50	253.30	99.70	147.75	130.55
54	Kong_1997_010_S2-4	S2-4	250	292	62.2	2.80	455.20	0.70	2.50	219.40	99.70	147.75	139.53
55	Kong_1997_011_S2-5	S2-5	250	292	62.2	2.80	455.20	0.93	2.50	282.10	132.93	164.74	150.30
56	Kong_1997_013_S3-1	S3-1	250	297	57.3	1.66	505.60	0.50	2.49	209.20	72.38	131.56	98.94
57	Kong_1997_014_S3-2	S3-2	250	297	57.3	1.66	505.60	0.50	2.49	178.00	72.38	131.56	107.74
58	Kong_1997_015_S3-3	S3-3	250	293	57.3	2.79	505.60	0.50	2.49	228.60	71.40	129.79	110.02
59	Kong_1997_016_S3-4	S3-4	250	293	57.3	2.79	505.60	0.50	2.49	174.90	71.40	129.79	124.56
60	Kong_1997_017_S3-5	S3-5	250	287	57.3	3.85	505.60	0.50	2.51	296.60	69.94	127.13	101.00
61	Kong_1997_018_S3-6	S3-6	250	287	57.3	3.85	505.60	0.50	2.51	282.90	69.94	127.13	103.69
62	Kong_1997_019_S4-1	S4-1	250	524	76.5	3.12	455.20	0.70	2.48	354.00	178.91	271.93	276.01
63	Kong_1997_021_S4-3	S4-3	250	332	76.5	2.97	455.20	0.70	2.50	243.40	113.35	172.29	167.05
64	Kong_1997_022_S4-4	S4-4	250	292	76.5	2.80	455.20	0.70	2.50	258.10	99.70	151.53	133.02
65	Kong_1997_024_S4-6	S4-6	250	198	76.5	2.79	455.20	0.70	2.53	202.90	67.60	102.75	83.69
66	Kong_1997_025_S5-1	S5-1	250	292	78.6	2.80	455.20	0.70	3.01	241.70	99.70	151.53	137.48
67	Kong_1997_026_S5-2	S5-2	250	292	78.6	2.80	455.20	0.70	2.74	259.90	99.70	151.53	132.93
68	Kong_1997_027_S5-3	S5-3	250	292	78.6	2.80	455.20	0.70	2.50	243.80	99.70	151.53	136.94
69	Kong_1997_031_S7-1	S7-1	250	278	64.4	4.73	455.20	0.47	3.40	217.20	63.28	126.09	119.05
70	Kong_1997_032_S7-2	S7-2	250	278	64.4	4.73	455.20	0.56	3.40	205.40	75.93	132.56	133.99
71	Kong_1997_033_S7-3	S7-3	250	278	64.4	4.73	455.20	0.70	3.40	246.50	94.92	142.26	141.09
72	Kong_1997_034_S7-4	S7-4	250	278	64.4	4.73	455.20	0.87	3.40	273.60	118.64	154.39	156.02
73	Kong_1997_035_S7-5	S7-5	250	278	64.4	4.73	455.20	1.00	3.40	304.40	135.59	163.05	163.80
74	Kong_1997_036_S7-6	S7-6	250	278	64.4	4.73	455.20	1.16	3.40	310.60	158.19	174.60	182.20
75	Kong_1997_037_S8-1	S8-1	250	292	64.2	2.80	455.20	0.47	2.50	272.10	66.46	132.30	100.29
76	Kong_1997_038_S8-2	S8-2	250	292	64.2	2.80	455.20	0.56	2.50	251.00	79.76	139.09	115.83
77	Kong_1997_039_S8-3	S8-3	250	292	64.2	2.80	455.20	0.70	2.50	309.60	99.70	149.28	118.85
78	Kong_1997_040_S8-4	S8-4	250	292	64.2	2.80	455.20	0.70	2.50	265.80	99.70	149.28	128.65
79	Kong_1997_041_S8-5	S8-5	250	292	64.2	2.80	455.20	0.87	2.50	289.20	124.62	162.02	143.03
80	Kong_1997_042_S8-6	S8-6	250	292	64.2	2.80	455.20	1.00	2.50	283.90	142.42	171.12	158.54
81	Krefeld_1966_010_26-1	26-1	254	456	32.1	2.23	273.10	0.45	3.87	206.83	101.20	163.32	163.87
82	Krefeld_1966_012_29b-1	29b-1	254	456	29.7	2.23	273.10	0.30	3.87	160.13	67.47	141.89	143.85

Test No.	Author/Beam name	Beam name	b_w [mm]	d [mm]	f_{ck} [MPa]	ρ_l [%]	f_{ywk} [MPa]	$\rho_w f_{ywk}$ [MPa]	a/d	V_{exp} [kN]	$V_{VSIM\text{-}L\theta}$ (X_k, γ) [kN]	V_{ACI} (X_k, γ) [kN]	$V_{MC\text{-}10(III)}$ (X_k, γ) [kN]
83	Krefeld_1966_015_29a-2	29a-2	254	456	29.2	2.23	297.93	0.32	3.87	216.62	73.60	144.20	131.28
84	Krefeld_1966_016_29b-2	29b-2	254	456	33.4	2.23	297.93	0.32	3.87	202.38	73.60	151.25	142.16
85	Krefeld_1966_017_29c-2	29c-2	254	456	16.1	2.23	297.93	0.32	3.87	161.46	73.60	118.53	120.08
86	Krefeld_1966_018_29d-2	29d-2	254	456	22.4	2.23	297.93	0.32	3.87	165.02	73.60	131.77	134.32
87	Krefeld_1966_021_29g-2	29g-2	254	456	7.7	2.23	297.93	0.32	3.87	149.90	73.60	96.28	97.75
88	Leonhardt_1962_002_ET2	ET2	150	300	15.8	1.40	251.14	0.86	3.50	130.94	72.40	69.85	73.42
89	Leonhardt_1963_010_TA12	TA12	160	375	18.2	0.75	352.38	1.10	3.33	267.69	115.67	110.48	115.06
90	Levi_1989/1993_001_RC 30 A1	RC 30 A1	120	940	17.0	1.07	384.00	3.22	4.04	676.00	283.99	443.63	651.33
91	Levi_1989/1993_002_RC 30 A2	RC 30 A2	120	940	17.0	1.07	384.00	3.22	4.04	688.00	283.99	443.63	649.38
92	Levi_1989/1993_003_RC 60 A1	RC 60 A1	120	940	39.0	1.26	384.00	3.22	4.04	990.00	491.94	482.19	624.90
93	Levi_1989/1993_004_RC 60 A2	RC 60 A2	120	940	39.0	1.26	384.00	3.22	4.04	938.00	491.94	482.19	631.72
94	Levi_1989/1993_005_RC 60 B1	RC 60 B1	120	940	42.0	1.67	384.00	4.83	4.04	1181.00	576.49	667.96	957.77
95	Levi_1989/1993_006_RC 60 B2	RC 60 B2	120	940	42.0	1.67	384.00	4.83	4.04	1239.00	576.49	667.96	949.04
96	Levi_1989/1993_007_RC 70 B1	RC 70 B1	120	940	52.0	1.67	384.00	4.83	4.04	1330.00	651.22	681.40	935.61
97	Maruyama_1988_001_RS2-WD	RS2-WD	86	398	32.1	0.14	516.00	1.19	2.89	126.00	79.72	73.80	50.59
98	Moayer_1974_002_P20	P20	150	279	32.7	0.47	248.28	0.53	3.50	120.10	43.19	62.77	50.55
99	Özden_1967_002_T6	T6	110	298	25.4	1.05	218.17	1.33	3.52	137.34	81.43	71.82	79.23
100	Özden_1967_003_T7	T7	110	298	22.5	1.05	218.17	1.33	3.52	141.26	76.44	70.29	77.05
101	Özden_1967_004_T9	T9	110	298	22.5	1.05	218.17	1.33	3.52	154.02	76.44	70.29	74.28
102	Ozcebe_1999_003_TS56	TS56	150	310	53.0	3.46	204.00	0.49	5.00	129.20	44.43	79.74	74.95
103	Ozcebe_1999_006_TS59	TS59	150	310	74.0	4.43	204.00	0.57	5.00	125.40	51.83	90.56	94.32
104	Ozcebe_1999_009_TS36	TS36	150	310	67.0	2.59	204.00	0.49	3.00	155.90	44.43	86.64	68.18
105	Ozcebe_1999_011_TH39	TH39	150	310	65.0	3.08	204.00	0.43	3.00	142.90	38.87	82.86	69.81
106	Ozcebe_1999_012_TS39	TS39	150	310	65.0	3.08	204.00	0.57	3.00	179.20	51.83	89.48	72.44
107	Petersson_1972_001_V1	V1	175	322	30.0	1.07	258.40	0.56	3.57	100.93	61.38	83.95	71.72
108	Petersson_1972_002_VL1	VL1	120	278	35.0	1.20	292.80	2.45	3.24	190.73	124.81	115.33	121.54
109	Quast_1999_001_1/1	1/1	260	355	39.3	1.33	512.80	0.46	3.27	154.37	83.93	140.88	126.60
110	Regan_1971_001_R8	R8	152	272	18.4	1.46	216.00	0.46	3.22	81.00	37.26	49.71	43.52
111	Regan_1971_004_R11	R11	152	272	17.9	1.95	216.00	0.46	3.22	91.00	37.26	49.34	44.14
112	Regan_1971_005_R12	R12	152	254	25.5	4.17	216.00	0.46	3.45	112.00	34.79	51.13	47.15
113	Regan_1971_011_R20	R20	152	272	34.3	1.46	216.00	0.46	3.22	92.00	37.26	60.17	48.67
114	Regan_1971_012_R21	R21	152	254	39.4	4.17	224.00	0.90	3.45	153.00	68.05	75.84	75.74
115	Regan_1971_013_R22	R22	152	272	21.1	3.89	216.00	0.46	4.36	81.00	37.26	51.76	55.91
116	Regan_1971_016_R25	R25	152	254	22.4	4.17	216.00	0.46	3.45	107.00	34.79	49.17	46.24
117	Regan_1971_021_T3	T3	152	272	20.9	0.36	216.00	0.46	3.28	105.00	37.26	51.59	39.47
118	Regan_1971_022_T4	T4	152	272	26.3	0.48	216.00	0.46	3.28	110.00	37.26	55.27	45.02
119	Regan_1971_025_T7	T7	152	264	19.9	0.75	224.00	0.48	3.37	109.00	37.50	50.09	45.21
120	Regan_1971_026_T8	T8	152	254	23.7	1.04	224.00	0.48	3.50	124.00	36.08	50.70	44.82
121	Regan_1971_029_T13	T13	152	272	5.4	0.36	216.00	0.46	3.28	90.00	27.89	37.23	31.31
122	Regan_1971_030_T15	T15	152	254	25.1	1.04	216.00	0.46	7.10	104.00	34.79	50.88	48.64
123	Regan_1971_032_T17	T17	152	254	27.3	1.04	224.00	0.90	7.10	134.00	68.05	69.22	73.77

Test No.	Author/Beam name	Beam name	b_w [mm]	d [mm]	f_{ck} [MPa]	ρ_l [%]	f_{ywk} [MPa]	$\rho_w f_{ywk}$ [MPa]	a/d	V_{exp} [kN]	$V_{VSIM\text{-}L\theta}$ (X_k, γ) [kN]	V_{ACI} (X_k, γ) [kN]	$V_{MC\text{-}10(III)}$ (X_k, γ) [kN]
124	Regan_1971_033_T19	T19	152	254	22.2	1.04	216.00	0.46	5.30	106.00	34.79	49.07	46.35
125	Regan_1971_034_T20	T20	152	254	23.7	1.04	224.00	0.90	5.30	138.00	68.05	66.99	70.77
126	Regan_1971_038_T25	T25	152	272	44.7	0.36	216.00	0.46	3.28	114.00	37.26	65.76	46.88
127	Regan_1971_039_T26	T26	152	254	43.9	1.04	224.00	0.90	3.50	179.00	68.05	77.99	72.27
128	Regan_1971_046_T34	T34	152	254	23.3	2.08	216.00	0.46	5.30	112.00	34.79	49.79	45.80
129	Regan_1971_047_T35	T35	152	254	23.3	0.59	216.00	0.46	5.30	115.00	34.79	49.79	45.18
130	Rehm_1978_001_RsIS / BQ II 0	RsIS / BQ II 0	250	430	16.5	1.10	448.00	3.41	3.00	594.78	286.55	441.97	570.52
131	Rehm_1978_004_RnIIS	RnIIS	450	548	14.1	0.64	445.60	1.50	3.00	744.73	455.35	531.88	523.78
132	Reineck_1991_001_Stb III	Stb III	77	590	52.6	1.25	412.00	4.92	4.27	536.67	265.39	279.24	390.49
133	Reineck_1991_002_Stb I	Stb I	77	589	52.6	1.44	439.20	7.37	4.27	681.73	286.95	389.67	571.75
134	Roller_1990_007_7	7.00	457	762	64.4	1.88	356.14	0.56	2.91	787.83	384.42	666.35	599.93
135	Roller_1990_009_9	9.00	457	762	117.3	2.35	356.14	0.56	2.91	749.40	384.42	676.47	681.94
136	Roller_1990_010_10	10.00	457	762	117.3	2.89	356.14	0.83	2.91	1172.14	567.47	770.03	757.42
137	Sarsam_1992_007_BL2-H	BL2-H	180	233	67.7	2.82	656.00	0.61	4.00	138.30	50.11	83.39	72.11
138	Sarsam_1992_008_BS2-H	BS2-H	180	233	65.9	2.82	656.00	0.61	2.50	223.50	50.11	82.81	55.01
139	Sarsam_1992_010_BS4-H	BS4-H	180	233	72.1	2.82	656.00	1.22	2.50	206.90	100.22	109.00	95.70
140	Sarsam_1992_011_CL2-H	CL2-H	180	233	62.1	3.51	656.00	0.61	4.00	147.20	50.11	81.18	72.98
141	Sarsam_1992_013_CS3-H	CS3-H	180	233	66.2	3.51	656.00	0.92	2.50	247.20	75.16	95.74	74.33
142	Sarsam_1992_014_CS4-H	CS4-H	180	233	67.7	3.51	656.00	1.22	2.50	220.70	100.22	109.00	98.89
143	Shin_1999_009_MHB 2.5-25	MHB 2.5-25	125	215	44.0	3.77	292.73	0.86	2.45	98.80	45.35	53.30	53.04
144	Shin_1999_010_MHB 2.5-50	MHB 2.5-50	125	215	44.0	3.77	292.73	1.72	2.45	149.32	90.70	76.48	78.72
145	Shin_1999_021_HB 2.5-25	HB 2.5-25	125	215	65.0	3.77	292.73	0.86	2.45	115.72	45.35	59.58	54.65
146	Shin_1999_022_HB 2.5-50	HB 2.5-50	125	215	65.0	3.77	292.73	1.72	2.45	149.32	90.70	82.76	83.53
147	Soerensen_1974_001_T-21	T-21	110	298	24.5	1.05	182.86	0.95	3.52	130.95	61.25	59.09	59.71
148	Soerensen_1974_003_T-23	T-23	110	298	26.2	1.05	279.39	0.96	3.52	140.76	61.41	60.10	58.68
149	Soerensen_1974_007_T-2-B	T-2-B	110	298	16.9	1.05	317.84	0.97	3.52	130.95	57.60	55.21	55.93
150	Soerensen_1974_009_T-4-B	T-4-B	110	298	16.7	1.05	317.84	0.65	3.52	108.39	41.59	44.55	42.12
151	Stroband_1997_002_2	2.00	90	647	79.4	1.10	480.00	3.25	2.56	528.00	347.92	269.50	304.74
152	Stroband_1997_003_3	3.00	90	647	80.3	1.62	504.00	7.68	2.56	886.27	466.38	527.35	656.06
153	Taylor_1966_004_HSS-1-B	HSS-1-B	114	257	11.5	1.26	350.34	1.14	4.44	86.98	43.63	51.26	60.76
154	Yoon_1996_009_H2-N	H2-N	375	655	79.0	2.86	344.00	0.81	3.23	721.00	390.63	538.06	538.09
155	Rosenbusch_2003_001_1.3-1	1.3/1	200	260	41.2	3.55	544.00	0.38	3.37	120.80	38.64	76.23	72.93
156	Rosenbusch_2003_002_1.4-1	1.4/1	200	260	39.9	3.55	544.00	0.76	3.37	170.61	77.28	95.10	94.60
157	Rosenbusch_2003_004_1.7-1	1.7/1	200	260	42.4	3.55	440.00	2.46	3.37	190.46	214.46	185.02	240.27
158	Kautsch_2010_001_A2	A2	155	719	22.8	0.68	484.00	2.09	2.68	657.10	309.77	324.85	325.61
159	Kautsch_2010_002_B2	B2	155	719	23.4	0.68	484.00	1.57	2.68	571.22	283.47	267.55	264.61
160	Tanimura_2005_031_41	41.00	300	400	12.6	2.20	310.40	1.63	2.50	324.00	209.20	270.09	332.49